Technical Report Documentation Page

1. Report No. FHWA/TX-10/5-4124-01-2	2. Government Accession No.	3. Recipient's Catalog No.
4. Title and Subtitle Field Test and Finite Element of I-345 Bridge in Dallas		5. Report Date July 2009 6. Performing Organization Code
7. Author(s) Amy Smith Barrett, Hyeong Kim and Karl H. Frank		8. Performing Organization Report No. 5-4124-01-2
9. Performing Organization Name and Address Center for Transportation Research The University of Texas at Austin 3208 Red River, Suite 200 Austin, TX 78705-2650		10. Work Unit No. (TRAIS) 11. Contract or Grant No. 5-4124-01
12. Sponsoring Agency Name and Address Texas Department of Transportation Research and Technology Implementation Office P.O. Box 5080 Austin, TX 78763-5080		13. Type of Report and Period Covered Technical Report 14. Sponsoring Agency Code

15. Supplementary Notes
Project performed in cooperation with the Texas Department of Transportation and the Federal Highway Administration.

16. Abstract

This report documents a field test to determine the stresses at areas where fatigue cracks had formed in the bridges. Two bridges were instrumented and subjected to controlled truck traffic. In addition, the service fatigue stresses were evaluated by monitoring the stresses for a 1 week period after the controlled truck testing. A three dimensional finite element model was constructed of each bridge. The stresses from the field tests and the model were compared. The floor beams were found to behave as composite with the bridge deck when the truck loads were near floor beams. The local stress at the critical sections was in reasonable agreement between the field and analytical results. Proposed retrofit schemes were evaluated in the analytical model. In general, the proposed schemes appear to reduce the stresses at the critical locations, however high stresses are generated in other areas that have not cracked. The unsymmetrical support conditions of some of the girder units cause twisting of bridge section. Adding of additional supports to make the bridge support symmetrical will also improve fatigue performance of the bridge.

17. Key Words bridges, steel, fatigue, retrofit, analysis, and field test	18. Distribution Statement No restrictions. This document is available to the public through the National Technical Information Service, Springfield, Virginia 22161; www.ntis.gov.

19. Security Classif. (of report) Unclassified	20. Security Classif. (of this page) Unclassified	21. No. of pages 170	22. Price

Form DOT F 1700.7 (8-72) Reproduction of completed page authorized

Field Test and Finite Element of I-345 Bridge in Dallas

Amy Smith Barrett
Hyeong Kim
Karl H. Frank

CTR Technical Report:	5-4124-01-2
Report Date:	July 10, 2009
Project:	5-4124-01
Project Title:	Field Test and Finite Element of I-345 Bridge in Dallas
Sponsoring Agency:	Texas Department of Transportation
Performing Agency:	Center for Transportation Research at The University of Texas at Austin

Project performed in cooperation with the Texas Department of Transportation and the Federal Highway Administration.

Center for Transportation Research
The University of Texas at Austin
3208 Red River
Austin, TX 78705

www.utexas.edu/research/ctr

Disclaimers

Author's Disclaimer: The contents of this report reflect the views of the authors, who are responsible for the facts and the accuracy of the data presented herein. The contents do not necessarily reflect the official view or policies of the Federal Highway Administration or the Texas Department of Transportation (TxDOT). This report does not constitute a standard, specification, or regulation.

Patent Disclaimer: There was no invention or discovery conceived or first actually reduced to practice in the course of or under this contract, including any art, method, process, machine manufacture, design or composition of matter, or any new useful improvement thereof, or any variety of plant, which is or may be patentable under the patent laws of the United States of America or any foreign country.

Engineering Disclaimer

NOT INTENDED FOR CONSTRUCTION, BIDDING, OR PERMIT PURPOSES.

Project Engineer: Karl H. Frank
Professional Engineer License State and Number: Texas No. 48953
P. E. Designation: Research Supervisor

Acknowledgments

The authors wish to express appreciation to the TxDOT Dallas District and to Lloyd Wolf and Dr. Yuan Zhao for their guidance, help, and useful comments.

Table of Contents

List of Figures

List of Tables

Chapter 1. Introduction

1.1 Bridge Information

The bridge under study is an elevated section of I-345 near the interchange of I-45 and I-30 in downtown Dallas. This is a very busy interchange that plays a vital role in transporting vehicles to and from downtown Dallas. The bridge consists of two twin steel plate girder structures, one northbound and one southbound. Transverse floor beams frame over the two main girders and support the concrete slab, which is post-tensioned in both the longitudinal and transverse directions. Both the floor beams and the girders were designed to act non-compositely. The bridge was designed according to the 1965 and 1969 AASHTO Specifications.

1.2 History of Cracking

The original cracking on the bridge occurred at the connection of the floor beams to the girders. A detail of the connection is shown in Figure 1.1.

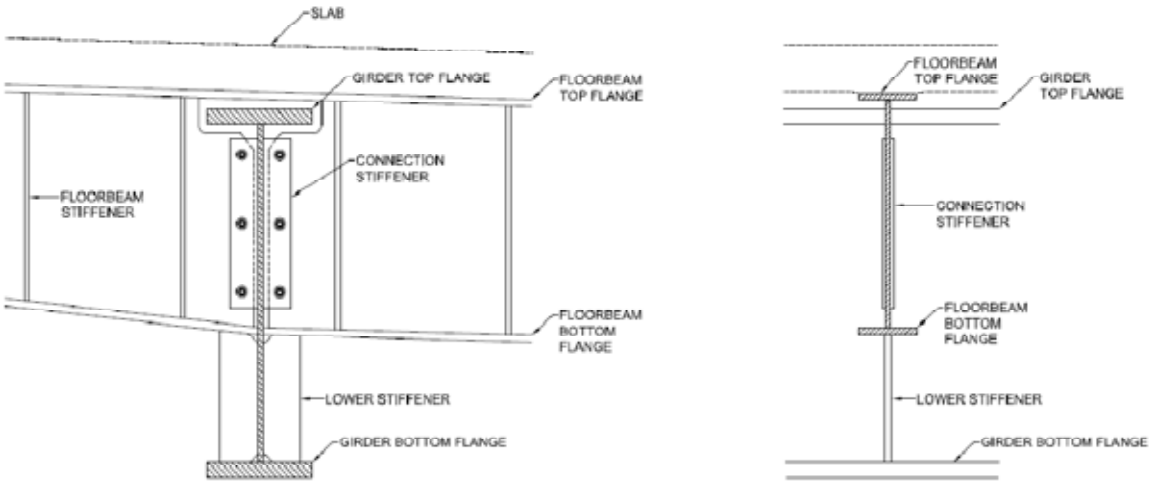

Figure 1.1: Typical Connection of Floor Beam to Girder

Cracking occurred in the girder web where the bottom floor beam flange is welded to the girder web. When the floor beam is at a pier the floor beam flanges frame into the web between the bearing stiffeners (Figure 1.2). The resulting small gap between the stiffener and flange welds causes high stresses to occur at the weld toes from displacement of the floor beam flange. These cracks typically formed an arc shape in the girder web around the edges of the bottom floor beam flange. Figure 1.3 shows the cracking that occurred at these locations. Cracking also occurred on the girder web in the gap between the top flange of the girder and the web of the connecting floor beam. The stiffener connecting the floor beam and girder webs is not attached to the top flange of the girder. This creates a small gap in the girder web where differential deflection between the two girders causes the floor beam to rotate creating very high stresses. Figure 1.4 shows an example of cracking at this location.

Figure 1.2: Floor Beam to Girder Connection at Pier

Figure 1.3: Cracked Weld Repair in Gap between Bearing Stiffener and Bottom Flange of Floor Beam

Figure 1.4: Crack in Web Gap

A retrofit was performed in 2004 in an attempt to mitigate the cracking. Many of the cracks were welded and arrestor holes were drilled at the crack tips to relieve the stress. This repair can be seen in Figure 1.3. The retrofit also consisted of adding retrofit stiffeners on top of the stiffeners connecting the floor beams to the girders. These stiffeners were welded to the top flange of the girder in order to close the previously mentioned gap where cracking had occurred. Figures 1.5 and 1.6 show a detail and picture of a retrofitted connection. Some of the welds were also subjected to ultrasonic impact treatment to improve their fatigue performance.

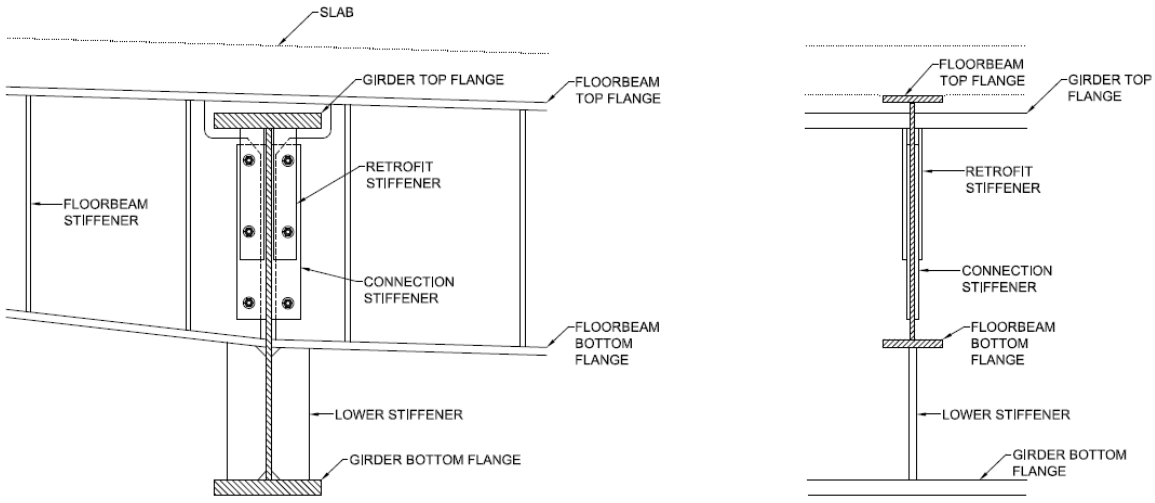

Figure 1.5: Typical Retrofitted Connection of Floor Beam to Girder

Figure 1.6: Retrofitted Connection

Since the retrofit, new cracks have developed at the connections. Figures 1.7 through 1.9 show three types of new cracks that formed where retrofit stiffeners were placed. New cracks also developed in the area between the bearing stiffeners and the bottom flange of the floor beams. Figure 1.10 shows an example of this type of crack that formed at the toe of the bearing stiffener weld. This type of crack formed due to the rotation of the floor beams, creating a region of high stress in this small area.

Figure 1.7: Crack at Connection of Retrofit Stiffener to Top Girder Flange

Figure 1.8: Crack at Weld Connecting Existing Stiffener to Floor Beam Web

Figure 1.9: Crack at Weld Connecting Retrofit Stiffener to Existing Stiffener

Figure 1.10: Cracks between Bearing Stiffener and Bottom Flange of Floor Beam

1.3 Details of Test Locations

The purpose of this study is to determine the reasons for cracking in this bridge. In order to accomplish this, two sections of the bridge were examined as part of this study. These sections were chosen because they were easily accessible and because they had experienced cracking. The two sections differed in their support layouts, roadway geometry, and girder dimensions. By comparing the results from the two sections, the effect of these differences on the bridge behavior can be determined.

Section F14N is part of the northbound structure and is located just north of Pacific Avenue. It is a three span continuous system with 12 floor beams running between the two main girders. The post-tensioned deck was designed to act non-compositely with the floor beams. The girders are spaced 46 feet apart and have a five-degree horizontal curve. A layout of Section F14N and elevations of its girders are shown in Figures 1.11 and 1.12, respectively. Floor beam two was studied in this section. An elevation of floor beam two can be seen in Figure 1.13.

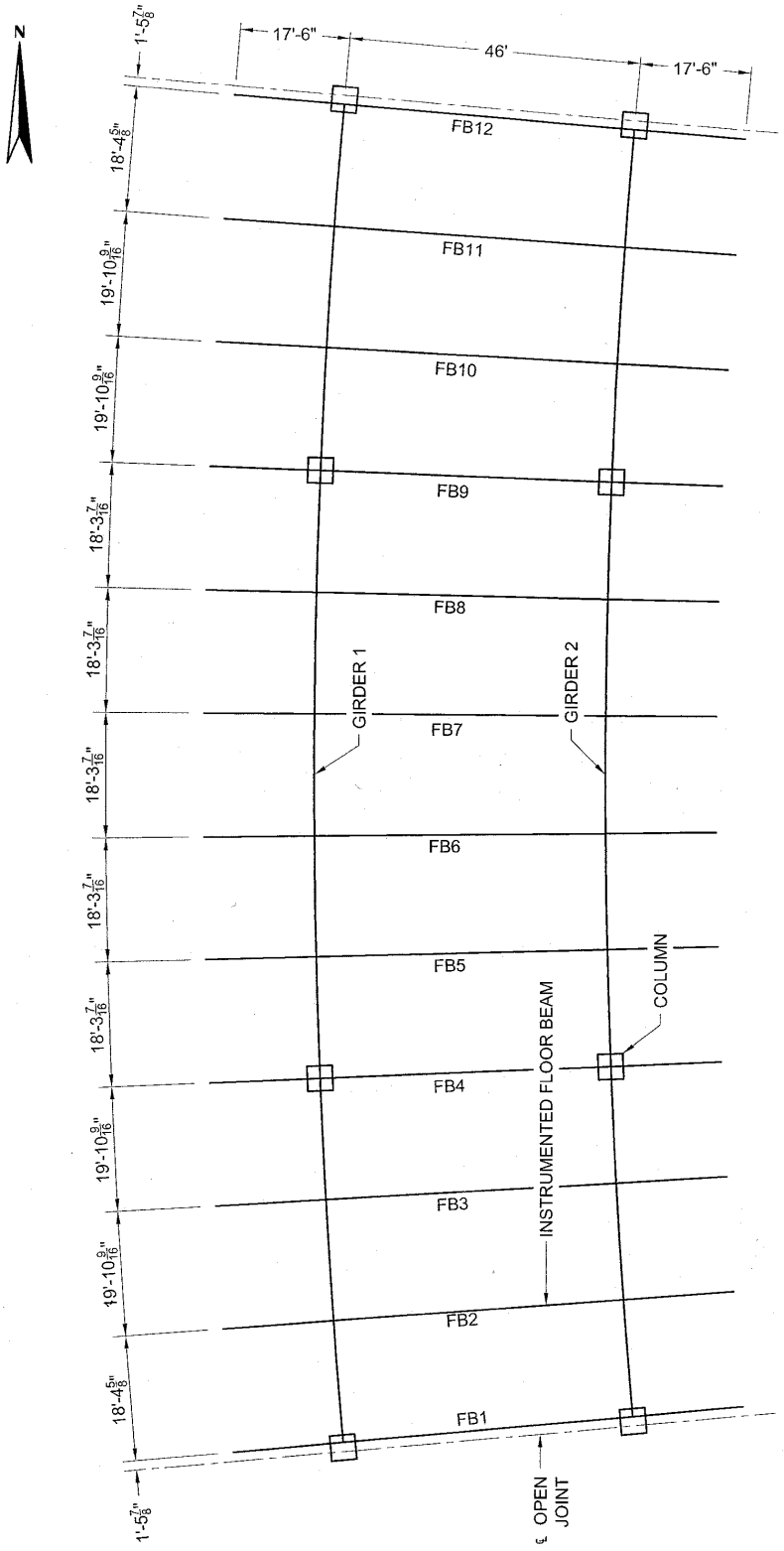

Figure 1.11: Section F14N Layout

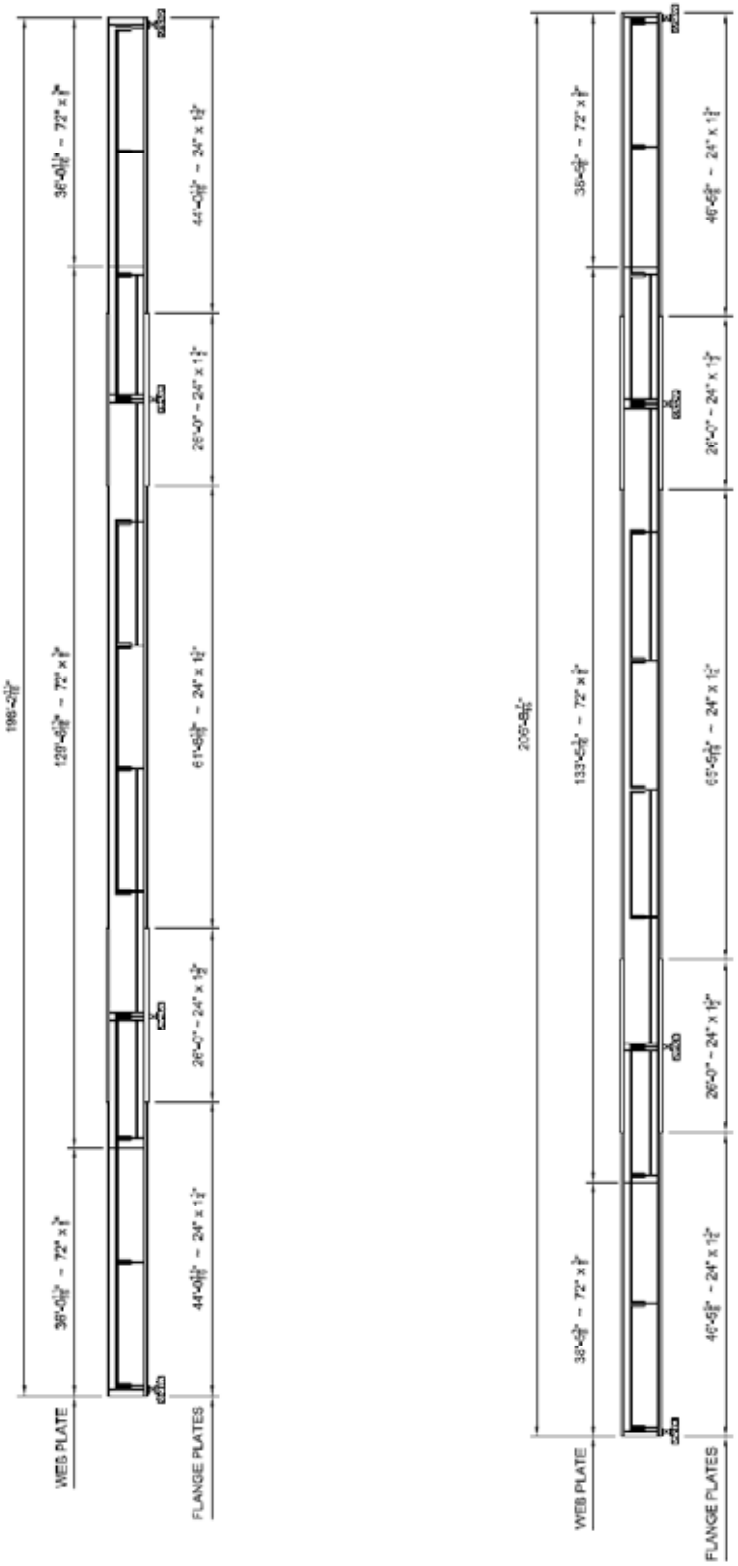

Figure 1.12: Section F14N Girder Elevations

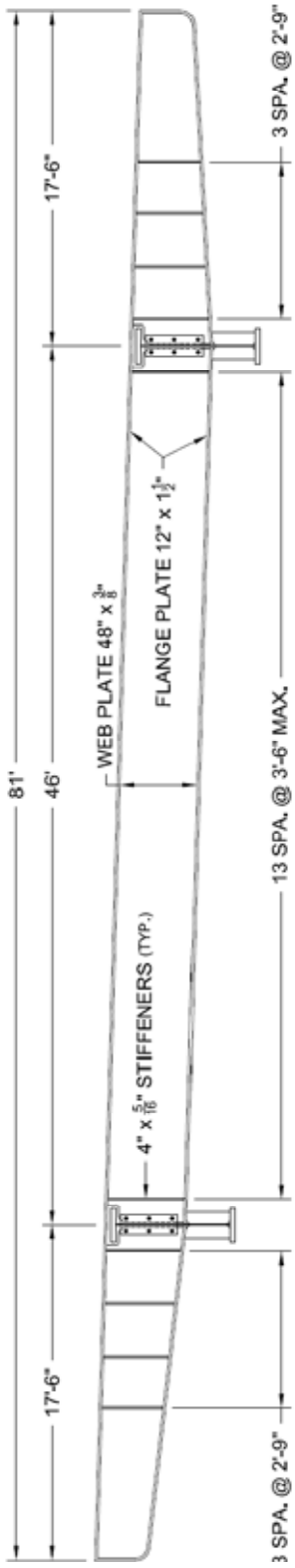

Figure 1.13: Sections F14N Floor Beam 2 Elevation

Section F17S is part of the southbound structure and is located just south of Live Oak Street. This section was chosen in part because of its asymmetrical support layout (see Figure 1.14). The support columns are placed in such a way as to accommodate the roadways underneath the bridge. This results in several locations where the girder at one end of a floor beam is supported by a column, but the girder at the other end is not. Girder two has two haunches as can be seen in Figure 1.14.

Figure 1.14: Asymmetrical Columns and Haunches of Section F17S

There are a total of 32 floor beams running between the two main girders. The post-tensioned deck was designed to act non-compositely with the floor beams. The bridge is flared at the north end to accommodate an entrance ramp. The girders are spaced from about 59’-9” at the north end to 42’ feet apart at the sound end. The horizontal curve of the section ranges from about 2.2 degrees to 7.5 degrees. A layout of Section F17S and elevations of its girders are shown in Figures 1.15 through 1.18. Floor beams 16 and 18 were studied in this section. Elevations of these floor beams can be seen in Figure 1.19.

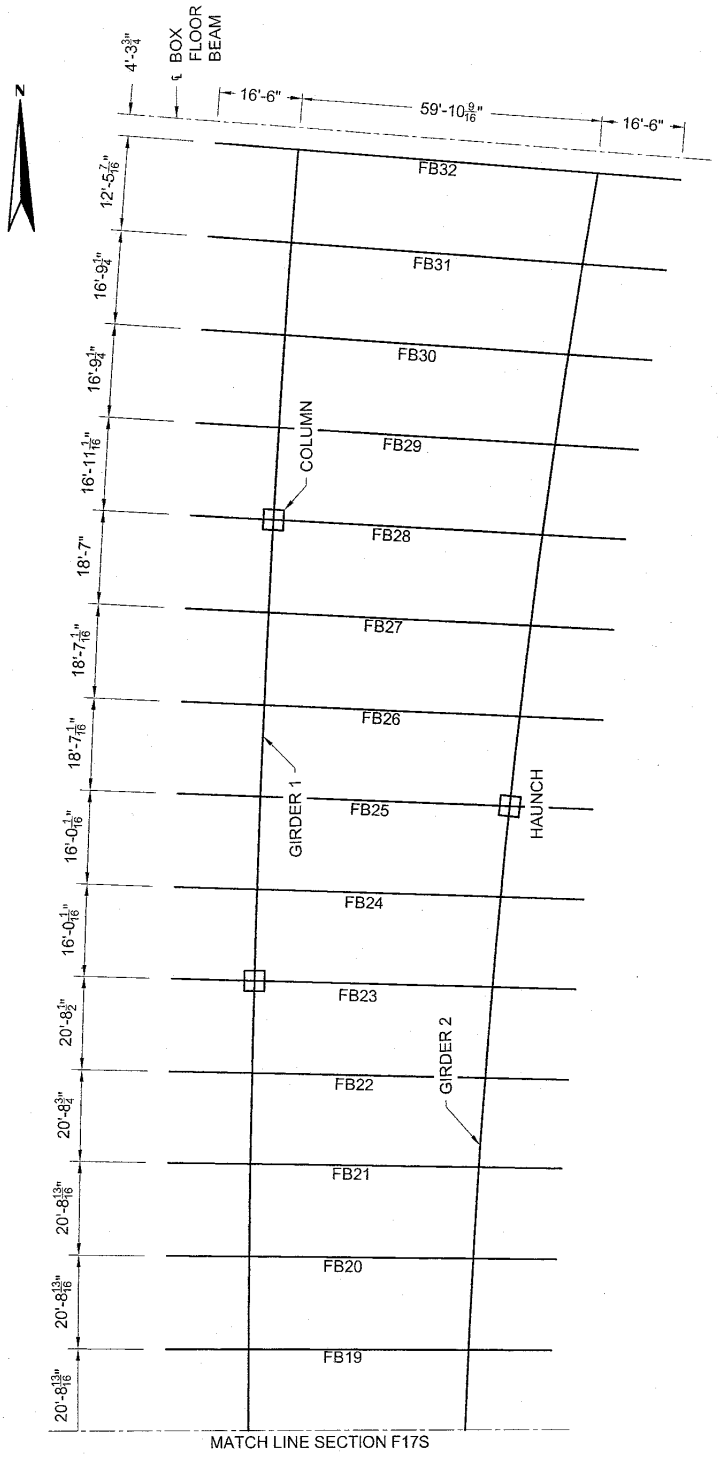

Figure 1.15: Section F17S Layout (North End)

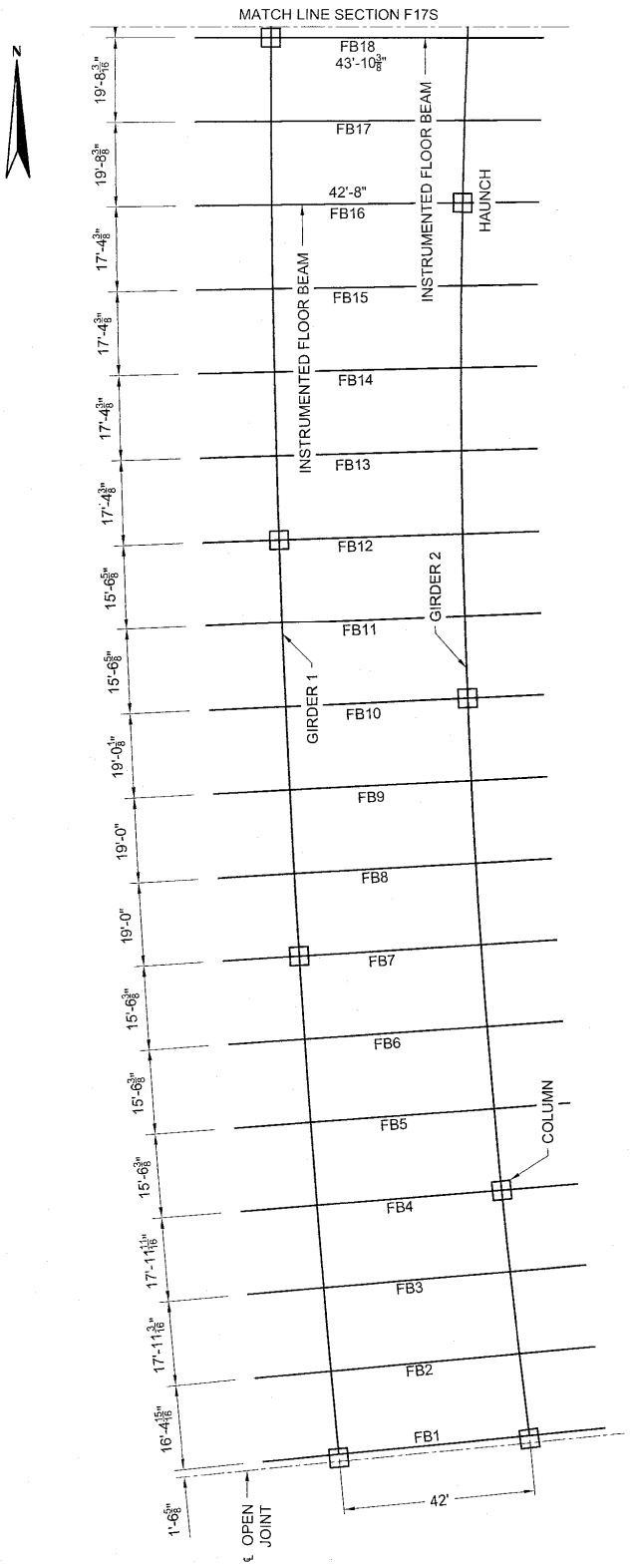

Figure 1.16: Section F17S Layout (South End)

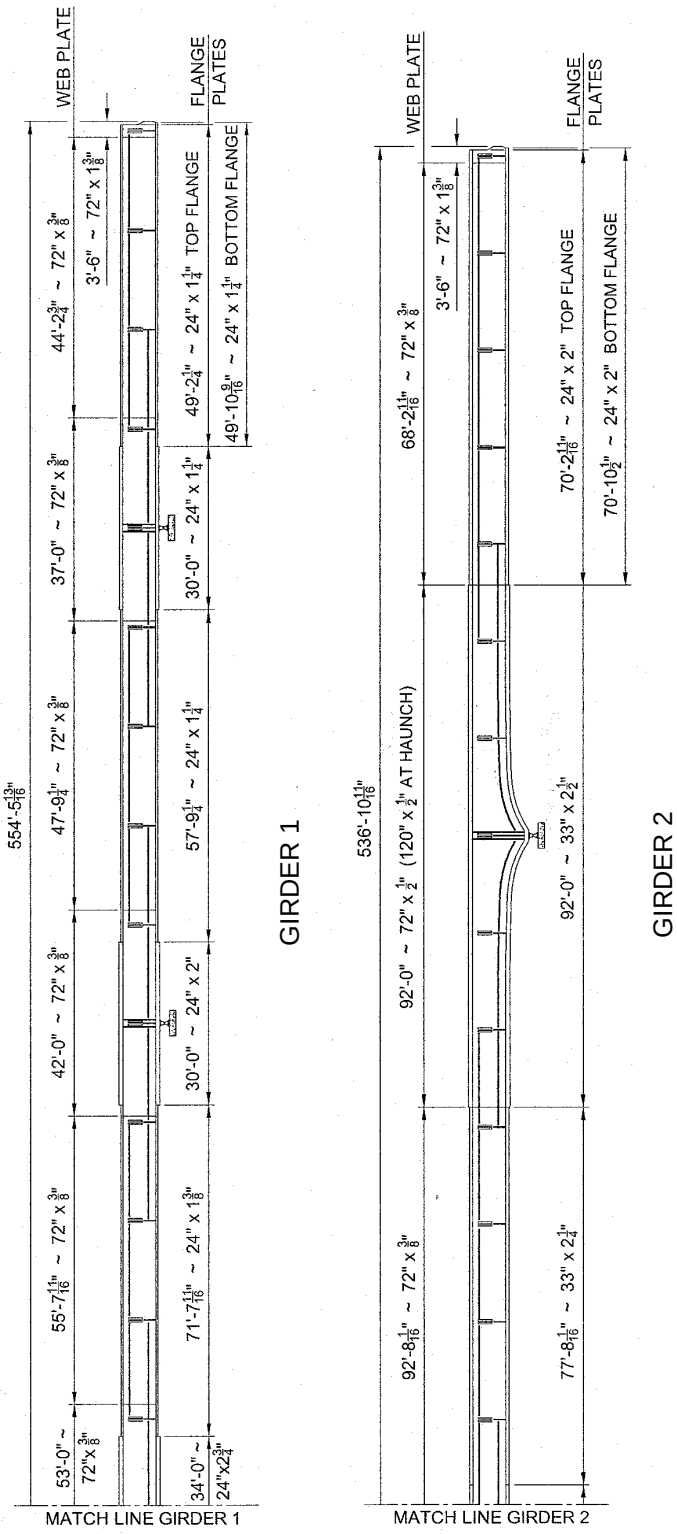

Figure 1.17: Section F17S Girder Elevations (North End)

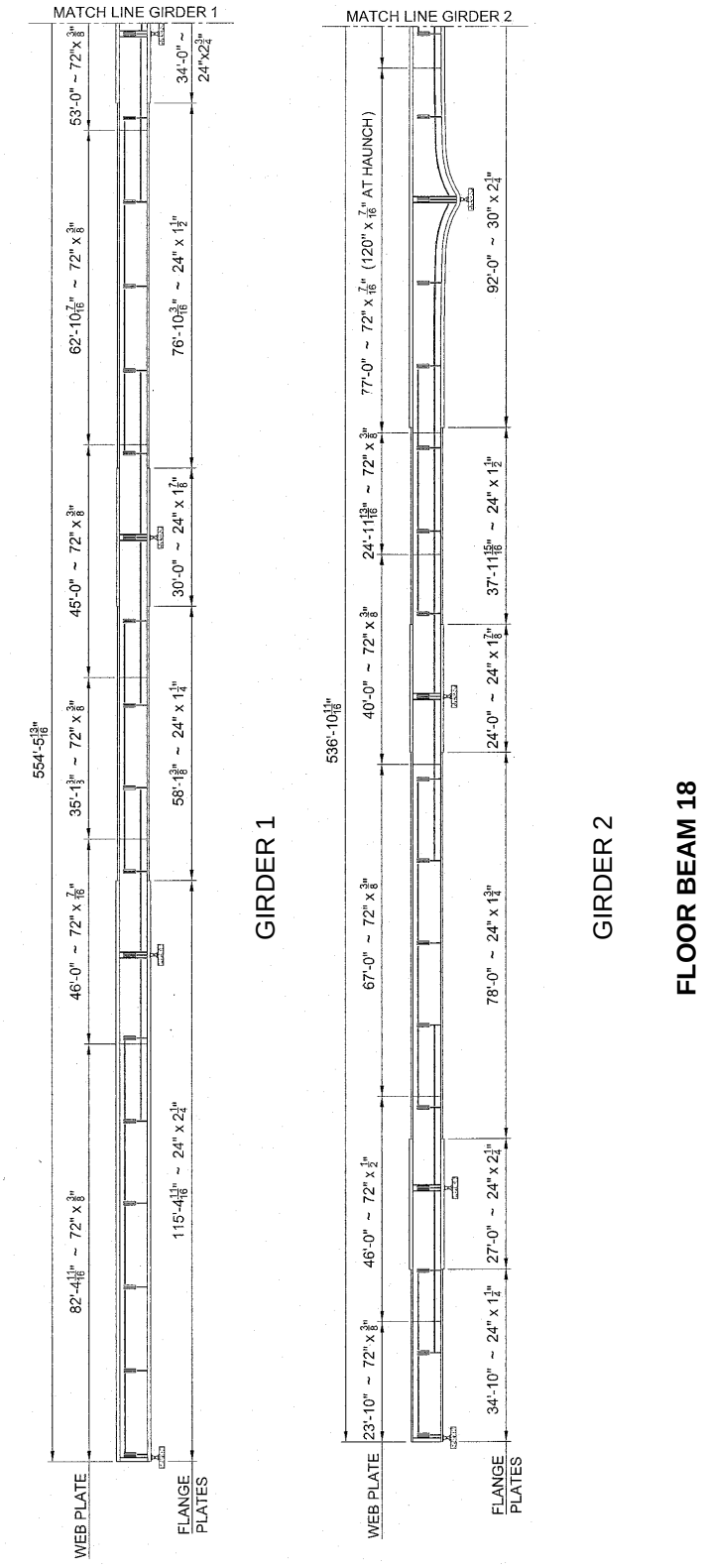

Figure 1.18: Section F17S Girder Elevations (South End)

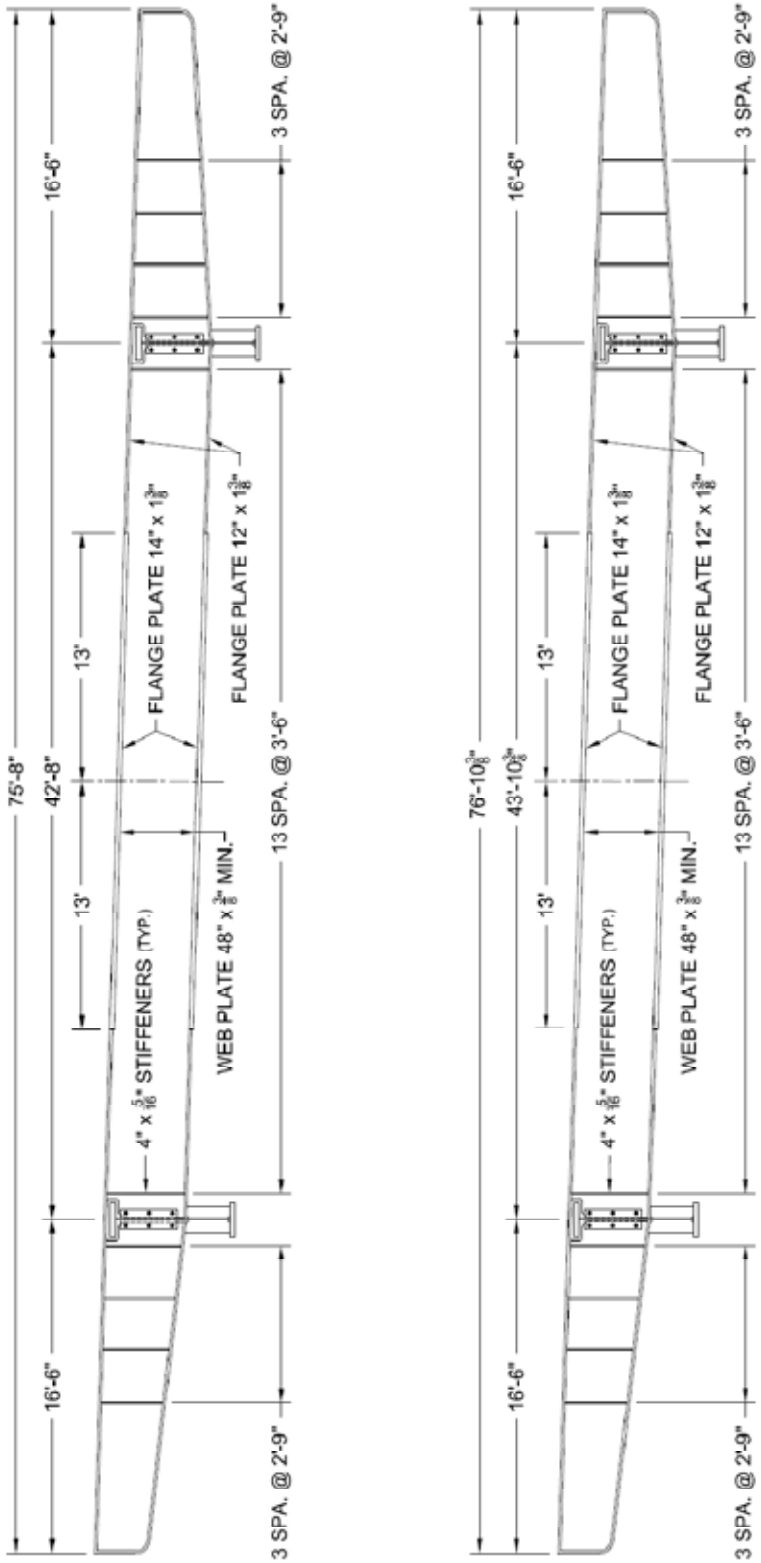

Figure 1.19: Section F17S Floor Beam Elevations

Chapter 2. Instrumentation and Testing

2.1 Introduction

This section details the type of instrumentation used and the field tests that were performed in order to gather data from the bridge. Strain gages were used to monitor the strains in the floor beams and girders under traffic loads. String potentiometers (or string pots) were used to measure the vertical deflection of each end of the floor beams near the connections to the girders. Data from two types of tests were collected. The first test consisted of running one and two dump trucks of known weight over the bridge in various locations. The second test monitored strain ranges in the floor beams and girders over a period of seven days.

2.2 Strain Gages

The strain gages used were model CEA-06-250UN-350 from Vishay Micro Measurements. These general purpose gages, shown in Figure 2.1, have a resistance of 350 ohms, a strain range of ±3%, and are self-temperature-compensated for use with mild steels. This gage has an overall length and width of 0.415” and 0.120”, respectively. The three wires from each gage were connected to a data acquisition system.

Figure 2.1: Vishay Micro Measurements CEA-06-250UN-350 Strain Gage

2.3 String Potentiometers

The string pots used were model number PG-2A from Patriot Sensors and Controls Corporation. The string pots were capable of measuring deflections of up to five inches. A typical string pot is shown in Figure 2.2.

Figure 2.2: Patriot Sensor and Controls PG-2A String Potentiometer

2.4 Data Acquisition System

The data acquisition system used to collect the information from the strain gages and string pots was the CR5000 Datalogger manufactured by Campbell Scientific. The CR5000,

shown in Figure 2.3, is capable of collecting data from 20 differential sensors at one time. Due to the number of gages applied to the bridge and the distance between them, a total of five dataloggers were used during the tests. The system was set to collect readings every 50 milliseconds from the strain gages. The settling time, which is the time from when an excitation voltage is applied to when the datalogger records the value, was set to 200 milliseconds. The integration time, which refers to the time the datalogger integrates a channel being measured, was set to 250 milliseconds. The longer the integration time, the less noise is recorded during the reading.

Figure 2.3: Campbell Scientific CR5000 Datalogger

2.5 Strain Gage Procedures

Bucket trucks provided by the Texas Department of Transportation (TxDOT) were used to reach the areas to be instrumented. These trucks can be seen in Figure 2.4. First, a paint-stripping tool was used to remove the paint in the areas where gages were to be placed. Then, grinders and sanders were used to create a smooth surface for the gages. The areas were then cleaned with acetone to remove all impurities. M-Bond 200 Catalyst-C made my Vishay Micro Measurements was painted on the back of the gages in order to speed up the setting of the adhesive. The adhesive used was type CN-Y from Texas Measurements. Gages were then applied to the bridge in pre-determined locations. Figure 2.5 shows a gage applied to the bridge. M-Coat W-1 wax from Vishay Micro Measurements was then brushed over the gages for waterproofing. Once installed, the gages were attached to the dataloggers that were anchored to the girder flanges (see Figure 2.6).

Figure 2.4: Bucket Trucks used to Place Strain Gages

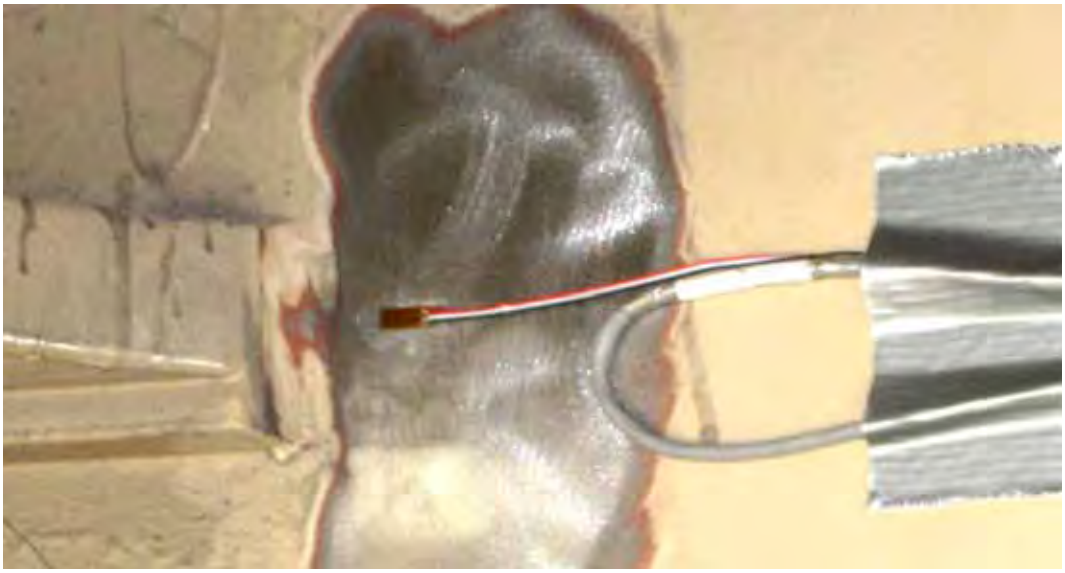

Figure 2.5: Strain Gage prior to adding Waterproof Wax

Figure 2.6: Datalogger on Girder Flange

2.6 Strain Gage Locations

Strain gages were applied to the girders at the floor beam-to-column connections as well as to the floor beams. The strain gages were applied in areas where cracking had occurred in order to determine the stresses at these locations under traffic loads.

In section F14N, floor beam two was instrumented. This location was chosen because of the symmetrical layout of support columns and because it had not been previously retrofitted. Two gages were placed on both sides of the girder web in the gap between the top girder flange and the connecting floor beam web. These gages will be referred to as the web gap gages. Gages were also placed on both sides of the girder web adjacent to the bottom flange of the connecting floor beam. These gages will be referred to as the bottom flange gages. A detail of the connection of the floor beam to the girder as well as the locations of the gages can be seen in Figure 2.7. These gages were placed so as to determine the reasons for cracking in these areas.

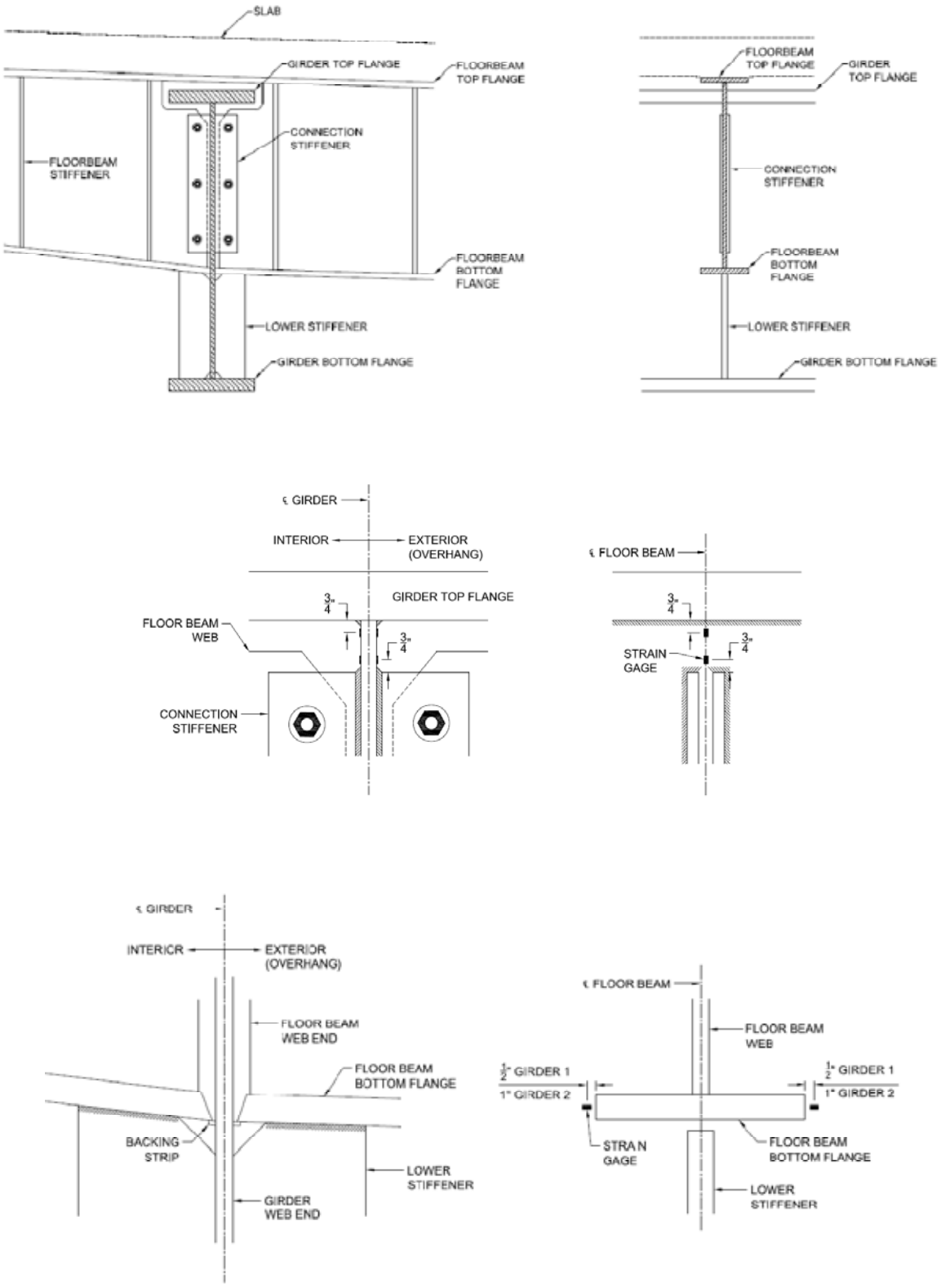

Figure 2.7: Section F14N Floor Beam Two Connection Detail and Strain Gage Locations

In section F17S, floor beams 16 and 18 were instrumented. The girders at these floor beams are supported on only one end of each floor beam. The asymmetric support condition, which causes larger floor beam rotations under traffic along with the tight gap between the floor beam flange and the bearing stiffeners, is suspected of being the cause of the cracking at these locations. Girder 2 is haunched at floor beam 16. The connections at floor beams 16 and 18 had been retrofitted. A gage was placed on the exposed side of both retrofit stiffeners on the interior side of the girder. These gages will be referred to as the retrofit stiffener gages. Gages were also placed on both sides of the girder web adjacent to the bottom flange of the connecting floor beam. These gages were placed so as to determine the reasons for cracking in these areas. The connections of floor beam 16 to girder 2 and floor beam 18 to girder 1 are at supports and, therefore, include bearing stiffeners. These stiffeners made it difficult to place the gages adjacent to the bottom flange of the connecting floor beam. Because of this and the existence of repair welds in this area, there were no gages placed on the girder web south of floor beam 16. Figure 2.8 shows the gap at this location. Details of the connections at floor beams 16 and 18 as well as the locations of the gages can be seen in Figures 2.9 through 2.12.

Figure 2.8: Gap between Bottom Flange of Floor Beam 16 and Bearing Stiffener

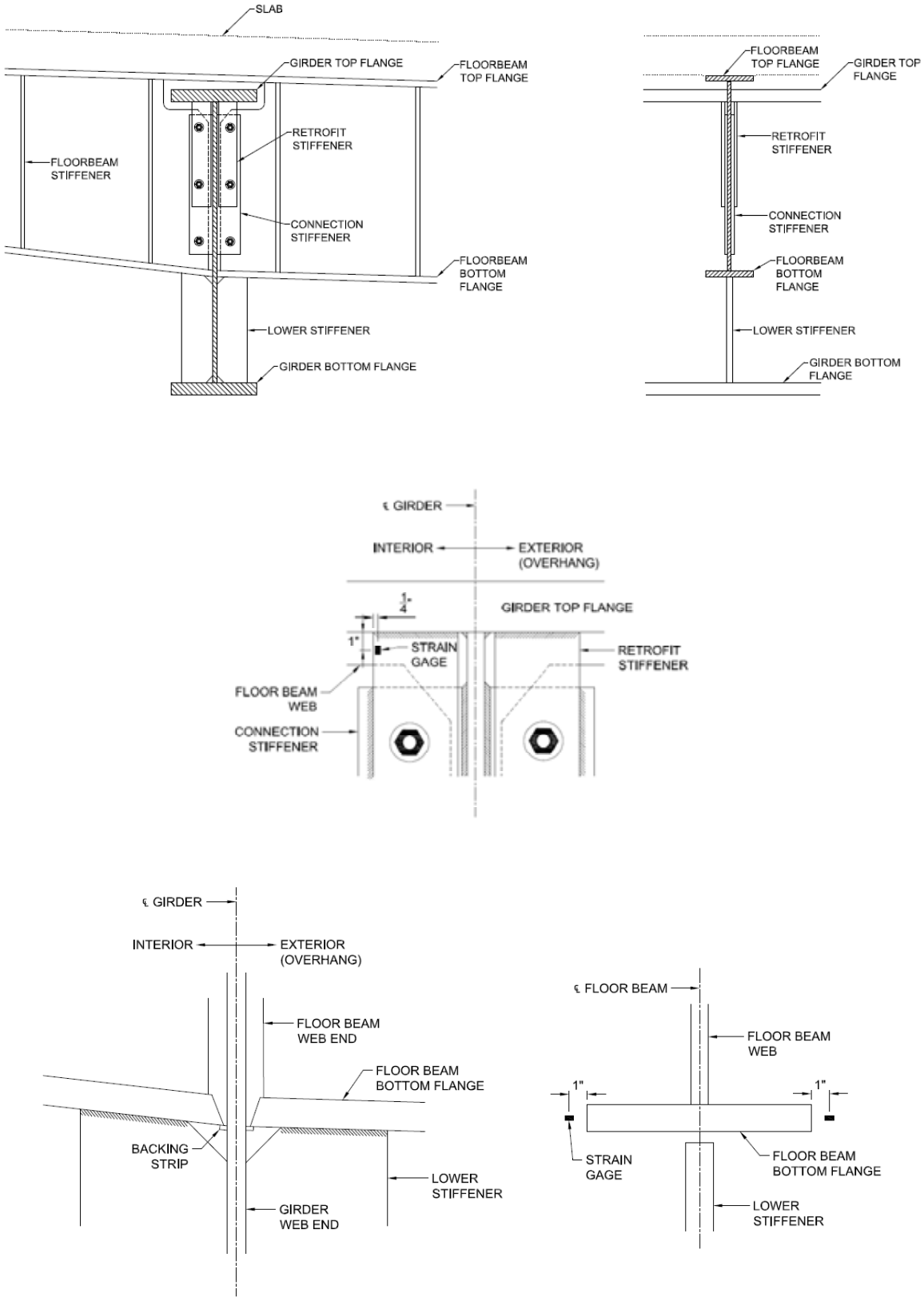

Figure 2.9: Section F17S Floor Beam 16 - Girder 1 Connection Detail and Strain Gage Locations

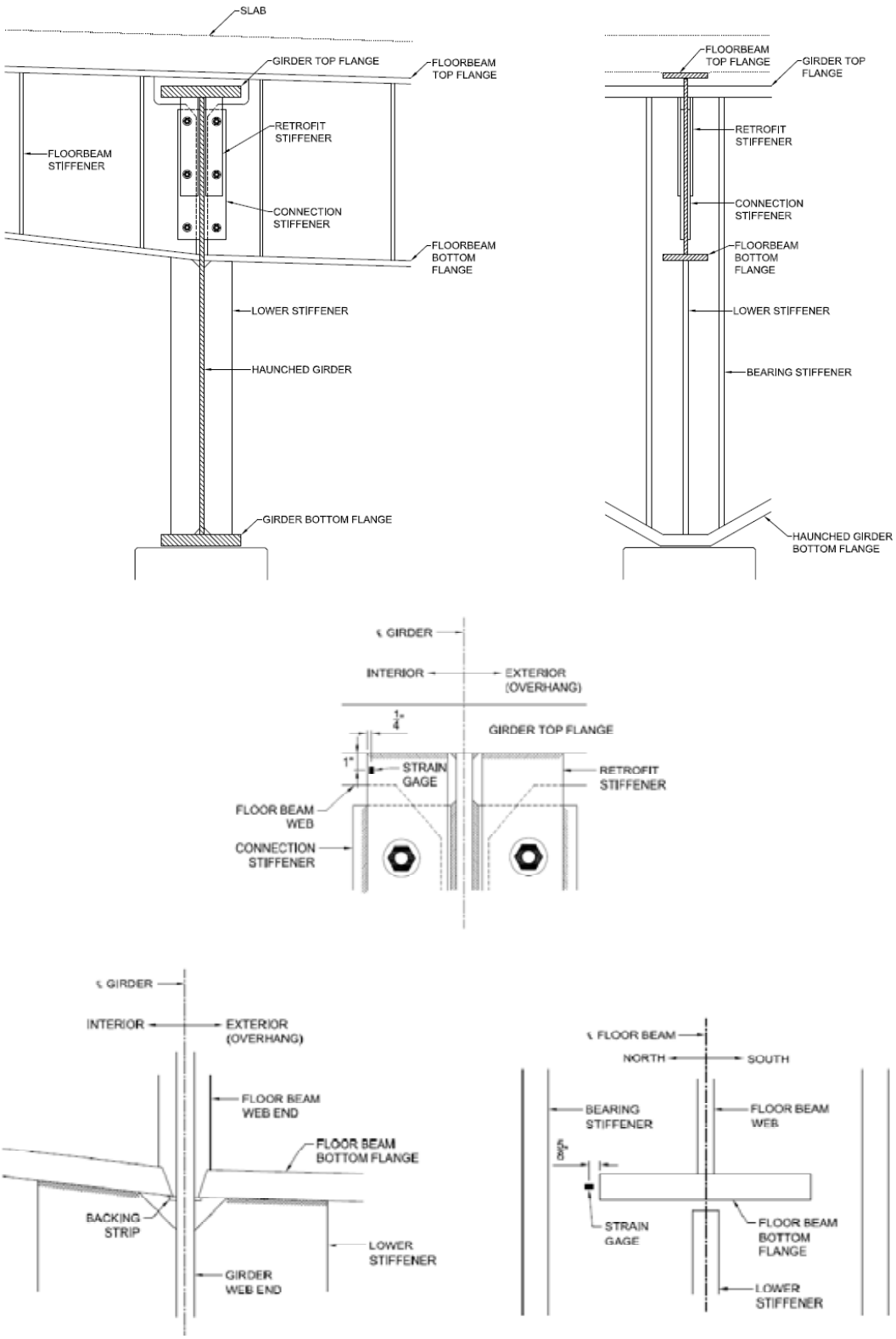

Figure 2.10: Section F17S Floor Beam 16 - Girder 2 Connection Detail and Strain Gage Locations

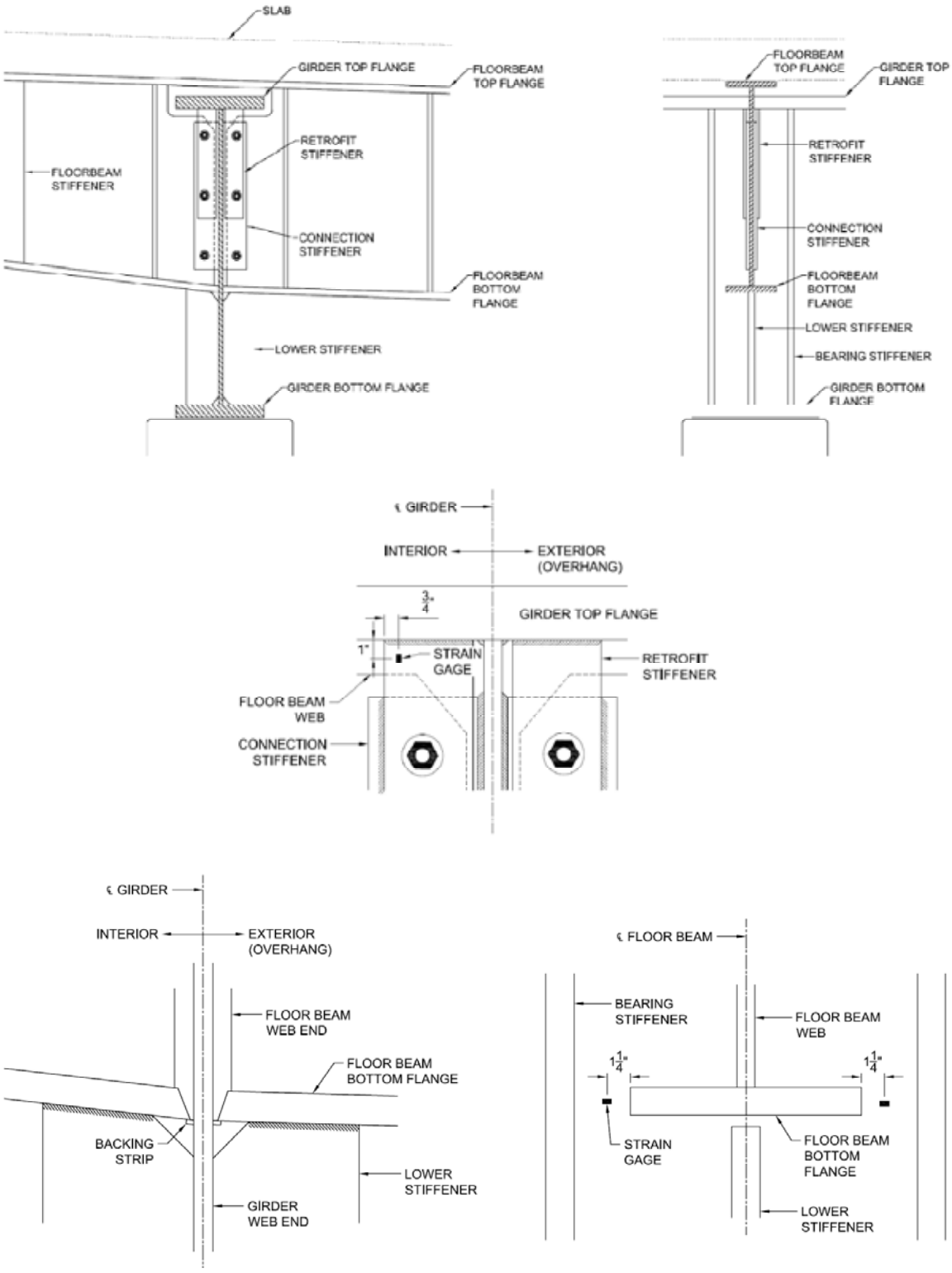

Figure 2.11: Section F17S Floor Beam 18 - Girder 1 Connection Details and Strain Gage Locations

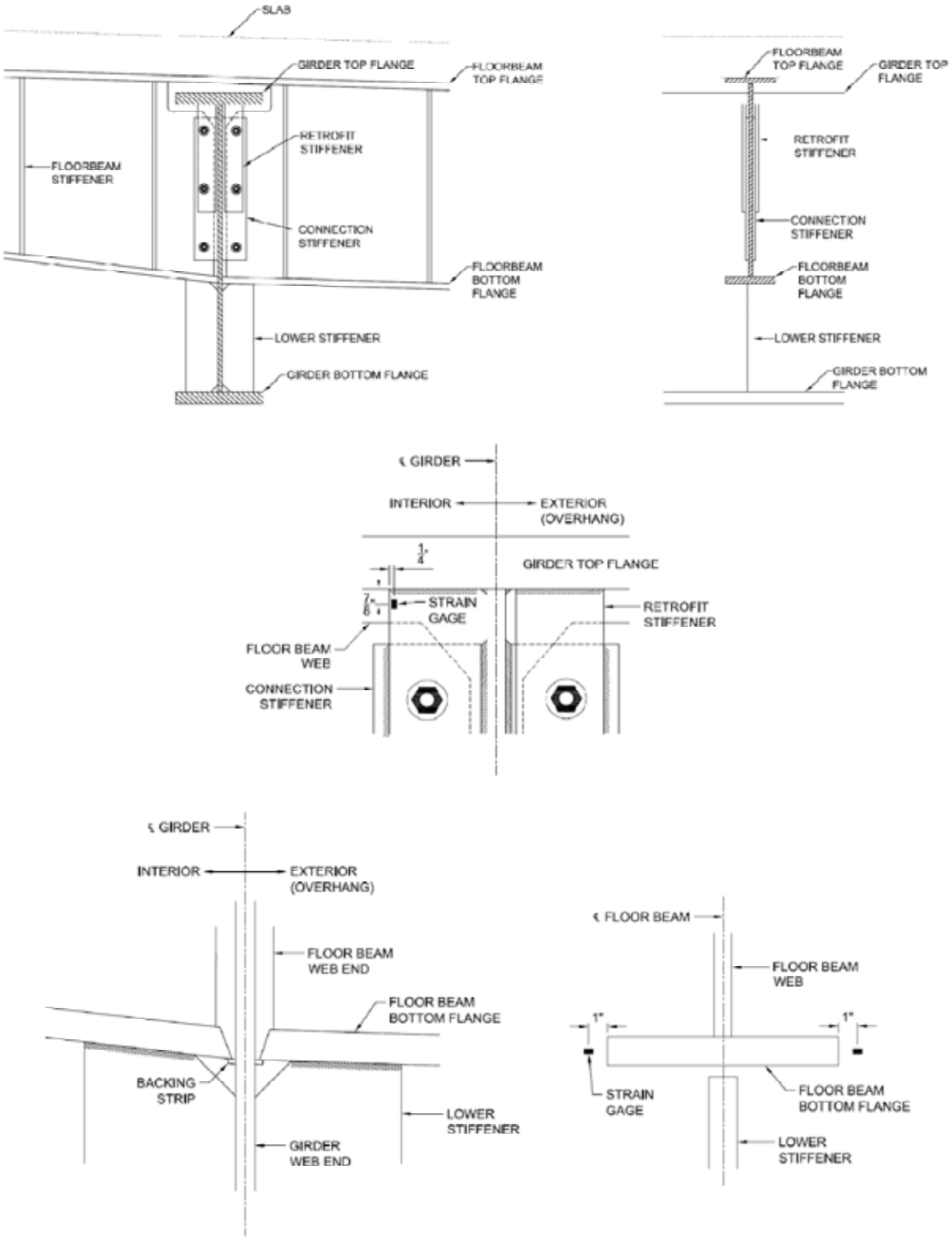

Figure 2.12: Section F17S Floor Beam 18 - Girder 2 Connection Detail and Strain Gage Locations

Gages were also placed on the top and bottom flanges of all three floor beams at both ends and in the middle. These gages were placed so as to determine the stresses in the floor beams and how they react to traffic loads. Figure 2.13 shows the locations of these gages.

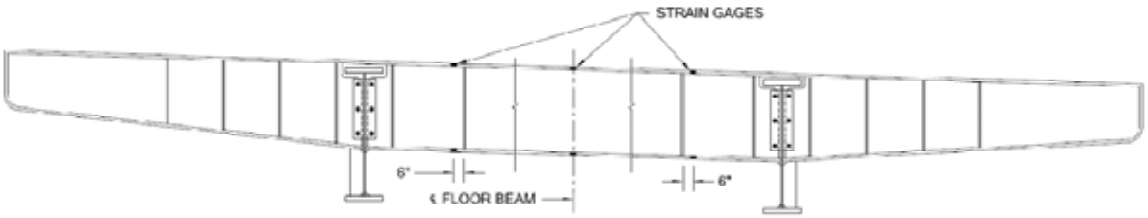

Figure 2.13: Location of Floor Beam Strain Gages

2.7 String Potentiometer Locations

String pots were placed on either end of the interior portion of the floor beams near the connections to the girders as seen in Figure 2.14. The string pots were fastened to the bottom of the bottom flange at each location. Cinderblocks with hooks glued to the top were placed on the ground under each string pot. The string from the string pots was drawn down from the floor beam and attached to the hook on the cinderblock.

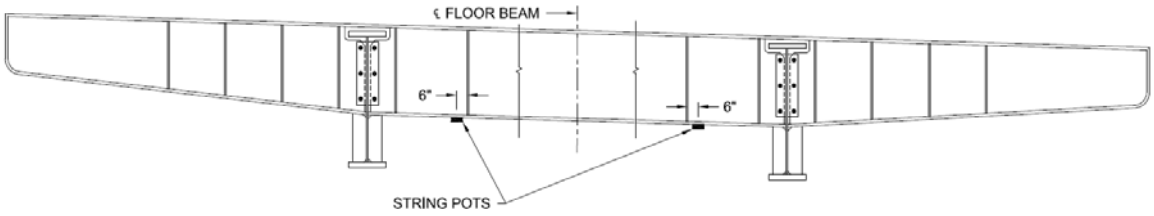

Figure 2.14: Location of String Potentiometers on Floor Beam

2.8 Controlled Live Load Tests

Two identically sized dump trucks of known weight were used in a controlled live load test of the bridge. The trucks were run over the bridge while data was collected from the strain gages. The details of the two dump trucks, which were filled with sand, are shown in Table 2.1 and Figure 2.15:

Table 2.1: Weights of Test Trucks

	Truck	**Truck**
Steer Axle Weight (lbs)	10440	10740
Drive Axles Weight	30360	27740
Gross Weight (lbs)	40800	38480

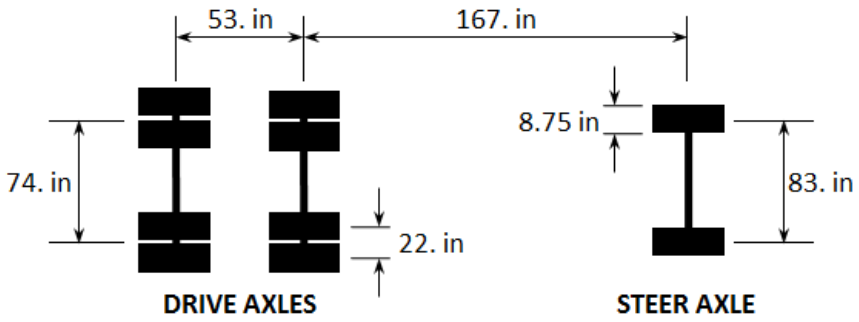

Figure 2.15: Dimensions of Test Trucks

There were two live load tests performed. The first test was performed on Monday July 7th from approximately 8:00 to 9:00 in the evening on section F14N. The second test was performed on Tuesday July 8th from approximately 8:00 to 10:00 in the evening on section F17S.

A moving road block provided by TxDOT vehicles was used to keep all traffic off of the road except for the test trucks. There were a total of 6 runs. The first run consisted of one truck in the far right lane. The second run had one truck in the far left lane. The third run had two trucks side by side in the two right lanes and the fourth run had two trucks side by side in the two left lanes. The fifth and sixth runs were a repeat of runs one and two, respectively. During each run, the truck(s) kept a steady pace around 5 mph and stopped for approximately 10 seconds when the first drive axle was directly above the instrumented floor beam. Having the trucks stop over the floor beams provides a steady state in which static stresses can be determined. Radios were used for communication between the test trucks, the road block, and the people monitoring the data acquisition system. A photograph of one truck driving over the bridge during the live load test can be seen in Figure 2.16.

Figure 2.16: Controlled Live Load Test of Section F17S

2.9 Fatigue Data Acquisition

Once the live load tests were complete, the data acquisition systems were reconfigured for rainflow counting to collect fatigue data. The data acquisition systems were left on all the gages on the two floor beams in section F17S and half of the gages on floor beam two of section F14N for one week. The rainflow counting program tallied the number of times the gages experienced strain ranges within specified values. Thus, the resulting data shows a histogram of strain ranges for each strain gage. From these values, the effective stress range and fatigue life can be determined.

The minimum and maximum strain limits in the rainflow counting program were set to -700 and +700 microstrain. These limits were set after looking at the data from the live load tests. The number of bins was set to 40. Therefore, the first bin tallies the number of times a gage experienced stress ranges from 0 to 35 microstrain (0 to 1.015 ksi), the second bin from 35 to 70 microstrain (1.015 to 2.03 ksi), and so on. The tally was reset every hour so that traffic patterns could be established.

Chapter 3. Data Reduction Techniques

3.1 Noise Reduction

In order to reduce some of the noise that was recorded by the gages, a moving average technique was used. This technique involved averaging the readings for every group of five data points. An example of the moving average technique can be seen in Table 3.1.

Table 3.1: Example of Moving Average Technique

TIME (s)	STRESS (psi)	AVERAGED VALUES	AVERAGED STRESS (psi)
0	40.3		40.30
0.1	38.1		41.03
0.2	44.7		40.08
0.3	37.8		38.66
0.4	39.5		39.42
0.5	33.2		37.76
0.6	41.9		37.34
0.7	36.4		37.56
0.8	35.7		38.74
0.9	40.6		38.47
1	39.1		39.10

Using this method significantly reduced the noise in some of the gages. Figures 3.1 and 3.2 show data before and after using the moving average technique.

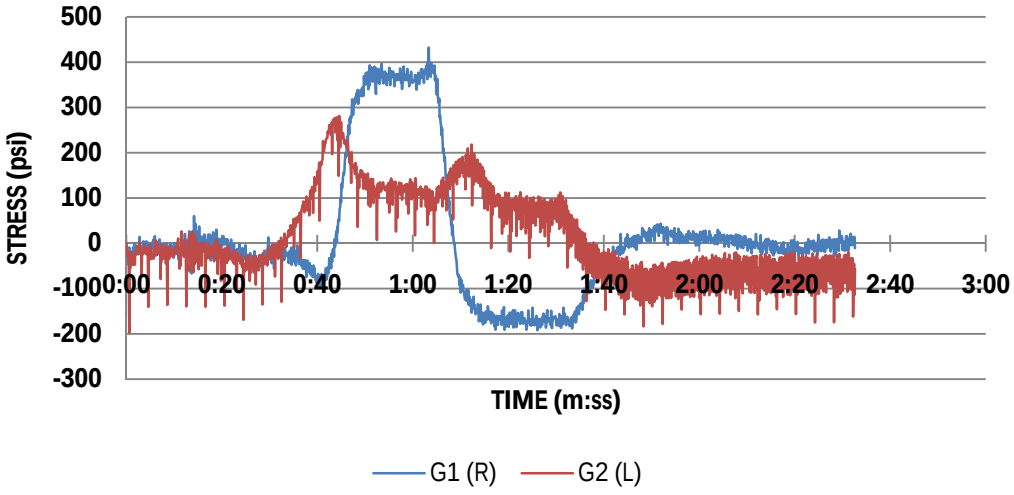

Figure 3.1: Raw Strain Gage Data

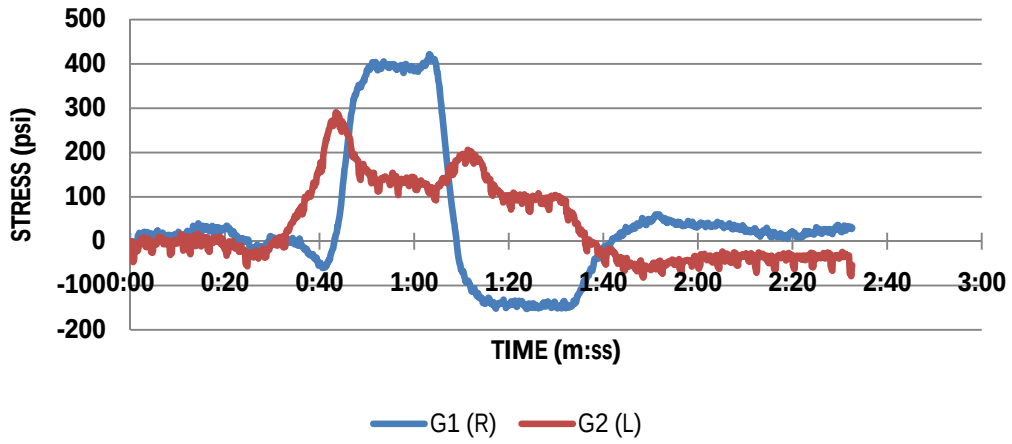

Figure 3.2: Strain Gage Data using the Moving Average Technique

3.2 In-Plane and Out-of-Plane Bending

The strain gages were placed on the bridge elements in pairs, such that each gage had an opposite. For example, there were gages placed at the same location on opposite sides of the floor beam flanges and opposite sides of the girder web. This was done in order to differentiate between in-plane and out-of-plane bending of the member. In-plane bending stresses vary linearly down the depth of the cross section. With respect to the gages placed on the girder web, in-plane stresses are the stresses caused by vertical bending of the girder in the plane of the web. These stresses are the largest at the top and bottom of the cross section and are assumed to be constant across the width of the member. Out-of-plane stresses vary linearly across the width of the member and are caused by bending out of the plane of the member. Figure 3.3 shows a diagram of the in-plane and out-of-plane stress distributions along the girder web and the equations used to calculate them.

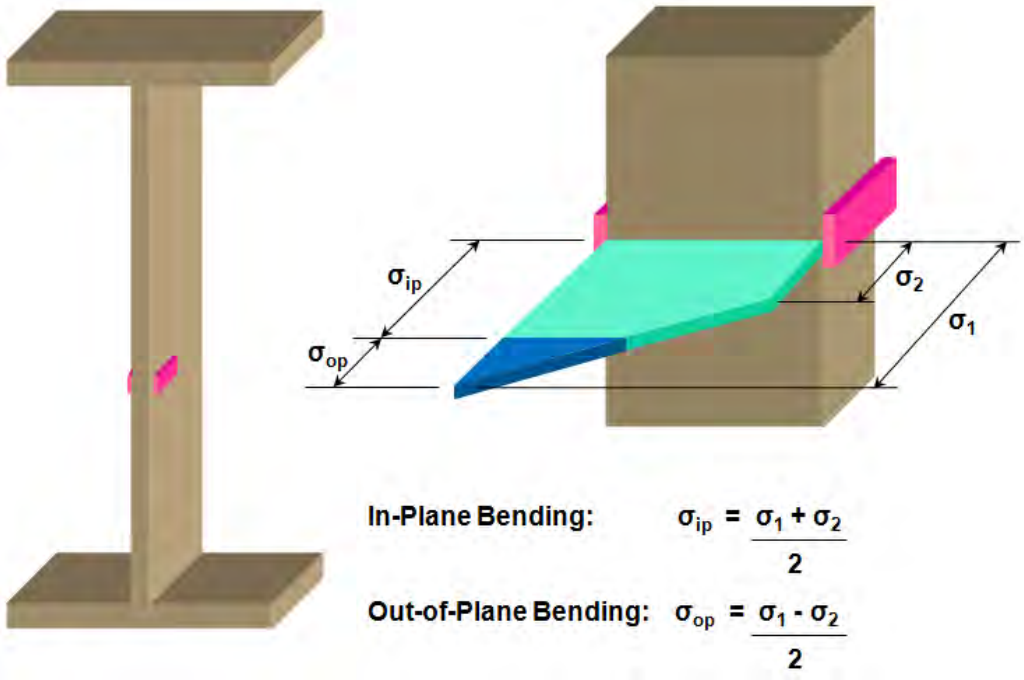

Figure 3.3: In-Plane and Out-of-Plane Bending Stresses

3.3 Bending Stress Sign Conventions

3.3.1 Positive and Negative Stress

The strain gages measured the strain in the member, which was then converted into stress. Both positive and negative values were recorded by the gages. Positive values are associated with positive strain, which indicates that the member is elongating. When converted into stress, positive strain values correspond to positive, or tensile, stress. Negative values correspond to negative strain, which means that the member is shortening and corresponds to negative, or compressive, stress.

3.3.2 Floor Beam Gages

The gages on opposite sides of the floor beam flanges were used to differentiate between in-plane and out-of-plane bending. In-plane bending corresponds to vertical bending of the floor beam in the plane of the web. Out-of-plane bending corresponds to lateral bending of the floor beam out of the plane of the web. The out-of-plane bending stresses for the floor beams were calculated in such a way that if the resulting stress is positive, the floor beam is bending toward the north, and if it is negative, the floor beam is bending toward the south. Figure 3.4 is a plan view of a floor beam showing a schematic of the sign convention for the floor beam gages.

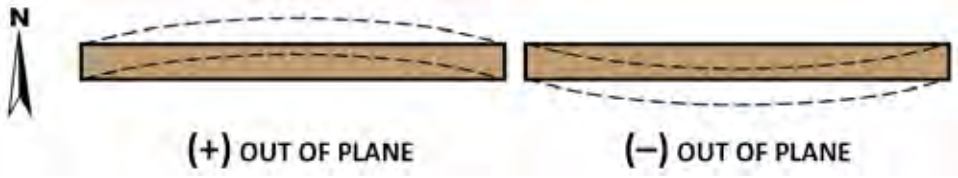

Figure 3.4: Plan View of Floor Beam Showing Out-of-Plane Bending Stress Sign Convention

3.3.3 Bottom Flange Gages

The stresses in the gages on opposite sides of the girder web were used to differentiate between in-plane and out-of-plane bending of the girder web. For all of the floor beam-to-column connections that were tested, with the exception of the haunched girder at floor beam 16, the bottom flange of the floor beam frames into the girder below the girder's neutral axis. Therefore the bottom flange gages that were adjacent to the bottom flange of the floor beam were also located below the girder's neutral axis. Positive in-plane stress recorded by the gages suggests that the bottom half of the girder is in tension. For connections that were not supported by a column, a positive in-plane stress value suggests that the girder is deflecting downward in the plane of the web. A negative in-plane stress value implies that the bottom half of the girder is in compression and is therefore deflecting upward.

The out-of-plane component of the bending stress was calculated in such a way that if the result is positive, the girder is bending inward toward the center of the bridge. If the result is negative, the girder is bending toward the outside of the bridge. Figure 3.5 is a plan view of the girders showing a schematic of the sign convention for the bottom flange gages.

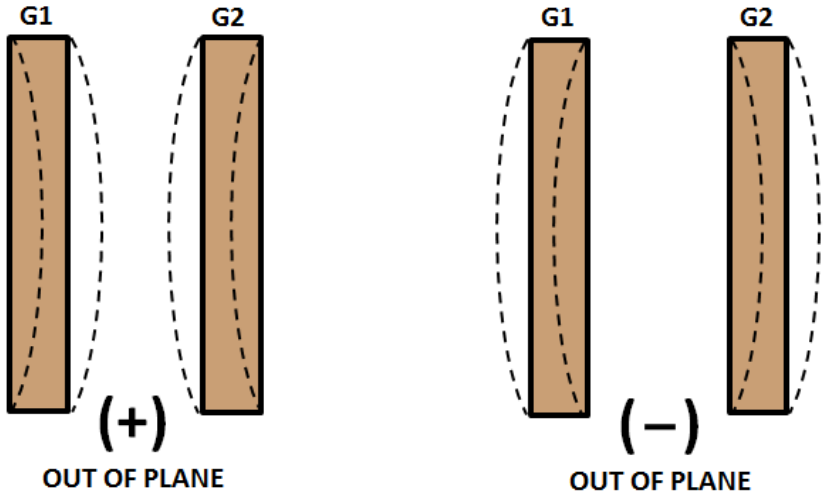

Figure 3.5: Plan View of Girders Showing Out-of-Plane Bending Stress Sign Convention

3.3.4 Web Gap Gages

The web gap gages were placed vertically along the web of the girder and, therefore, indicate how the girder web is bending out-of-plane. The data from the gages on opposite sides of the web were used to determine in which direction the girder web was bending. If the girder is bending out of the plane of the web, the gages on opposite sides of the web will experience

strains that are opposite in sign. This can be seen in Figure 3.6, which shows that the girder web bends toward the gage that records positive or tensile strain.

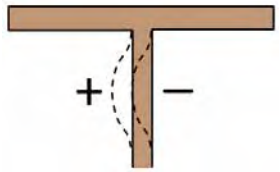

Figure 3.6: Out-of-Plane Bending of Girder Web Gap

3.3.5 Retrofit Stiffener Gages

The stresses in the gages on opposite sides of the retrofit stiffeners were used to differentiate between in-plane and out-of-plane bending of the stiffeners. In-plane bending corresponds to bending in the plane of the stiffener. Out-of-plane bending stress corresponds to the stress generated from the stiffener bending out of plane. The gages on the retrofit stiffeners were placed on the outer top corner of the stiffeners on either side of the floor beam web. Therefore, if the gage records positive in-plane stresses, the stiffener would be bending as shown in Figure 3.7(a). If the gage records negative out-of-plane stresses, the stiffener would be bending as shown in Figure 3.7(b).

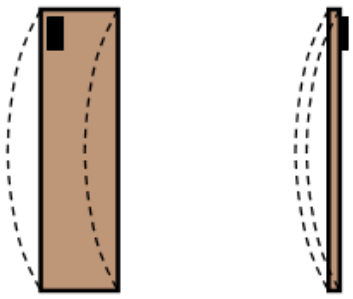

Figure 3.7: In-Plane (a) and Out-of-Plane (b) Bending of the Retrofit Stiffeners

3.4 Composite Action of Floor Beams and Slab

The floor beams and slab of this bridge were designed to act non-compositely. In order to verify this, the neutral axis of the floor beam was calculated using the strain in the top and bottom flanges of the floor beam. The neutral axis of a section is the point at which the strain is equal to zero. If the slab and floor beam were acting non-compositely, the strain in the top and bottom flange of the floor beam would be equal in magnitude but opposite in sign and the neutral axis of the floor beam would be at the centroid, or mid-height, of the section. The strain in the slab would be independent of the strain in the floor beam. This can be seen in Figure 3.8(a). If the slab and floor beam were acting compositely, the strain in the bottom flange would be greater in magnitude than the strain in the top flange, moving the neutral axis above the centroid of the floor beam. The strain distribution would continue linearly into the slab as seen in Figure 3.8(b).

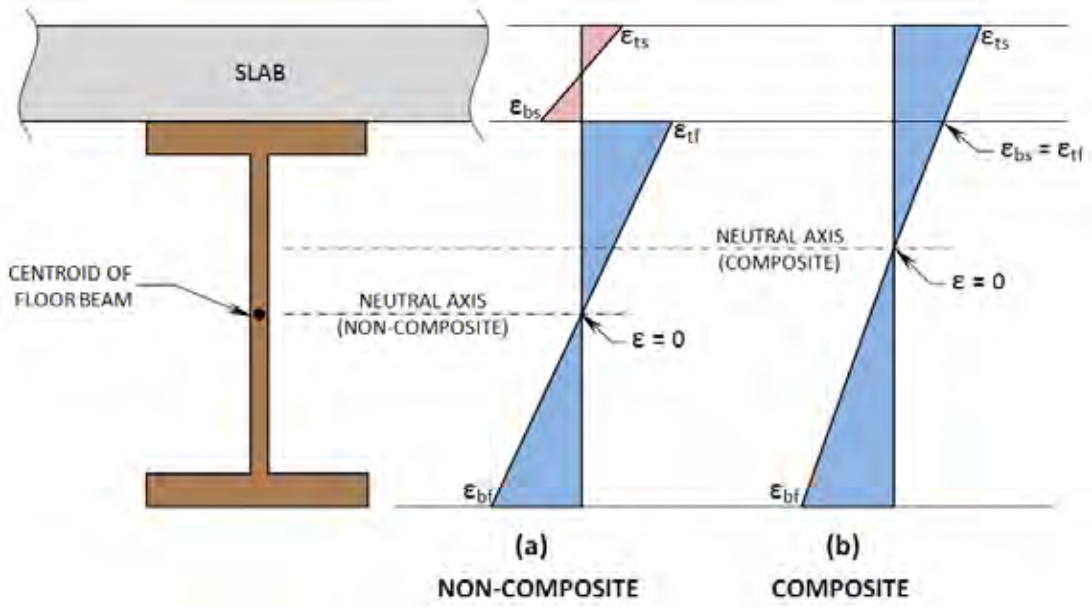

Figure 3.8: Strain Distribution Diagrams for Non-Composite and Composite Action of Slab and Floor Beam

As stated, the location of the neutral axis is dependent upon the strain in the top and bottom flanges. When the floor beam is experiencing very little strain, the neutral axis calculation is very sensitive to any slight changes in the strain values. This causes the location of the neutral axis to appear highly variable. For this reason, limits were placed on the location of the neutral axis when doing the calculations. A lower limit of zero inches above the bottom flange and an upper limit of 60 inches above the bottom flange were used. Because the floor beams were typically about 50 inches tall, the upper limit of 60 inches places the neutral axis in the slab.

Chapter 4. Controlled Live Load Test Results for Section F14N Floor Beam 2

4.1 Introduction

This section summarizes the results from the controlled live load field tests for Section F14N. The instrumented floor beam in this section was unsupported on both ends and has not been retrofitted. The gages were grouped into four main categories: deflection gages, floor beam gages, bottom flange gages, and web gap gages. The results from the four live load tests will be discussed below for each group of gages.

The figures from the deflection gages are plots of the deflection measured by the gages as a function of time as the trucks move along the bridge. The figures from the rest of the gages plot the stress calculated from the strain gages as a function of time. The deflection and stress values are taken relative to the values in the gages when there is no traffic on the bridge. Therefore, the values plotted are changes in deflection and stress due to the applied live load. The circles and squares plotted along the horizontal axis in some of the figures represent the approximate times when the truck came onto the floor beam and left the floor beam being tested. The plateaus in the plots signify the time when the truck was stationary over the floor beam. The deflection and stress at the plateaus will be referred to as the static deflection and static stress. In each of the plots, the colors of the lines correspond to a specific strain gage, the location of which is depicted on the details within each of the figures.

4.2 Live Load Test Results: 1 Truck Right

4.2.1 Deflection Gages

Deflection gages, also referred to as string potentiometers, were placed on the bottom flange of the floor beam at each end near the connection to the girder. These gages were used to determine how much the floor beam deflected under the weight of the trucks. Figure 4.1 shows the deflection of both ends of the floor beam due to one truck on the right side of the bridge. It can be seen that the right side of the floor beam deflects downward under the weight of the truck while the left side does not deflect. The total deflection on the right side of the floor beam is relatively small, measuring only 0.04 inches. The right side of the floor beam seems to stay partially deflected even after the truck leaves the floor beam. From this data, the deflected shape of the floor beam due to the static loading can be determined. This shape is represented by the dashed line in the detail of the floor beam within Figure 4.1.

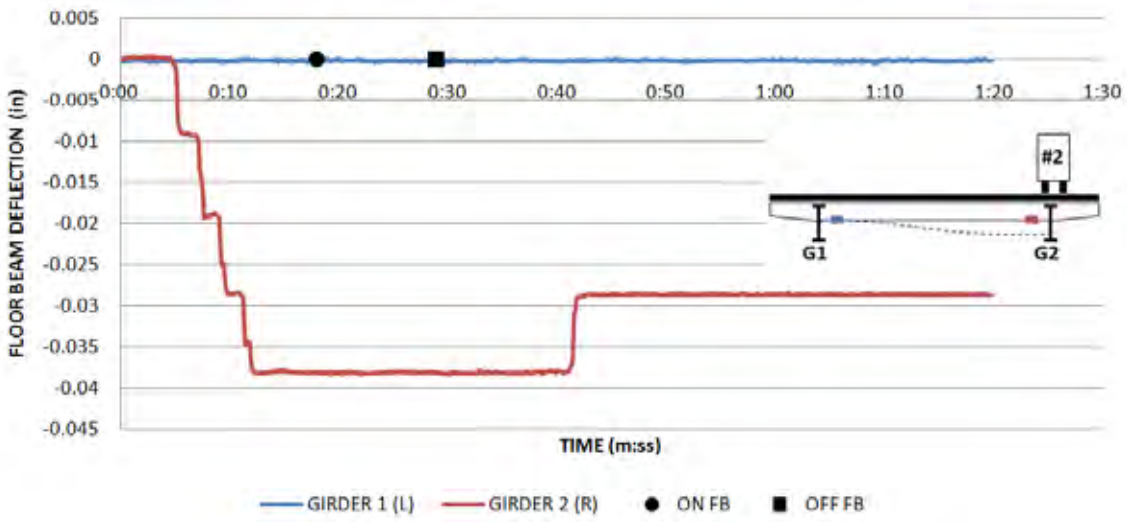

Figure 4.1: Deflection of Floor Beam due to One Truck on the Right

4.2.2 Floor Beam Gages

Using the data gathered from the strain gages on the flanges of the floor beam, it is possible to determine how the floor beam moves under the weight of traffic. Figure 4.2 shows the in-plane bending stresses recorded on both ends of the bottom flange of the floor beam versus time while one truck was in the right lane. It can be seen that the truck causes the strain gage on right side of the floor beam to have positive static stress values, meaning it is in tension. If the bottom flange of the floor beam is in tension, it means that the floor beam is deflecting downward at that location. The left side has a negative static stress value, which means it is in compression. This change in sign of the stress indicates that the floor beam is bending in double curvature. From this data, the deflected shape of the floor beam can be assumed and is shown by the dashed line in the detail of the floor beam within Figure 4.2. This assumed deflected shape matches the one determined from the deflection gages in Figure 4.1. If the floor beam was bending in perfect double curvature, it would be expected that the magnitude of the static stress would be the same on both ends with opposite signs. This is not the case, however. The magnitude of the stress under the truck is about two thirds of the stress on the other end.

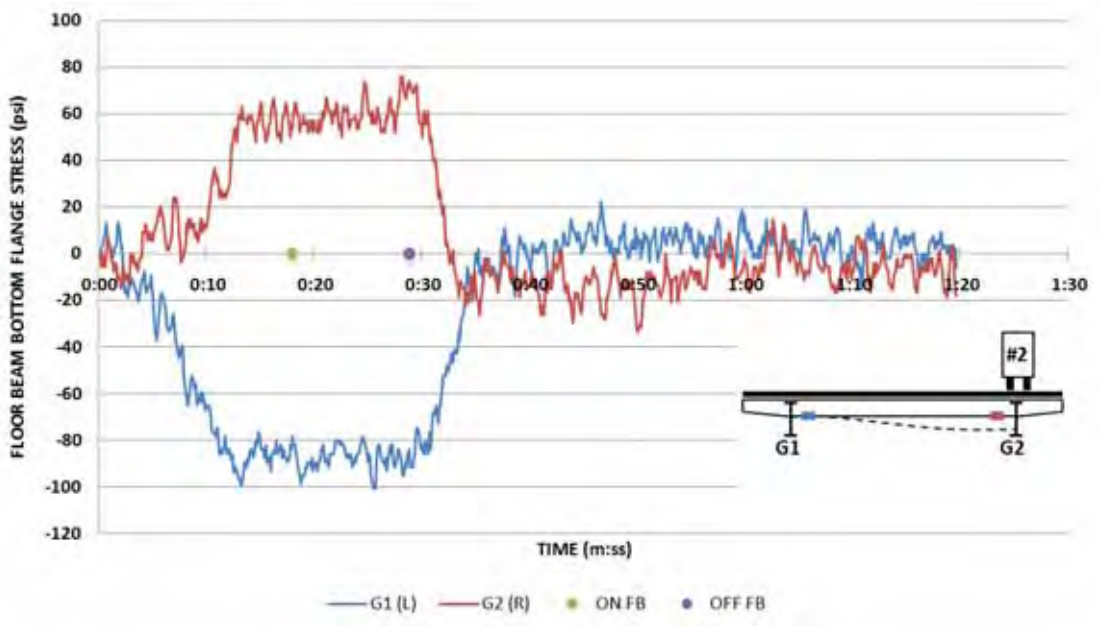

Figure 4.2: Stress in the Bottom Flange of the Floor Beam due to one Truck on the Right

To gain a better understanding of how the floor beam is moving under the truck load, the in-plane and out-of-plane stresses were determined as discussed in Section 3.2 and plotted. Figure 4.3 shows the stresses in the top and bottom flange near Girder 1. It can be seen that there is a large in-plane compressive stress in the bottom flange. There is very little in-plane bending of the top flange or out-of-plane bending of either flange. Figure 4.4 shows the stresses in the top and bottom flange near Girder 2. For this case, there is in-plane bending in both the top and bottom flanges as well as relatively large out-of-plane bending in the bottom flange. The top flange is restrained by the deck, so it is expected that there would be little to no lateral movement of the top flange. The out-of-plane bending of the bottom flange suggests that the floor beam is deflecting laterally as the truck moves over the bridge. This lateral movement of the floor beam under the truck seems to alleviate some of the in-plane bending stress, which could be one of the reasons why the in-plane bending stress in the bottom flange of the floor beam near Girder 2 is less than the stress near Girder 1. Overall, the stresses in the floor beam due to one truck in the right lane are relatively small, reaching a maximum of 0.1 ksi. When the truck leaves the floor beam, the stresses in the floor beam flanges go to zero.

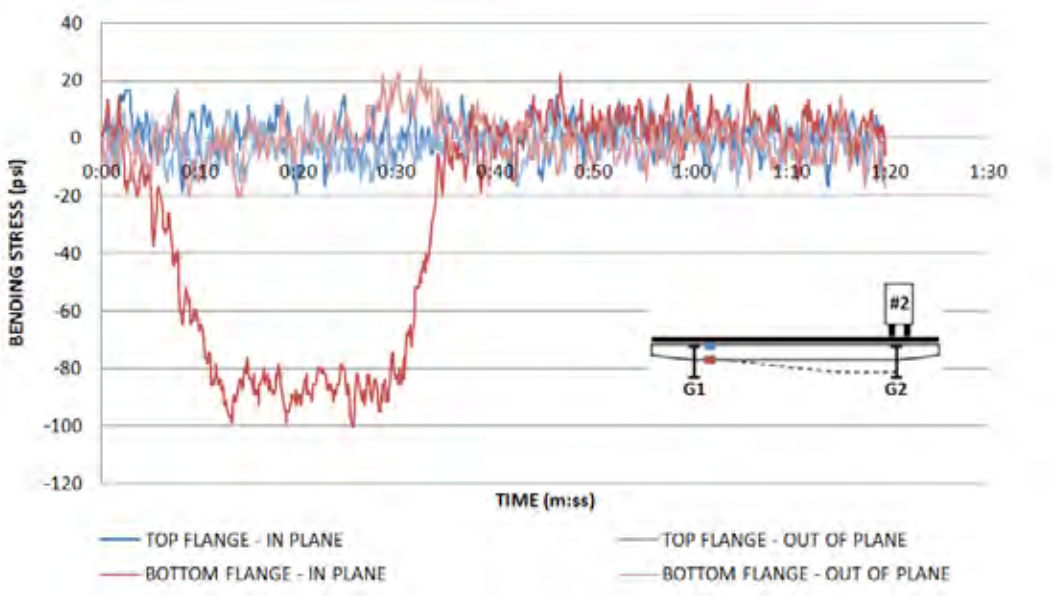

Figure 4.3: In-Plane and Out-of-Plane Stress of the Floor Beam near Girder 1 due to one Truck on the Right

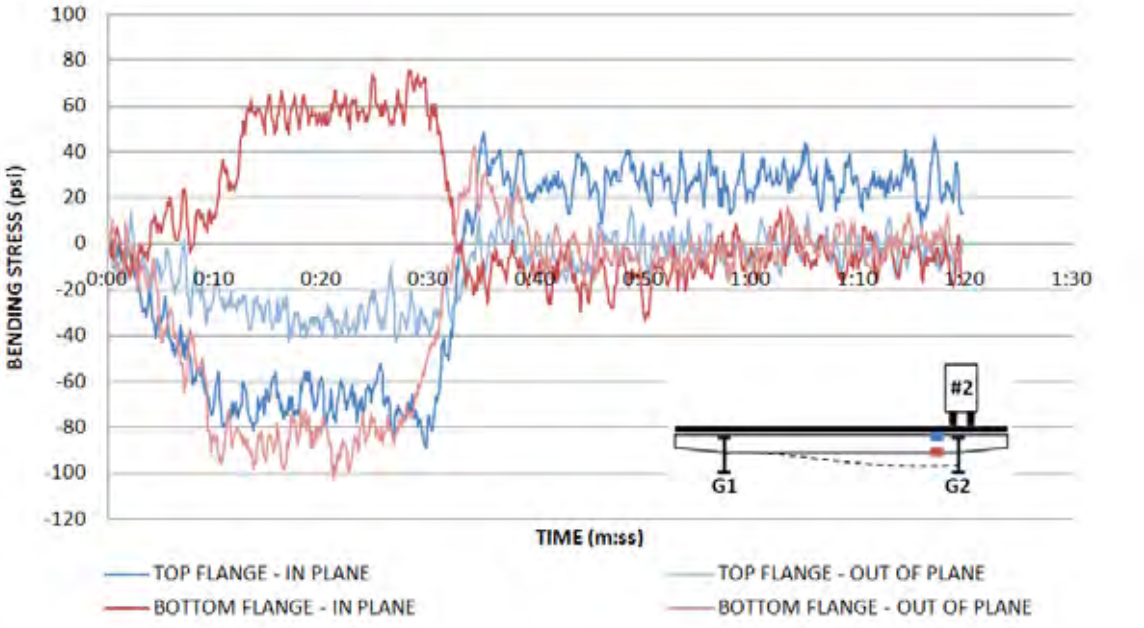

Figure 4.4: In-Plane and Out-of-Plane Stress of the Floor Beam near Girder 2 due to one Truck on the Right

4.2.3 Bottom Flange Gages

Using the data from the gages installed on the girder web adjacent to the bottom flange of the floor beam, the response of this area to traffic loads can be determined.

Figures 4.5 and 4.6 show the in-plane and out-of-plane bending stress of the girder web due to one truck in the right lane at Girder 1 and Girder 2, respectively. At Girder 1, it can be seen that there is very little in-plane bending of the girder web when the truck is on the opposite side. This suggests that this girder is not deflecting vertically. The plot shows slight positive out-of-plane bending of the girder web on the north side of the floor beam and negative out-of-plane bending on the south side. These stresses, however, are relatively small in magnitude when compared to the stresses in Girder 2 under the truck, as seen in Figure 4.6.

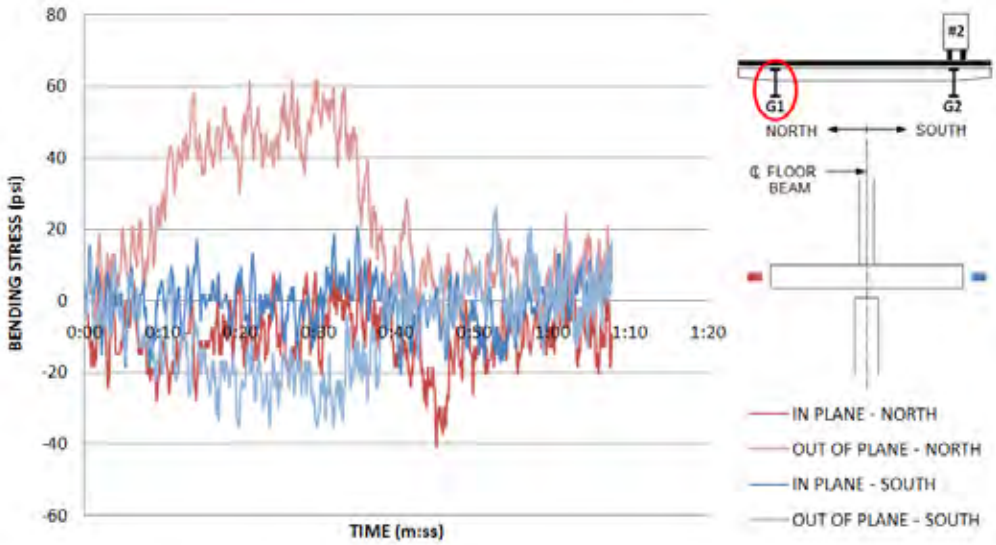

Figure 4.5: In-Plane and Out-of-Plane Bending Stresses of Girder 1 Web due to one Truck on the Right

Figure 4.6 shows significant positive in-plane bending of Girder 2, which means it is deflecting downward under the weight of the truck, as discussed in Section 3.3.3. There is also out-of-plane bending of the web toward the exterior of the bridge. Note that there is a distinct point at which the stresses reverse in sign. This is believed to happen when the truck moves onto the next span.

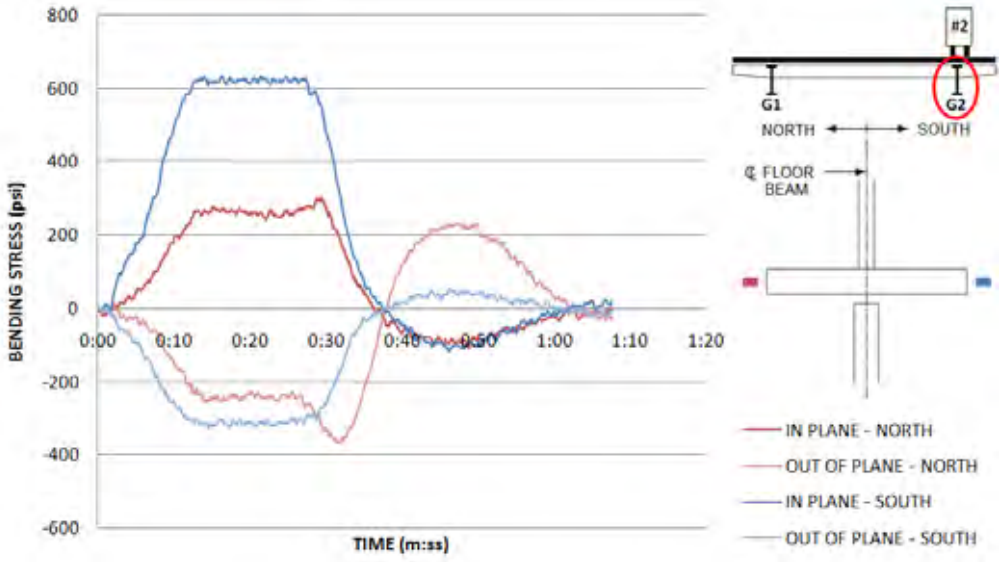

Figure 4.6: In-Plane and Out-of-Plane Bending Stresses of Girder 2 Web due to one Truck on the Right

4.2.4 Web Gap Gages

The expected behavior of the web gap was that the top flange of the girder and the connection stiffeners would behave has rigid constraints for this small gap. Therefore, if there was bending in this area, it would be in double curvature as seen in Figure 4.7(a). If this was the case, the gages on opposite sides of the girder web and the gages on the same side of the web would have opposite signs. This, however, is not what was recorded. The gages on the same side of the girder web showed the same sign, meaning the gap was bending in single curvature. This could only be possible if the top flange of the girder was rotating or the movement of the floor beam was causing the web to bend as seen in Figure 4.7(b).

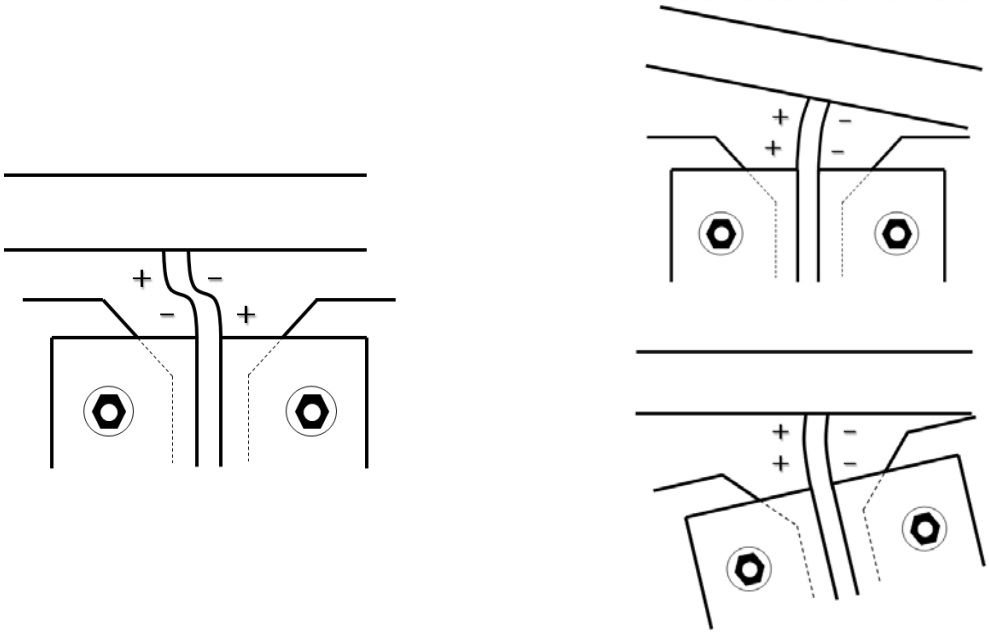

(a) ASSUMMED BEHAVIOR (b) RECORDED BEHAVIOR

Figure 4.7: Assumed versus Recorded Behavior of Web Gap

Figure 4.8 shows the stress in the web gap gages on Girder 1 when the truck is on the right side of the bridge. It can be seen that the gages on the interior side of the web have compressive static stress values and the gages on the exterior side of the web have tensile static stress values. This suggests that the web gap is bending in single curvature toward the exterior of the bridge. The gages in the top of the web gap recorded higher stresses than the gages in the bottom of the gap meaning there is more bending in the top of the gap. There are three distinct sections in this plot created by stress reversals in the gages. It is believed that the gages experience reversals in stress as the truck moves over the three spans of the bridge.

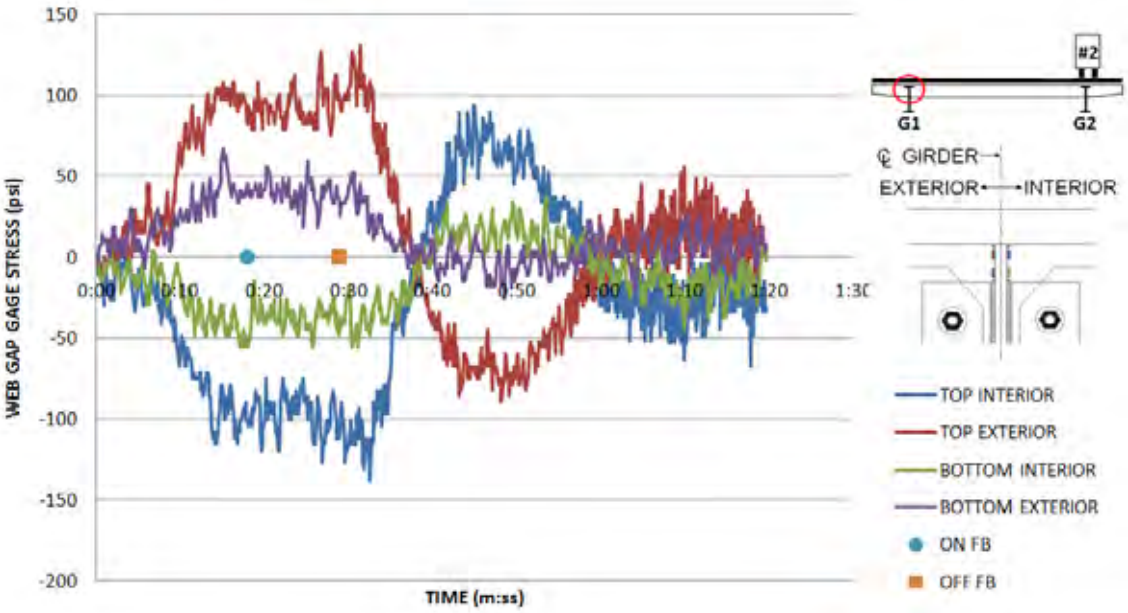

Figure 4.8: Stress in Web Gap Gages on Girder 1 due to one Truck on the Right

Figure 4.9 shows the stress in the web gap gages on Girder 2 under the truck. The bottom gage on the exterior side of the web was found to be defective; therefore it is not shown on the plot. The three sections caused by stress reversals are apparent in this plot as well. The top gages show that the web gap is bending in single curvature toward the interior of the bridge when the truck is on the floor beam. However, once the truck leaves the floor beam, it looks as though the gap begins to bend in double curvature. This starts when the green line, representing the bottom interior gage, begins to follow the red line, representing the top exterior gage. It should also be noted that the stresses in the web gap are much higher in the girder under the truck than they are in the other girder.

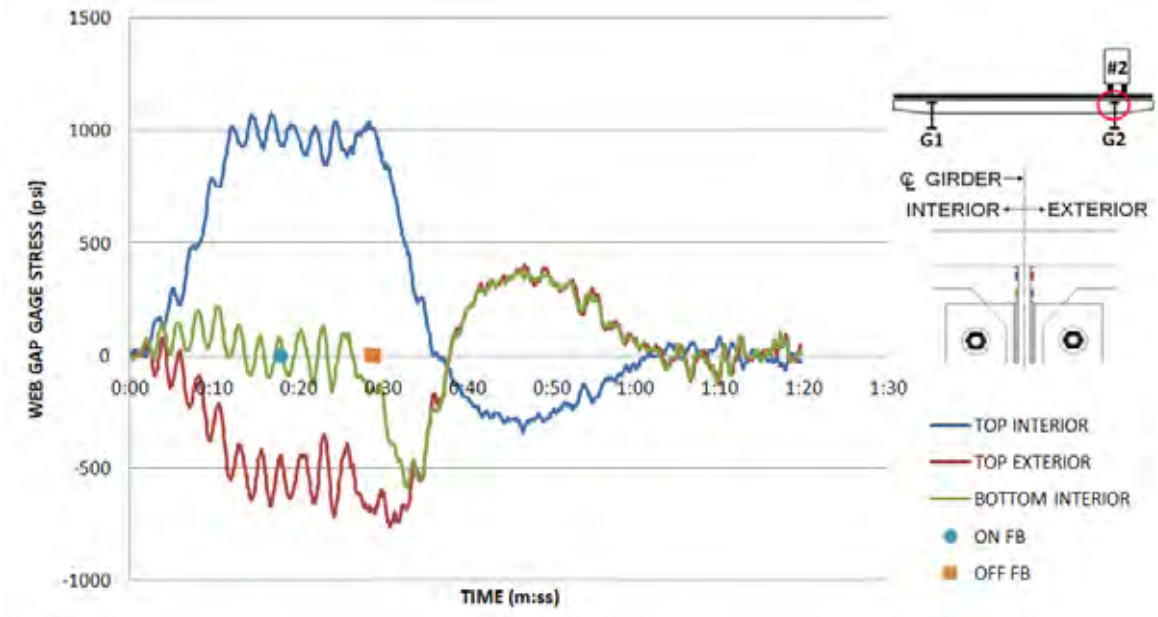

Figure 4.9: Stress in Web Gap Gages on Girder 2 due to one Truck on the Right

4.3 Live Load Test Results

4.3.1 Deflection Gages

Figure 4.10 shows the deflection of both ends of the floor beam due to two trucks on the right side of the bridge. The right side of the bridge deflects downward under the weight of the trucks while the left side remains stationary. The total static deflection of the right side is small, measuring only 0.08 inches. This is twice the deflection that was seen with the single truck. The assumed deflected shape of the floor beam under static loads is represented by the dashed line on the detail of the floor beam within Figure 4.10. Once the trucks leave the floor beam, it returns to its original undeflected status.

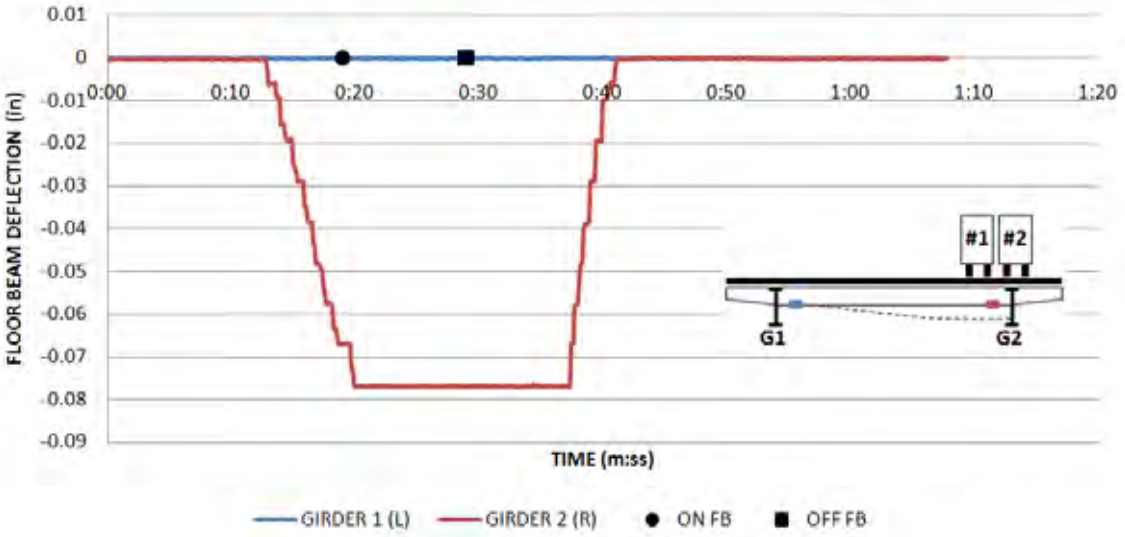

Figure 4.10: Deflection of Floor Beam due to Two Trucks on the Right

4.3.2 Floor Beam Gages

Figure 4.11 shows the stresses in the bottom flange of the floor beam when two trucks were in the two right-most lanes. It would be expected that doubling the load would double the stress in the floor beam. However, if Figure 4.11 is compared to Figure 4.2, it can be seen that the static tensile stress in the floor beam under two trucks is ten times the value under one truck. The behavior of the left side of the floor beam is very interesting. It has little to no stress until just before the truck reaches the floor beam at which point it experiences tensile stresses. Therefore, right before the trucks reach the floor beam, the floor beam seems to be bending in single curvature. Once the truck is on the floor beam, the left side shows a small compressive stress, suggesting it is bending in double curvature. To determine why the tensile stress under the trucks is much greater than the compressive stress on the other side of the floor beam, the in-plane and out-of-plane bending stresses were calculated and are plotted in Figures 4.12 and 4.13.

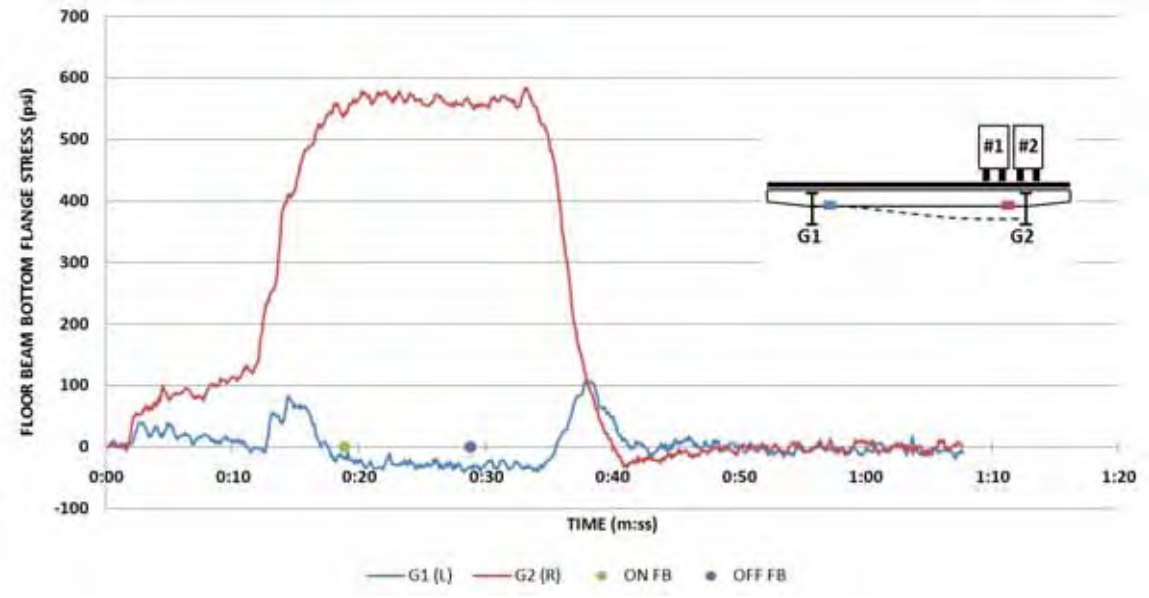

Figure 4.11: Stress in the Bottom Flange of the Floor Beam due to 2 Trucks on the Right

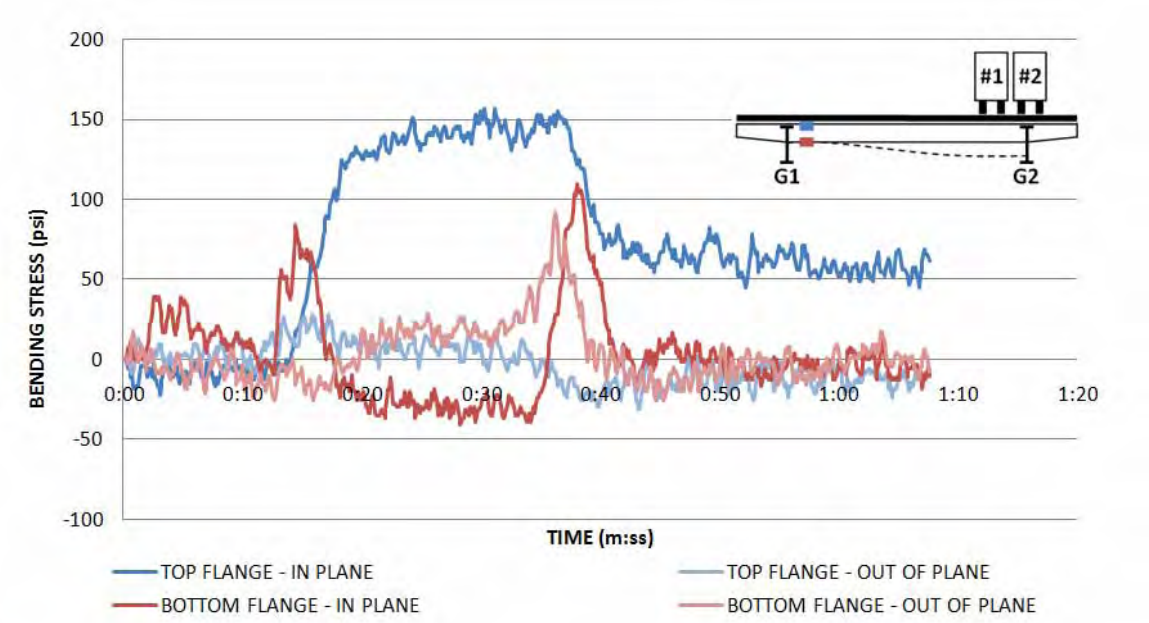

Figure 4.12: In-Plane and Out-of-Plane Stress of the Floor Beam near Girder 1 due to two Trucks on the Right

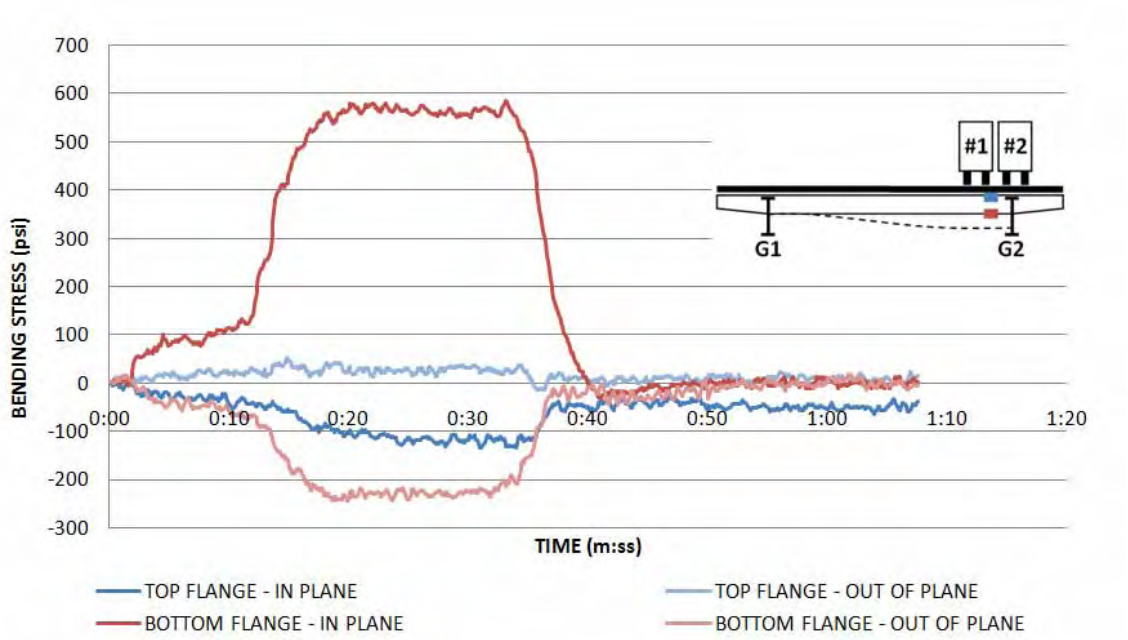

Figure 4.13: In-Plane and Out-of-Plane Stress of the Floor Beam near Girder 2 due to two Trucks on the Right

Figure 4.12 shows the in-plane and out-of-plane bending stresses in the floor beam near Girder 1 due to two trucks in the right lanes and Figure 4.13 shows the stresses near Girder 2. The plots show that there is practically no out-of-plane bending of the floor beam on the side opposite the trucks, but there is out-of-plane bending of the bottom flange under the trucks. This doesn't seem to explain why the stress on the side opposite the trucks is much less than under the trucks. Another possible explanation for this could be rotation of the girder as will be discussed in the following section with the bottom flange and web gap gage results.

4.3.3 Bottom Flange Gages

Figure 4.14 shows the in-plane and out-of-plane bending stresses in Girder 1 on either side of the floor beam framing into the girder. The in-plane stresses are positive while the truck is over the floor beam indicating that the girder is deflecting downward. The out-of-plane stresses are also positive, which suggests that the girder is bending inward toward the center of the bridge. When these results are compared with Figure 4.5, which shows the results from the single truck test for Girder 1, it can be seen that the stresses are much higher. One truck in the right lane caused little to no stress in Girder 1 whereas doubling the load to two trucks caused Girder 1 to bend both in and out of plane. After the truck leaves the floor beam, the gages show that the girder is bending out of plane in different directions on either side of the floor beam. On the north side of the floor beam, the girder is bending inward and on the south side, the girder is bending outward. This is most likely caused by lateral bending of the floor beam. The out-of-plane bending of Girder 1 could explain why the stress on the left side of the floor beam was much smaller than the stress on the right side, as seen in Figure 4.11. The out-of-plane rotation of the floor beam-to-Girder 1 connection could have alleviated some of the stress in the bottom flange of the floor beam near that connection.

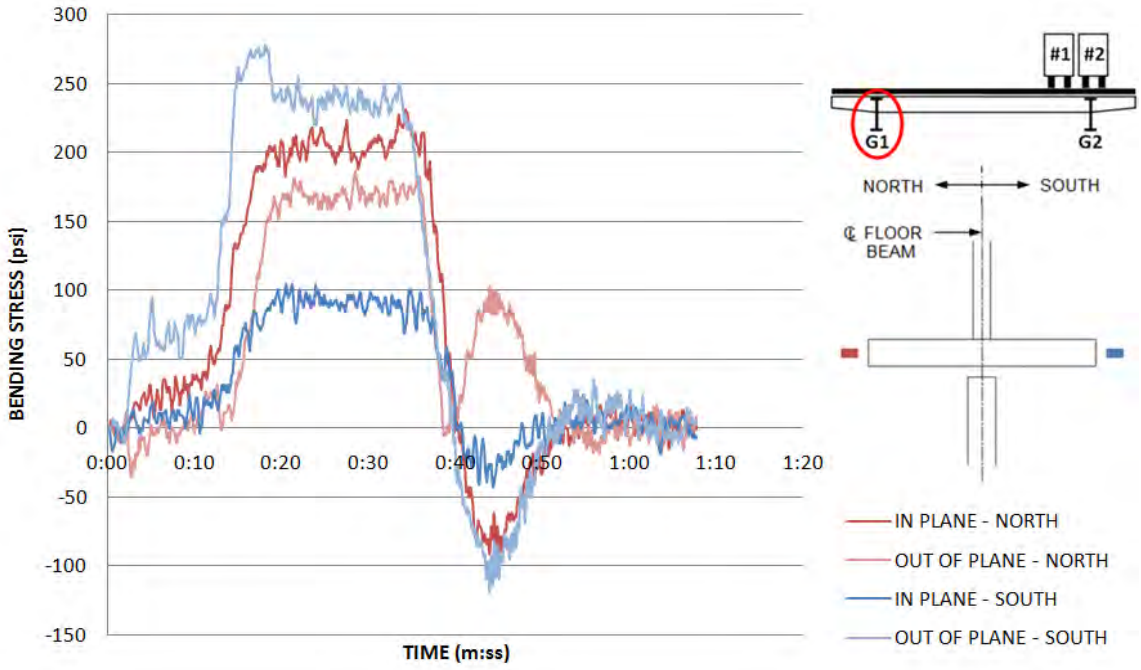

Figure 4.14: In-Plane and Out-of-Plane Bending Stresses of Girder 1 Web due to two Trucks on the Right

Figure 4.15 shows the in-plane and out-of-plane bending stresses in Girder 2 on either side of the floor beam framing into the girder due to two trucks in the right lanes. This plot shows the three sections seen in the web gap plots created from stress reversals as the trucks move over the three spans of the section. During this test, the trucks were directly over Girder 2. The plot shows that while the trucks were over the floor beam, the girder is deflecting downward creating tensile stresses in the gages. The out-of-plane bending stresses were negative indicating that the girder is bending outward toward the exterior of the bridge. When the trucks move onto the second span, the in-plane stresses are negative suggesting the girder is deflecting upward and the out-of-plane stresses are positive suggesting the girder is bending inward toward the interior of the bridge. These stresses are then reversed as the trucks move over the third span.

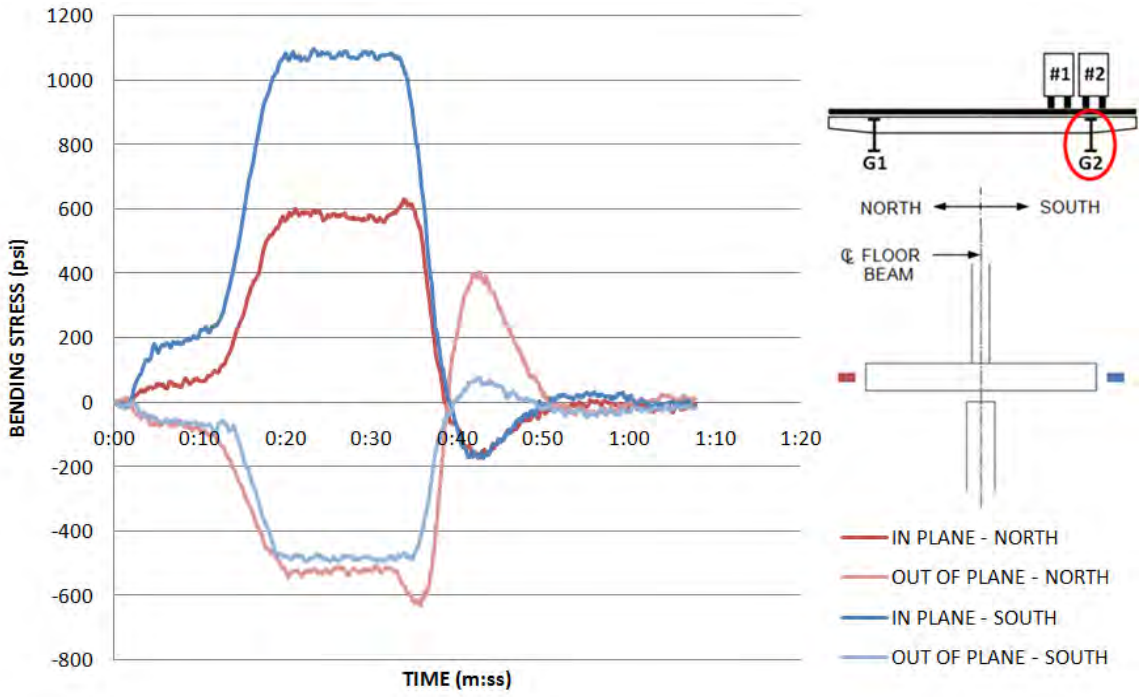

Figure 4.15: In-Plane and Out-of-Plane Bending Stresses of Girder 2 Web due to two Trucks on the Right

4.3.4 Web Gap Gages

Using the data from the gages installed in the web gap, it is possible to determine how this area of the girder responds to traffic loads. The following two figures show the stress in the web gap gages as a function of time for the tests with two trucks in the right lanes. Figure 4.16 shows the stresses for the web gap gages on Girder 1. The plot shows the stress reversals that were seen in previous plots caused by movement of the truck over the three spans. As the trucks are on the first span, which includes floor beam two, the exterior gages produced tensile stresses and the interior gages produced compressive stresses. This suggests that the girder web is bending out of plane toward the exterior of the bridge. This bending is reversed once the trucks are on the middle span, and then reversed again when the trucks reach the third span.

Figure 4.17 shows the stresses in the web gap gages on Girder 2 while two trucks are in the right lanes. This plot also shows the three sections created from stress reversals as the trucks move over the three spans. Looking at the gages at the top of the web gap when the trucks are over floor beam two, the interior gage produces tensile stresses and the exterior gage produces compressive stresses. This suggests that the girder web is bending out of plane toward the interior of the bridge. Once the trucks move into the middle span, the top exterior and the bottom interior gages show the same stresses. This implies that the web gap is bending in double curvature. When comparing the static stresses in the two girders due to the two trucks, it can be seen that the stresses in the top of the gap of Girder 2 are slightly higher than in Girder 1. This is because the trucks are directly over Girder 2.

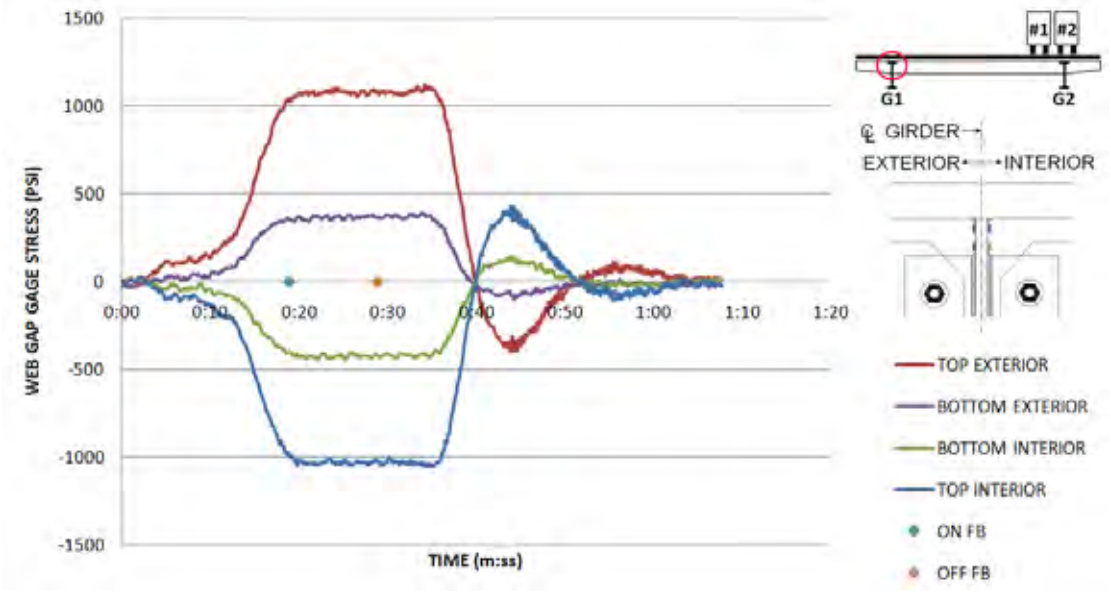

Figure 4.16: Stress in Web Gap Gages on Girder 1 due to 2 Trucks on the Right

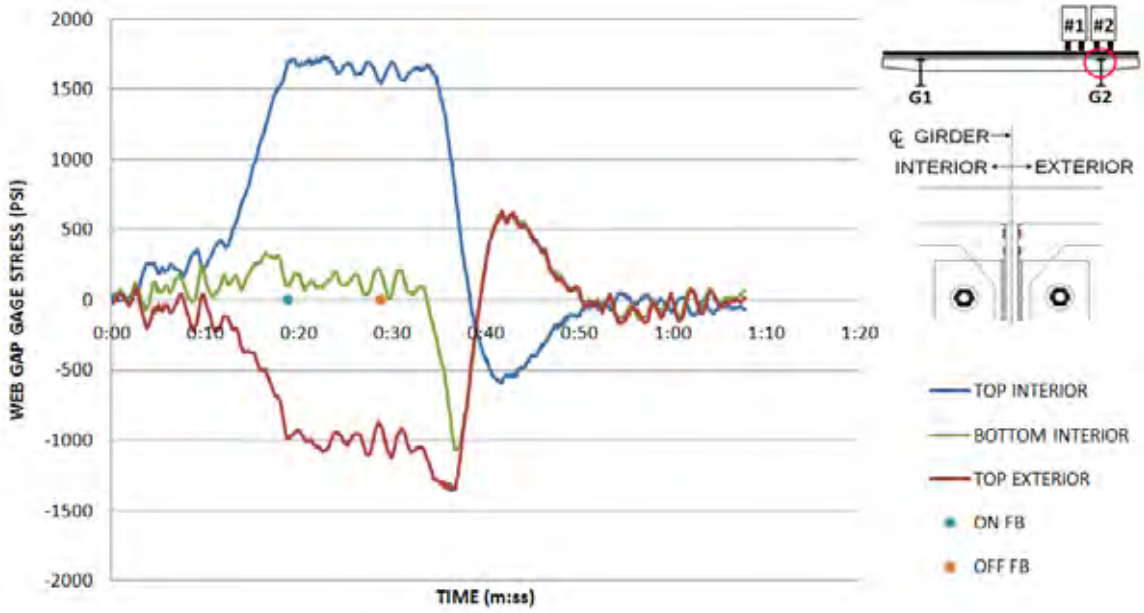

Figure 4.17: Stress in Web Gap Gages on Girder 2 due to 2 Trucks on the Right

4.4 Live Load Test Results: 1 Truck Left

4.4.1 Deflection Gages

Figure 4.18 shows the deflection at either end of the floor beam due to one truck on the left side of the bridge. The left side of the bridge deflects downward a total of 0.008 inches under the weight of the truck while the right side of the bridge remains undeflected. The assumed deflected shape of the floor beam under static loads is represented by the dashed line on the

detail of the floor beam within Figure 4.18. The left side of the floor beam seems to stay deflected even after the truck leaves the floor beam. This could have been caused by the deflection gage sticking in the deflected position.

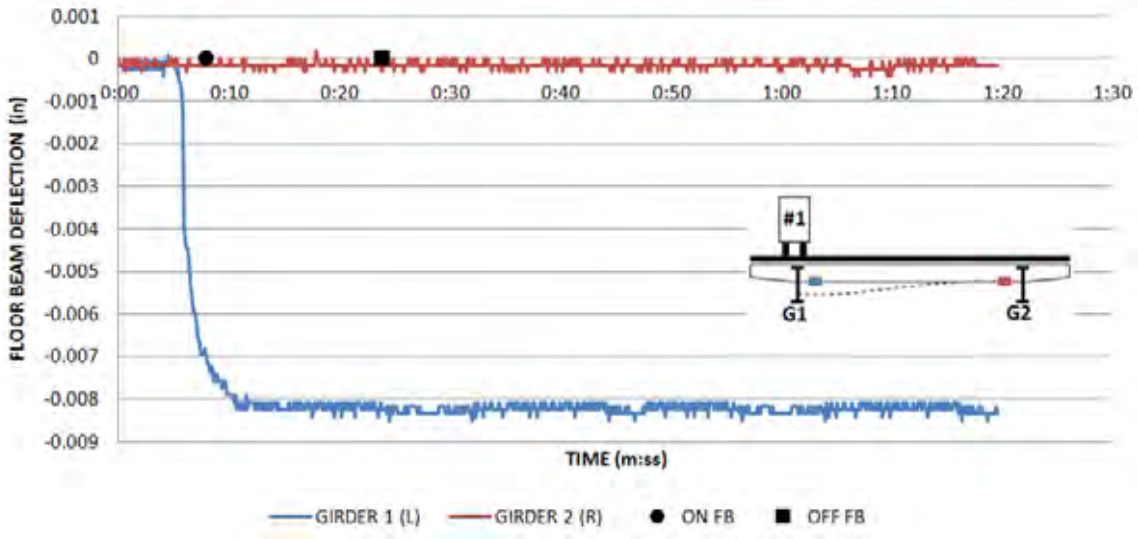

Figure 4.18: Deflection of Floor Beam due to One Truck on the Left

4.4.2 Floor Beam Gages

Figure 4.19 shows the stress at both ends of the bottom flange of the floor beam due to one truck in the left lane. It can be seen that the truck causes the left side of the floor beam to deflect downward creating tensile stresses in the bottom flange. The right side of the beam is in compression, which creates double curvature in the beam. When comparing Figures 4.2 and 4.19, it would be expected that with the symmetry of the bridge, the stresses caused by the two single truck tests would be opposite, but similar in magnitude. This was not the case. It can be seen that the tensile stresses caused by the two single truck tests are quite different. The stress in the left side of the beam caused by one truck on the left is almost three times the stress in the right side of the beam due to one truck on the right. The reason for this could be partially due to the fact that the truck that was run on the left side weighed about one ton more than the truck on the right side. Also, the left girder (Girder 1) is along the outer edge of the horizontal curve of the bridge. This creates a larger tributary area for Girder 1, which would increase the stress in the floor beams on that side of the bridge.

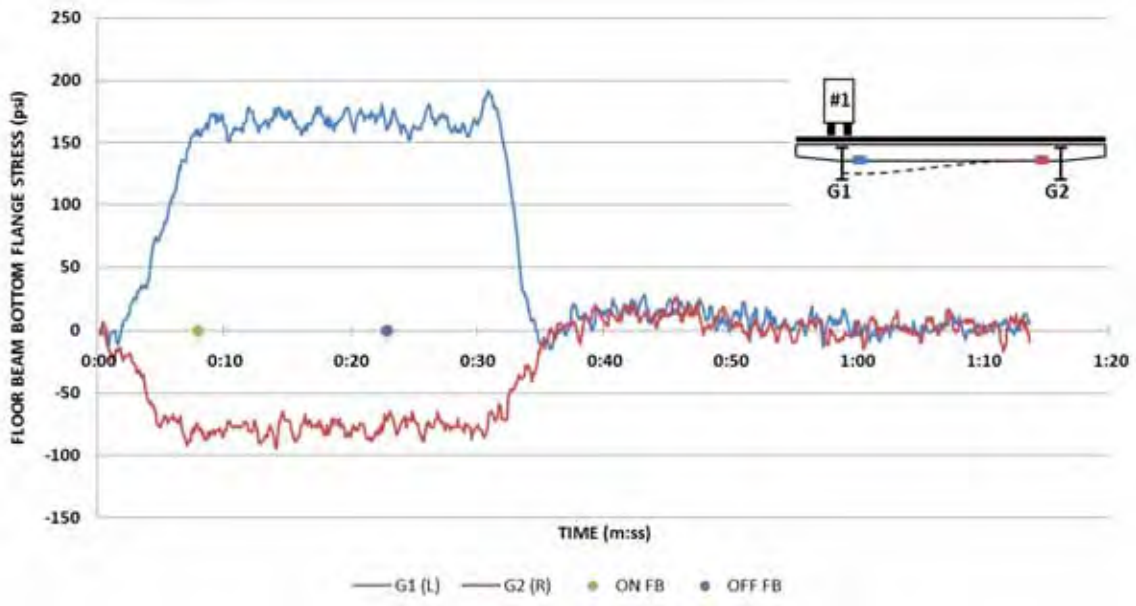

Figure 4.19: Stress in the Bottom Flange of the Floor Beam due to 1 Truck on the Left

The discrepancies between the two single truck tests could also be a result of the lateral bending of the floor beam. Figures 4.20 and 4.21 show the in-plane and out-of-plane bending of the floor beam due to one truck on the left side. If Figures 4.4 and 4.20, which plot the bending stresses underneath the single trucks, are compared, it can be seen that there is much more out-of-plane bending when the truck is on the right side. The out-of-plane bending of the floor beam due to one truck on the right seems to have alleviated some of the in-plane bending, which would explain the difference in values between the single truck tests.

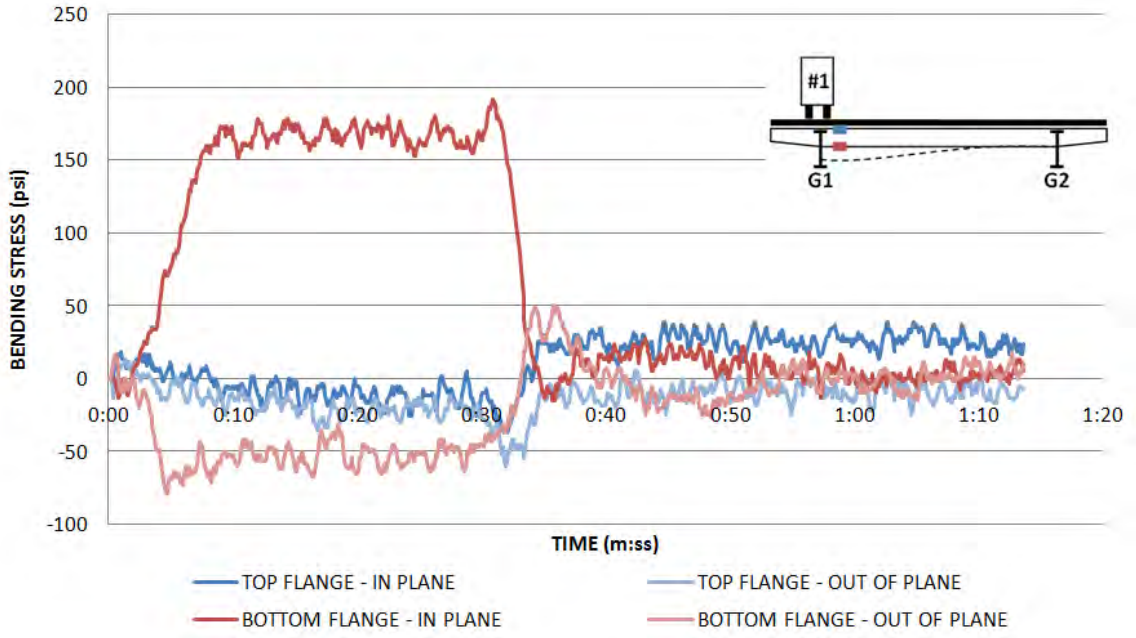

Figure 4.20: In-Plane and Out-of-Plane Stress of the Floor Beam near Girder 1 due to one Truck on the Left

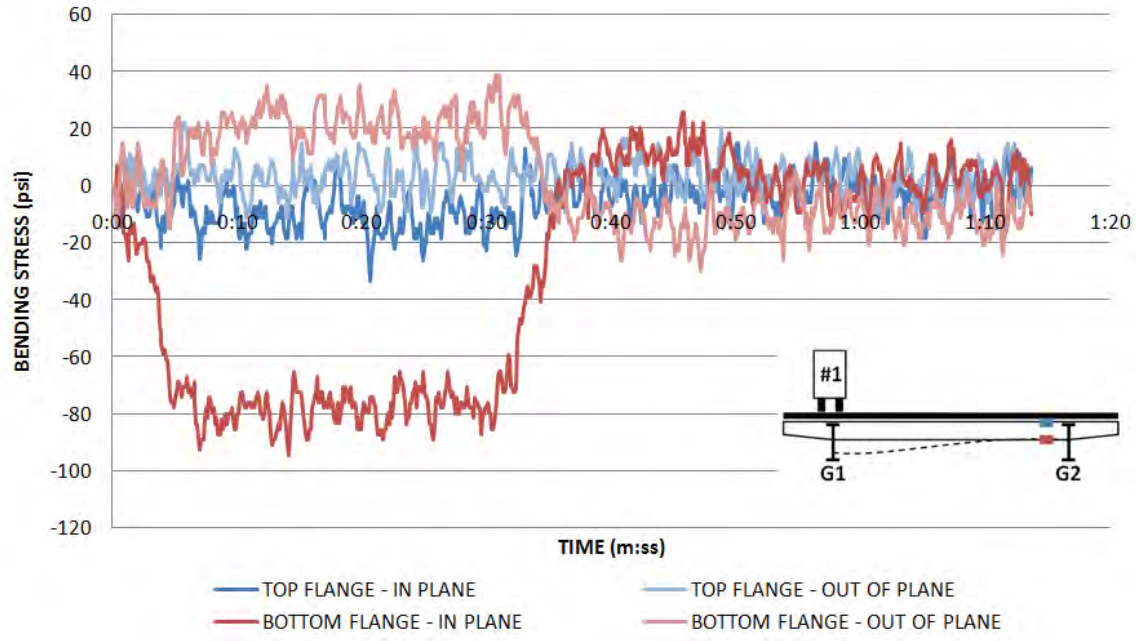

Figure 4.21: In-Plane and Out-of-Plane Stress of the Floor Beam near Girder 2 due to one Truck on the Left

4.4.3 Bottom Flange Gages

Figures 4.22 and 4.23 show the in-plane and out-of-plane bending measured in Girder 1 and Girder 2, respectively, due to one truck on the left side of the bridge. The plots show that Girder 1 has positive in-plane bending, which suggests it is deflecting downward and positive out-of-plane bending, which suggests it is also bending inward toward the center of the bridge. Once the truck leaves the floor beam, the girder shows negative in-plane stresses, indicating that there is uplift of the girder when the truck is over the middle span. At this point, the girder also starts to bend out-of-plane in different directions on either side of the floor beam indicating that there is lateral movement of the floor beam. Girder 2 has a relatively large out-of-plane bending stress on the south side of the floor beam and practically no in-plane stresses. These stresses, however, are very small when compared to the stress in the girder under the truck.

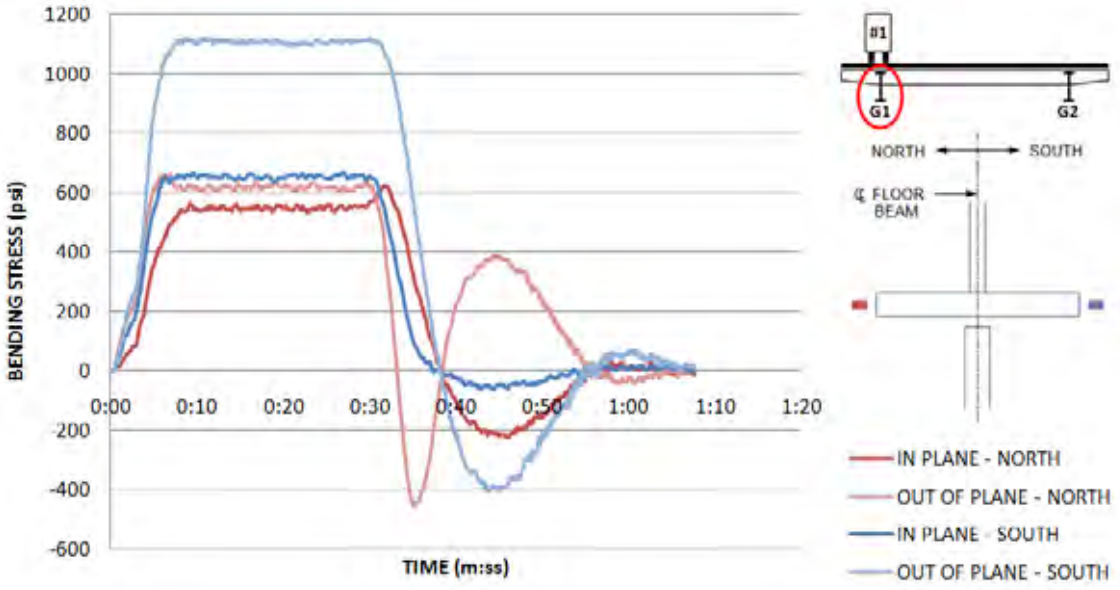

Figure 4.22: In-Plane and Out-of-Plane Bending Stresses of Girder 1 Web due to one Truck on the Left

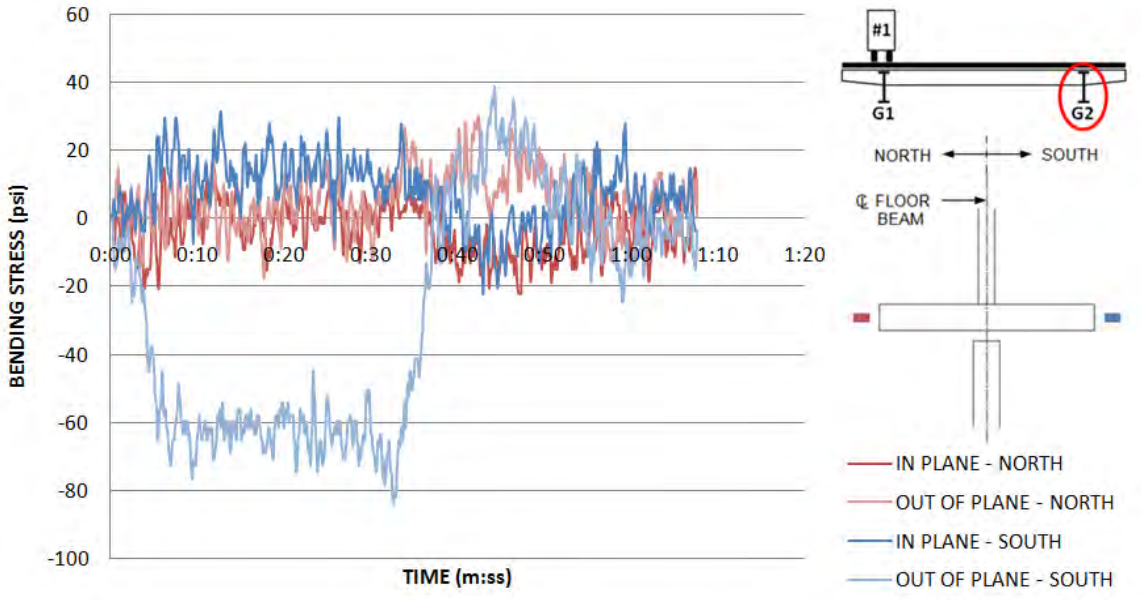

Figure 4.23: In-Plane and Out-of-Plane Bending Stresses of Girder 2 Web due to one Truck on the Left

4.4.4 Web Gap Gages

Figure 4.24 shows the stress in the web gap of Girder 1 due to one truck on the left side of the bridge. For this run, the truck is directly over the girder, which creates high stresses in the gap. The exterior gages experienced tensile stresses while the interior gages experienced compressive stresses. Therefore, the gap is bending in single curvature toward the exterior of the bridge. The stress recorded by the top gages is more than twice that of the bottom gages, which means there is more bending toward the top of the gap. The three sections signifying the three spans of the bridge are also apparent in this plot. The web gap bends in the opposite direction when the truck is on the middle span and bends back the other way when the truck is on the last span.

Figure 4.25 shows the stress in the web gap of Girder 2 due to one truck on the left side of the bridge. The plot shows significant noise in the data. However, the values of the stress that were recorded were very low. Therefore, the web gap experiences very little stress when the truck is on the other side of the bridge.

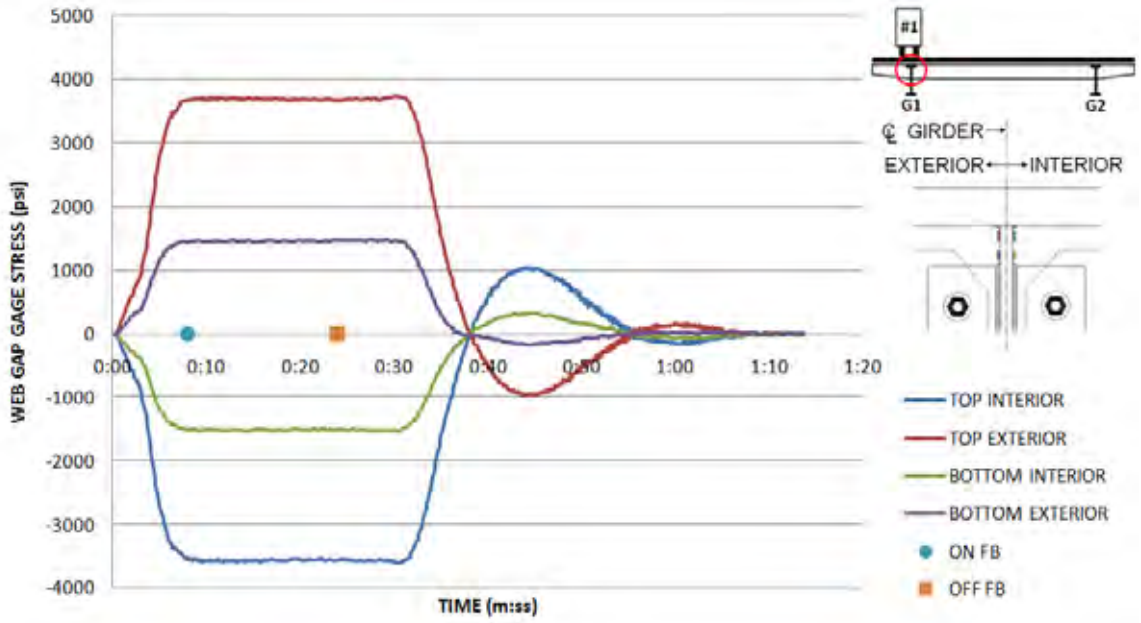

Figure 4.24: Stress in Web Gap Gages on Girder 1 due to 1 Truck on the Left

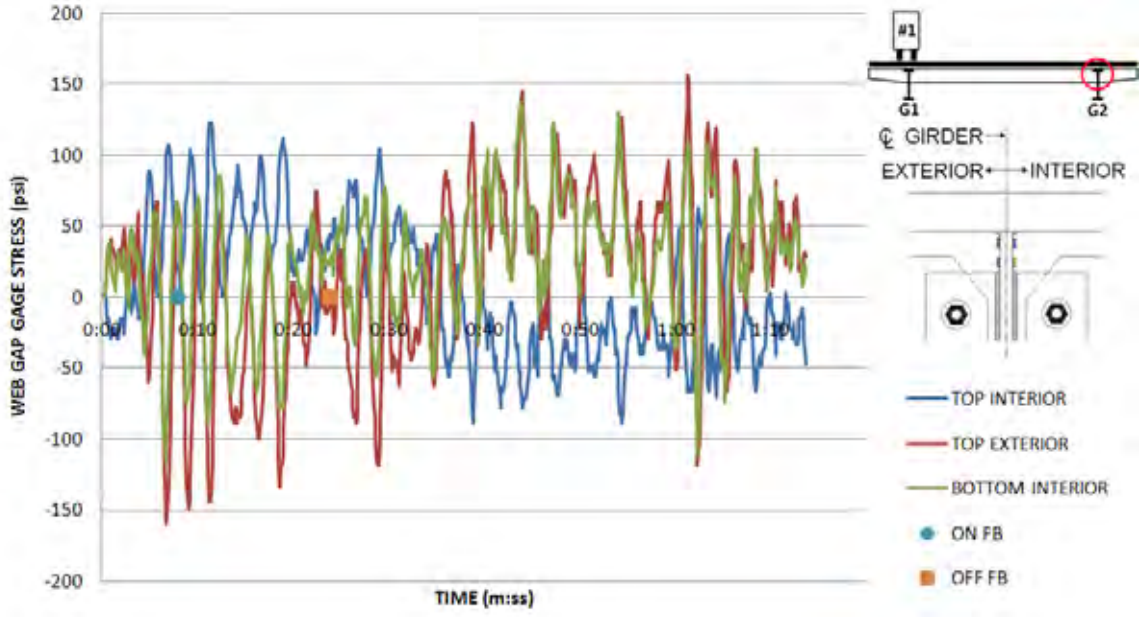

Figure 4.25: Stress in Web Gap Gages on Girder 2 due to 1 Truck on the Left

4.5 Live Load Test Results: 2 Trucks Left

4.5.1 Deflection Gages

Figure 4.26 shows the deflection at either end of the floor beam due to two trucks on the left side of the bridge. The left side of the bridge deflects downward a total of 0.03 inches under the weight of the trucks. This deflection is almost four times the deflection seen with one truck

on the left. The figure also shows that the right side of the floor beam deflects downward a very small amount. The floor beam seems to stay deflected even after the trucks leave the floor beam, which could have been caused by a sticky deflection gage.

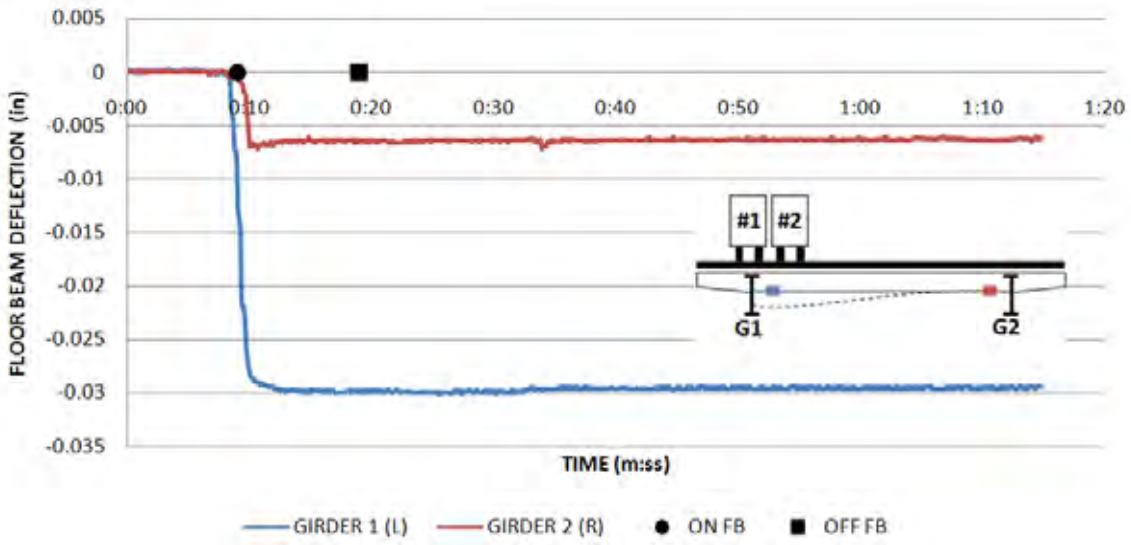

Figure 4.26: Deflection of Floor Beam due to Two Trucks on the Left

4.5.2 Floor Beam Gages

Figure 4.27 shows the stress at both ends of the bottom flange of the floor beam when two trucks are in the two left-most lanes. The trucks cause the left end of the floor beam to deflect vertically downward, creating tensile stresses in the bottom flange. The static tensile stress on the left side of the floor beam is almost four times the value due to one truck. The plot shows the same change to single curvature after the truck leaves the floor beam as was seen with the two trucks on the right. It can also be seen that there is a slight decrease in the compressive stress in the bottom flange of the floor beam on the side opposite the trucks from the single left truck test.

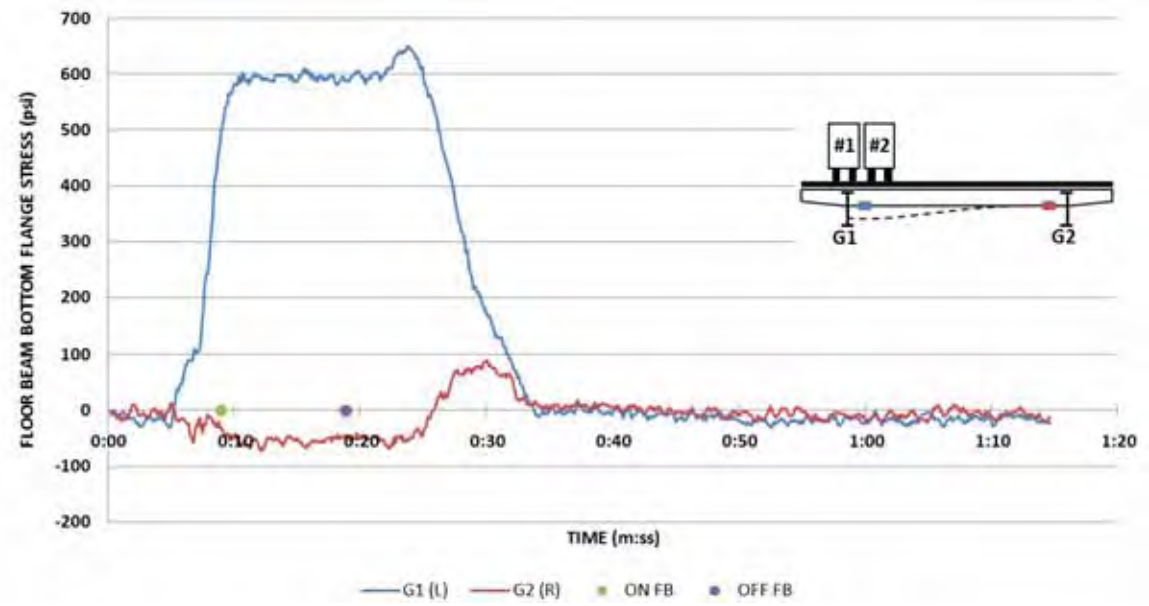

Figure 4.27: Stress in the Bottom Flange of the Floor Beam due to 2 Trucks on the Left

Figures 4.28 and 4.29 show the in-plane and out-of-plane bending of the floor beam due to two trucks on the left side of the bridge. As can be seen, the in-plane stress in the bottom flange dominates the other stresses and there is very little out-of-plane bending on either side of the floor beam. Therefore, the decrease in the compressive stress in the bottom flange of the floor beam on the side opposite the trucks is most likely not due to lateral bending of the floor beam. Another explanation could be out-of-plane bending of the girder at the floor beam to girder connection. To determine if this is the case, the results from the bottom flange gages will be discussed.

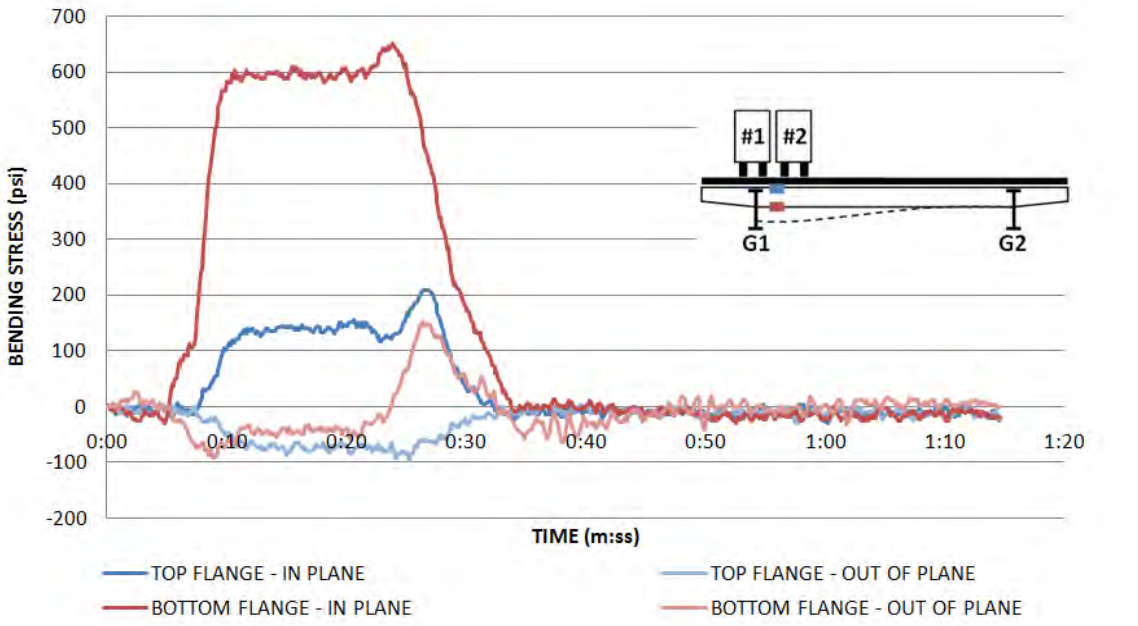

Figure 4.28: In-Plane and Out-of-Plane Stress of the Floor Beam near Girder 1 due to two Trucks on the Left

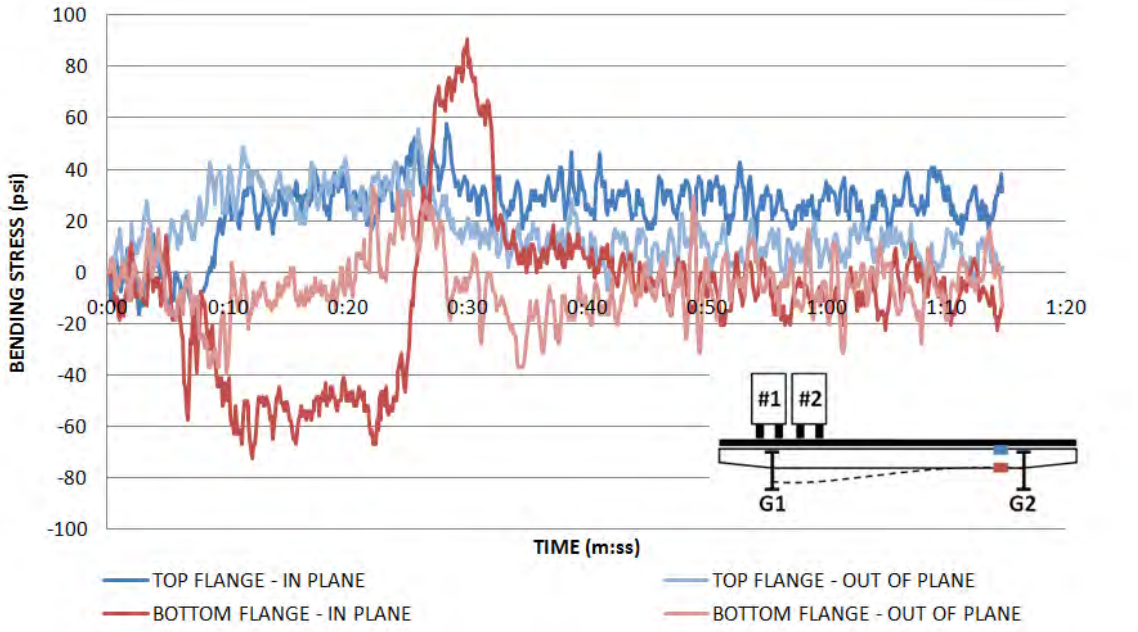

Figure 4.29: In-Plane and Out-of-Plane Stress of the Floor Beam near Girder 2 due to two Trucks on the Left

4.5.3 Bottom Flange Gages

Figure 4.30 shows the stress in the bottom flange gages on the web of Girder 1 due to two trucks on the left side of the bridge. Both in-plane and out-of-plane stresses are positive when the trucks are over the floor beam, which means the girder is deflecting both downward and inward toward the center of the bridge. When the trucks are on the middle span, the girder deflects upwards and bends out-of-plane in different directions on either side of the floor beam. On the last span, the girder reverses the directions in which it bends.

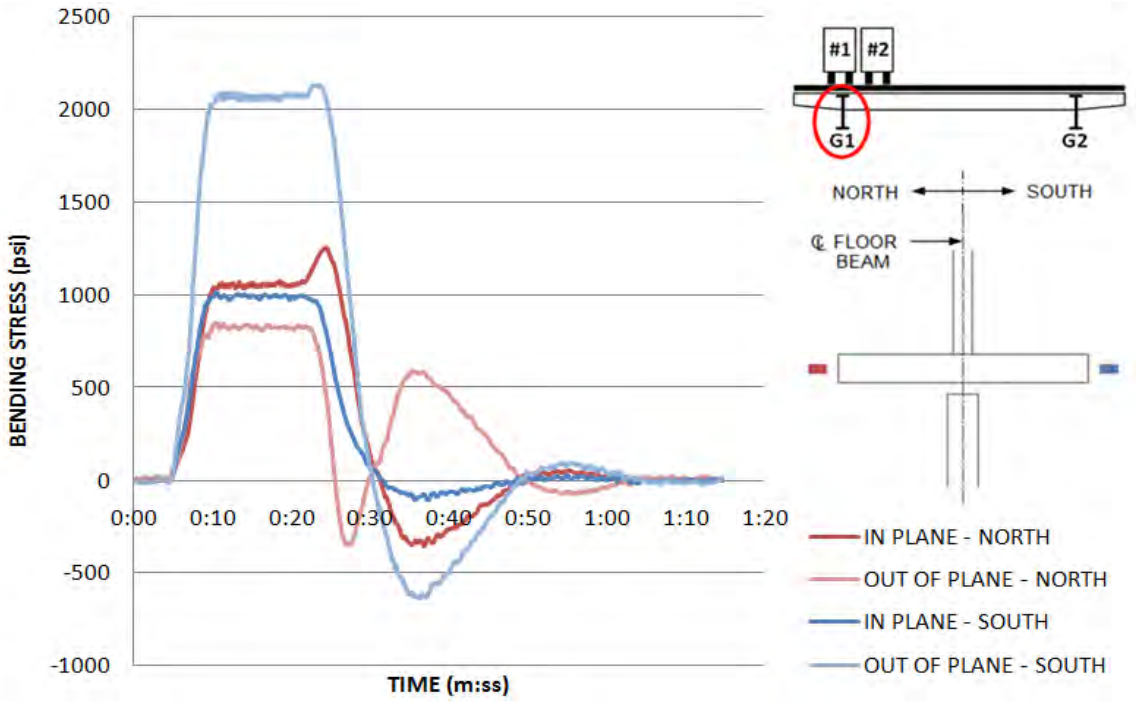

Figure 4.30: In-Plane and Out-of-Plane Bending Stresses of Girder 1 Web due to two Trucks on the Left

Figure 4.31 shows the stress in the bottom flange gages on the web of Girder 2 due to two trucks on the left side of the bridge. The in-plane stresses are positive, which means the girder is deflecting downward when the trucks are on the floor beam. The out-of-plane bending stresses are negative, which means the truck is bending outward toward the exterior of the bridge. These stresses reverse whenever the truck moves onto the next span.

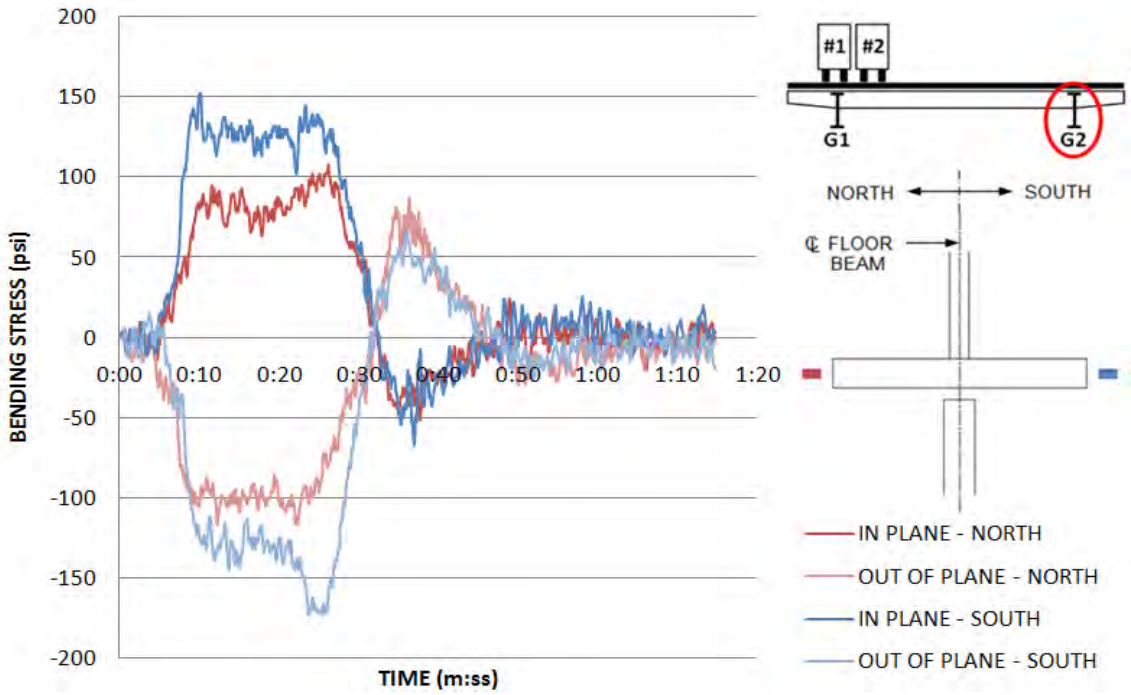

Figure 4.31: In-Plane and Out-of-Plane Bending Stresses of Girder 2 Web due to two Trucks on the Left

When comparing the stress in the bottom flange gages from both of the two truck tests, it was determined that the girders bend out-of-plane in the same direction regardless of the location of the trucks. Girder 1 always bends inward toward the center of the bridge and Girder 2 always bends outward toward the exterior of the bridge. It was thought that because the floor beam bends and deflects differently depending on the location of the trucks, this would cause the girder web to do the same. This, however, was not the case. These results seem to suggest that the bending of the girders depends on more than just the movement of the floor beam.

4.5.4 Web Gap Gages

Figure 4.32 is a plot of the stress in the web gap of Girder 1 due to two trucks on the left. The exterior gages show tensile stresses and the interior gages show compressive stresses. This indicates that the web gap is bending in single curvature toward the exterior of the bridge. When the truck is on the middle span, the web gap bends toward the interior of the bridge and bends back toward the exterior of the bridge on the last span. The stresses measured in the web gap of Girder 1 were the largest stresses measured anywhere along this floor beam and the girder connections.

Figure 4.33 shows the stresses in the web gap of Girder 2 due to two trucks on the left. The top gages show that the web gap is bending inward toward the center of the bridge. Again, the bending is reversed every time the trucks move onto the next span.

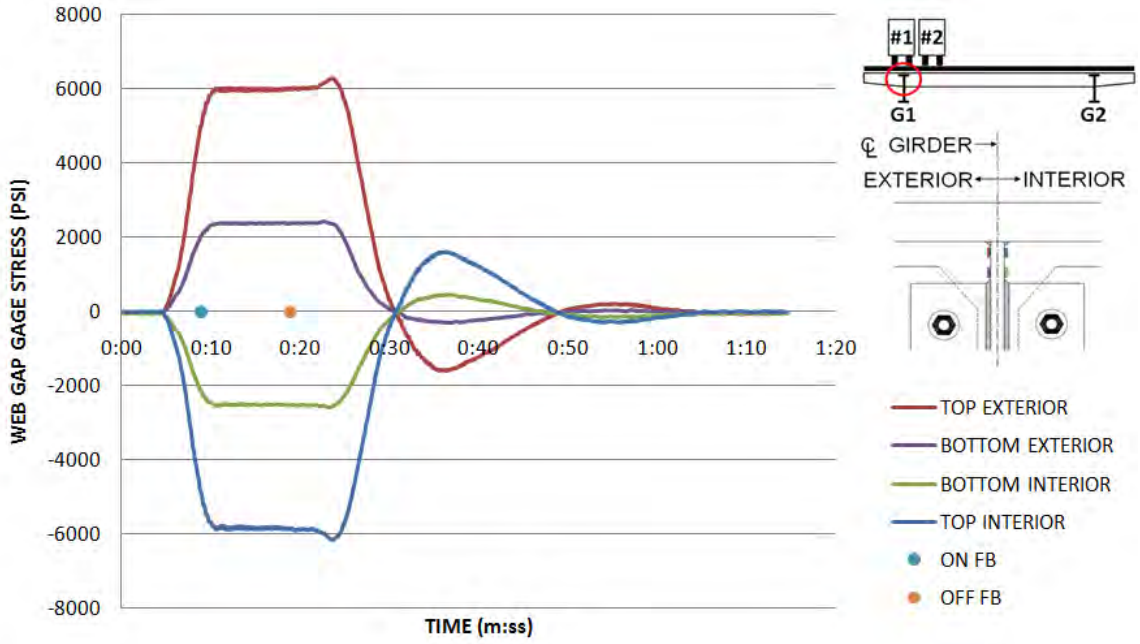

Figure 4.32: Stress in Web Gap Gages on Girder 1 due to 2 Trucks on the Left

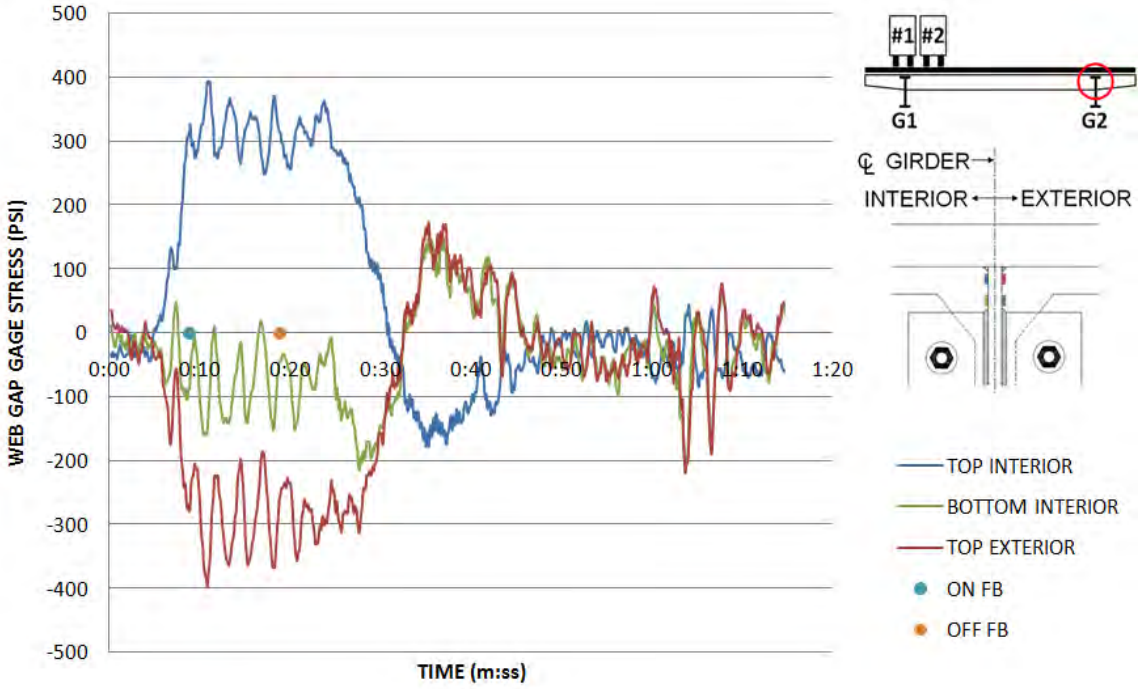

Figure 4.33: Stress in Web Gap Gages on Girder 2 due to 2 Trucks on the Left

4.6 Composite Action of Floor Beams and Slab

In order to verify whether or not the floor beam and slab were acting compositely, the neutral axis of the floor beam was calculated using the method described in Section 3.4. The neutral axis was plotted versus time for each of the four truck runs and can be seen in Figures 4.34 through 4.37. The neutral axis was calculated at each of the three gage locations along the length of the floor beam. The three gage locations, shown on the figure of the floor beam in each plot, correspond to the three lines plotted in the figures. The vertical axis of the plots is the distance between the calculated neutral axis and the bottom of the floor beam. Because the cross sectional height of the floor beam was 51 inches, the neutral axis was expected to be at about 25.5 inches.

For each of the plots, there is significant noise in the data until the truck reaches the floor beam. The reason for this is because the strain in the floor beam was practically zero when there were no trucks on the floor beam. Therefore, any small change in the strain during this time would drastically change the location of the neutral axis. When the trucks reached the floor beam, the strain in the flanges was large enough that the calculation of the neutral axis was more accurate and produced less noise in the plot. The majority of the results show that the neutral axis is well above the centroid of the cross section when the trucks were over the floor beams. At times, the neutral axis was calculated to be more than 51 inches, which means that the neutral axis extended into the concrete slab. These results suggest that the slab and the floor beam are acting compositely when the trucks are over the floor beam. It is thought that the weight of the trucks produces a friction force between the floor beams and slab, creating the composite action.

There are two anomalies in the data. The first is the location of the neutral axis on the right side of the floor beam when one truck is on the right (see Figure 4.34). The neutral axis was calculated to be about 23 inches above the bottom flange. This is slightly below the expected neutral axis if the floor beam and slab were to act non-compositely. In addition, the truck was very close to these gages. It would be expected that this would increase the friction force between the slab and floor beam, which would in turn increase the composite action between the two components. One explanation for this could be that when the truck came onto the floor beam, its weight caused the slab and floor beam to slip past one another, releasing the friction and causing non-composite action. Figure 4.4 shows that the in-plane bending stresses in the top and bottom flange on the right side of the floor beam are practically equal, which does suggest non-composite action as shown in Figure 3.8(a). The second anomaly occurred on the left side of the floor beam when two trucks are on the right (see Figure 4.35). The neutral axis at this location was calculated to be about ten inches above the bottom flange. The reason for this is that the stress measured in the top flange is much greater than the stress measured in the bottom flange (see Figure 4.12). This could be due to the fact that there was a lot of out-of-plane bending of Girder 1 during this run (see Figure 4.14), which may have decreased the stress in the bottom flange of the floor beam and caused the calculated neutral axis to be abnormally low.

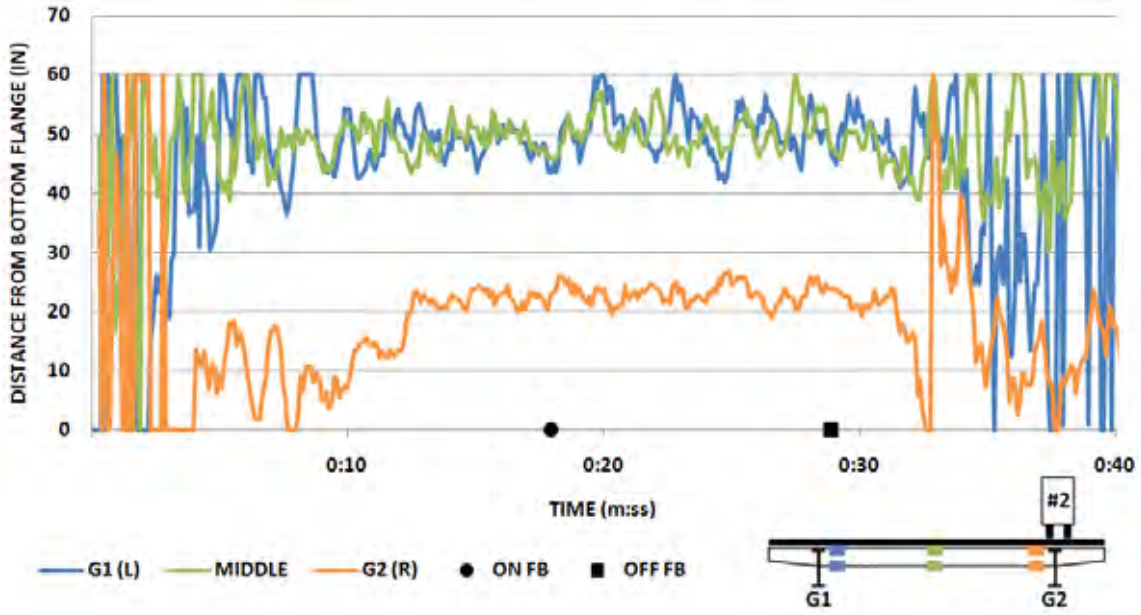

Figure 4.34: Axis of the Floor Beam versus Time due to One Truck on the Right

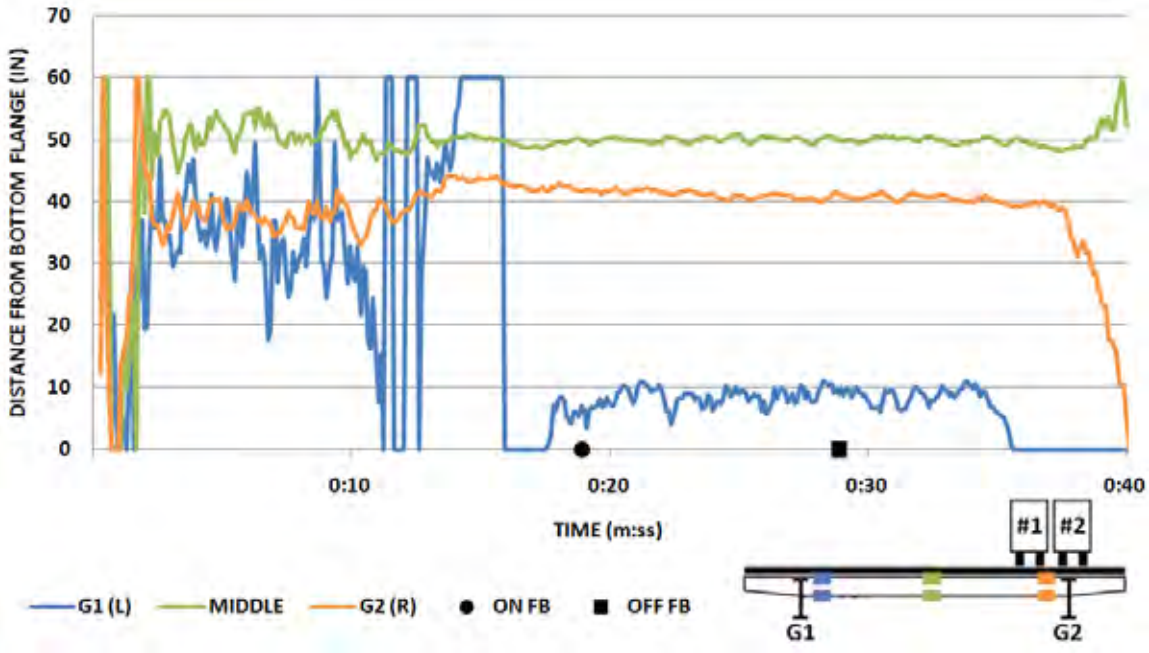

Figure 4.35: Neutral Axis of the Floor Beam versus Time due to Two Trucks on the Right

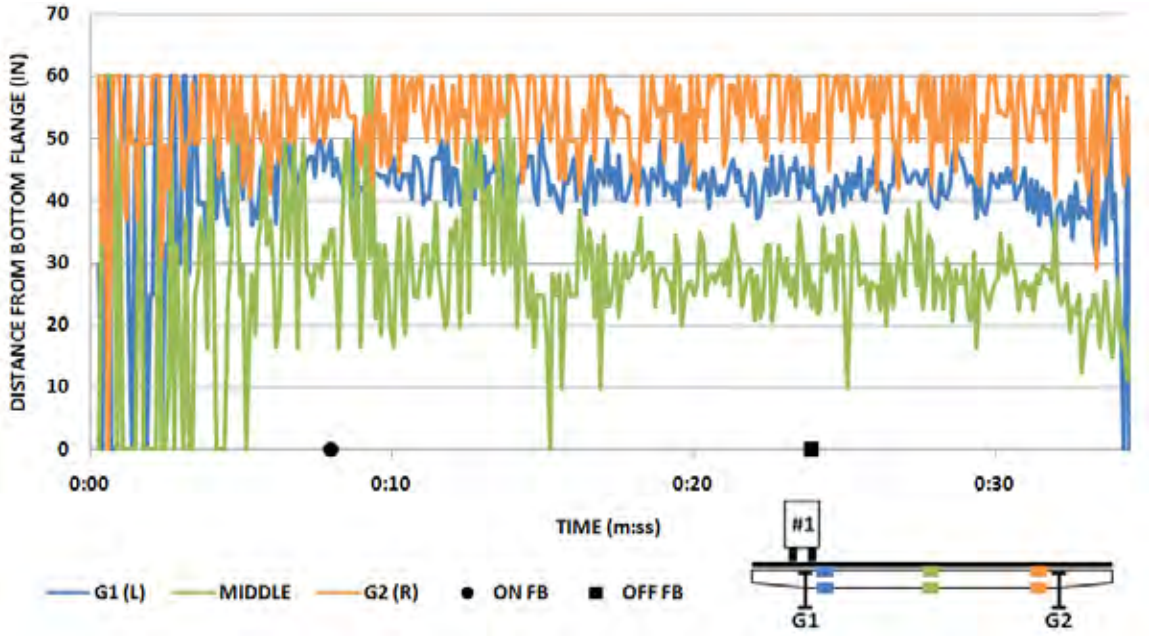

Figure 4.36: Neutral Axis of the Floor Beam versus Time due to One Truck on the Left

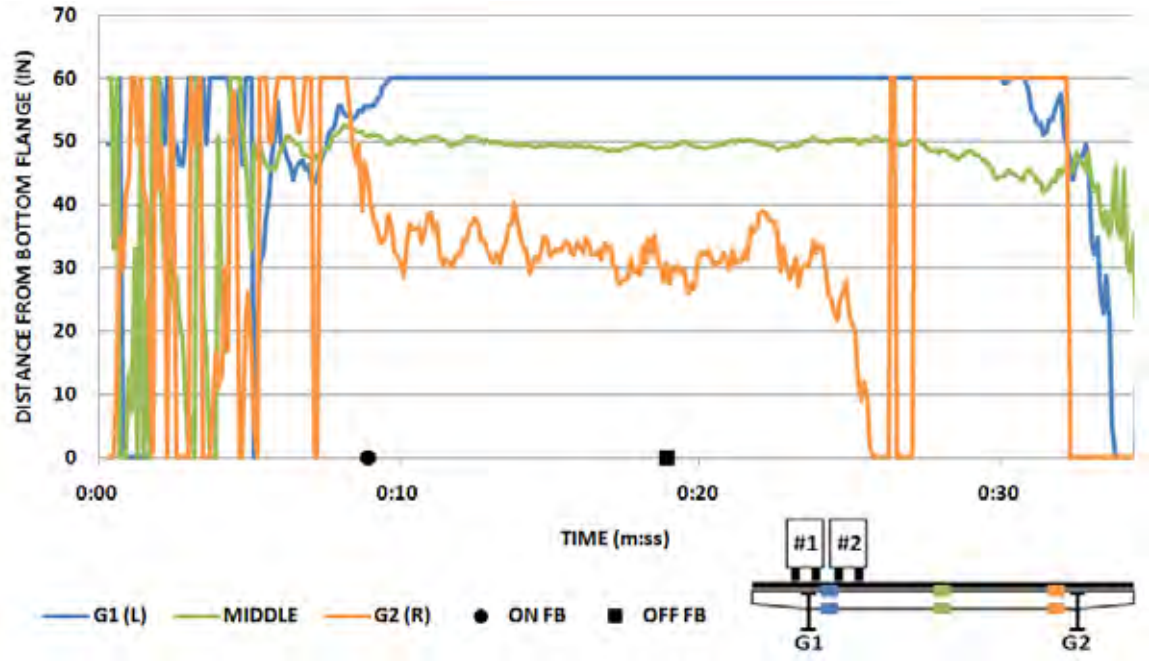

Figure 4.37: Neutral Axis of the Floor Beam versus Time due to Two Trucks on the Left

4.7 Summary

4.7.1 Floor Beams

For this floor beam, which was unsupported on both sides, the side of the floor beam where the trucks are located deflects downward vertically. The other side of the floor beam generally does not deflect in either direction. From the strain gage results, it can be determined that the floor beams bend in double curvature between the girders. In addition to bending in the plane of the web, the floor beam also bends out of plane. The out-of-plane bending generally occurs in the bottom flange of the floor beam because it is not restricted from moving by the slab as is the top flange. The out-of-plane bending is generally much larger in the floor beam directly underneath the trucks. The stress in the floor beam caused by the two truck tests was found to be greater than twice that caused by the single truck tests. Once the trucks leave the floor beam, the stress in that floor beam drops to zero.

4.7.2 Girder (Bottom Flange Gages)

The girder was found to bend both in and out of the plane of the web at the location where the bottom flange of the floor beam frames into the girder. The girder deflects downward in the plane of the web under the weight of the trucks. When the trucks move to the middle span, the girder deflects upward, and when the trucks are on the last span, the girder deflects downward. The girders bend out of the plane of the web in the same direction regardless of which side of the bridge the trucks were located. However, there is very little out-of-plane bending in the girder on the opposite side of the bridge from the trucks. Each time the trucks move to the next span, the girder bends in the opposite direction. At times, the girder bends out of plane in different directions on either side of the floor beam.

4.7.3 Girder (Web Gap Gages)

The web gap of the girder was found to bend in single curvature with the stress at the top of the gap being greater than the stress at the bottom of the gap. As was seen with the bottom flange gages, the web gap bends in the same direction regardless of which side of the bridge the trucks were located. The girder directly under the trucks experienced much greater stresses than the girder on the opposite side of the bridge. Each time the trucks move onto the next span, the web gap bends in the opposite direction.

4.7.4 Composite Actions of Floor Beams and Slab

The extent of composite action between the slab and floor beam was determined by calculating the neutral axis of the floor beam using the stresses in the top and bottom flanges. The neutral axis was found to be very high on the floor beam or in the slab when the trucks were near the floor beam. It is believed that the weight of trucks creates a frictional force between the floor beams and slab causing them to act compositely.

Chapter 5. Controlled Live Load Test Results for Section F17S Floor Beam 16

5.1 Introduction

This section summarizes the results from the controlled live load field tests for Floor Beam 16 in Section F17S. Floor Beam 16 was unsupported on one end and supported with a haunched girder on the other end. The floor beam-to-girder connections in this section had been retrofitted. The strain gages were grouped into four main categories: deflection gages, floor beam gages, bottom flange gages, and retrofit stiffener gages. The results from the two live load tests with two trucks will be discussed below for each group of gages. These tests were chosen because they produced similar trends as the single truck tests, but with larger stresses.

The figures in this chapter plot the deflection and stress calculated from the strain gages as a function of time as the trucks move along the bridge. The deflection and stress values are taken relative to the values in the gages when there is no traffic on the bridge. Therefore, the values plotted are changes in deflection and stress due to the applied live load. The circles and squares plotted along the horizontal axis in some of the figures represent the approximate times when the truck came onto the floor beam and left the floor beam being tested. The plateaus in the plots signify the time when the truck was stationary over the floor beam. The values at the plateaus will be referred to as the static deflection and static stress. In each of the plots, the colors of the lines correspond to a specific strain gage, the location of which is depicted on the details within each of the figures.

5.2 Live Load Test Results: 2 Trucks Right

5.2.1 Deflection Gages

Deflection gages, also referred to as string potentiometers, were placed on the bottom flange of the floor beam at each end near the connection to the girder. These were used to determine how much the floor beam deflected under the weight of the trucks. The string pot that was placed near Girder 2 was determined to be defective. However, because this location was near the supported girder, it was not expected to deflect significantly. Figure 5.1 shows the deflection on the right side of the floor beam due to two trucks on the right side of the bridge. The right side of the floor beam deflected upward when the trucks were nearing Floor Beam 18 and deflected downward when the trucks were over Floor Beam 16. From this data, the deflected shape of Floor Beam 16 due to the stationary trucks can be determined and is represented by the dashed line in the detail of the floor beam within Figure 5.1. The right side of the floor beam deflects downward under the weight of the trucks while the left side is restrained from deflecting by the column.

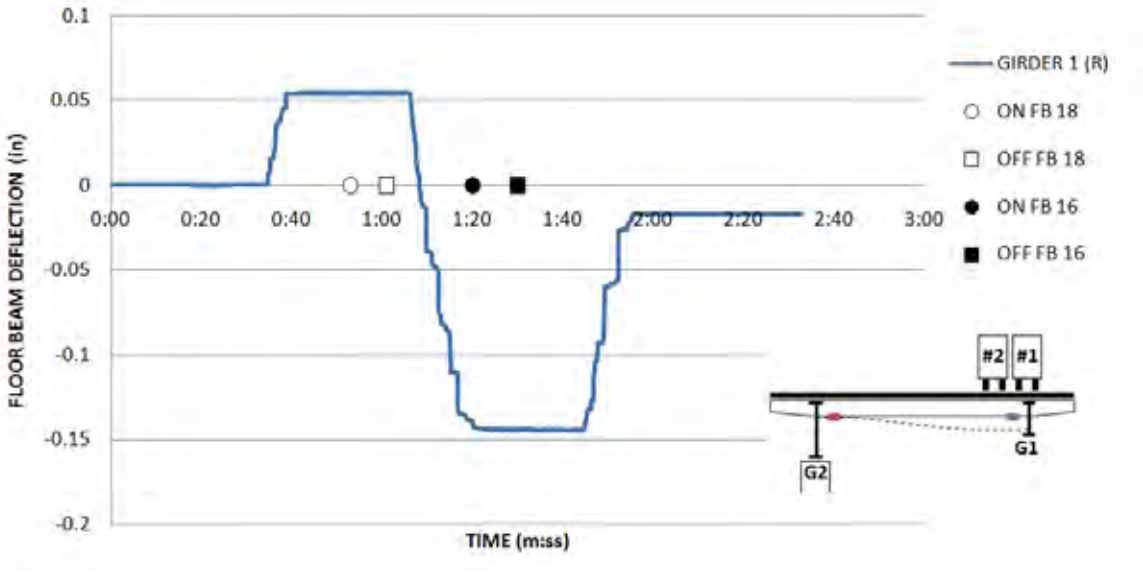

Figure 5.1: Deflection of Floor Beam due to Two Trucks on the Right

5.2.2 Floor Beam Gages

To determine how Floor Beam 16 responds to traffic loads, the stress in the floor beam gages was plotted versus time. Figure 5.2 shows the in-plane and out-of-plane bending stresses in the top and bottom flanges of the floor beam near Girder 1 due to two trucks on the right side of the bridge. When the trucks were over Floor Beam 18, there is very little stress in Floor Beam 16. This is because Girder 1 is supported by a column at Floor Beam 18. Therefore, the weight of the trucks was transferred through the girder to the column, not to the surrounding floor beams. When the trucks are over Floor Beam 16, it can be seen that the in-plane bending stress of the bottom flange is very large compared to the other stresses. The tensile stress in the bottom flange is a result of the weight of the trucks deflecting the right side of the floor beam downward. There is slight out-of-plane movement of the top flange when the trucks are over the floor beam and in both flanges when the trucks leave the floor beam. These stresses, however, are relatively small compared to the in-plane stress of the bottom flange.

One of the gages placed on the bottom flange of the floor beam near Girder 2 was defective. Therefore, it is not possible to determine whether the stress in the floor beam flange at this location is in plane or out of plane. Figure 5.3 shows the in-plane and out-of-plane bending stresses in the top flange near Girder 2 as well as the stress on one side of the bottom flange due to two trucks on the right side of the bridge. Before the trucks reach Floor Beam 18, the bottom flange of Floor Beam 16 shows a slight tensile stress. The left side of the floor beam is restrained from deflecting due to the column. Therefore, this tensile stress is most likely caused by the right side deflecting upward from the weight of the trucks on the previous span. When the trucks are stationary over Floor Beam 16, there is tensile stress in the top flange and compressive stress in the bottom flange. This is consistent with the assumed deflected shape determined from Figure 5.1. The left side is restrained from deflecting due to the support from the column and the right side is deflecting downward under the weight of the trucks. This results in the floor beam bending in double curvature. After the trucks leave the floor beam, the bottom flange shows a slight tensile stress.

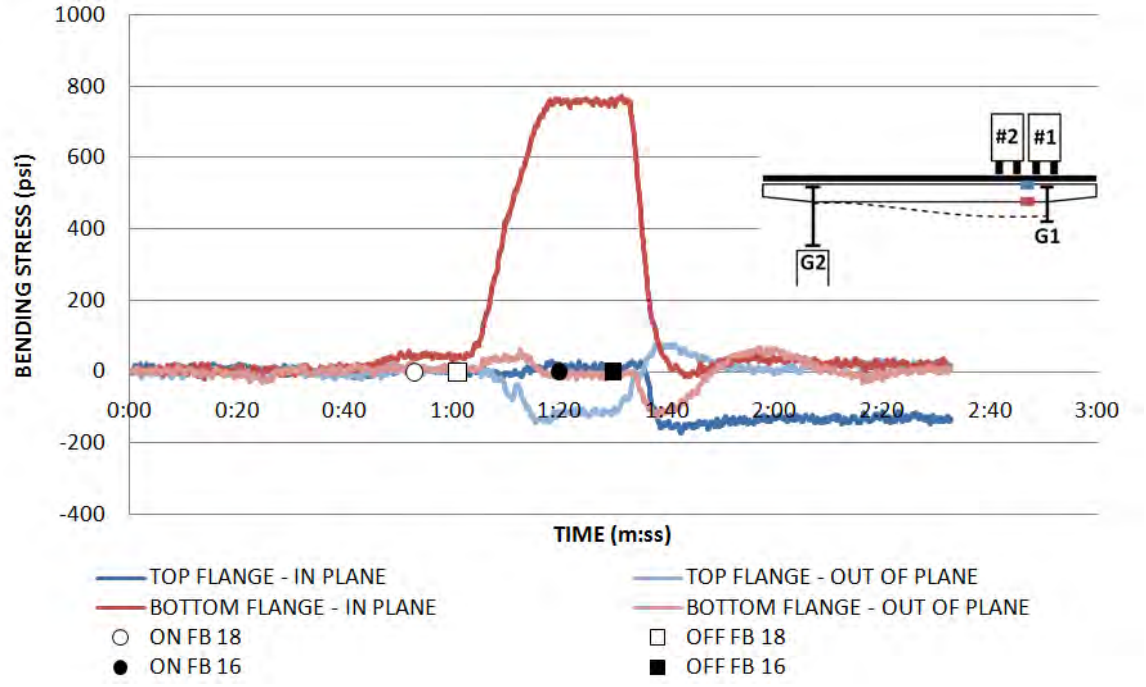

Figure 5.2: In-Plane and Out-of-Plane Stress of the Floor Beam near Girder 1 due to two Trucks on the Right

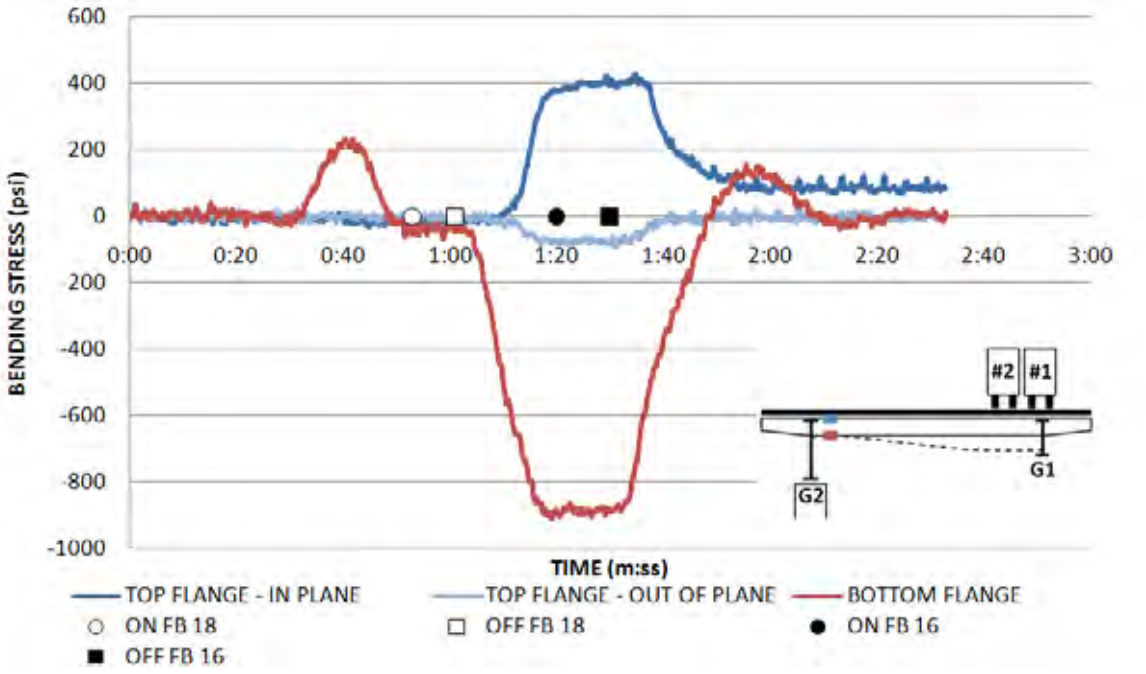

Figure 5.3: In-Plane and Out-of-Plane Stress of the Floor Beam near Girder 2 due to two Trucks on the Right

5.2.3 Bottom Flange Gages

The stress recorded by the bottom flange gages can be plotted versus time to determine how the girder moves under live load. Figure 5.4 shows the in-plane and out-of-plane stress in Girder 1 adjacent to the bottom flange of the floor beam due to two trucks on the right side of the bridge. Before the trucks reach Floor Beam 18, Girder 1 experiences compressive in-plane stresses, which suggests that the girder is deflecting upward. When the trucks stop at Floor Beam 18, the stresses are zero. This is due to the fact that the trucks are over the connection of Floor Beam 18 to Girder 1, which is supported by a column. Therefore, no stress is being transferred to other floor beams. When the trucks stop over Floor Beam 16, the in-plane stresses in the girder are tensile due to the downward deflection of the girder under the weight of the trucks. The out-of-plane stresses are in different directions on either side of the floor beam. When the trucks leave the floor beam, the girder bends in the opposite direction.

Figure 5.5 shows the stress in Girder 2 adjacent to the bottom flange of the floor beam due to two trucks in the right lanes. Girder 2 is haunched and supported by a column at this location. The girder has bearing stiffeners on either side of the floor beam that create a very small gap in which to place the strain gages. Because of this and the presence of repair welds, it was not possible to place gages on the interior or exterior side of the girder on the south side of the floor beam. The haunch of Girder 2 causes the bottom flange of the floor beam to frame into the girder above the girder's neutral axis. Figure 5.5 shows that the girder is experiencing in and out-of-plane stresses just before the trucks reach Floor Beam 18. Again, the stresses are practically zero when the trucks stop over Floor Beam 18. When the trucks stop over Floor Beam 16, the girder experiences tensile in-plane and out-of-plane stresses. This suggests that the girder is deflecting downward on either side of the column creating tension at the location where the floor beam frames into the girder above the column. The positive out-of-plane stress suggests that the girder is also bending inward toward the center of the bridge. The out-of-plane stress is significantly higher that the in-plane stress at this location. This is most likely due to the fact that the girder is supported by the column and is, therefore, restrained from deflecting vertically. The increased height of the girder due to the haunch creates a more slender web that may be more susceptible to out-of-plane bending. Comparing Figures 5.4 and 5.5, it can be seen that the stress in Girder 2 is much greater than the stress in Girder 1. This is due to the presence of bearing stiffeners on Girder 2. The bearing stiffeners create a very small gap next to the bottom flange of the floor beam, which results in very high stress concentrations in this area. These stress concentrations are most likely the cause of cracking at this location.

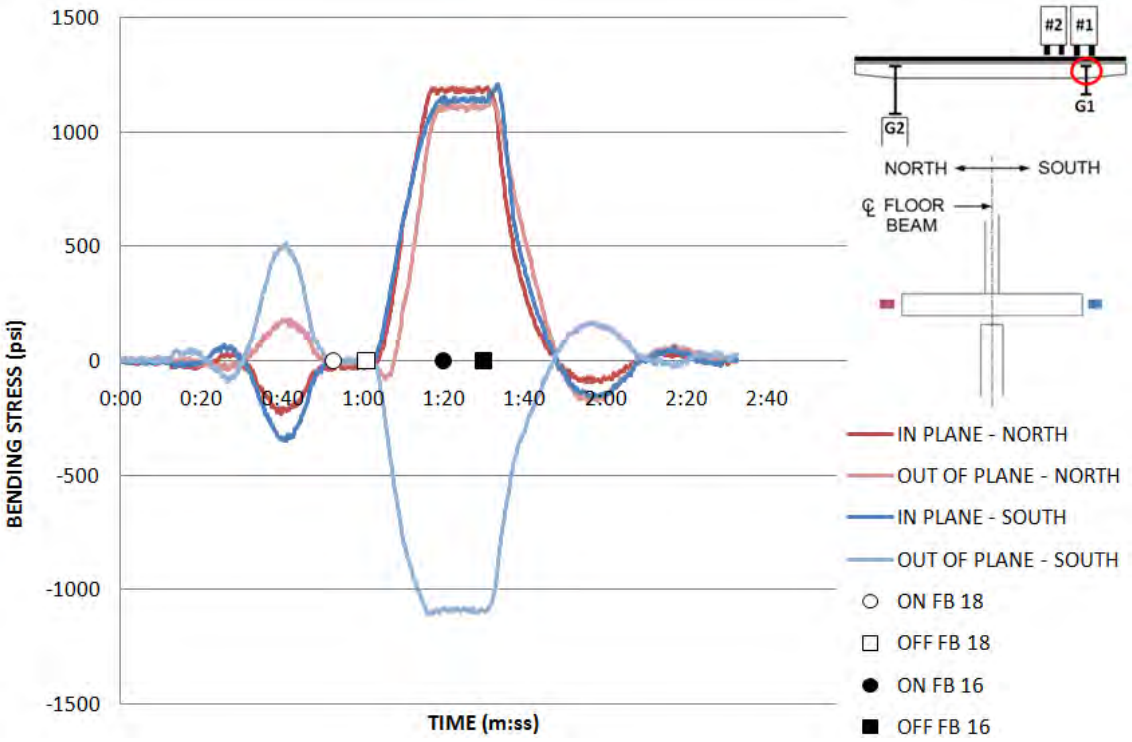

Figure 5.4: In-Plane and Out-of-Plane Bending Stresses of Girder 1 Web due to two Trucks on the Right

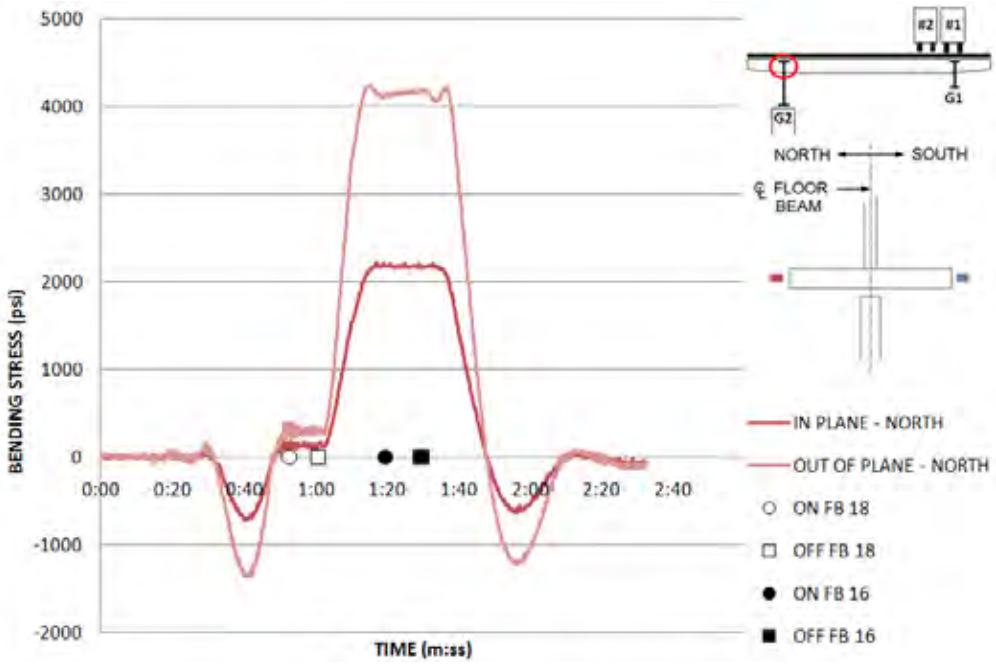

Figure 5.5: In-Plane and Out-of-Plane Bending Stresses of Girder 2 Web due to two Trucks on the Right

5.2.4 Retrofit Stiffener Gages

This section of the bridge was part of the 2004 retrofit in which stiffeners extending to the top flange of the girder were placed over the existing connection stiffeners. One stiffener was installed on each side of the connecting floor beam web and on both the interior and exterior side of the girder. One strain gage was placed on the exposed side of each of the two interior retrofit stiffeners. The results from these two strain gages were used to determine the in-plane and out-of-plane bending stresses in the retrofit stiffeners using the method described in Section 3.2. In-plane stresses refer to the stresses caused by bending in the plane of the stiffener. Out-of-plane stresses refer to the stresses caused by bending out of the plane of the stiffener. Movement of the retrofit stiffeners is also an indication of the movement of the top flange of the girder due to the welded connection between the two components.

Figure 5.6 shows the results from the retrofit stiffeners at Girder 1 for the live load test with two trucks on the right. It can be seen that the stiffeners experienced in-plane and out-of-plane bending prior to the trucks reaching Floor Beam 18. When the trucks stop at Floor Beam 18, the stresses are practically zero. Similar to the trends seen with the bottom flange gages, this is due to the fact that the trucks are over the connection of Floor Beam 18 to Girder 1, which is supported by a column. Therefore, no stress is being transferred to other floor beams. When the trucks stop on Floor Beam 16, the in-plane stresses are far greater than the out-of-plane stresses, which are practically zero. At this point, the trucks are directly over the connection and are causing no out-of-plane movement of the stiffeners.

Figure 5.7 shows the results from the retrofit stiffeners at the haunched Girder 2 for the live load test with two trucks on the right. The gage attached to the retrofit stiffener on the south side of the floor beam was found to be defective and is therefore not plotted in the figure. The plotted line corresponds to the stress recorded by the gage on the stiffener on the north side of the floor beam. There are compressive stresses in the girder prior to the trucks reaching Floor Beam 18, at which time the stress is zero. When the trucks are over Floor Beam 16, there are very high stresses in the stiffener. This is similar to what was seen in the bottom flange gages on Girder 2 when the trucks were on the right side (see Figure 5.5). Girder 2 seems to attract much of the stress due to its haunched section.

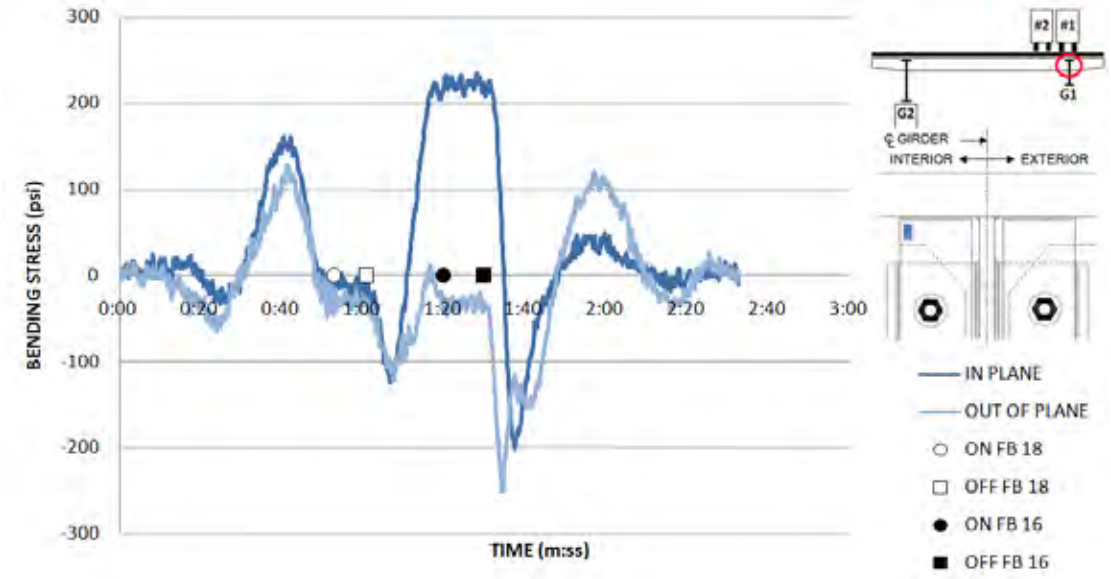

Figure 5.6: Stress in Girder 1 Retrofit Stiffeners due to two Trucks on the Right

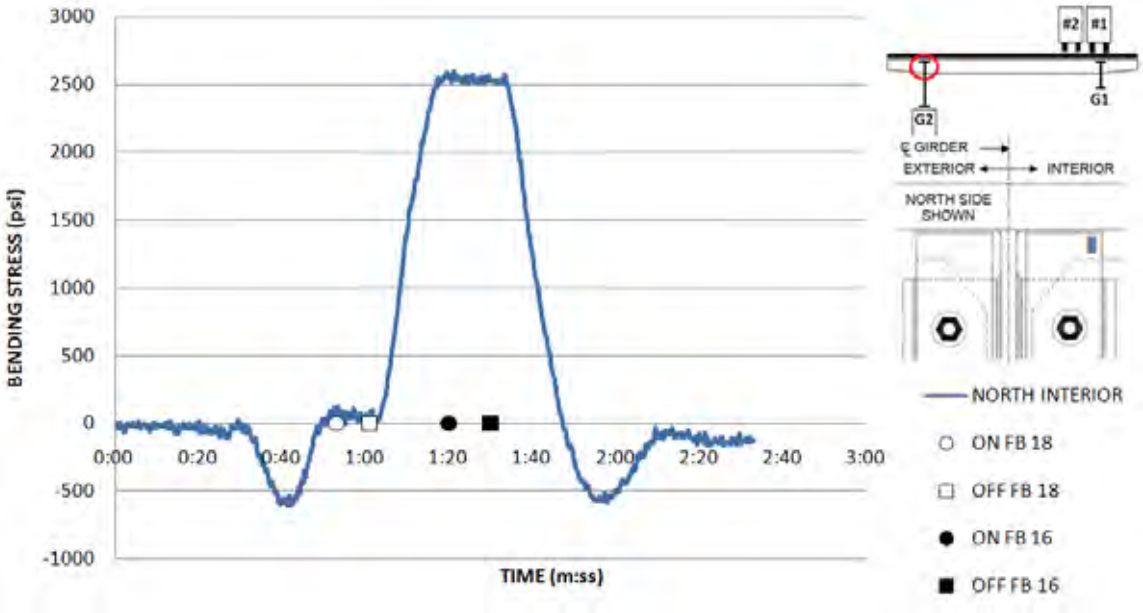

Figure 5.7: Stress in Girder 2 Retrofit Stiffeners due to two Trucks on the Right

5.3 Live Load Test Results: 2 Trucks Left

5.3.1 Deflection Gage

Figure 5.8 shows the deflections measured at the right side of the floor beam due to two trucks on the left side of the bridge. The string pot on the left side was defective, but it is assumed that the left side does not deflect due to the support of the column. The figure shows that the right side of the floor beam does not deflect. Because of the narrow shoulder on the left side of this bridge, the two trucks are centered over Girder 2 as can be seen in the detail within

Figure 5.8. Therefore, the trucks are completely supported by Girder 2 and do not cause the right side of the floor beam to deflect.

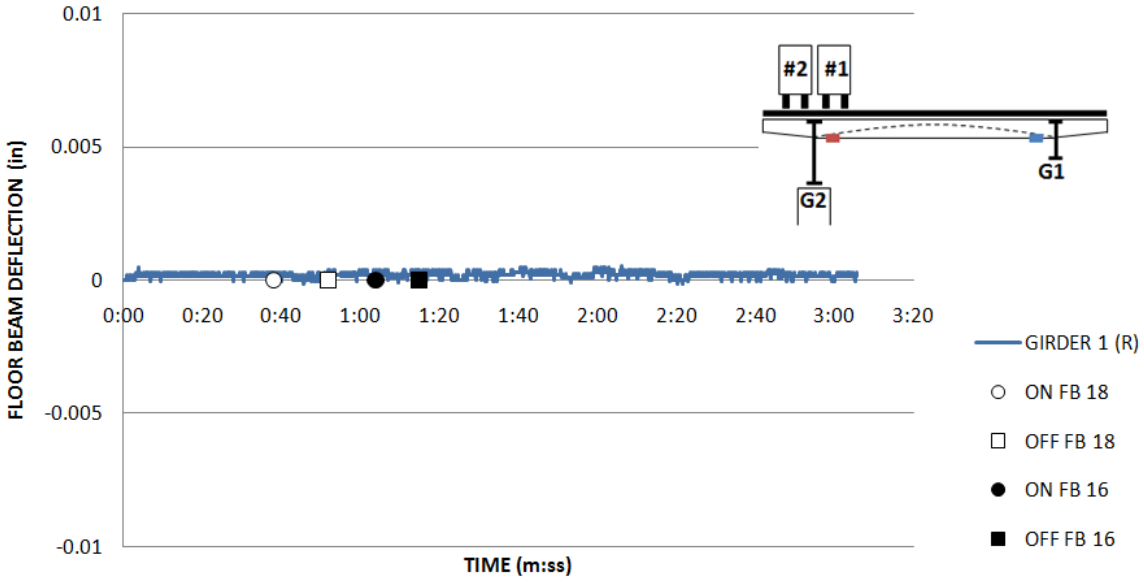

Figure 5.8: Deflection of Floor Beam due to Two Trucks on the Left

5.3.2 Floor Beam Gages

Figure 5.9 shows the in-plane and out-of-plane stresses in Floor Beam 16 near Girder 1 when two trucks were on the left side of the bridge. It can be seen that the stresses at this location are very low with the maximum recorded stress being only about 0.09 ksi. This is due to the fact that when the trucks are on the left side of Floor Beam 16, they are directly over the haunched girder, which is supported by a column. Therefore, the majority of the stress caused by the trucks is taken by the support and is not transmitted to the girder on the other side of the floor beam.

Figure 5.10 shows the in-plane and out-of-plane stresses in Floor Beam 16 near Girder 2 when two trucks were on the left side of the bridge. One of the gages placed on the bottom flange of the floor beam near Girder 2 was defective. Therefore, it is not possible to determine whether the stress in the floor beam flange at this location is in plane or out of plane. The top flange experiences very little stress until the trucks reach Floor Beam 16, at which point the flange experiences in-plane tensile stresses. The bottom flange recorded compressive stresses. This suggests that the floor beam is deflecting upward in between the two girders. This makes sense if the location of the trucks is considered. The left shoulder on Section F17S is narrow, measuring only four feet wide. Therefore, when the trucks are on the left side of the road, one of the trucks is actually driving on the overhang. This seems to create enough downward force on the overhang to cause the middle section of the floor beam to bend upward, as can be seen from the dashed line in the details of the previous figures.

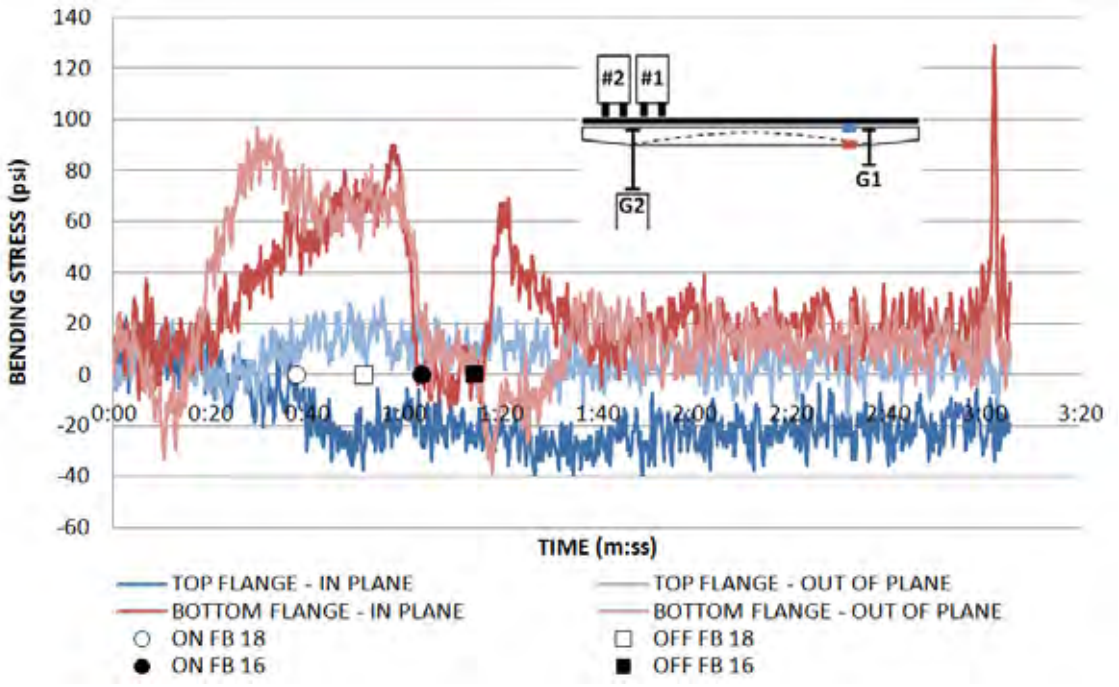

Figure 5.9: In-Plane and Out-of-Plane Stress of the Floor Beam near Girder 1 due to two Trucks on the Left

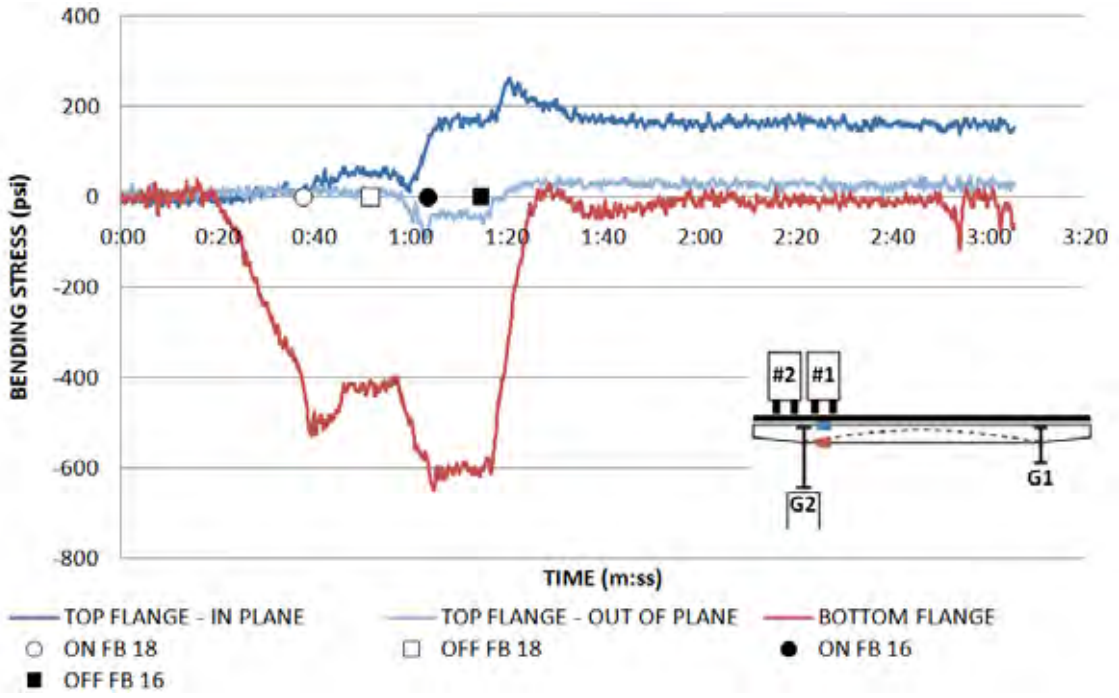

Figure 5.10: In-Plane and Out-of-Plane Stress of the Floor Beam near Girder 2 due to two Trucks on the Left

5.3.3 Bottom Flange Gages

Figure 5.11 shows the stress in the web of Girder 1 due to two trucks on the left side of the bridge. Overall, the stresses are very low. This is because the trucks are directly over Girder 2, which is supported by a column. Therefore, no stress is being transferred to Girder 1. There is some out-of-plane bending of Girder 1 when the trucks are over Floor Beam 18 as well as when the trucks leave Floor Beam 16. The opposite signs of the out-of-plane stresses suggest that the girder web is bending in different directions on either side of the floor beam. These stresses, however, are all relatively low.

Figure 5.12 shows the stress in the web of Girder 2 due to two trucks on the left side of the bridge. Girder 2 is haunched and supported by a column at this location. The girder has bearing stiffeners on either side of the floor beam, which create a very small gap in which to place the strain gages. Because of this and the presence of repair welds, it was not possible to place gages on the interior or exterior side of the girder on the south side of the floor beam. Therefore, Figure 5.12 shows the in-plane and out-of-plane stresses in the girder web on the north side of Floor Beam 16. The haunch of Girder 2 causes the bottom flange of the floor beam to frame into the girder above the girder's neutral axis. Seeing as how the girder is supported by a column at this location, the in-plane stress would be expected to be tensile. This is true until the point when the trucks reach Floor Beam 16 where the in-plane stresses are negative. The girder bends out of plane toward the interior of the bridge when the trucks are over Floor Beam 18 and bends outward toward the exterior of the bridge when the trucks are over Floor Beam 16.

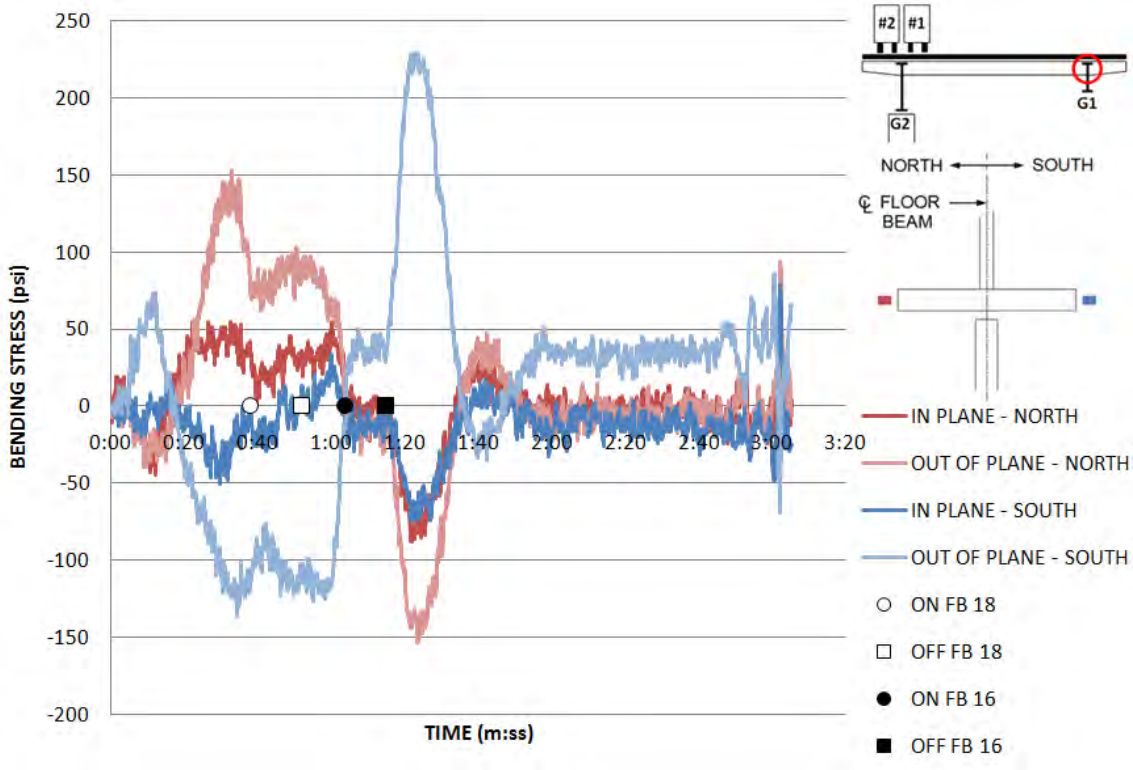

Figure 5.11: In-Plane and Out-of-Plane Bending Stresses of Girder 1 Web due to two Trucks on the Left

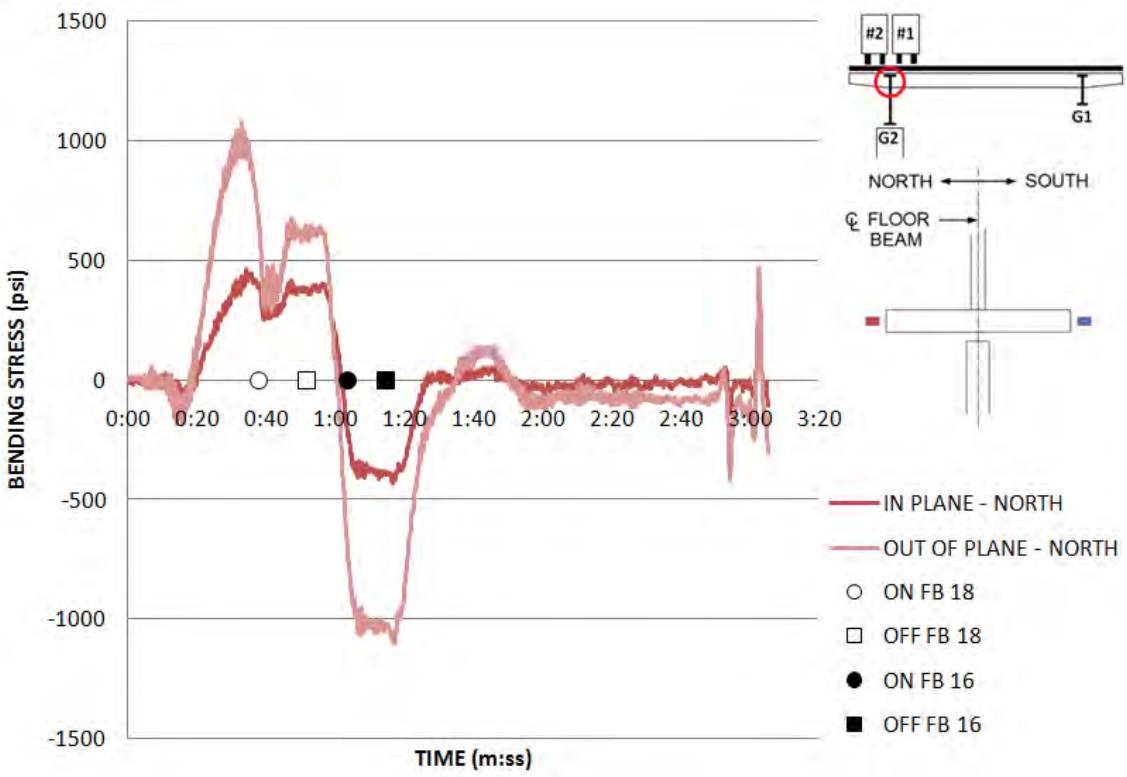

Figure 5.12: In-Plane and Out-of-Plane Bending Stresses of Girder 2 Web due to two Trucks on the Left

5.3.4 Retrofit Stiffener Gages

Figure 5.13 is a plot of the in-plane and out-of-plane stresses in the retrofit stiffeners on Girder 1 due to two trucks on the left side of the bridge. The plot shows that the stress in the stiffeners is very low, with the maximum being about 0.1 ksi. This is due to the fact that when the trucks are on the left side of Floor Beam 16, they are directly over the haunched girder that is supported by a column. Therefore, the majority of the stress caused by the trucks is taken by the support and is not transmitted to the girder on the other side of the floor beam. This is similar to what was seen with the floor beam and bottom flange gages.

Figure 5.14 shows a plot of the in-plane and out-of-plane bending stresses in the retrofit stiffeners on Girder 2 due to two trucks on the left side of the bridge. The gage attached to the retrofit stiffener on the south side of the floor beam was found to be defective and is therefore not plotted in the figure. The plotted line corresponds to the stress recorded by the gage on the stiffener on the north side of the floor beam. Because there was only one gage, it is not possible to determine whether the stress is due to in-plane or out-of-plane bending. The gage recorded tensile stresses when the trucks were over Floor Beam 18 and a greater tensile stress when the trucks were over Floor Beam 16.

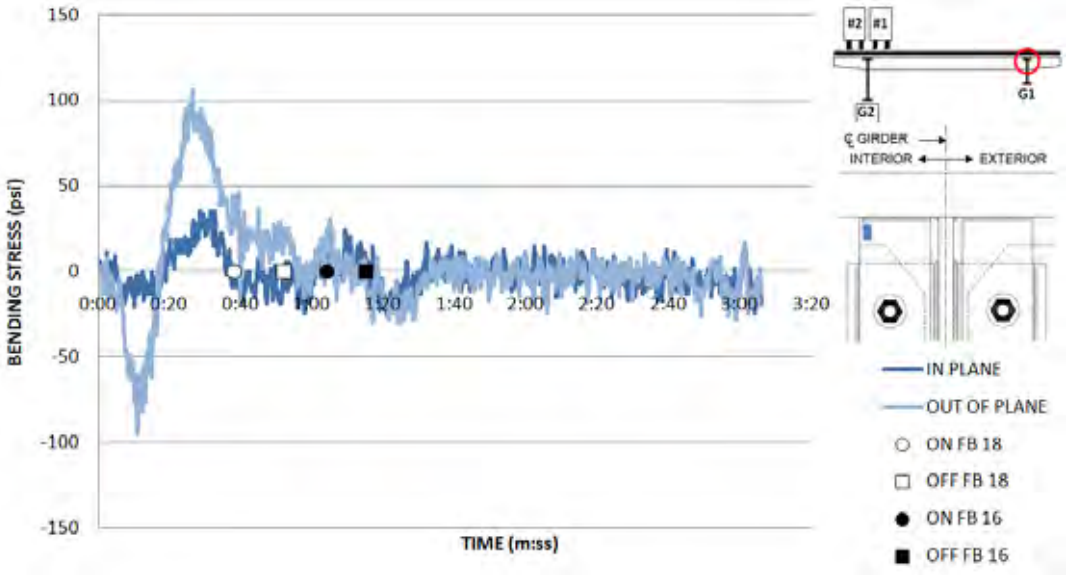

Figure 5.13: Stress in Girder 1 Retrofit Stiffeners due to two Trucks on the Left

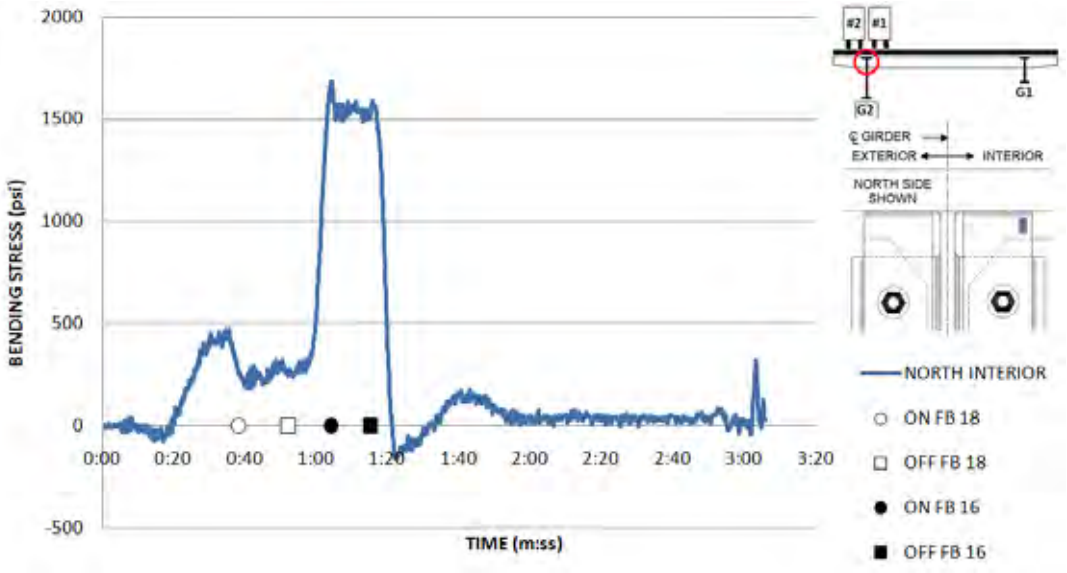

Figure 5.14: Stress in Girder 2 Retrofit Stiffeners due to two Trucks on the Left

5.4 Composite Action of Floor Beams and Slab

In order to determine whether or not the floor beams and slab were acting compositely, the location of the neutral axis of the floor beam was calculated using the method described in Section 3.4. If the slab and floor beam were acting non-compositely, the strain in the top and bottom flange of the floor beam would be equal in magnitude and the neutral axis of the floor beam would be at the centroid, or mid-height, of the section. This can be seen in Figure 3.8(a). If the slab and floor beam were acting compositely, the strain in the bottom flange would be greater in magnitude than the strain in the top flange, moving the neutral axis above the centroid of the floor beam, as seen in Figure 3.8(b). The neutral axis was calculated at both ends of the floor

beam near the connections to the girders as well as in the center of the floor beam. The horizontal axis of the following figures was adjusted to show the period of time around when the trucks were stationary over the floor beam. The reason for this is because the strain in the floor beam was practically zero when there were no trucks near the floor beam. Therefore, any small change in the strain during this time would drastically change the location of the neutral axis. This is illustrated by the significant noise at the beginning and end of the following two plots.

Figure 5.15 shows the location of the neutral axis versus time as two trucks move along the right side of the bridge. The figure shows that underneath the trucks, the neutral axis of the floor beam is about 50 inches above the bottom flange, which is in the top flange of the floor beam. Therefore, it would seem as though the floor beam and slab were acting compositely at that location. On the left side of the floor beam, the side opposite the trucks, the neutral axis is about 26 inches above the bottom flange of the floor beam, which is very near the center of the section. Therefore, it would seem as though the floor beam and slab were acting non-compositely at this location. In the middle of the floor beam, the neutral axis is located about 40 inches above the bottom flange which is in the top half of the web. It is believed that the weight of the trucks produces a friction force between the floor beams and slab, creating the composite action. On the side opposite the trucks, there is no weight to create friction between the floor beam and slab. As a result, they are free to slip past one another causing non-composite action.

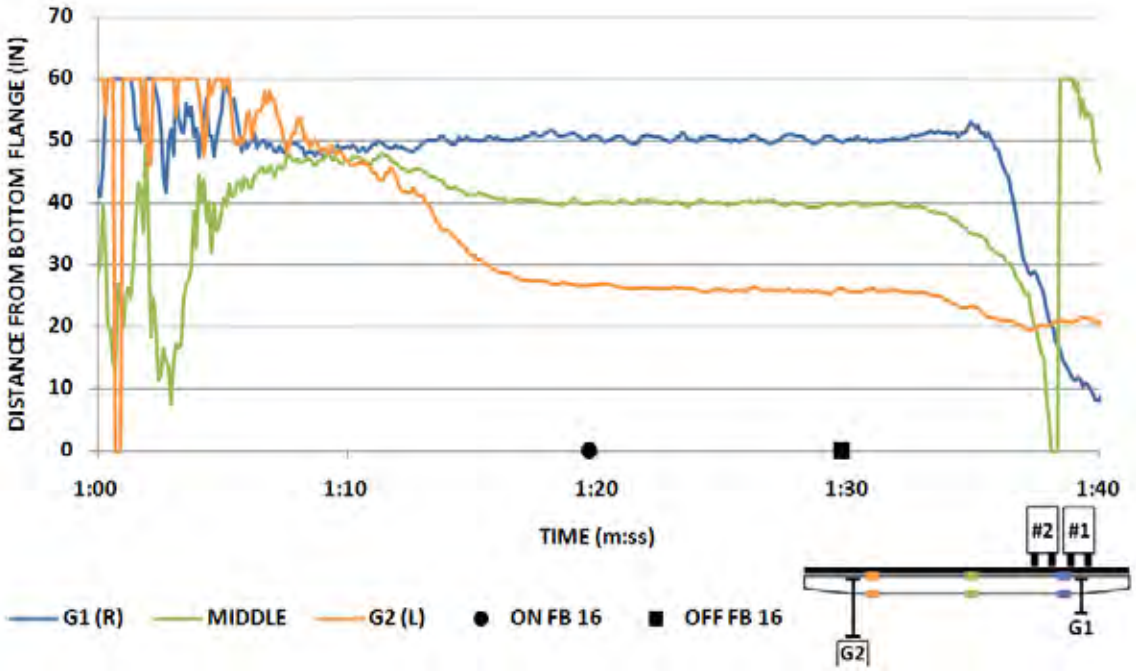

Figure 5.15: Neutral Axis of the Floor Beam versus Time due to Two Trucks on the Right

Figure 5.16 shows the location of the neutral axis of the floor beam versus time as two trucks move along the left side of the bridge. During this run, the two trucks were directly over Girder 2, which is supported by a column at Floor Beam 16. Due to the support of the column, there was very little stress transferred to the middle and right side of the floor beam. When the stress values are very small, the calculation of the neutral axis is very sensitive to any changes in stress. This makes the location of the neutral axis highly variable. This is the reason for the

scatter in the data of Figure 5.16 for the middle and right side of the floor beam. On the left side of the floor beam, directly under the trucks, the neutral axis was calculated to be about 32 inches above the bottom flange, which is slightly above the centroid. This suggests very minor composite action between the floor beam and slab. Because the supported girder is taking much of the stress from the trucks, there is little weight transferred to the floor beams. Therefore, there is very little friction to cause the floor beam and slab to act compositely.

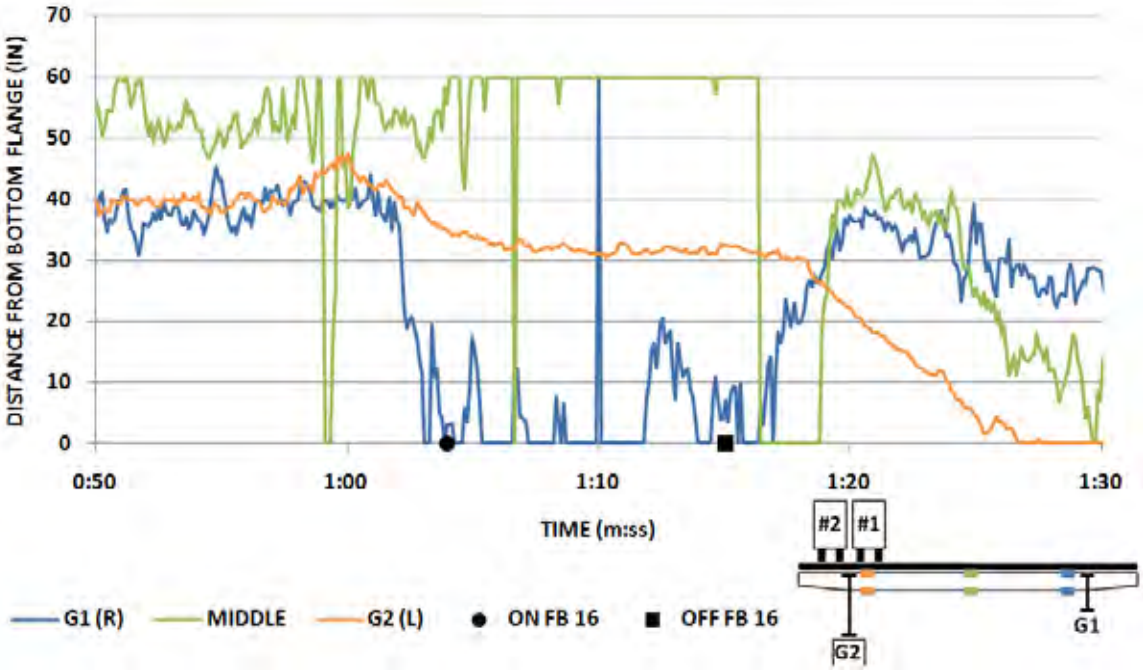

Figure 5.16: Neutral Axis of the Floor Beam versus Time due to Two Trucks on the Left

5.5 Summary

5.5.1 Floor Beams

The left side of Floor Beam 16 is connected to a haunched girder, which is supported by a column. The right side of the floor beam is connected to a girder that is neither haunched nor supported by a column. This creates a situation in which one side of the floor beam has a very stiff, rigid connection while the other side is fairly free to move. The data shows that the floor beam bends in double curvature when the trucks were run on the right side of the road over the unsupported girder. During this run, the right side of the floor beam deflects both upward and downward depending on the location of the trucks along the bridge. The haunched girder on the left side of the floor beam creates a very stiff connection that attracts stress caused by the trucks. When the trucks are directly over the haunch, very little stress is transferred to the other side of the floor beam. When the trucks are on the opposite side, the side of the floor beam near the haunch still experiences higher stresses than the side of the floor beam under the trucks. There is also very little lateral bending of this floor beam. The asymmetric support layout in this section of the bridge allows the floor beams to deflect in such a way that creates a twisting motion in the bridge.

5.5.2 Girder (Bottom Flange Gages)

The girder was found to bend both in and out of the plane of the web at the location where the bottom flange of the floor beam frames into the girder. The haunched girder was restricted from deflecting vertically due to the column. Therefore, the majority of the bending in this girder was out of the plane of the web. The out-of-plane stress was highest in the haunched girder when the trucks were on the other side of the bridge. The other girder deflected both in and out of the plane of the web. The in-plane and out-of-plane bending of girders was found to change directions as the trucks moved along the multiple spans of the bridge.

5.5.3 Retrofit Stiffeners

The retrofit stiffeners were found to bend both in and out of the plane of the stiffener. In-plane bending was most likely caused by rotation of the floor beam-to-column connection due to deflection of the floor beams. Out-of-plane bending of the stiffeners was most likely due to vertical movement of the girder in the plane of the girder web. The highest stresses occurred in the stiffeners attached to the haunched girder.

5.5.4 Composite Action of Floor Beams and Slab

The extent of composite action between the slab and floor beam was determined by calculating the neutral axis of the floor beam using the stresses in the top and bottom flanges. It was found that the floor beam and slab behaved more compositely near the location of the trucks. It is believed that the weight of trucks creates a frictional force between the floor beams and slab causing the composite action.

Chapter 6. Controlled Live Load Test Results for Section F175 Floor Beam 1S

6.1 Introduction

This section summarizes the results from the controlled live load field tests for Floor Beam 18 in section F17S. Floor Beam 18 was unsupported on one end and supported by a column on the other end. The floor beam-to-column connections in this section had been retrofitted. The strain gages were grouped into four main categories: deflection gages, floor beam gages, bottom flange gages and retrofit stiffener gages. The results from the two live load tests with two trucks will be discussed below for each group of gages. These tests were chosen because they produced similar trends as the single truck tests, but with larger stresses.

The figures in this chapter plot the deflection and stress calculated from the strain gages as a function of time as the trucks move along the bridge. The deflection and stress values are taken relative to the values in the gages when there is no traffic on the bridge. Therefore, the values plotted are changes in deflection and stress due to the applied live load. The circles and squares plotted along the horizontal axis in some of the figures represent the times when the truck came onto the floor beam and left the floor beam being tested. The plateaus in the plots signify the time when the truck was stationary over the floor beam. The values at the plateaus will be referred to as the static deflection and static stress. In each of the plots, the colors of the lines correspond to a specific strain gage, the location of which is depicted on the details within each of the figures.

6.2 Live Load Test Results: 2 Trucks Right

6.2.1 Deflection Gages

Deflection gages, also referred to as string potentiometers, were placed on the bottom flange of the floor beam at each end near the connection to the girder. These were used to determine how much the floor beam deflected under the weight of the trucks. Figure 6.1 shows the deflection on either side of the floor beam due to two trucks on the right side of the bridge. The right side of the floor beam was near Girder 1, which was supported by a column. Therefore, this side of the floor beam was restrained from deflecting. Due to the position of truck 2, which was on the interior side of Girder 1, the left side of the floor beam deflected downward 0.04 inches when the trucks were over the floor beam. When the trucks continue onto Floor Beam 16, the right side of the floor beam deflects upward 0.01 inches, which increases to 0.02 inches after the trucks leave Floor Beam 16. From these results, the deflected shape of the floor beam can be determined and is represented by the dashed line in the detail within Figure 6.1.

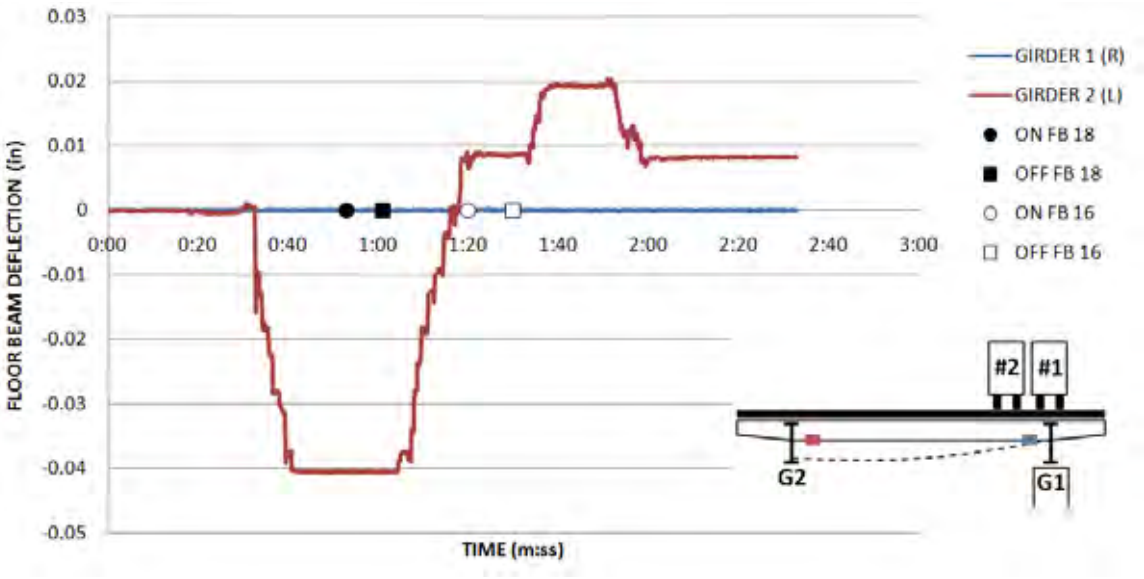

Figure 6.1: Deflection of Floor Beam due to Two Trucks on the Right

6.2.2 Floor Beam Gages

Figure 6.2 shows the in-plane and out-of-plane bending of the floor beam near Girder 1 due to two trucks on the right side of the bridge. The top and bottom flanges of the floor beam experienced tensile in-plane stresses where the stress in the bottom flange was almost twice that in the top flange. There is slight out-of-plane bending of the bottom flange when the trucks were over the floor beam. The top flange did not bend out of plane. These stresses changed direction when the trucks moved to Floor Beam 16. The in-plane stresses decreased while the out-of-plane bending of the bottom flange increased.

Figure 6.3 shows the in-plane and out-of-plane bending stresses of the floor beam near Girder 2 due to two trucks on the right side of the bridge. There is a lot of noise in this plot due to the small values of the stresses. With the trucks were over Girder 1, which was supported by a column, there was little stress transferred to the other side of the floor beam. The gages recorded small tensile in-plane stresses in the top and bottom flanges and out-of-plane stresses in different directions. The in-plane stress in the bottom flange is shown to be greater than that in the top flange except when it suddenly decreases when the trucks are over the floor beam. The reason for this could be that the stress on the left side of the floor beam is temporarily alleviated when the trucks are directly over the column on the right side. The stress then increases once the trucks leave the column. When the trucks moved onto Floor Beam 16, the stresses on this side of the floor beam generally went to zero.

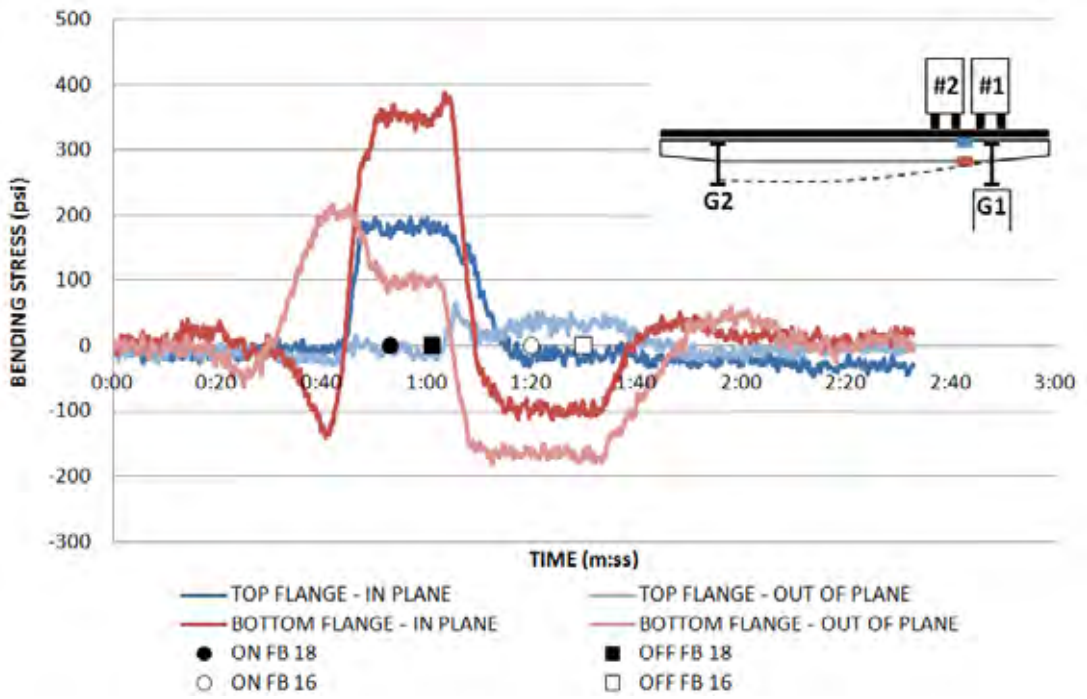

Figure 6.2: In-Plane and Out-of-Plane Stress of the Floor Beam near Girder 1 due to two Trucks on the Right

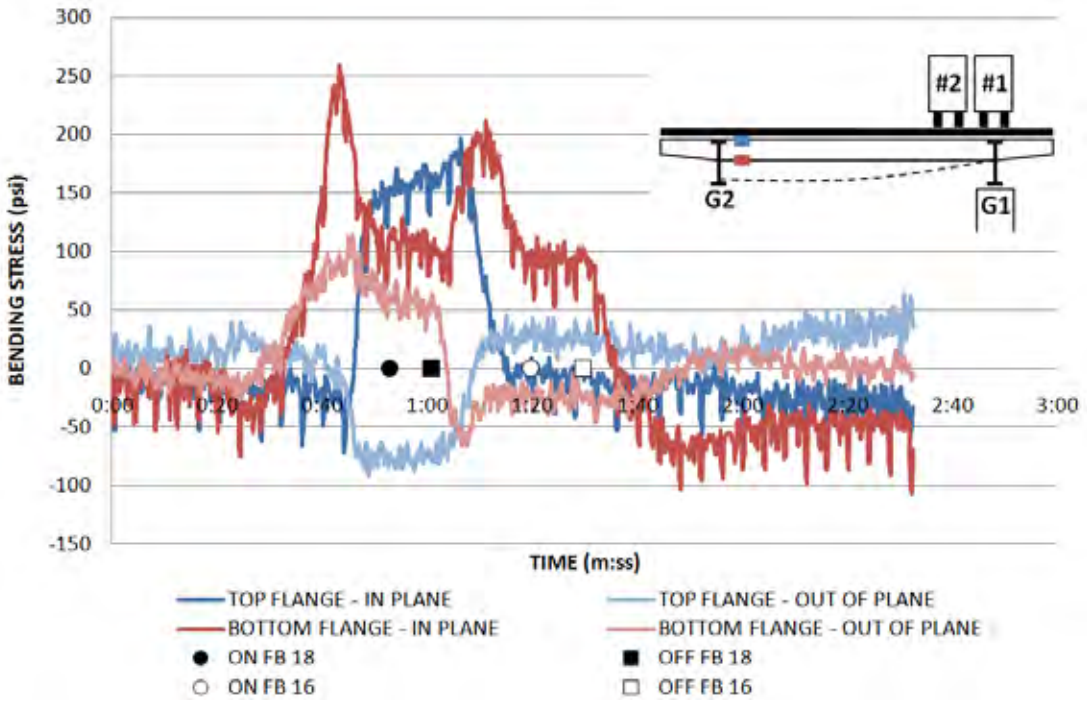

Figure 6.3: In-Plane and Out-of-Plane Stress of the Floor Beam near Girder 2 due to two Trucks on the Right

6.2.3 Bottom Flange Gages

Figure 6.4 shows the in-plane and out-of-plane bending of the Girder 1 web adjacent to the bottom flange of the floor beam when two trucks were on the right side of the bridge. The bottom flange of the floor beam frames into the girder below the girder's neutral axis. Because Girder 1 is supported by a column at this location, the in-plane bending stress recorded by these gages was expected to be compressive. However, the figure shows that the in-plane stresses are tensile when the trucks are over the floor beam. The out-of-plane static stresses are very large and show that the girder is bending inward toward the interior of the bridge. When the truck is over Floor Beam 16, the in-plane stresses in the girder show different signs on either side of the floor beam. This suggests that the girder is deflecting upward on the north side of the floor beam and downward on the south side of the floor beam, which is the side closest to Floor Beam 16. There is also some out-of-plane bending of the girder on the north side of the floor beam when the trucks are over Floor Beam 16.

Figure 6.5 shows the in-plane and out-of-plane bending of the Girder 2 web adjacent to the bottom flange of the floor beam when two trucks were on the right side of the bridge. The stresses recorded in Girder 2 were relatively small due to the fact that the trucks were supported by a column on the right side. There is out-of-plane bending of the girder before the trucks reach Floor Beam 18 and when the trucks are over Floor Beam 16. In both of these cases, the girder is bending out of plane in different directions on either side of the floor beam.

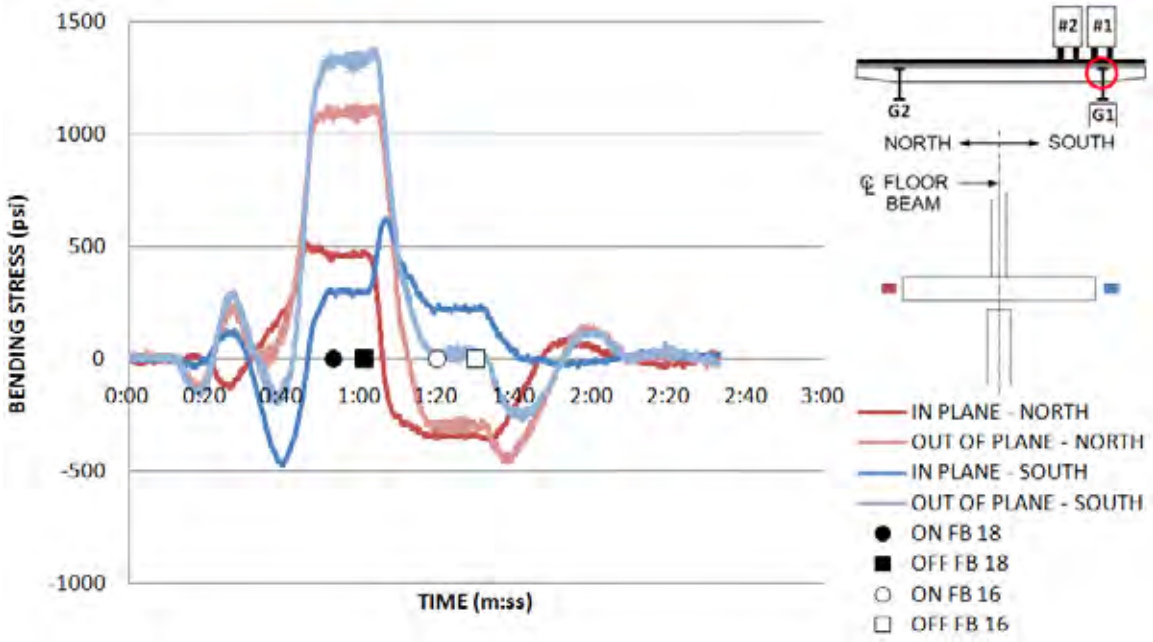

Figure 6.4: In-Plane and Out-of-Plane Bending Stresses of Girder 1 Web due to two Trucks on the Right

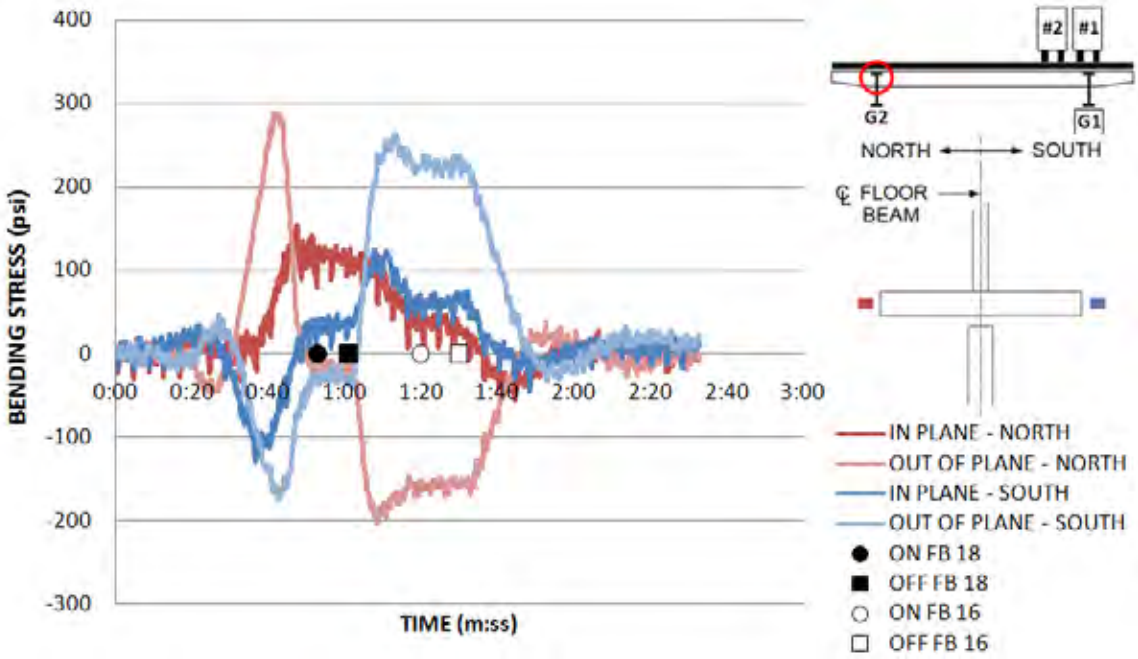

Figure 6.5: In-Plane and Out-of-Plane Bending Stresses of Girder 2 Web due to two Trucks on the Right

6.2.4 Retrofit Stiffener Gages

Figure 6.6 shows the in-plane and out-of-plane bending stresses of the Girder 1 retrofit stiffeners due to two trucks on the right side of the bridge. The stiffeners bend out of plane prior to the trucks reaching the floor beam, but then bend completely in-plane when the trucks are on the floor beam. The static in-plane stress is relatively high due to the trucks location directly over the girder. Once the trucks leave the floor beam, the stiffeners bend out-of-plane.

Figure 6.7 shows the in-plane and out-of-plane bending stresses of the Girder 2 retrofit stiffeners due to two trucks on the right side of the bridge. The stiffeners bend both in and out of plane before the trucks reach the floor beam. When the trucks are on the floor beam, the stiffeners bend mostly in plane. When the trucks are over Floor Beam 16, the stiffeners bend in plane in the opposite direction with slight out-of-plane bending.

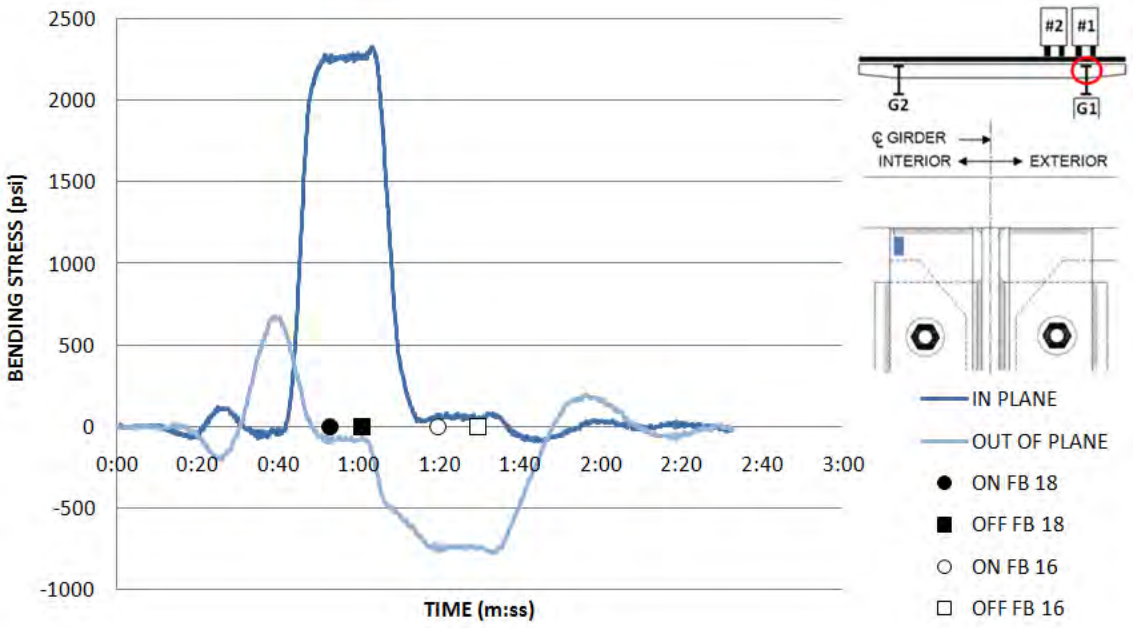

Figure 6.6: Stress in Girder 1 Retrofit Stiffeners due to two Trucks on the Right

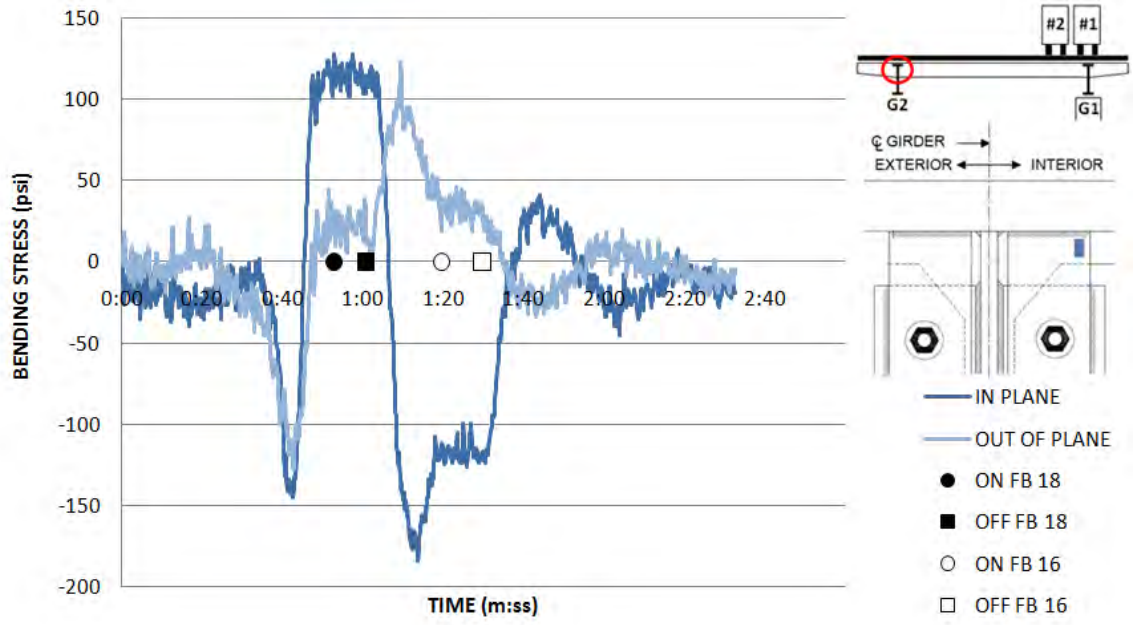

Figure 6.7: Stress in Girder 2 Retrofit Stiffeners due to two Trucks on the Right

6.3 Live Load Test Results: 2 Trucks Left

6.3.1 Deflection Gages

Figure 6.8 plots the deflection at both ends of the floor beam due to two trucks on the left side of the bridge. Girder 1 is restrained from deflecting due to the column. Therefore, the string pot on the right side of the floor beam shows no deflection. The left side of the floor beam deflects upward just before the trucks reach Floor Beam 18. When the trucks are on Floor Beam 18, the left side of the floor beam deflects downward under the weight of the trucks. The maximum deflection was recorded to be about 0.3 inches. When the trucks move onto Floor Beam 16, there is no deflection in Floor Beam 18. This is because the trucks are supported by the column at the connection of Girder 2 and Floor Beam 16. When the trucks leave Floor Beam 16, the left side of Floor Beam 18 deflects upward. From these results, the deflected shape of the floor beam due to static loading can be determined and is represented by the dashed line in the detail of the floor beam within Figure 6.8.

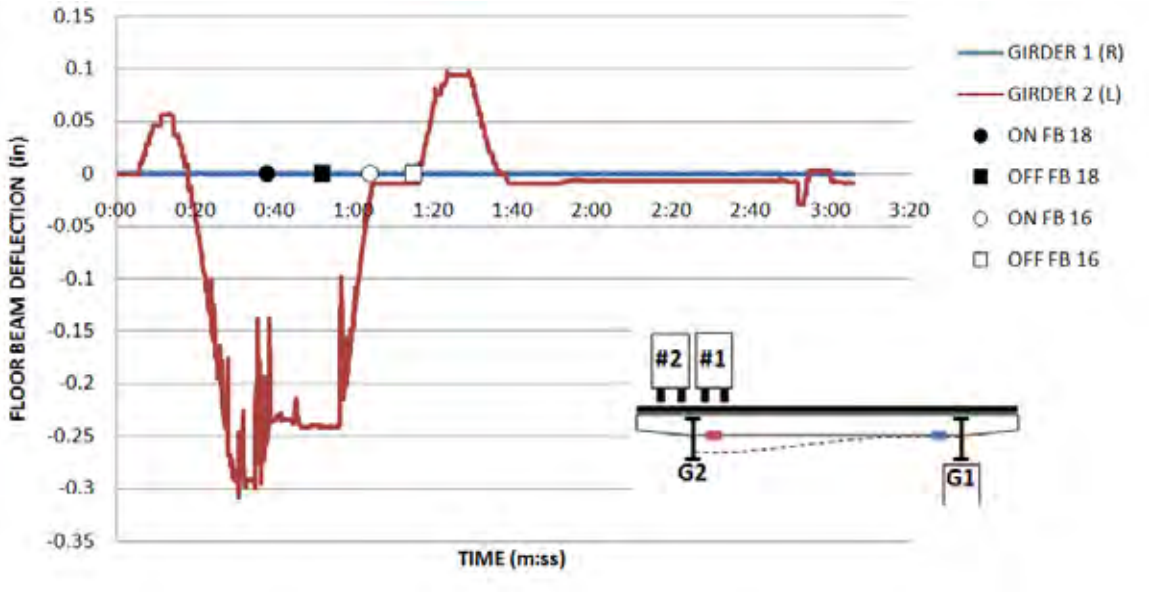

Figure 6.8: Deflection of Floor Beam due to Two Trucks on the Left

6.3.2 Floor Beam Gages

Figure 6.9 shows the in-plane and out-of-plane bending of the floor beam near Girder 1 due to two trucks on the left side of the bridge. There is slight in-plane and out-of-plane bending of the bottom flange before the trucks reach the floor beam. When the trucks are stationary over the floor beam, there is a relatively large in-plane compressive stress in the bottom flange with very little out-of-plane bending. The top flange has a small tensile in-plane stress. After the trucks leave Floor Beam 16, the bottom flange experiences tensile stresses. This data correlates with the deflection data from Figure 6.8, which shows that the left side of the bridge deflects downward under the weight of the trucks and causes compressive stresses in the bottom flange on the opposite side of the floor beam. When the trucks move past Floor Beam 16, the left side of Floor Beam 18 deflects upward as seen in Figure 6.8, which creates tensile stresses in the bottom flange on the opposite side of the floor beam.

Figure 6.10 shows the in-plane and out-of-plane bending stresses in the floor beam near Girder 2 due to two trucks on the left. Before the trucks reach the floor beam, there are high out-of-plane bending stresses in the bottom flange, which suggest that the floor beam is deflecting laterally. When the trucks are over the floor beam, this out-of-plane stress is decreased as the in-plane bending stress increases. The in-plane stress is positive on the bottom flange when the trucks move onto the floor beam indicating that the floor beam is deflecting downward under the weight of the trucks. This data correlates well with the deflection data from Figure 6.8 that shows that the left side of the floor beam is deflecting downward due to the trucks. The stress in the bottom flange on the left side of the floor beam is generally less than that on the right side of the floor beam. This seems to suggest that the supporting column is attracting the majority of the stress caused by the trucks even when they are on the other side of the bridge.

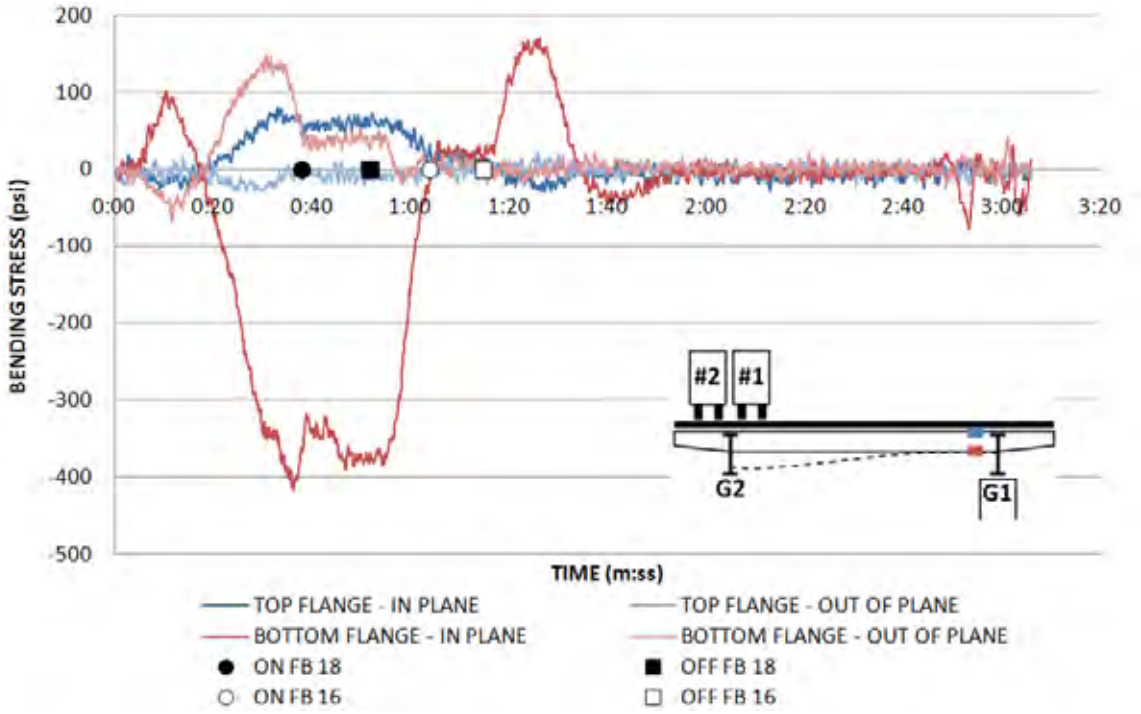

Figure 6.9: In-Plane and Out-of-Plane Stress of the Floor Beam near Girder 1 due to two Trucks on the Left

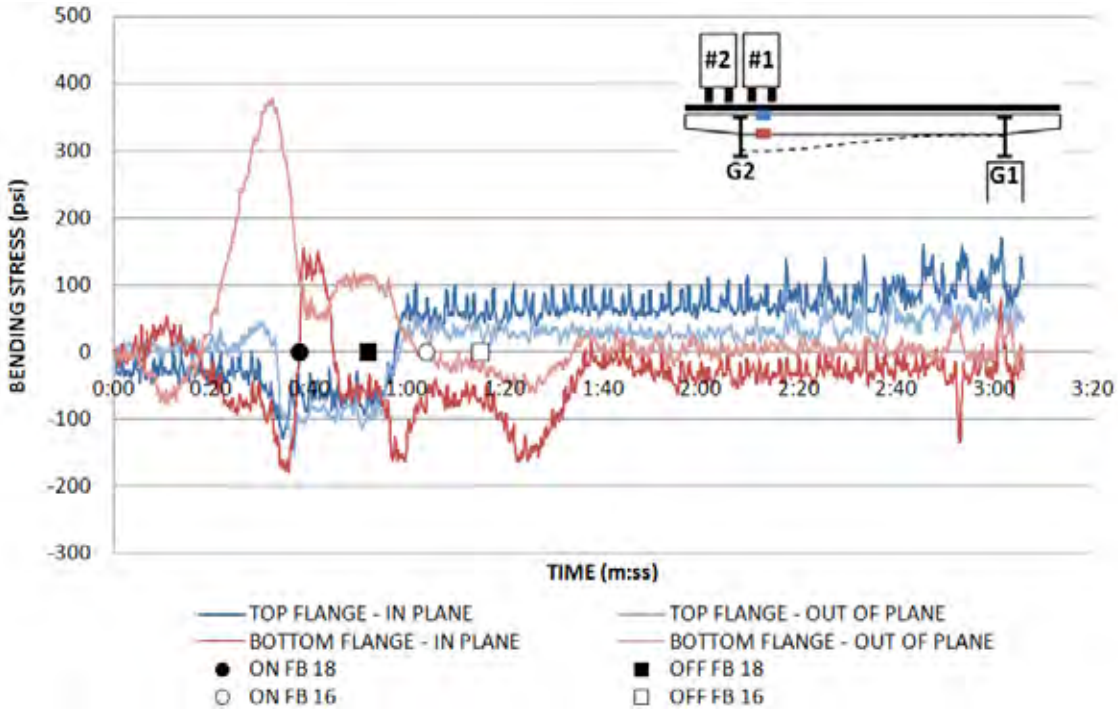

Figure 6.10: In-Plane and Out-of-Plane Stress of the Floor Beam near Girder 2 due to two Trucks on the Left

6.3.3 Bottom Flange Gages

Figure 6.11 shows the in-plane and out-of-plane bending stresses in the web of Girder 1 adjacent to the bottom flange of Floor Beam 18 due to two trucks on the left side of the bridge. Because the girder at this location is supported by a column, it is assumed that the girder would not deflect vertically. This would cause the in-plane bending stresses to be very low. Figure 6.11 confirms this assumption. The figure shows that the in-plane bending stresses on either side of the floor beam flange are, in fact, small compared to the out-of-plane stresses. Before the trucks reach Floor Beam 18, the out-of-plane stresses are negative indicating that the girder is bending outward toward the exterior of the bridge. When the trucks are over the floor beam, the out-of-plane stresses are positive, which indicate that the girder is bending inward toward the center of the bridge. When the trucks are over Floor Beam 16, which is supported by a column on the left side, there is very little in-plane or out-of-plane stresses in the girder. After the trucks leave Floor Beam 16, the girder bends in the opposite direction, toward the exterior of the bridge.

Figure 6.12 shows the in-plane and out-of-plane bending stresses in the web of Girder 2 adjacent to the bottom flange of Floor Beam 18 due to two trucks on the left side of the bridge. Girder 2 is not supported by a column at this location. Therefore, it is expected that the girder would deflect downward under the weight of the trucks. Figure 6.12 shows that the in-plane stresses on both sides of the floor beam are positive when the trucks are over Floor Beam 18, meaning that the bottom half of the girder is in tension. This confirms the assumption that the girder deflects downward, which would create tension in the bottom half of the girder. The out-of-plane stresses are small compared to the in-plane stresses, so there is very little lateral bending when the trucks are over the floor beam. Prior to the trucks reaching Floor Beam 18, the in-plane stresses on either side of the floor beam have different signs. On the north side of the floor beam,

which is the direction from which the trucks approach the floor beam, the tensile stress suggests that the girder is deflecting downward. On the south side of the floor beam, the compressive stress suggests that the girder is deflecting upward. When the trucks are on Floor Beam 16, which is supported by a column on the left side, the stress in the girder near Floor Beam 18 is very small. Once the trucks leave Floor Beam 16, the in-plane stresses are negative suggesting that the girder is deflecting upward. The small out-of-plane stresses are opposite in sign on either side of the floor beam, which means that it is deflecting laterally in different directions.

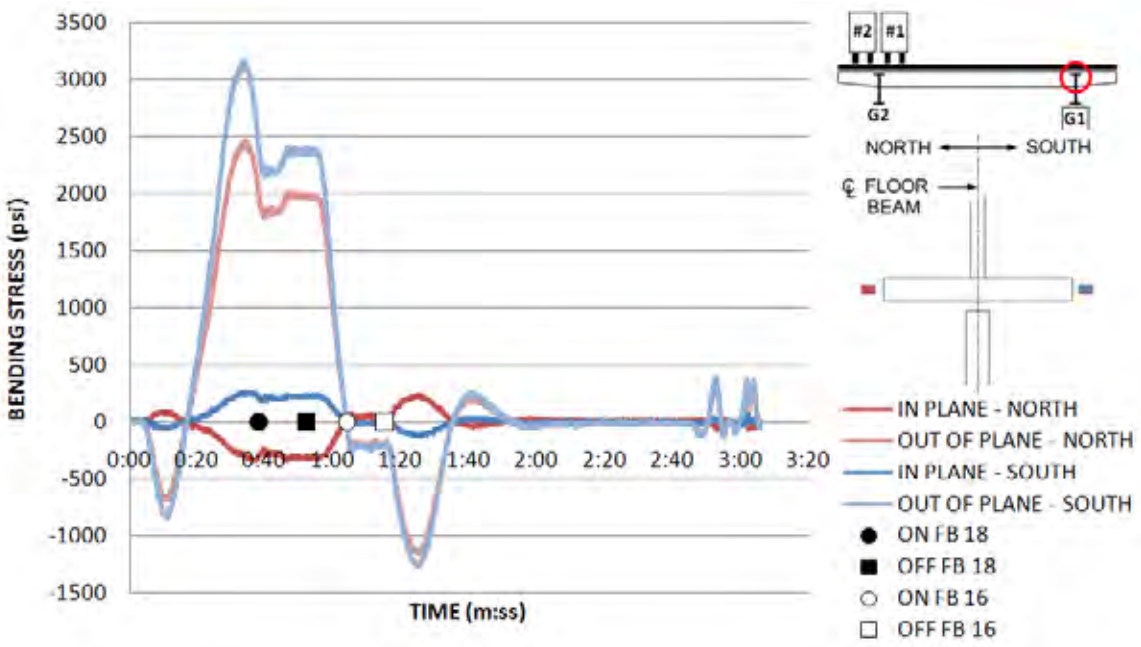

Figure 6.11: In-Plane and Out-of-Plane Bending Stresses of Girder 1 Web due to two Trucks on the Left

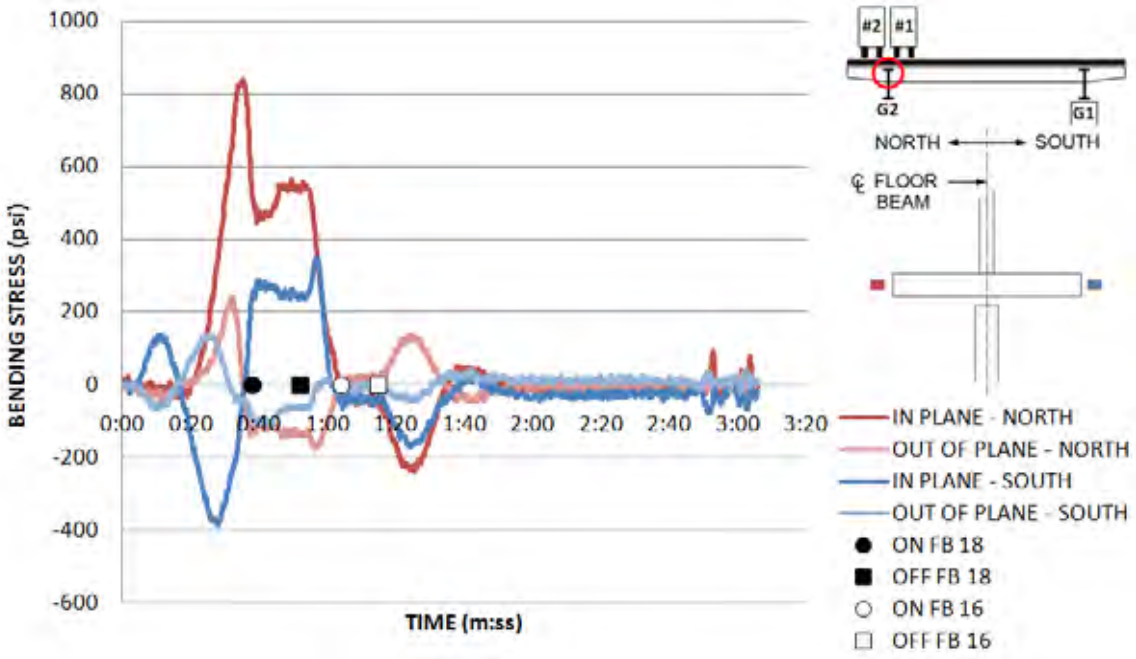

Figure 6.12: In-Plane and Out-of-Plane Bending Stresses of Girder 2 Web due to two Trucks on the Left

6.3.4 Retrofit Stiffener Gages

Figure 6.13 shows the in-plane and out-of-plane bending stress in the retrofit stiffeners on Girder 1 due to two trucks in the left lanes. The figure shows that while the trucks are stationary over the girder, the stiffeners have a large positive in-plane stress, suggesting that they are bending in the plane of the stiffener. The trucks on the left side of the bridge are causing the floor beam-to-column connection on the right side of the bridge to bend out of the plane of the girder as seen in Figure 6.11. This is what is causing the in-plane bending of the stiffeners. When the trucks are over Floor Beam 16, which is supported by a column on the left side, there is very little stress in the stiffeners on Floor Beam 18. Once the trucks leave Floor Beam 16, the stiffeners experience compressive in-plane stress, which indicates they are bending in the opposite direction that they were bending when the trucks were over the floor beam. As the trucks continue to move along the bridge, the stress in the stiffeners goes to zero.

Figure 6.14 shows the in-plane and out-of-plane bending stress in the retrofit stiffeners on Girder 2 due to two trucks in the left lanes. The figure shows that the stiffeners experience a very large out-of-plane bending stress before the trucks reach the floor beam. This suggests that they are bending out of the plane of the stiffener. The reason for this could be due to the movement of the girder, which bends vertically in different directions on either side of the floor beam, as seen in Figure 6.12. When the trucks are over the floor beam, the stiffeners experience only in-plane stresses due to the movement of the floor beam. When the trucks reach Floor Beam 16, the stress in the stiffeners is zero because the trucks are supported by a column at that location. Once the trucks leave Floor Beam 16, the stiffeners experience both in-plane and out-of-plane stress.

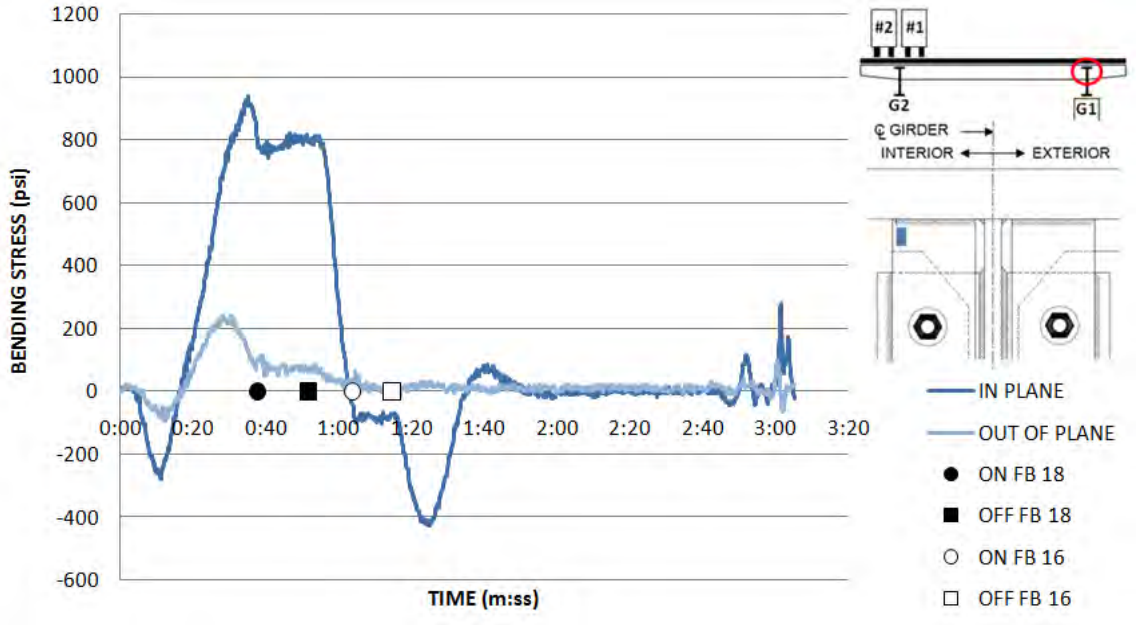

Figure 6.13: Stress in Girder 1 Retrofit Stiffeners due to two Trucks on the Left

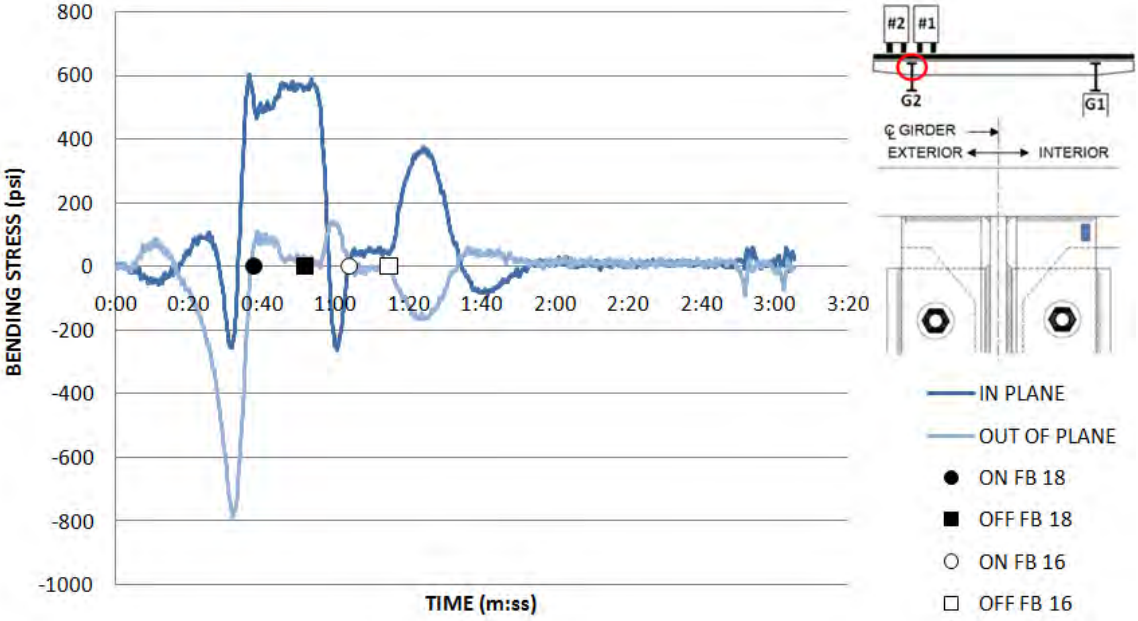

Figure 6.14: Stress in Girder 2 Retrofit Stiffeners due to two Trucks on the Left

6.4 Composite Action of Floor Beams and Slab

In order to determine whether or not the floor beams and slab were acting compositely, the location of the neutral axis of the floor beam was calculated using the method described in Section 3.4. If the slab and floor beam were acting non-compositely, the strain in the top and bottom flange of the floor beam would be equal in magnitude and the neutral axis of the floor beam would be at the centroid, or mid-height, of the section. This can be seen in Figure 3-8(a). If

the slab and floor beam were acting compositely, the strain in the bottom flange would be greater in magnitude than the strain in the top flange, moving the neutral axis above the centroid of the floor beam, as seen in Figure 3-8(b). The neutral axis was calculated at both ends of the floor beam near the connections to the girders as well as in the center of the floor beam. The horizontal axis of the figure was adjusted to show the period of time around when the trucks were stationary over the floor beam. The reason for this is because the strain in the floor beam was practically zero when there were no trucks near the floor beam. Therefore, any small change in the strain during this time would drastically change the location of the neutral axis. This is illustrated by the significant noise at the beginning and end of the following two plots.

Figure 6.15 shows the location of the neutral axis versus time as two trucks move along the right side of the bridge. During this run, the trucks were directly over Girder 1, which is supported by a column at Floor Beam 18. Looking at the right side of the floor beam near the trucks, the figure shows that the neutral axis was calculated to be at the imposed limit of 60 inches from the bottom flange. This suggests that the stress in the bottom flange is much greater than the stress in the top flange. Figure 6.2 shows the stress in the flanges of the floor beam near the right side of the floor beam during this run. It can be seen that both the top and bottom flanges are experiencing tensile stress when the trucks are stationary, with the stress in the bottom flange greater than that in the top flange. Therefore, the neutral axis cannot be located within the floor beam and, therefore, must be in the slab, implying composite action.

In the middle of the floor beam, the neutral axis was calculated to be at about 33 inches from the bottom flange, which is slightly above the centroid. This suggests that there is slight composite action between the floor beam and slab. On the left side of the floor beam, opposite the trucks, the figure shows the neutral axis to be above the centroid of the section except for the time around when the trucks were stationary over the floor beam at which time the neutral axis drops suddenly to the bottom of the section. Figure 6.3 shows the stresses in the top and bottom flanges on the left side of the floor beam. Both the top and bottom flanges are experiencing tensile stresses when the trucks are near the floor beam. The stress in the bottom flange is shown to be greater than that in the top flange except when it suddenly decreases when the trucks are over the floor beam. This is the cause for the sudden jump in the location of the neutral axis in Figure 6.15. The reason for this could be that the stress on the left side of the floor beam is temporarily alleviated when the trucks are directly over the column on the right side. The stress then increases once the trucks leave the column.

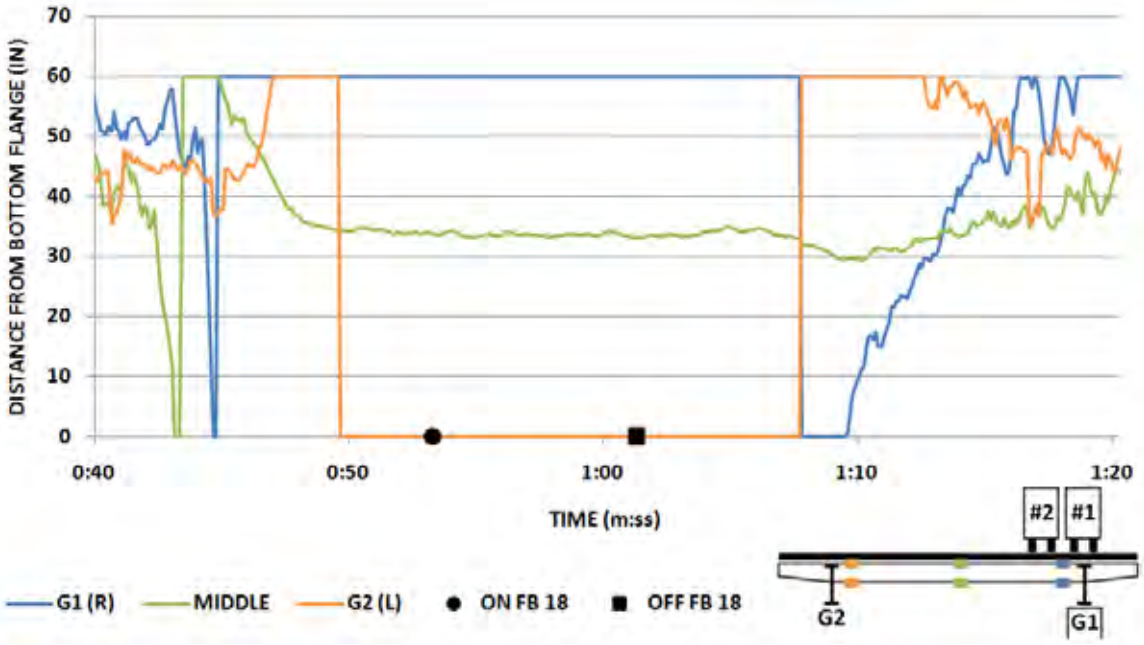

Figure 6.15: Neutral Axis of the Floor Beam versus Time due to Two Trucks on the Right

Figure 6.16 shows the location of the neutral axis versus time as two trucks move along the left side of the bridge. The figure shows that the location of the neutral axis at the middle and left side of the floor beam is somewhat steady when the trucks stop on the floor beam, but then becomes highly variable. Figure 6.10 shows the stress in the left side of the floor beam during this run. It can be seen that the in-plane stress in the bottom flange is positive when the trucks first stop on the floor beam and the stress in the top flange is slightly negative. Then the stress in the bottom flange suddenly becomes negative even though the trucks are stationary. At this point, the stresses in the top and bottom flanges are essentially equal in sign and magnitude, which makes calculating the neutral axis impossible and is the cause of the variability in the plot shown in Figure 6.16. However, prior to this point, the neutral axis was calculated to be above the centroid for each of the three gage locations and, therefore, suggests composite action between the floor beam and slab.

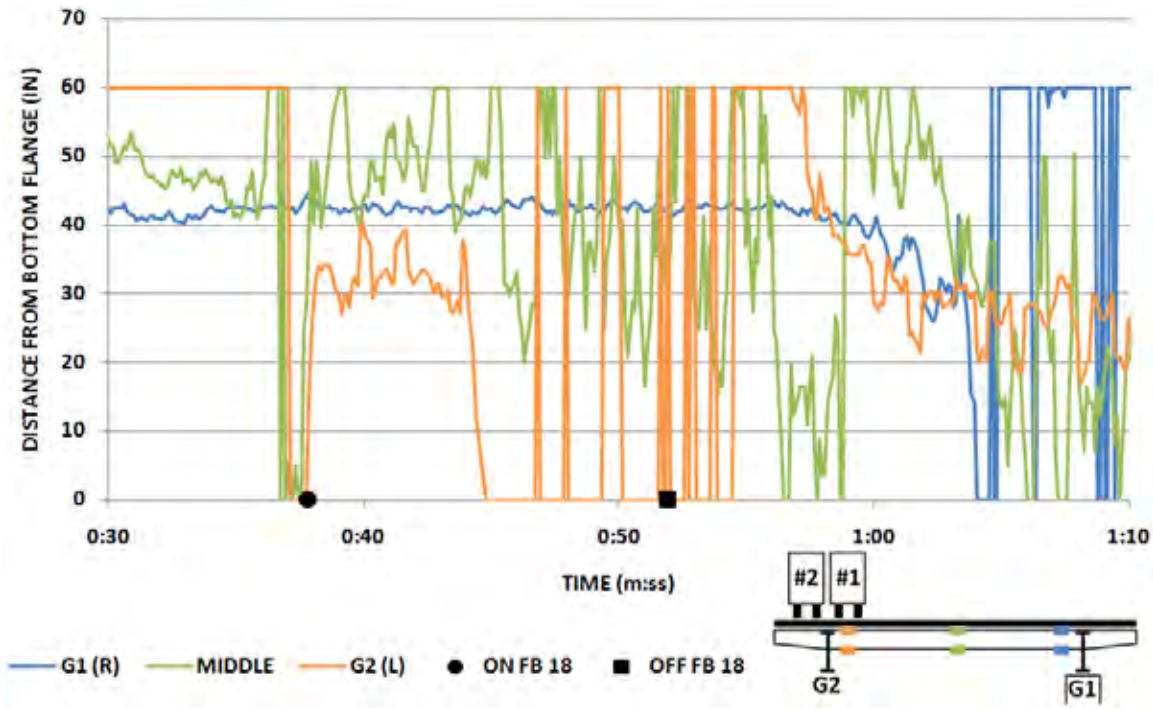

Figure 6.16: Neutral Axis of the Floor Beam versus Time due to Two Trucks on the Left

6.5 Summary

6.5.1 Floor Beams

The right side of Floor Beam 18 is connected to a girder, which is supported by a column while the left side of the floor beam is connected to a girder that is not supported by a column. This creates a situation in which one side of the floor beam is restrained by the support while the other side is fairly free to move. The data shows that the left side of the floor beam deflects both upward and downward depending on the location of the trucks along the bridge. The supported girder on the right side of the floor beam creates a much stiffer connection that attracts stress caused by the trucks. When the trucks are directly over the column, very little stress is transferred to the other side of the floor beam. When the trucks are on the opposite side, the side of the floor beam near the column still experiences higher stresses than the side of the floor beam under the trucks. There is also some lateral bending of this floor beam, which is usually higher when the trucks are away from the floor beam. The asymmetric support layout in this section of the bridge allows the floor beams to deflect in such a way that creates a twisting motion in the bridge.

6.5.2 Girder (Bottom Flange Gages)

The girder was found to bend both in and out of the plane of the web at the location where the bottom flange of the floor beam frames into the girder. The supported girder was restricted from deflecting vertically due to the column. Therefore, the majority of the bending in this girder was out of the plane of the web. The out-of-plane stress was highest in the supported girder when the trucks were on the other side of the bridge. The other girder deflected both in and out of the plane of the web. The in-plane bending was greatest when the trucks were over the

floor beam while the out-of-plane bending was greatest when the trucks were away from the floor beam. The in-plane and out-of-plane bending of girders was found to change directions as the trucks moved along the multiple spans of the bridge.

6.5.3 Retrofit Stiffeners

The retrofit stiffeners were found to bend both in and out of the plane of the stiffener. In-plane bending was most likely caused by rotation of the floor beam-to-column connection due to deflection of the floor beams. Out-of-plane bending of the stiffeners was most likely due to vertical movement of the girder in the plane of the girder web. The highest stresses occurred in the stiffeners attached to the supported girder.

6.5.4 Composite Action of Floor Beams and Slab

The extent of composite action between the slab and floor beam was determined by calculating the neutral axis of the floor beam using the stresses in the top and bottom flanges. It was found that the floor beam and slab generally behaved more compositely near the location of the trucks. It is believed that the weight of trucks creates a frictional force between the floor beams and slab causing the composite action.

Chapter 7. Fatigue Test Results

7.1 Introduction

7.1.1 Fatigue Test

The data acquisition systems were reconfigured after the live load tests for rainflow counting to collect fatigue data. The data acquisition systems were left connected to all the gages on the two floor beams in section F17S and half of the gages on Floor Beam 2 of section F14N for one week. The rainflow counting program tallies the number of times the gages experience strain ranges within specified values. Thus, the resulting data shows a histogram of strain ranges for each strain gage. From these values, the effective stress range and fatigue life can be determined.

7.1.2 Effectiveness Stress Range Calculation

A rainflow counting program counts the number of times a strain gage experiences a strain range within specified values. These strain ranges can then be converted into stress ranges and an effective stress range can be calculated. The effective stress range is a weighted average of all of the stress ranges experienced by the strain gage. Equation 7.1 was used to calculate the effective stress range for each strain gage.

$$S_{R,eff} = \left(\sum_i \frac{n_i}{N} \cdot {S_{R,i}}^3\right)^{\frac{1}{3}} \qquad \text{Equation 7.1}$$

In this equation, $S_{R,eff}$ is the effective stress range, $S_{R,i}$ is an individual stress range, n_i is the number of cycles within the stress range $S_{R,i}$, and N is the total number of cycles recorded over all stress ranges. The effective stress range can then be used to calculate the fatigue life of a structure.

7.1.3 Fatigue Life Calculations

The fatigue life of a structure is based on the effective stress range, number of cycles, and the details of the structure. The American Association of State Highway and Transportation Officials (AASHTO) has determined various categories based on the type of detail being tested. The categories are based on the direction of the stress being measured, the thickness of the member, whether or not there are connecting members, and how those members are connected. The first step in determining the fatigue life of a structure is to determine the number of cycles to failure using Equation 7.2.

$$N = A \cdot {S_{R,eff}}^{-3} \qquad \text{Equation 7.2}$$

In this equation, N is the total number of cycles to failure, A is a constant given by AASHTO based on the structural detail, and $S_{R,eff}$ is the effective stress range calculated above.

Once the number of cycles to failure is determined, this number is compared with the number of cycles recorded by the rainflow counting program over a known period of time to determine the fatigue life in years.

7.1.4 Results Summary Tables

Figures 7.1, 7.2, 7.4 through 7.6, and 7.8 through 7.10 show a summary of values calculated using the fatigue data collected from the three floor beams. Each of the columns in the tables represents a particular strain gage that was placed on the structure. The color of the column heading matches the color of that gage shown in the diagram above the table. For each gage, there are three values tabulated. The first value, $S_{R,eff}$, is the effective stress range calculated as discussed in Section 7.1.2. The second value, $S_{R,max}$, is the maximum stress range recorded by the rainflow counting program for that gage. The last number, N, is the number of cycles recorded. For each gage, these three values were determined for each day the program collected data as well as for the entire week. This was done so that traffic trends could be observed.

7.2 Section F14N Floor Beam 2 Results

7.2.1 Fatigue Test Results

Figures 7.1 and 7.2 show a summary of the effective stress range, maximum stress range, and number of cycles for each of the gages on Floor Beam 2. The first group of gages shown is the web gap gages. The calculations show that the gages at the top of the gap experienced the highest stress ranges. The maximum stress ranges recorded were between 12 and 15 ksi. However, the effective stress range was calculated to be only about 1.5 ksi. This is because there were only a few cycles in the very high stress ranges while the majority of the cycles were in very low stress ranges. The gages on the bottom of the gap recorded lower stress ranges with the maximum recorded around 4.5 ksi and the effective stress range around 0.8 ksi.

The bottom flange gages are summarized next. Three of the four gages recorded very similar numbers. The maximum stress range for these gages was 3.55 ksi and the effective stress range was around 0.73 ksi. The interior gage on the south side of the floor beam recorded slightly higher stresses at 5.58 ksi and 0.93 ksi for the maximum and effective stress ranges, respectively.

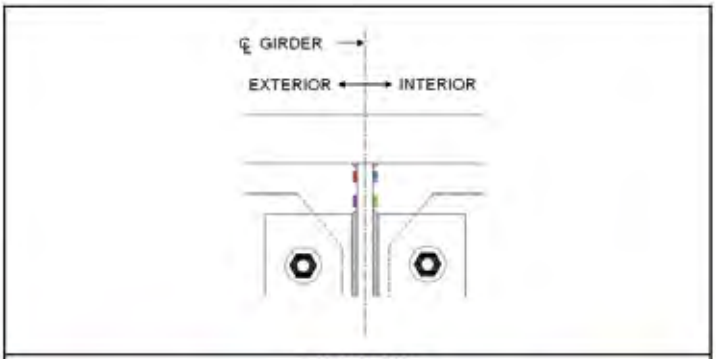

	WEB GAP GAGES											
	TOP						BOTTOM					
	EXTERIOR			INTERIOR			EXTERIOR			INTERIOR		
	$S_{R,eff}$	$S_{R,max}$	N	$S_{R,eff}$	$S_{R,max}$	N	$S_{R,eff}$	$S_{R,max}$	N	$S_{R,eff}$	$S_{R,max}$	N
Wed Jul 9	1.66	12.69	133,714	1.66	12.69	153,167	0.76	3.55	30,074	0.78	3.55	63,221
Thu Jul 10	1.62	12.69	220,104	1.63	14.72	253,187	0.77	3.55	45,277	0.81	4.57	101,972
Fri Jul 11	1.61	11.67	220,811	1.63	11.67	255,101	0.78	3.55	44,389	0.82	4.57	103,039
Sat Jul 12	1.30	10.66	166,901	1.28	10.66	207,799	0.75	2.54	19,910	0.73	3.55	55,440
Sun Jul 13	1.06	9.64	125,465	1.05	10.66	168,601	0.68	2.54	8,755	0.68	3.55	30,786
Mon Jul 14	1.63	12.69	208,096	1.64	12.69	240,718	0.79	3.55	42,089	0.83	4.57	95,983
Tue Jul 15	1.64	12.69	216,917	1.65	12.69	249,861	0.79	4.57	43,734	0.84	4.57	100,161
Wed Jul 16	1.63	12.69	217,835	1.64	12.69	249,422	0.78	3.55	44,179	0.81	4.57	101,325
Thu Jul 17	1.56	11.67	90,804	1.61	12.69	104,010	0.79	3.55	16,698	0.83	3.55	41,459
TOTALS FOR WEEK	1.56	12.69	1,600,647	1.57	14.72	1,881,866	0.78	4.57	295,105	0.81	4.57	693,386

Stress range values in ksi

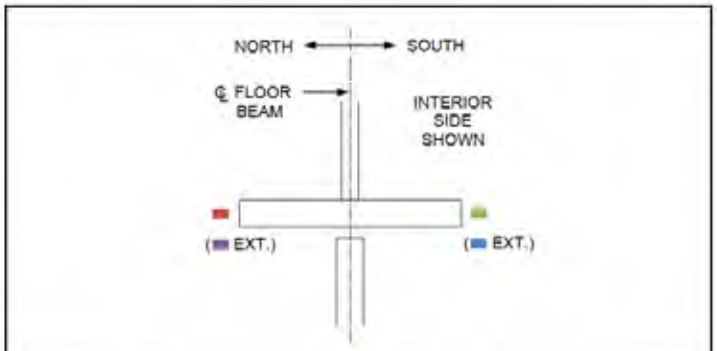

	GIRDER WEB GAGES ADJACENT TO BOTTOM FLANGE OF FLOOR BEAM											
	NORTH						SOUTH					
	EXTERIOR			INTERIOR			EXTERIOR			INTERIOR		
	$S_{R,eff}$	$S_{R,max}$	N	$S_{R,eff}$	$S_{R,max}$	N	$S_{R,eff}$	$S_{R,max}$	N	$S_{R,eff}$	$S_{R,max}$	N
Wed Jul 9	0.75	3.55	43,794	0.73	2.54	20,264	0.73	3.55	40,080	0.96	5.58	57,263
Thu Jul 10	0.75	3.55	67,520	0.74	2.54	31,300	0.73	3.55	60,014	0.95	5.58	86,340
Fri Jul 11	0.75	3.55	67,686	0.73	2.54	30,475	0.72	3.55	59,473	0.94	5.58	85,581
Sat Jul 12	0.67	3.55	34,345	0.70	2.54	13,634	0.68	2.54	28,134	0.84	4.57	46,206
Sun Jul 13	0.65	2.54	18,826	0.67	2.54	6,554	0.64	2.54	14,011	0.76	4.57	25,840
Mon Jul 14	0.74	3.55	63,000	0.74	3.55	29,513	0.73	3.55	56,583	0.95	5.58	81,472
Tue Jul 15	0.75	3.55	65,440	0.74	3.55	31,414	0.73	3.55	59,174	0.96	5.58	83,860
Wed Jul 16	0.75	3.55	66,926	0.74	2.54	31,189	0.73	3.55	59,667	0.95	5.58	85,906
Thu Jul 17	0.73	3.55	26,702	0.72	3.55	12,428	0.72	3.55	22,715	0.92	5.58	33,207
TOTALS FOR WEEK	0.74	3.55	454,239	0.73	3.55	206,771	0.72	3.55	399,851	0.93	5.58	585,675

Stress range values in ksi

Figure 7.1: Stress Range Summary for Gages Near Connection of Floor Beam 2 to Girder 1

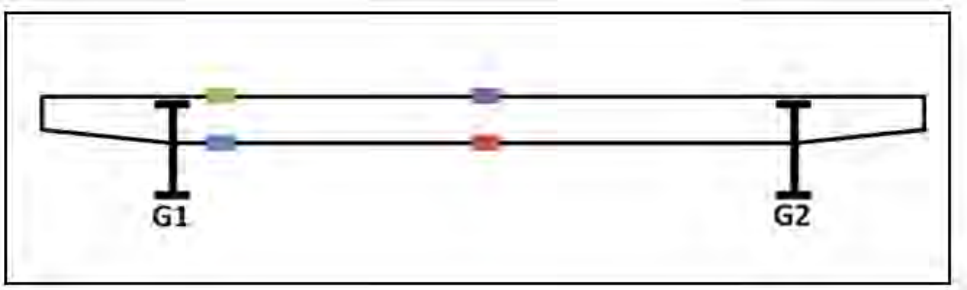

	NEAR GIRDER 1											
	TOP						BOTTOM					
	NORTH			SOUTH			NORTH			SOUTH		
	$S_{R,eff}$	$S_{R,max}$	N	$S_{R,eff}$	$S_{R,max}$	N	$S_{R,eff}$	$S_{R,max}$	N	$S_{R,eff}$	$S_{R,max}$	N
Wed Jul 9	0.57	1.52	461	0.58	1.52	767	0.62	2.54	19,222	0.58	1.52	11,412
Thu Jul 10	0.57	2.54	775	0.58	2.54	1,121	0.62	2.54	28,420	0.58	2.54	17,190
Fri Jul 11	0.59	1.52	715	0.58	1.52	1,033	0.62	2.54	27,740	0.58	1.52	17,032
Sat Jul 12	0.51	0.51	195	0.53	1.52	347	0.60	1.52	11,658	0.56	1.52	6,780
Sun Jul 13	0.51	0.51	52	0.51	0.51	144	0.61	2.54	5,021	0.56	1.52	2,802
Mon Jul 14	0.53	1.52	621	0.53	1.52	973	0.62	2.54	25,937	0.58	1.52	16,118
Tue Jul 15	-	-	-	0.53	1.52	958	0.62	2.54	28,714	0.58	1.52	18,910
Wed Jul 16	-	-	-	0.56	1.52	1,082	0.62	2.54	28,197	0.58	1.52	17,605
Thu Jul 17	-	-	-	0.56	1.52	347	0.62	2.54	11,080	0.58	1.52	6,885
TOTALS FOR WEEK	0.56	2.54	2,819	0.56	2.54	6,772	0.62	2.54	185,989	0.58	2.54	114,734

Stress range values in ksi

	MIDDLE OF FLOOR BEAM											
	TOP						BOTTOM					
	NORTH			SOUTH			NORTH			SOUTH		
	$S_{R,eff}$	$S_{R,max}$	N	$S_{R,eff}$	$S_{R,max}$	N	$S_{R,eff}$	$S_{R,max}$	N	$S_{R,eff}$	$S_{R,max}$	N
Wed Jul 9	0.65	1.52	315	0.66	1.52	225	0.87	5.58	28,968	0.86	4.57	28,430
Thu Jul 10	0.66	2.54	453	0.69	2.54	308	0.87	5.58	46,224	0.86	6.60	45,307
Fri Jul 11	0.71	2.54	437	0.73	2.54	279	0.86	6.60	47,437	0.85	5.58	45,513
Sat Jul 12	0.58	1.52	110	0.63	1.52	56	0.75	3.55	26,743	0.76	4.57	24,786
Sun Jul 13	0.51	0.51	33	0.51	0.51	15	0.69	3.55	17,039	0.69	3.55	15,125
Mon Jul 14	0.53	1.52	366	0.54	1.52	244	0.84	5.58	42,797	0.83	4.57	41,221
Tue Jul 15	0.69	3.55	422	0.75	3.55	238	0.86	7.61	47,546	0.85	7.61	46,062
Wed Jul 16	0.67	2.54	412	0.66	2.54	268	0.87	6.60	45,603	0.86	4.57	44,147
Thu Jul 17	0.69	1.52	152	0.65	1.52	91	0.87	3.55	19,039	0.86	4.57	18,674
TOTALS FOR WEEK	0.66	3.55	2,700	0.68	3.55	1,724	0.85	7.61	321,396	0.84	7.61	309,265

Stress range values in ksi

Figure 7.2: Stress Range Summary for Gages on Floor Beam 2

Figure 7.2 shows the summary of values for the gages that were placed on the flanges of the floor beam. The top flange gage near Girder 1 on the north side of the floor beam became defective after six days of data collection. Therefore, the total values for the week were determined from only those six days. All of the gages near the connection to Girder 1 experienced maximum stress ranges of 2.54 ksi and effective stress ranges around 0.6 ksi. The gages in the middle of the floor beam recorded slightly higher stress ranges with the bottom flange gages experiencing higher stresses than those gages on the top flange. The reason for the increase in stress range in the middle gages is believed to be because these gages are nearer to the right side of the bridge. The large trucks that create the highest stress ranges usually drive on the right side of the road. Therefore, the gages on the right side of the bridge would be expected to record higher stress ranges.

7.2.2 Fatigue Life

The fatigue life for the three details being studied – the floor beam flange, the girder web adjacent to the bottom flange of the floor beam, and the girder web gap – was calculated using the procedure explained in Section 7.1.3. The information recorded by the gage experiencing the maximum effective stress range for each of the three details was used in the calculation. Table 7.1 summarizes the values used in the calculation of the fatigue life as well as the estimated fatigue life in years.

Table 7.2 shows the same calculations as Table 7.1; however these calculations were made ignoring the cycles recorded in the first bin of stress ranges. The first bin includes stress ranges from practically zero to about 1 ksi. Therefore, the number of cycles recorded in this bin could have been inflated by noise experienced by the strain gage. Ignoring the first bin results in a higher effective stress range, but lower number of cycles, and typically increased the fatigue life slightly.

This bridge has been in service for approximately 40 years. With the typical design life of a bridge being about 75 years, this bridge has approximately 35 years of service life left. Examining the data from the two tables shows that fatigue is not a concern for the floor beam flanges, where the fatigue life was estimated to be around 1000 years. The bottom flange gages, on the other hand, have a much smaller fatigue life. Including the first bin, the fatigue life was estimated to be around 16 years, and ignoring the first bin brought this number up to 73 years. Both of these numbers are below the typical design life of the bridge, with the 16 year estimate below the current age of the bridge. This short fatigue life is a result of the high stresses created in the region around the connection of the bottom flange of the floor beam to the girder. Also, this detail is a Category E according to AASHTO, which is a very poor fatigue detail. The web gap gages also show very poor fatigue performance with fatigue life estimates of 12 and 2 years. This was one of only two cases where ignoring the first bin of stress ranges actually decreased the fatigue life. Similar to the bottom flange gages, the short fatigue life is a result of very high stress ranges and a poor fatigue detail.

Table 7.1: Calculation of Estimated Fatigue Life for Floor Beam 2 Including First Bin

Gage Location	Calculated from Test Results			From AASHTO		(Eqn. 7-2)	
	$S_{R,EFF}$ (ksi)	Avg. Cycles per Week	Avg. Cycles per Year	Detail Category	A (ksi^3)	N (cycles)	Est. Life (years)
Floor Beam	0.85	321,396	16,712,592	B	1.20E+10	1.95E+10	1169
Bottom Flange	0.93	585,675	30,455,100	E'	3.90E+08	4.85E+08	16
Web Gap	1.57	1,881,866	97,857,032	C	4.40E+09	1.14E+09	12

Table 7.2: Calculation of Estimated Fatigue Life for Floor Beam 2 Excluding First Bin

Gage Location	Calculated from Test Results			From AASHTO		(Eqn. 7-2)	
	$S_{R,EFF}$ (ksi)	Avg. Cycles per Week	Avg. Cycles per Year	Detail Category	A (ksi^3)	N (cycles)	Est. Life (years)
Floor Beam	2.16	24,171	1,256,892	B	1.20E+10	1.19E+09	947
Bottom Flange	1.56	27,128	1,410,656	E'	3.90E+08	1.03E+08	73
Web Gap	4.51	440,705	22,916,660	C	4.40E+09	4.80E+07	2

7.2.3 Comparison of Fatigue Data to Controlled Live Load Test Data

Figure 7.3 shows the maximum stress ranges recorded for each gage from both the rainflow counting program as well as the four controlled live load tests. It can be seen that the stress ranges from each of the tests are different, but the general trends in the stress ranges for the gages are similar for all of the tests. All of the tests found that the top web gap gages experienced the highest stress ranges.

For the gages located near the left side of the bridge, it would be expected that the highest stress ranges recorded during the live load tests would occur during the test where there were two trucks on the left side of the road. Figure 7.3 confirms this expectation. The two trucks left test is followed by the single truck left, two trucks right, and single truck right tests.

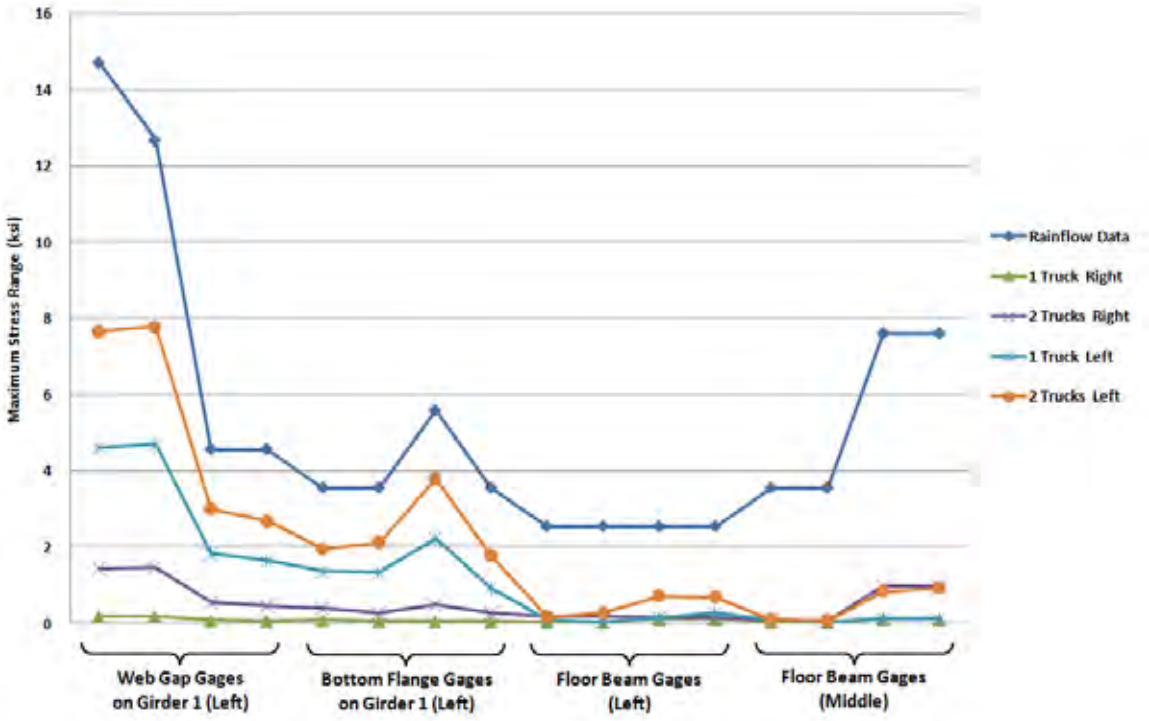

Figure 7.3: Comparison of Rainflow Data to Live Load Test Data for Floor Beam 2

The stress ranges recorded by the rainflow counting program are significantly higher than the stress ranges calculated from the live load tests. It is important to remember that the trucks were moving very slowly during the live load tests and were, in fact, stationary when over the instrumented floor beams. Therefore, the stresses that were recorded during these tests were essentially static stresses. Conversely, during the fatigue test, the traffic was moving at its normal pace. The fast-moving vehicles create a dynamic effect that amplifies the stresses felt by the bridge members.

7.3 Section F17S Floor Beam 16 Results

7.3.1 Fatigue Test Results

Figures 7.4 through 7.6 show a summary of the effective stress range, maximum stress range, and number of cycles for each of the gages on Floor Beam 16. Figure 7.4 shows the gages located at the connection of Floor Beam 16 to Girder 2, which is on the left side of the bridge. There were only two working gages at this connection. The first is the retrofit stiffener gage. This gage recorded a maximum stress range of 6.6 ksi and an effective stress range of 0.97 ksi. If compared to the retrofit stiffeners on Girder 1, which is shown in Figure 7.6, it can be seen that the stiffeners on Girder 2 experienced higher stress ranges. This is due to the fact that Girder 2 is haunched and was shown in Chapter 5 to attract greater stress than Girder 1.

The bottom flange gage on Girder 1 (Figure 7.4) experienced an effective stress range of 0.91ksi. This is higher than the bottom flange gages on Girder 2 (Figure 7.6), whose effective stress ranges average 0.64 ksi. Again, this is due to the haunch of Girder 2 attracting high stresses.

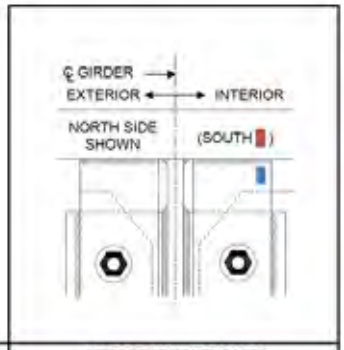

	RETROFIT STIFFENER GAGES			
	INTERIOR			
	NORTH			SOUTH
	$S_{R,eff}$	$S_{R,max}$	N	$S_{R,eff}$ $S_{R,max}$ N
Wed Jul 9	1.01	5.58	42,331	NO DATA
Thu Jul 10	1.00	5.58	62,396	
Fri Jul 11	0.97	6.60	62,831	
Sat Jul 12	0.87	5.58	40,645	
Sun Jul 13	0.85	4.57	29,698	
Mon Jul 14	1.00	5.58	60,848	
Tue Jul 15	1.00	6.60	62,779	
Wed Jul 16	0.94	4.57	9,586	
Thu Jul 17	-	-	-	
TOTALS FOR WEEK	0.97	6.60	371,114	

Stress range values in ksi

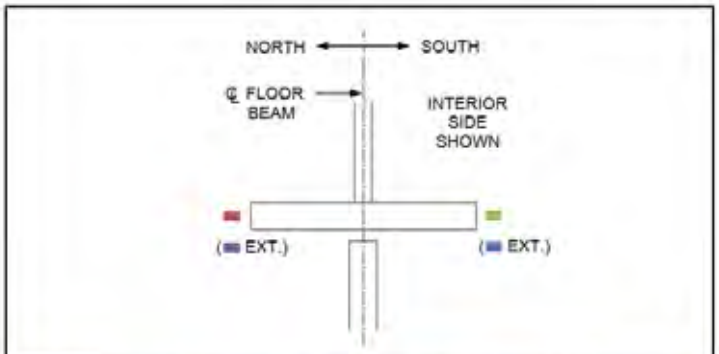

	GIRDER WEB GAGES ADJACENT TO BOTTOM FLANGE OF FLOOR BEAM											
	NORTH						SOUTH					
	EXTERIOR			INTERIOR			EXTERIOR			INTERIOR		
	$S_{R,eff}$	$S_{R,max}$	N	$S_{R,eff}$	$S_{R,max}$	N	$S_{R,eff}$	$S_{R,max}$	N	$S_{R,eff}$	$S_{R,max}$	N
Wed Jul 9	0.93	4.57	45,481	NO DATA			NO DATA			NO DATA		
Thu Jul 10	0.93	4.57	69,442									
Fri Jul 11	0.91	4.57	69,950									
Sat Jul 12	0.83	4.57	44,443									
Sun Jul 13	0.81	3.55	32,689									
Mon Jul 14	0.94	4.57	69,418									
Tue Jul 15	0.94	4.57	69,187									
Wed Jul 16	0.89	4.57	12,396									
Thu Jul 17	-	-	-									
TOTALS FOR WEEK	0.91	4.57	413,006									

Stress range values in ksi

Figure 7.4: Stress Range Summary for Gages Near Connection of Floor Beam 16 to Girder 2

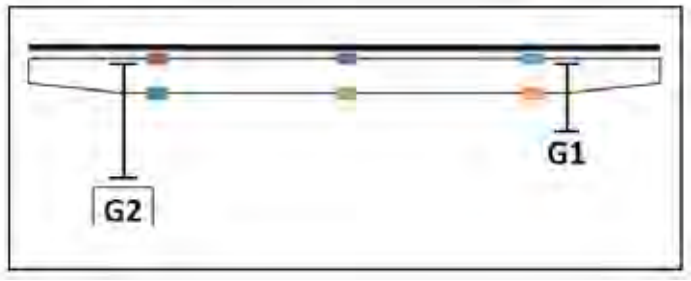

	NEAR GIRDER 2											
	TOP						BOTTOM					
	NORTH			SOUTH			NORTH			SOUTH		
	$S_{R,eff}$	$S_{R,max}$	N	$S_{R,eff}$	$S_{R,max}$	N	$S_{R,eff}$	$S_{R,max}$	N	$S_{R,eff}$	$S_{R,max}$	N
Wed Jul 9	0.55	1.52	846	0.55	1.52	1,255				0.60	2.54	9,374
Thu Jul 10	0.53	1.52	3,338	0.54	2.54	3,476				0.60	2.54	13,519
Fri Jul 11	0.54	1.52	1,863	0.55	1.52	2,224				0.58	2.54	13,073
Sat Jul 12	0.54	1.52	1,328	0.55	1.52	1,411				0.59	2.54	5,520
Sun Jul 13	0.52	1.52	2,270	0.53	1.52	2,163	NO DATA			0.60	1.52	3,226
Mon Jul 14	0.54	1.52	2,525	0.54	1.52	2,870				0.59	2.54	13,039
Tue Jul 15	0.54	1.52	1,775	0.54	1.52	2,188				0.59	2.54	13,344
Wed Jul 16	0.54	1.52	930	0.55	1.52	744				0.59	1.52	1,548
Thu Jul 17	-	-	-	-	-	-				-	-	-
TOTALS FOR WEEK	0.54	1.52	14,875	0.54	2.54	16,331				0.59	2.54	72,643

Stress range values in ksi

	MIDDLE OF FLOOR BEAM											
	TOP						BOTTOM					
	NORTH			SOUTH			NORTH			SOUTH		
	$S_{R,eff}$	$S_{R,max}$	N	$S_{R,eff}$	$S_{R,max}$	N	$S_{R,eff}$	$S_{R,max}$	N	$S_{R,eff}$	$S_{R,max}$	N
Wed Jul 9	0.53	1.52	3,875	0.57	2.54	5,889	0.85	4.57	18,361	0.84	3.55	20,321
Thu Jul 10	0.53	2.54	6,658	0.56	2.54	5,707	0.87	4.57	22,335	0.86	4.57	24,068
Fri Jul 11	0.57	1.52	629	0.62	1.52	849	0.85	3.55	20,088	0.83	3.55	22,792
Sat Jul 12	0.57	1.52	474	0.61	1.52	852	0.79	3.55	12,023	0.78	3.55	13,501
Sun Jul 13	0.55	1.52	457	0.59	1.52	897	0.77	3.55	10,023	0.77	3.55	10,911
Mon Jul 14	0.58	1.52	1,318	0.65	2.54	1,804	0.87	3.55	19,897	0.85	3.55	22,387
Tue Jul 15	0.58	2.54	750	0.63	2.54	945	0.87	3.55	20,112	0.86	4.57	23,006
Wed Jul 16	0.58	1.52	665	0.63	2.54	905	0.87	4.57	19,591	0.85	3.55	22,415
Thu Jul 17	0.56	1.52	223	0.58	1.52	649	0.88	3.55	7,061	0.85	3.55	8,677
TOTALS FOR WEEK	0.55	2.54	15,049	0.59	2.54	18,497	0.85	4.57	149,491	0.84	4.57	168,078

Stress range values in ksi

	NEAR GIRDER 1											
	TOP						BOTTOM					
	NORTH			SOUTH			NORTH			SOUTH		
	$S_{R,eff}$	$S_{R,max}$	N	$S_{R,eff}$	$S_{R,max}$	N	$S_{R,eff}$	$S_{R,max}$	N	$S_{R,eff}$	$S_{R,max}$	N
Wed Jul 9	0.51	0.51	117	0.53	1.52	543	0.56	2.54	14,385	0.55	1.52	5,257
Thu Jul 10	0.52	1.52	572	0.51	1.52	3,101	0.56	3.55	21,309	0.55	2.54	8,820
Fri Jul 11	0.51	0.51	184	0.52	1.52	648	0.55	2.54	19,237	0.55	1.52	6,278
Sat Jul 12	0.51	0.51	15	0.55	1.52	212	0.55	2.54	7,697	0.53	1.52	2,611
Sun Jul 13	0.51	0.51	7	0.51	0.51	164	0.54	1.52	4,760	0.53	1.52	1,737
Mon Jul 14	0.51	0.51	107	0.53	1.52	649	0.55	2.54	18,881	0.55	1.52	6,733
Tue Jul 15	0.54	1.52	114	0.53	1.52	651	0.56	2.54	20,019	0.55	1.52	7,037
Wed Jul 16	0.51	0.51	78	0.52	1.52	489	0.55	2.54	19,315	0.55	2.54	6,678
Thu Jul 17	0.51	0.51	27	0.51	0.51	177	0.57	1.52	6,901	0.58	1.52	2,464
TOTALS FOR WEEK	0.52	1.52	1,221	0.52	1.52	6,634	0.56	3.55	132,504	0.55	2.54	47,615

Stress range values in ksi

Figure 7.5: Stress Range Summary for Gages on Floor Beam 16

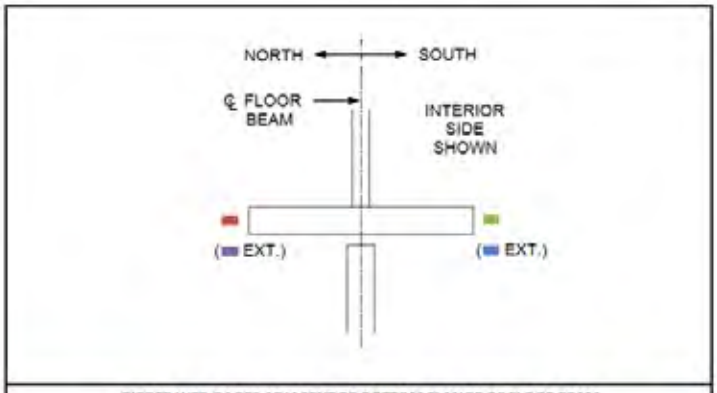

	GIRDER WEB GAGES ADJACENT TO BOTTOM FLANGE OF FLOOR BEAM											
	NORTH						SOUTH					
	INTERIOR			EXTERIOR			INTERIOR			EXTERIOR		
	$S_{R,eff}$	$S_{R,max}$	N	$S_{R,eff}$	$S_{R,max}$	N	$S_{R,eff}$	$S_{R,max}$	N	$S_{R,eff}$	$S_{R,max}$	N
Wed Jul 9	0.74	4.57	28,873	0.52	1.52	3,176	0.51	1.52	1,837	0.83	4.57	27,786
Thu Jul 10	0.73	4.57	42,243	0.51	1.52	4,455	0.51	1.52	2,661	0.82	5.58	41,363
Fri Jul 11	0.71	3.55	42,203	0.51	1.52	4,428	0.51	1.52	2,484	0.79	3.55	40,564
Sat Jul 12	0.69	3.55	20,325	0.51	1.52	1,381	0.51	0.51	648	0.75	5.58	22,842
Sun Jul 13	0.71	3.55	11,451	0.51	0.51	751	0.51	0.51	480	0.76	3.55	14,324
Mon Jul 14	0.73	4.57	38,815	0.52	1.52	3,735	0.51	0.51	2,024	0.82	4.57	39,010
Tue Jul 15	0.73	7.61	41,028	0.52	1.52	4,139	0.51	1.52	2,442	0.83	8.63	40,607
Wed Jul 16	0.73	3.55	40,325	0.52	1.52	3,983	0.51	1.52	2,153	0.81	4.57	40,005
Thu Jul 17	0.74	3.55	13,765	0.51	1.52	1,431	0.51	0.51	769	0.82	3.55	14,649
TOTALS FOR WEEK	0.73	7.61	279,028	0.52	1.52	27,479	0.51	1.52	15,498	0.81	8.63	281,150

Stress range values in ksi

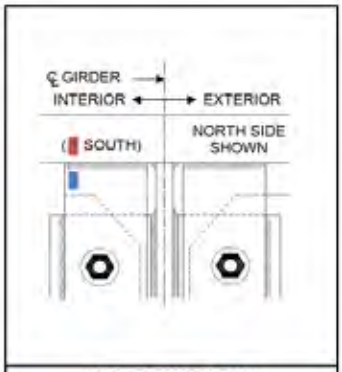

	RETROFIT STIFFENER GAGES					
	INTERIOR					
	NORTH			SOUTH		
	$S_{R,eff}$	$S_{R,max}$	N	$S_{R,eff}$	$S_{R,max}$	N
Wed Jul 9	0.51	1.52	1,626	0.51	0.51	141
Thu Jul 10	0.52	1.52	3,335	0.51	1.52	1,062
Fri Jul 11	0.51	1.52	4,931	0.51	1.52	4,613
Sat Jul 12	0.51	1.52	1,481	0.51	0.51	697
Sun Jul 13	0.51	0.51	671	0.51	0.51	31
Mon Jul 14	0.51	1.52	2,302	0.52	1.52	334
Tue Jul 15	0.51	1.52	2,512	0.51	0.51	376
Wed Jul 16	0.52	1.52	2,548	0.52	1.52	523
Thu Jul 17	0.53	1.52	867	0.51	0.51	99
TOTALS FOR WEEK	0.51	1.52	20,273	0.51	1.52	7,876

Stress range values in ksi

Figure 7.6: Stress Range Summary for Gages Near Connection of Floor Beam 16 to Girder 1

Figure 7.5 shows the summary of values for the gages that were placed on the flanges of the floor beam. In general, these stresses were very low, ranging from 0.52 to 0.85 ksi. The maximum recorded stress range was typically higher for the bottom flange gages than the corresponding top flange gages. These results are consistent with the findings of Chapter 5, which suggest that the floor beam and slab are behaving compositely. The maximum stress ranges were found to be in the middle of the bottom flange of the floor beam.

7.3.2 Fatigue Life

The fatigue life for the three details being studied—the floor beam flange, the girder web adjacent to the bottom flange of the floor beam, and the retrofit stiffener—was calculated using the procedure explained in Section 7.1.3. The information recorded by the gage experiencing the maximum effective stress range for each of the three details was used in the calculation. Table 7.3 summarizes the values used in the calculation of the fatigue life as well as the estimated fatigue life in years. Table 7.4 shows the calculations made ignoring the first bin of stress ranges for the reason described in Section 7.2.2.

The data from the two tables shows that fatigue is not a concern for the floor beam flanges, where the fatigue life was estimated to be above 2000 years. The bottom flange gages, on the other hand, have a much smaller fatigue life. Including the first bin, the fatigue life was estimated to be around 24 years, and ignoring the first bin brought this number up to 29 years. Both of these numbers are below the current age of the bridge. As discussed for Floor Beam 2, this short fatigue life is a result of the high stresses created in this region and the poor fatigue detail. The fatigue of the retrofit stiffeners is shown to be of little concern with the fatigue life estimated to be above 250 years.

Table 7.3: Calculation of Estimated Fatigue Life for Floor Beam 16 Including First Bin

Gage Location	Calculated from Test Results			From AASHTO		(Eqn. 7-2)	
	$S_{R,EFF}$ (ksi)	Avg. Cycles per Week	Avg. Cycles per Year	Detail Category	A (ksi^3)	N (cycles)	Est. Life (years)
Floor Beam	0.84	168,078	8,740,056	B	1.20E+10	2.02E+10	2316
Bottom Flange	0.91	413,006	21,476,312	E'	3.90E+08	5.18E+08	24
Retrofit Stiffener	0.97	371,114	19,297,928	C'	4.40E+09	4.82E+09	250

Table 7.4: Calculation of Estimated Fatigue Life for Floor Beam 16 Excluding First Bin

Gage Location	Calculated from Test Results			From AASHTO		(Eqn. 7-2)	
	$S_{R,EFF}$ (ksi)	Avg. Cycles per Week	Avg. Cycles per Year	Detail Category	A (ksi^3)	N (cycles)	Est. Life (years)
Floor Beam	1.75	14,717	765,284	B	1.20E+10	2.24E+09	2926
Bottom Flange	1.89	38,917	2,023,684	E'	3.90E+08	5.78E+07	29
Retrofit Stiffener	2.03	35,567	1,849,484	C'	4.40E+09	5.26E+08	284

7.3.3 Comparison of Fatigue Data to Controlled Live Load Test Data

Figure 7.7 shows the maximum stress ranges recorded for each gage from both the rainflow counting program as well as the four controlled live load tests. The gages on the horizontal axis are arranged such that the gages on the left side of the bridge are shown on the left side of the plot and gages on the right side of the bridge are shown on the right.

It can be seen that the general trends in the stress ranges for the gages are similar for all of the tests. The largest stress ranges for the live load tests were recorded during the run with two trucks on the right side of the bridge. This is because the girder on the right side of this floor beam was not supported by a column. For each of the tests, the largest stress ranges were experienced by the bottom flange gages and the retrofit stiffener gage on Girder 2.

As discussed for Floor Beam 2, the stress ranges recorded by the rainflow counting program are significantly higher than the stress ranges calculated from the live load tests because of the dynamic effect created by the fast-moving traffic recorded during the fatigue tests.

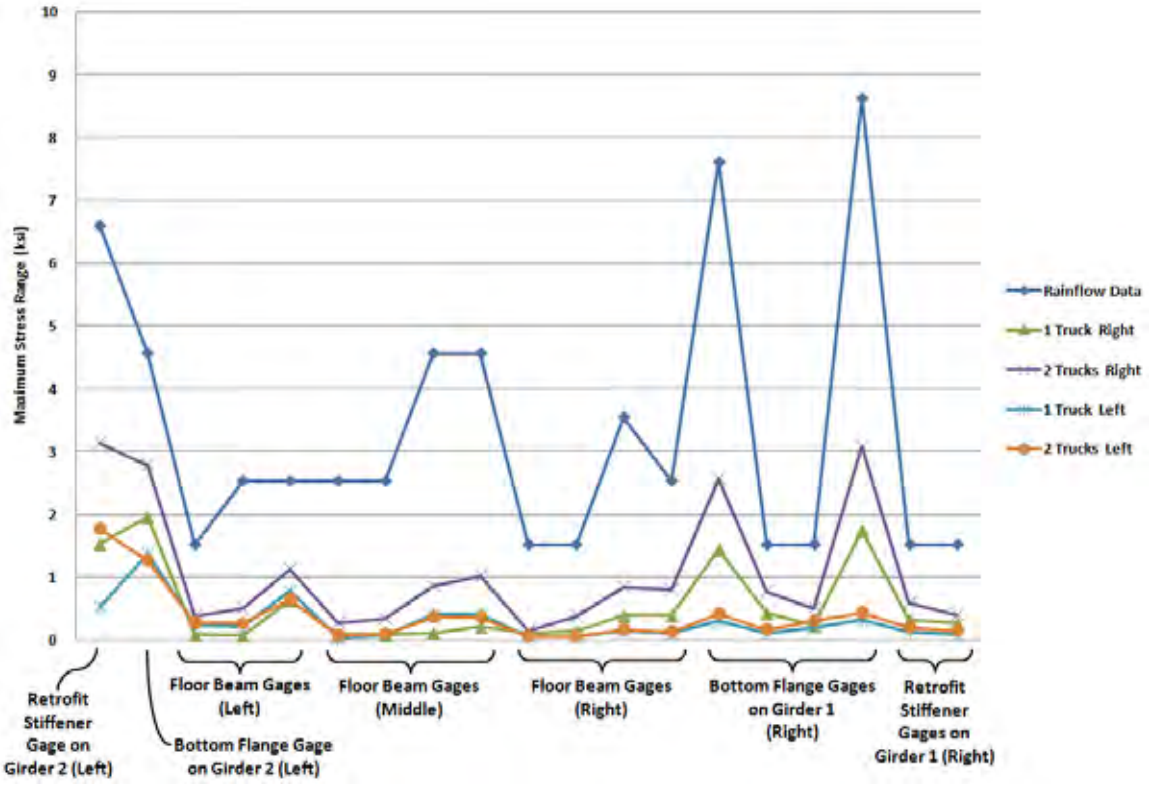

Figure 7.7: Comparison of Rainflow Data to Live Load Test Data for Floor Beam 16

7.4 Section F17S Floor Beam 18 Results

7.4.1 Fatigue Test Results

Figures 7.8 through 7.10 show a summary of the effective stress range, maximum stress range, and number of cycles for each of the gages on Floor Beam 18. Figure 7.8 shows the gages located at the connection of Floor Beam 18 to Girder 2, which is on the left side of the bridge. The first are the retrofit stiffener gages. The maximum stress range recorded by these gages

averaged about 2 ksi and the effective stress range averaged about 0.6 ksi. If compared to the retrofit stiffeners on Girder 1, which is shown in Figure 7.10, it can be seen that the stiffeners on Girder 1 experienced higher stress ranges. The average maximum and effective stress ranges for these gages were about 6.6 ksi and 0.9 ksi, respectively. This is due to the fact that Girder 1 is supported by a column and able to attract greater stress than Girder 2.

The bottom flange gages on Girder 2, shown in Figure 7.8, experienced average maximum and effective stress ranges of about 2.3 ksi and 0.58 ksi, respectively. These values are less than those on Girder 1, shown in Figure 7.10, whose values averaged 7.1 ksi and 1.1 ksi. Again, this is due to the fact that Girder 1 is supported by a column and is able to attract greater stresses.

Figure 7.9 shows the summary of values for the gages that were placed on the flanges of the floor beam. In general, these stresses were very low, ranging from 0.53 to 0.87 ksi. The maximum recorded stress range was typically higher for the bottom flange gages than the corresponding top flange gages. These results are consistent with the findings of Chapter 6, which suggest that the floor beam and slab are behaving compositely. The maximum stress ranges were found to be in the middle of the bottom flange of the floor beam.

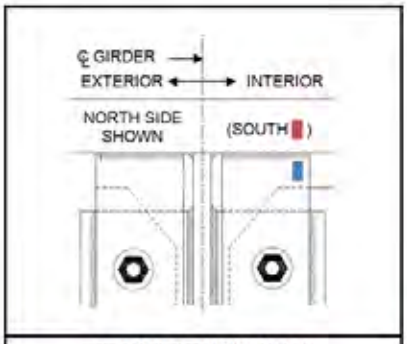

	RETROFIT STIFFENER GAGES					
	INTERIOR					
	NORTH			SOUTH		
	$S_{R,eff}$	$S_{R,max}$	N	$S_{R,eff}$	$S_{R,max}$	N
Wed Jul 9	0.68	2.54	4,767	0.55	1.52	8,036
Thu Jul 10	0.68	2.54	7,089	0.56	1.52	12,157
Fri Jul 11	0.67	1.52	6,572	0.54	1.52	11,015
Sat Jul 12	0.64	1.52	2,556	0.53	1.52	4,278
Sun Jul 13	0.60	1.52	1,964	0.53	1.52	2,632
Mon Jul 14	0.69	1.52	6,207	0.55	1.52	10,442
Tue Jul 15	0.67	2.54	6,747	0.55	1.52	11,235
Wed Jul 16	0.70	1.52	2,615	0.56	1.52	4,811
Thu Jul 17	-	-	-	-	-	-
TOTALS FOR WEEK	0.67	2.54	38,517	0.55	1.52	64,606

Stress range values in ksi

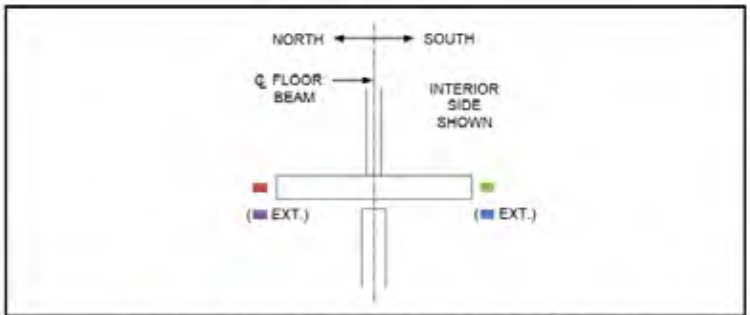

	GIRDER WEB GAGES ADJACENT TO BOTTOM FLANGE OF FLOOR BEAM											
	NORTH						SOUTH					
	EXTERIOR			INTERIOR			EXTERIOR			INTERIOR		
	$S_{R,eff}$	$S_{R,max}$	N	$S_{R,eff}$	$S_{R,max}$	N	$S_{R,eff}$	$S_{R,max}$	N	$S_{R,eff}$	$S_{R,max}$	N
Wed Jul 9	0.58	1.52	6,900	0.66	1.52	3,784	0.53	1.52	2,348	0.56	1.52	3,954
Thu Jul 10	0.59	2.54	10,506	0.68	1.52	5,547	0.53	1.52	3,463	0.56	1.52	5,655
Fri Jul 11	0.58	2.54	8,866	0.64	1.52	5,138	0.52	1.52	3,028	0.55	1.52	4,998
Sat Jul 12	0.56	2.54	3,989	0.63	1.52	2,111	0.53	1.52	1,078	0.55	1.52	1,980
Sun Jul 13	0.55	1.52	2,870	0.60	1.52	1,382	0.54	1.52	944	0.53	1.52	1,444
Mon Jul 14	0.58	2.54	8,966	0.66	1.52	5,135	0.53	1.52	2,956	0.55	1.52	5,143
Tue Jul 15	0.58	2.54	9,352	0.66	2.54	5,333	0.53	2.54	3,201	0.55	1.52	5,439
Wed Jul 16	0.58	2.54	4,467	0.66	1.52	2,397	0.53	1.52	1,391	0.55	1.52	2,379
Thu Jul 17	-	-	-	-	-	-	-	-	-	-	-	-
TOTALS FOR WEEK	0.58	2.54	55,916	0.66	2.54	30,827	0.53	2.54	18,409	0.55	1.52	30,992

Stress range values in ksi

Figure 7.8: Stress Range Summary for Gages Near Connection of Floor Beam 18 to Girder 2

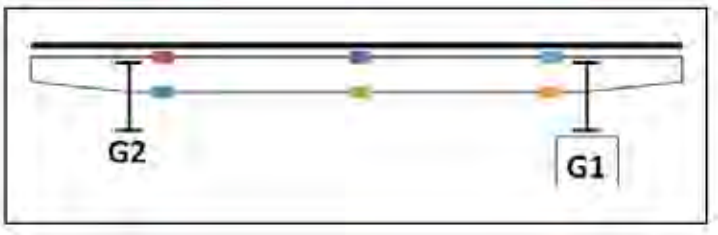

	NEAR GIRDER 2											
	TOP						BOTTOM					
	NORTH			SOUTH			NORTH			SOUTH		
	$S_{R,eff}$	$S_{R,max}$	N	$S_{R,eff}$	$S_{R,max}$	N	$S_{R,eff}$	$S_{R,max}$	N	$S_{R,eff}$	$S_{R,max}$	N
Wed Jul 9	0.54	1.52	1,458	0.54	1.52	1,088	0.72	3.55	7,899	0.65	3.55	11,633
Thu Jul 10	0.55	1.52	1,828	0.55	1.52	1,485	0.72	3.55	10,972	0.65	3.55	15,922
Fri Jul 11	0.54	1.52	1,627	0.53	1.52	1,191	0.70	3.55	11,018	0.63	2.54	14,990
Sat Jul 12	0.54	1.52	1,727	0.53	1.52	702	0.66	2.54	5,653	0.62	2.54	6,694
Sun Jul 13	0.53	1.52	1,279	0.53	1.52	465	0.65	2.54	4,179	0.60	2.54	4,611
Mon Jul 14	0.54	1.52	1,655	0.55	1.52	1,160	0.71	2.54	10,507	0.64	2.54	14,835
Tue Jul 15	0.55	1.52	1,737	0.55	1.52	1,260	0.71	2.54	11,658	0.64	2.54	15,633
Wed Jul 16	0.55	1.52	1,083	0.53	1.52	549	0.73	3.55	4,907	0.65	3.55	6,897
Thu Jul 17	-	-	-	-	-	-	-	-	-	-	-	-
TOTALS FOR WEEK	0.54	1.52	12,394	0.54	1.52	7,900	0.70	3.55	66,793	0.64	3.55	91,215

Stress range values in ksi

	MIDDLE OF FLOOR BEAM											
	TOP						BOTTOM					
	NORTH			SOUTH			NORTH			SOUTH		
	$S_{R,eff}$	$S_{R,max}$	N	$S_{R,eff}$	$S_{R,max}$	N	$S_{R,eff}$	$S_{R,max}$	N	$S_{R,eff}$	$S_{R,max}$	N
Wed Jul 9	0.58	2.54	2,682	0.70	2.54	1,070	0.89	3.55	22,712			
Thu Jul 10	0.56	2.54	7,427	0.62	2.54	5,914	0.89	5.58	34,212			
Fri Jul 11	0.55	2.54	5,819	0.73	2.54	1,361	0.85	4.57	33,055			
Sat Jul 12	0.56	1.52	420	0.66	1.52	501	0.80	3.55	18,369			
Sun Jul 13	0.54	1.52	707	0.56	1.52	674	0.78	3.55	14,840	NO DATA		
Mon Jul 14	0.63	2.54	1,684	0.72	2.54	1,371	0.88	3.55	30,140			
Tue Jul 15	0.65	2.54	1,163	0.72	2.54	1,279	0.90	5.58	30,712			
Wed Jul 16	0.65	2.54	1,087	0.72	2.54	1,191	0.89	4.57	29,936			
Thu Jul 17	0.58	1.52	435	0.67	1.52	506	0.92	3.55	11,559			
TOTALS FOR WEEK	0.58	2.54	21,424	0.67	2.54	13,867	0.87	5.58	225,535			

Stress range values in ksi

	NEAR GIRDER 1											
	TOP						BOTTOM					
	NORTH			SOUTH			NORTH			SOUTH		
	$S_{R,eff}$	$S_{R,max}$	N	$S_{R,eff}$	$S_{R,max}$	N	$S_{R,eff}$	$S_{R,max}$	N	$S_{R,eff}$	$S_{R,max}$	N
Wed Jul 9	0.54	1.52	1,238	0.54	1.52	1,840	0.53	1.52	9,354	0.54	1.52	10,132
Thu Jul 10	0.53	1.52	1,702	0.54	1.52	1,616	0.53	2.54	11,241	0.54	2.54	13,855
Fri Jul 11	0.52	1.52	1,039	0.54	1.52	1,018	0.53	1.52	10,232	0.54	1.52	11,521
Sat Jul 12	0.51	0.51	471	0.52	1.52	446	0.52	1.52	3,735	0.53	1.52	3,984
Sun Jul 13	0.52	1.52	718	0.52	1.52	736	0.52	1.52	3,384	0.53	1.52	3,220
Mon Jul 14	0.53	1.52	1,111	0.55	1.52	1,099	0.53	1.52	9,926	0.54	1.52	10,136
Tue Jul 15	0.54	1.52	1,181	0.54	1.52	1,142	0.53	1.52	10,771	0.55	2.54	10,973
Wed Jul 16	0.52	1.52	1,110	0.54	1.52	1,030	0.53	1.52	9,678	0.54	2.54	10,239
Thu Jul 17	0.53	1.52	472	0.54	1.52	447	0.53	1.52	4,348	0.56	1.52	4,351
TOTALS FOR WEEK	0.53	1.52	9,042	0.54	1.52	9,374	0.53	2.54	72,669	0.54	2.54	78,411

Stress range values in ksi

Figure 7.9: Stress Range Summary for Gages on Floor Beam 18

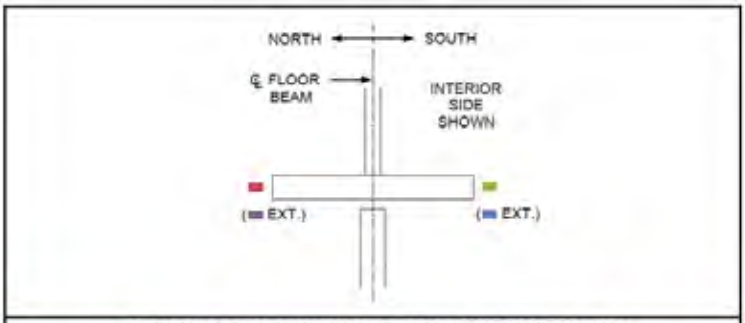

	GIRDER WEB GAGES ADJACENT TO BOTTOM FLANGE OF FLOOR BEAM											
	NORTH						SOUTH					
	INTERIOR			EXTERIOR			INTERIOR			EXTERIOR		
	$S_{R,eff}$	$S_{R,max}$	N	$S_{R,eff}$	$S_{R,max}$	N	$S_{R,eff}$	$S_{R,max}$	N	$S_{R,eff}$	$S_{R,max}$	N
Wed Jul 9	1.09	5.58	31,216	1.15	6.60	41,438	1.27	7.61	51,360	1.19	5.58	34,502
Thu Jul 10	1.09	6.60	44,919	1.15	6.60	59,613	1.27	8.63	74,533	1.20	6.60	49,251
Fri Jul 11	1.04	5.58	43,764	1.08	6.60	58,052	1.19	8.63	73,831	1.13	6.60	47,361
Sat Jul 12	0.93	5.58	26,958	0.97	5.58	34,742	1.06	6.60	46,068	1.01	4.57	28,716
Sun Jul 13	0.94	4.57	19,655	0.97	6.60	24,533	1.05	5.58	33,446	1.02	6.60	20,303
Mon Jul 14	1.06	5.58	42,558	1.11	6.60	55,197	1.23	7.61	69,908	1.16	5.58	44,591
Tue Jul 15	1.07	5.58	43,229	1.12	6.60	57,218	1.24	7.61	73,019	1.17	6.60	45,827
Wed Jul 16	1.08	5.58	41,572	1.13	6.60	54,295	1.25	8.63	70,674	1.17	5.58	43,804
Thu Jul 17	1.08	4.57	17,261	1.11	6.60	22,865	1.23	7.61	30,246	1.16	6.60	18,055
TOTALS FOR WEEK	1.05	6.60	311,132	1.10	6.60	407,953	1.22	8.63	523,085	1.15	6.60	332,410

Stress range values in ksi

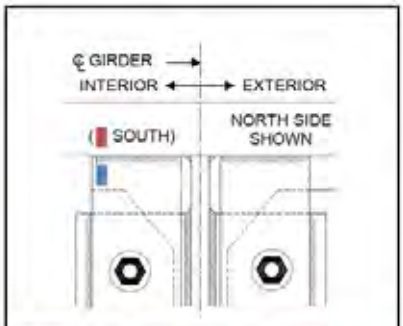

	RETROFIT STIFFENER GAGES					
	INTERIOR					
	NORTH			SOUTH		
	$S_{R,eff}$	$S_{R,max}$	N	$S_{R,eff}$	$S_{R,max}$	N
Wed Jul 9	0.93	4.57	21,189	0.88	4.57	30,120
Thu Jul 10	0.94	6.60	29,533	0.88	6.60	41,228
Fri Jul 11	0.90	4.57	28,821	0.85	4.57	38,290
Sat Jul 12	0.83	4.57	18,276	0.79	5.58	24,296
Sun Jul 13	0.83	3.55	13,267	0.78	3.55	17,628
Mon Jul 14	0.93	4.57	27,714	0.87	4.57	37,102
Tue Jul 15	0.94	4.57	28,450	0.88	5.58	38,514
Wed Jul 16	0.94	4.57	27,670	0.88	5.58	37,524
Thu Jul 17	0.97	4.57	10,925	0.90	4.57	15,926
TOTALS FOR WEEK	0.92	6.60	205,845	0.86	6.60	280,628

Stress range values in ksi

Figure 7.10: Stress Range Summary for Gages Near Connection of Floor Beam 18 to Girder 1

7.4.2 Fatigue Life

The fatigue life for the three details being studied—the floor beam flange, the girder web adjacent to the bottom flange of the floor beam, and the retrofit stiffener—was calculated using the procedure explained in Section 7.1.3. The information recorded by the gage experiencing the maximum effective stress range for each of the three details was used in the calculation. Table 7.5 summarizes the values used in the calculation of the fatigue life as well as the estimated fatigue life in years. Table 7.6 shows the calculations made ignoring the first bin of stress ranges for the reason described in Section 7.2.2.

The data from the two tables shows that fatigue is not a concern for the floor beam flanges, where the fatigue life was estimated to be above 1500 years. The bottom flange gages, on the other hand, have a much smaller fatigue life. Including the first bin, the fatigue life was estimated to be around 8 years, and ignoring the first bin brought this number up to 9 years. Both of these numbers are below the current age of the bridge. This was the other case in which ignoring the first bin of stress ranges actually lowered the fatigue life. As discussed for the two floor beams above, this short fatigue life is a result of the high stresses created in this region and the poor fatigue detail. The fatigue of the retrofit stiffeners is shown to be of little concern with the fatigue life estimated to be above 500 years.

Table 7.5: Calculation of Estimated Fatigue Life for Floor Beam 18 Including First Bin

Gage Location	Calculated from Test Results			From AASHTO		(Eqn. 7-2)	
	$S_{R,EFF}$ (ksi)	Avg. Cycles per Week	Avg. Cycles per Year	Detail Category	A (ksi^3)	N (cycles)	Est. Life (years)
Floor Beam	0.87	225,535	11,727,820	B	1.20E+10	1.82E+10	1554
Bottom Flange	1.22	523,085	27,200,420	E'	3.90E+08	2.15E+08	8
Retrofit Stiffener	0.92	205,845	10,703,940	C'	4.40E+09	5.65E+09	528

Table 7.6: Calculation of Estimated Fatigue Life for Floor Beam 18 Excluding First Bin

Gage Location	Calculated from Test Results			From AASHTO		(Eqn. 7-2)	
	$S_{R,EFF}$ (ksi)	Avg. Cycles per Week	Avg. Cycles per Year	Detail Category	A (ksi^3)	N (cycles)	Est. Life (years)
Floor Beam	1.89	18,231	948,012	B	1.20E+10	1.78E+09	1875
Bottom Flange	2.46	59,045	3,070,340	E'	3.90E+08	2.62E+07	9
Retrofit Stiffener	1.83	23,860	1,240,720	C'	4.40E+09	7.18E+08	579

7.4.3 Comparison of Fatigue Data to Controlled Live Load Test Data

Figure 7.11 shows the maximum stress ranges recorded for each gage from both the rainflow counting program as well as the four controlled live load tests. The gages on the horizontal axis are arranged such that the gages on the left side of the bridge are shown on the left side of the plot and gages on the right side of the bridge are shown on the right. It can be seen that the general trends in the stress ranges for the gages are similar for all of the tests. The largest stress ranges for the controlled live load tests were generally recorded during the run with

two trucks on the left side of the bridge. This is because the girder on the left side of the floor beam was not supported by a column. The plots show that the largest stress ranges were generally experienced by the bottom flange gages on Girder 1, which is the supported girder.

As discussed for the two floor beams above, the stress ranges recorded by the rainflow counting program are significantly higher than the stress ranges calculated from the live load tests because of the dynamic effect created by the fast-moving traffic recorded during the fatigue tests.

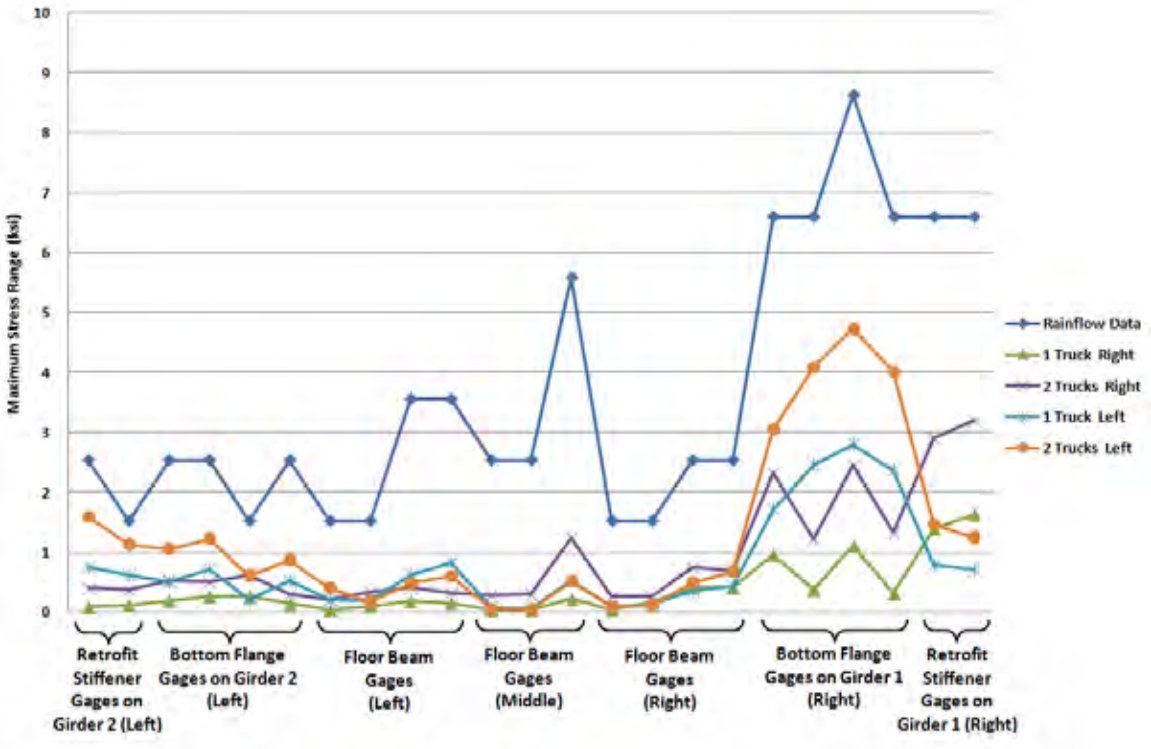

Figure 7.11: Comparison of Rainflow Data to Live Load Test Data for Floor Beam 18

7.5 Summary

In summary, the floor beams and retrofit stiffeners are of little concern with regard to fatigue. These details are experiencing relatively low stress ranges and perform fairly well under fatigue loading. The girder web details, including the small gap above the web of the connecting floor beam and adjacent to the bottom flange of the connecting floor beam, are details that perform very poorly under fatigue loading. These details are experiencing very high stress ranges that result in very short fatigue lives.

Chapter 8. Finite Element Model Results for Section F14N

8.1 Introduction

After completing the field testing, a finite element model of Section F14N was created. The purpose of the model was to provide a comparison to the field test results. The model was also used to test the effectiveness of one of the retrofit ideas for this section. This chapter will explain the details of the finite element model as well as compare the model results with the field test data. The effectiveness of the retrofit plan will also be discussed by comparing the model results before and after the retrofit.

8.2 Finite Element Model Details

The model was created using the finite element software Abaqus. First, a full model of the bridge (shown in Figure 8.1 without the slab) was created that included the concrete slab, girders with bearing stiffeners, and floor beams with transverse stiffeners. Longitudinal and transverse stiffeners were included in the girders near the connections of interest. Quadratic shell elements with reduced integration were used in the analysis of the model. The support conditions were imposed on the area between the bearing stiffeners at the bottom flanges of the girders. The supports along girder 1 were free to move in the longitudinal direction only except for the support at floor beam 4, which was restrained in all directions. The supports along girder 2 were all free to move in both the longitudinal and transverse directions.

As discussed in the previous sections, the field test results show that the slab and floor beams are most likely acting compositely due to a friction force between the slab and floor beams caused by a normal force on the interface from the traffic loads. Therefore, composite and non-composite models were created. The composite model used ties to connect the slab and floor beam elements together along the full length of the floor beam. In the non-composite model, the slab was not connected to any point along the first eleven floor beams and friction between the slab and those floor beams was set to zero. The slab was tied to the top flange of floor beam 12 so that rigid body motion of the slab is prevented during analysis. As floor beam 2, the floor beam of interest, is at the other end of the section, it is believed that these ties would not influence the result significantly. There was also a partially composite model created that differed from the non-composite model only in that the friction coefficient between the slab and floor beams was set to 0.5 rather than zero.

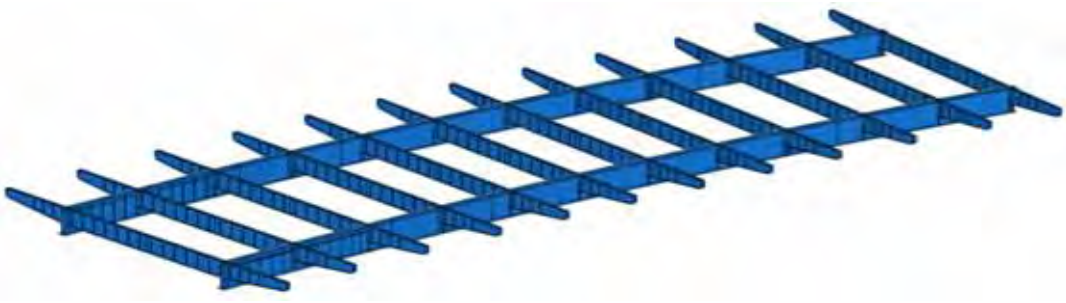

Figure 8.1: Full Finite Element Model of Section F14N

The model also tested various concrete strengths for the slab as the actual strength is unknown. The model used concrete strengths of 4000, 6000 and 8000 psi. Preliminary results showed little difference in the stress values near the connections of floor beam 2 to the girders for the different concrete strengths. As a result, 4000 psi concrete was used in the final model.

To better understand the behavior at the connection of the floor beams to the girders, a sub model was created that uses the displacement field generated in the full model to derive its boundary conditions. The sub model, shown in Figure 8.2, focuses on the connection of floor beam 2 to the two girders. The sub model included connection stiffener details and allowed for a finer mesh to be defined at the connections so that the behavior could be more accurately recorded. A closer view of the connection can be seen in Figure 8.3, showing the connection stiffener. Two 3/8" thick connection stiffeners connecting the front and back of the floor beam web were modeled as one connection stiffener with the thickness of ¾ in. This was done to avoid difficulties associated with including narrow gap between the connections stiffeners in the sub model. The edges of the connection stiffeners were tied to the floor beam web and the girder web along the welds to represent the welds that connect the stiffeners to the floor beam web and the girder web.

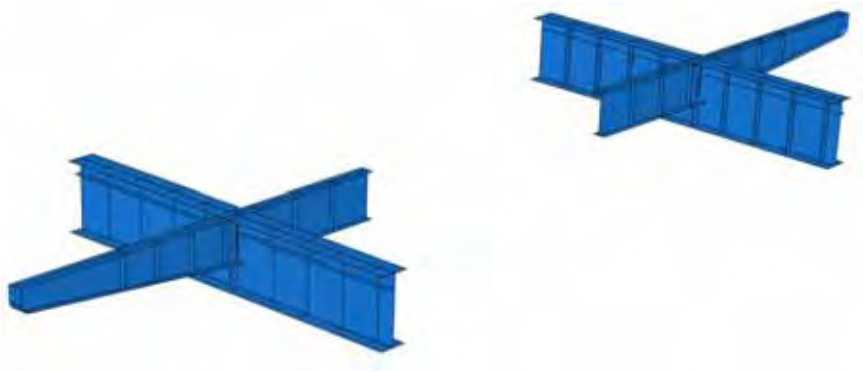

Figure 8.2: Sub Model Showing Connection of Floor Beam 2 to Girders 1 and 2

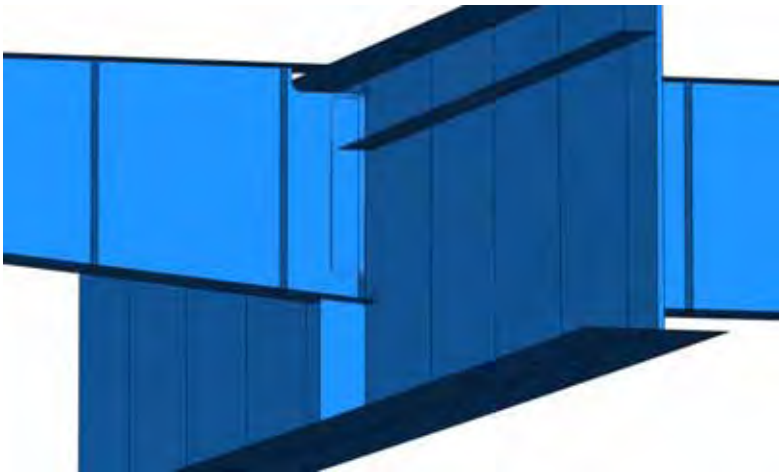

Figure 8.3: View of Connection of Floor Beam 2 to Girder 2

The sub model also incorporates one of the retrofit ideas that have been developed for this bridge. A detail of the retrofit can be seen in Figure 8.4. The retrofit consists of connecting the web of the floor beam and the top flange of the girder using angles. The angles are connected to the floor beam web using 7/8 inch A325 bolts and to the girder flange using 7/8 inch welded threaded studs. The detail shows that these angles would be installed adjacent to the existing retrofit stiffeners that were part of an earlier retrofit of the bridge. As was discussed in Chapter 1, there have been new cracks that have formed at the welds connecting the retrofit stiffener to the top flange of the girder and to the existing connection stiffener. Therefore, when the retrofit angles were incorporated into the finite element sub model, the retrofit stiffeners were not included. This assumes that the retrofit stiffeners have cracked and are no longer effective. Figure 8.5 shows the retrofit angles in the sub model. These angles are tied to the floor beam web and girder top flange at the locations were bolts and studs were specified in the details.

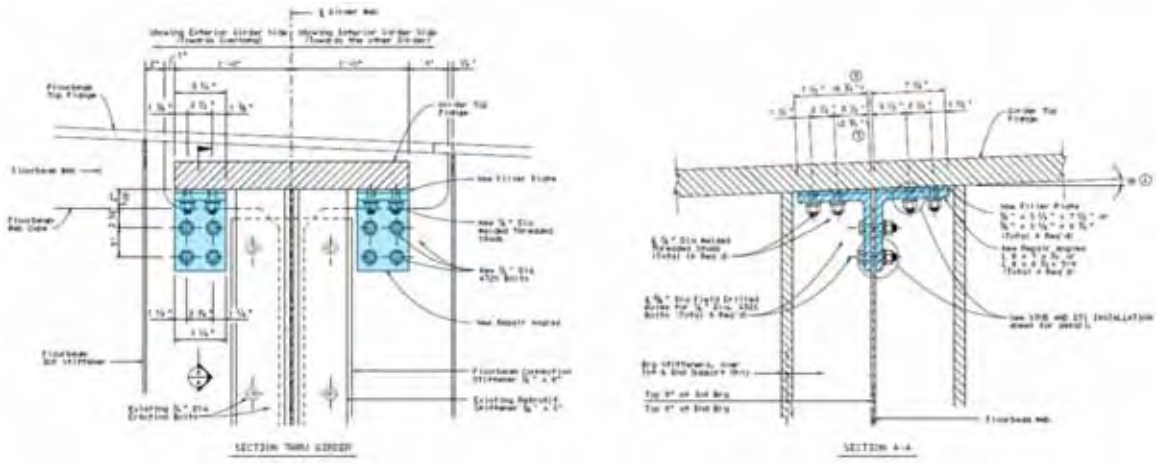

Figure 8.4: Detail Showing Proposed Retrofit Angles

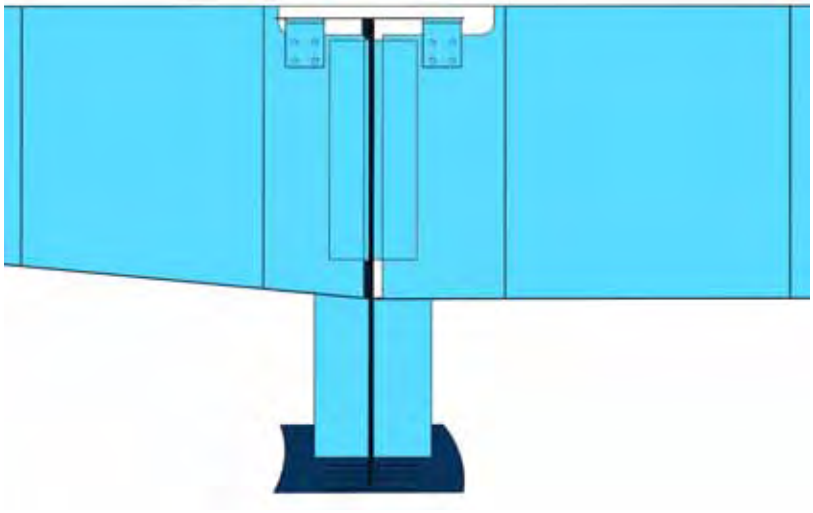

Figure 8.5: Finite Element Model with Retrofit Angles

To be able to simulate the four live load truck runs that were performed in the field, the weights of the truck axles and the distances between those axles were recorded and were shown

in Chapter 2. This information was then used to create loading conditions in the model that closely resembled the conditions in the field. This allowed for the model data and field data to be compared directly.

8.3 Finite Element Model Results

8.3.1 Comparison of Composite and Non-Composite Models

As previously mentioned, the slab and the floor beams were designed to act non-compositely. However, the field tests results show that they are behaving more compositely when there is live load over the floor beam. Therefore, both composite and non-composite finite element models were developed. To compare the two models, the stress at the locations where strain gages were placed during the field tests was determined using the models. These values were then plotted for the two two-truck load cases. Figure 8.6 shows the comparison between stress values for the case where two trucks were on the right side of the bridge and Figure 8.7 compares the values for the case where two trucks were on the left. Each data point in the figures corresponds to the stress measured at the location of a specific strain gage. The location of the strain gage is shown by the rectangle of the same color in the detail next to each group of data points.

As can be seen in both figures, the results from both of the models were close. The composite model does show a smaller stress in the web gap areas, which results from a smaller rotation of the floor beam due to the higher stiffness of the composite floor beam. Also, the non-composite model shows a larger stress in the top flange of the floor beam near the trucks, which would be expected with non-composite elements. However, the differences between the values from the two models are small at the locations of interest. The results from the partially composite model showed stress values that were typically between the fully-composite and non-composite values.

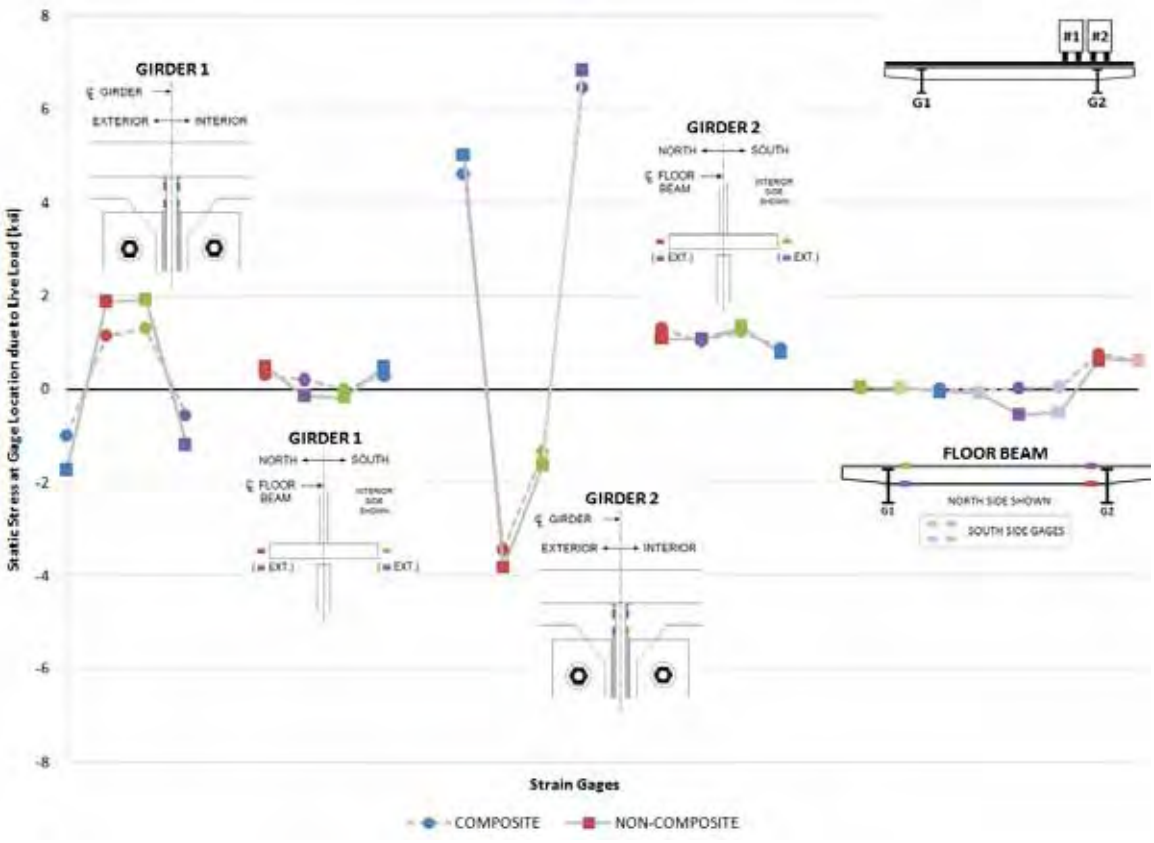

Figure 8.6: Comparison of Composite and Non-Composite Models for the Load Case with 2 Trucks on the Right

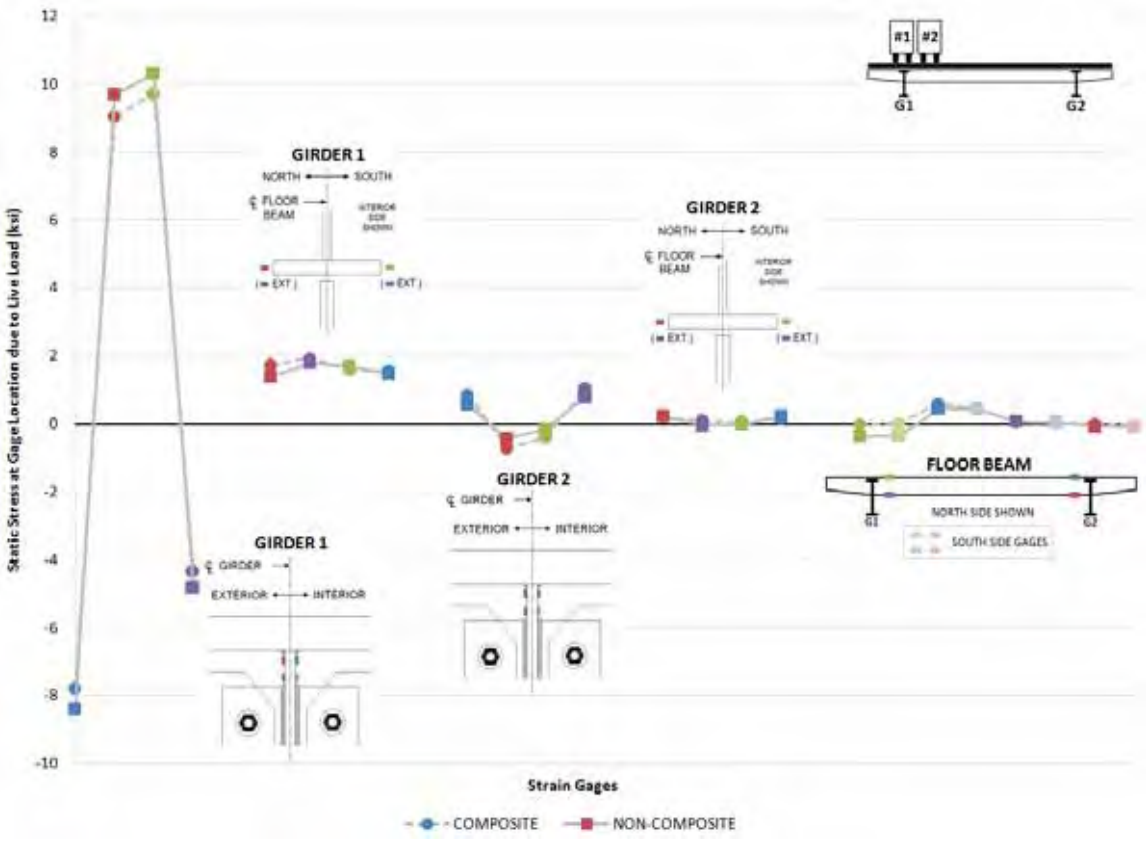

Figure 8.7: Comparison of Composite and Non-Composite Models for the Load Case with 2 Trucks on the Left

8.3.2 Comparison of Composite Model and Field Test Results

As was mentioned in the previous section, there was little difference between the results of the composite and non-composite models. Because the field test data shows that the slab and floor beams are most likely acting compositely, the composite model will be used as a comparison to the field test results. The results from the tests with two trucks on the right and two trucks on the left will be compared.

Figure 8.8 shows the comparison of the model to the field data for the test with two trucks on the right side of the bridge. One difference between the model and field data is that the model shows the web gap bending in double curvature. As was discussed in Chapter 4, this is what was expected to happen, but was not what was recorded during the field testing. All of the field test results showed the web gap bending in single curvature with the top of the gap recording higher stresses than the bottom of the gap. Another difference between the model and field data is that the model does not show as much out-of-plane bending of the girder web at the location where the bottom flange of the floor beam frames into the girder. The stresses in the gages on opposite sides of the web are much closer in value, which suggests that the majority of the stress is due to in-plane bending of the web. These differences are more prevalent at the connection of the floor beam to girder 2, which is where the trucks were located. The stress values measured in the floor beam during the field test were similar to the results from the computer model.

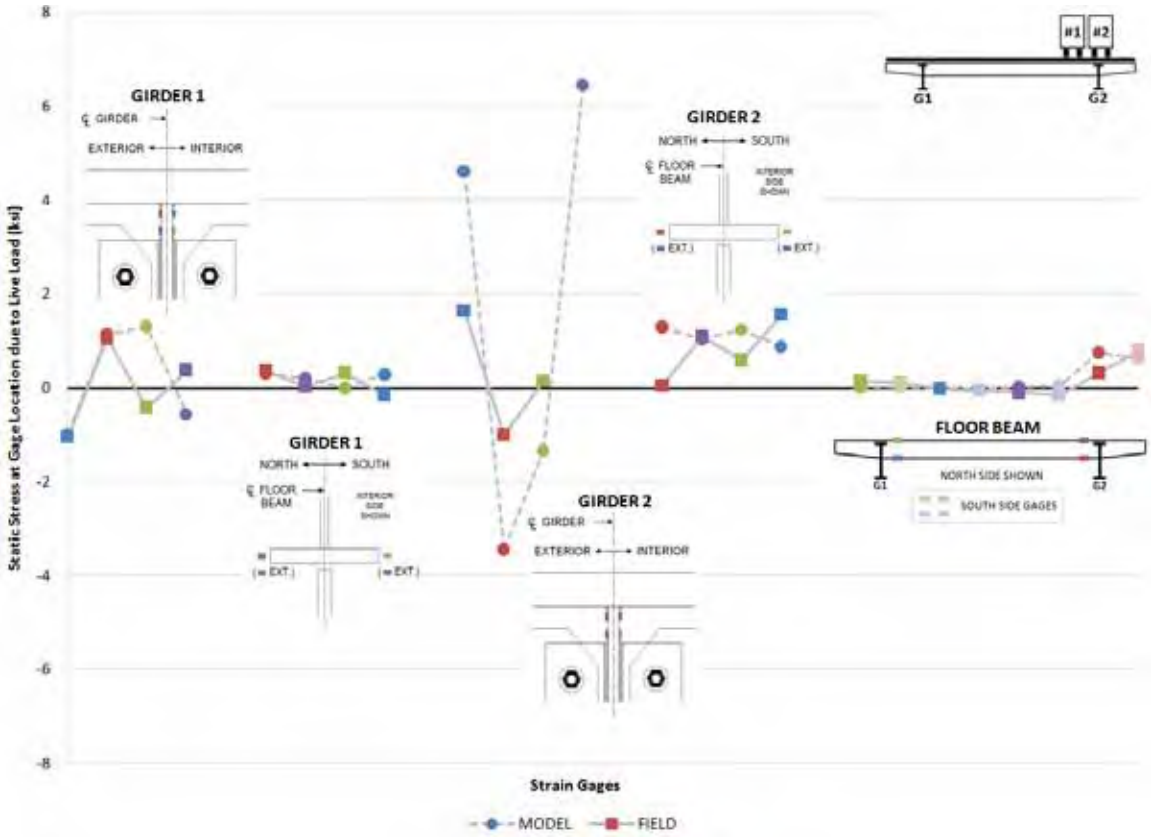

Figure 8.8: Comparison of Composite Model with Field Test Results for the Load Case with 2 Trucks on the Right

Figure 8.9 shows the deformed state of the entire bridge due to the weight of two trucks over girder 2. The slab has been removed from this image to provide a better view of the deformed shape of the girders and floor beams. The deformations have been magnified by a factor of 1500. Figure 8.10 shows a view of the connection in the deformed state. The double curvature of the web gap can be seen in this figure as well as the lack of significant out-of-plane bending in the girder web near the connection of the bottom flange of the floor beam. The high stress concentration at the web gap is shown in the figure (the top and bottom flanges are removed from the image to provide a better view).

Figure 8.9: Deformed State of Bridge due to 2 Trucks on the Right

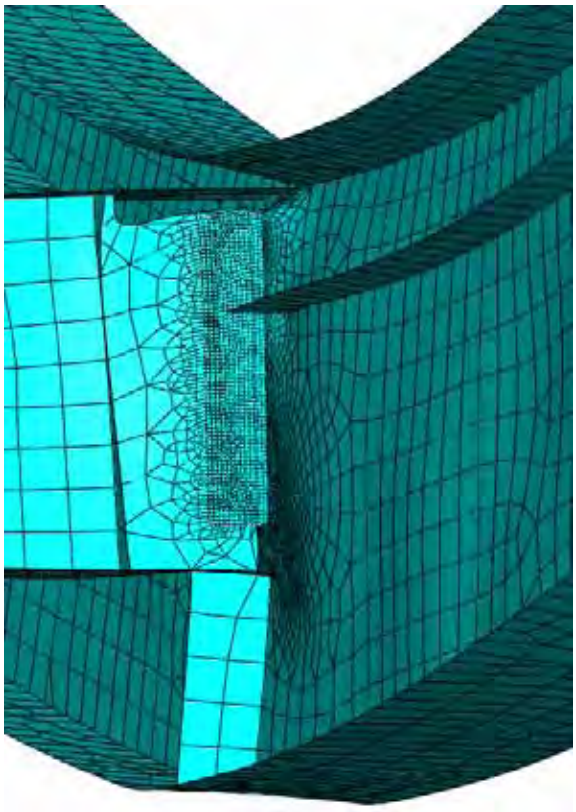

(a) Deformed shape

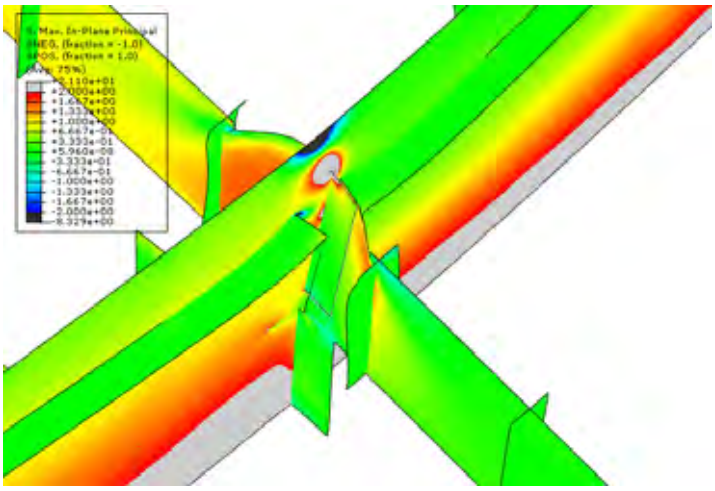

(b) Stress Contour

Figure 8.10: View of Connection in Deformed State

Figure 8.11 shows the comparison of the model to the field data for the test with two trucks on the left side of the bridge. These results show the same differences that were seen in the previous test. The model is showing double curvature in the web gap and virtually no out-of-plane bending in the girder web due to the movement of the floor beam in the connection under

the trucks. At the connection of the floor beam to the other girder, the results from the model closely resemble the field test results as do the results from the floor beam.

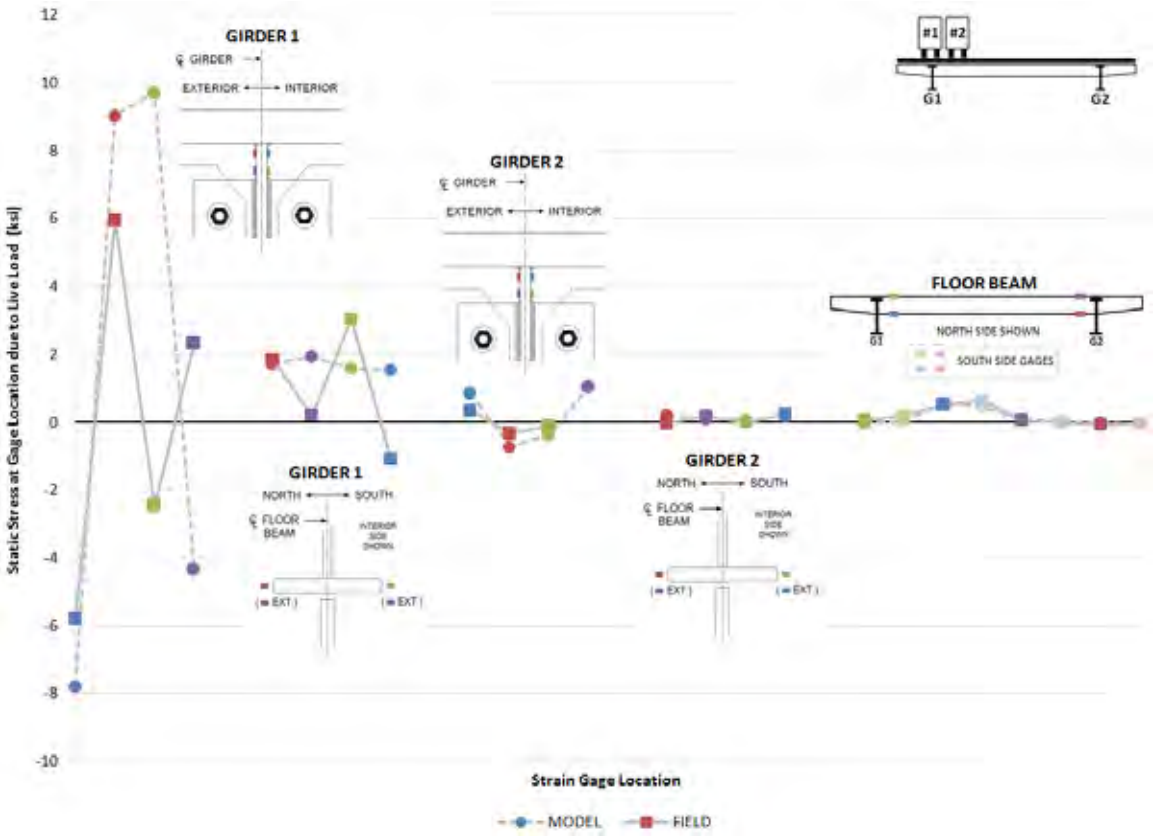

Figure 8.11: Comparison of Composite Model with Field Test Results for the Load Case with 2 Trucks on the Left

8.3.3 Effectiveness of Retrofit Angles

The results from the composite model before and after adding the retrofit angles will be compared to determine if this retrofit is effective in reducing the stress at the connection. Figures 8.12 and 8.13 show the results for the test with two trucks on the right and two trucks on the left, respectively. As can be seen from both figures, the retrofit angles are effective in reducing the stress in the web gaps. However, the stress in the girder web near the bottom flange of the floor beam is not affected by the angles.

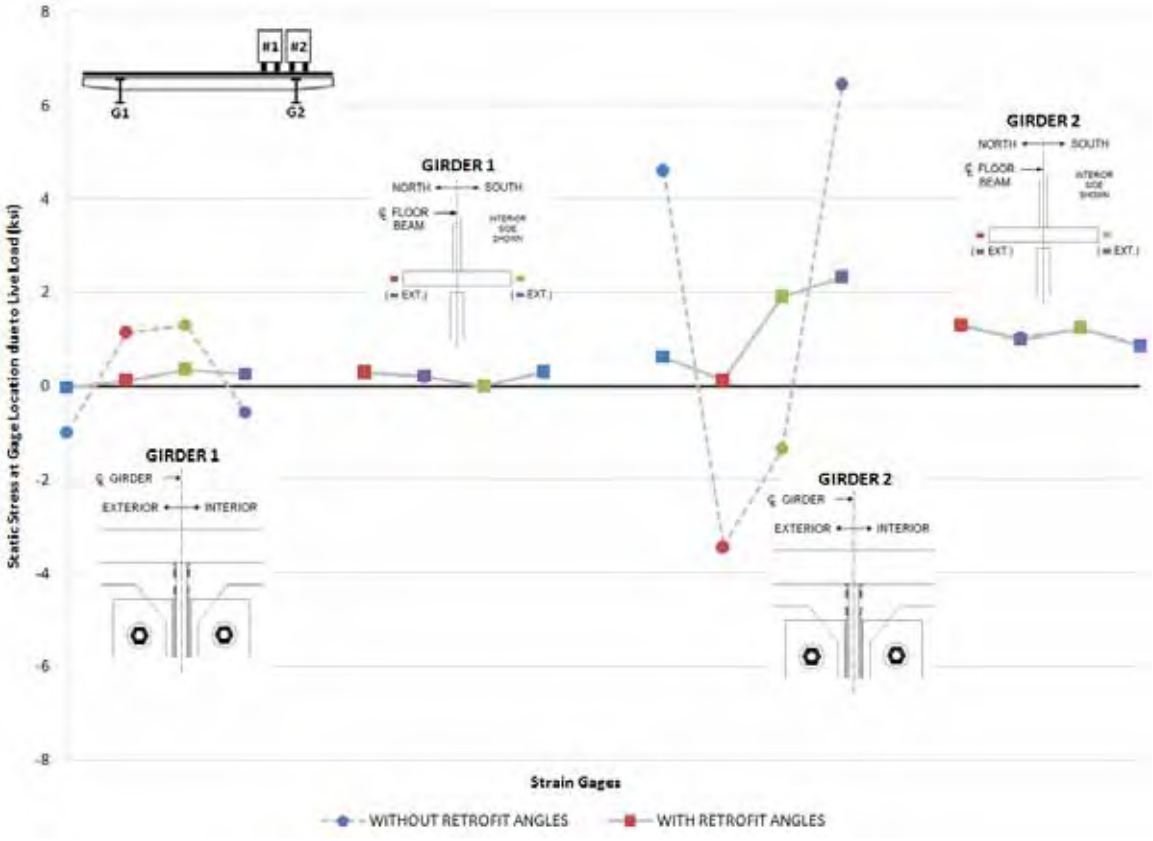

Figure 8.12: Comparison of Model Results with and without Retrofit Angles for Load Case with 2 Trucks on the Right

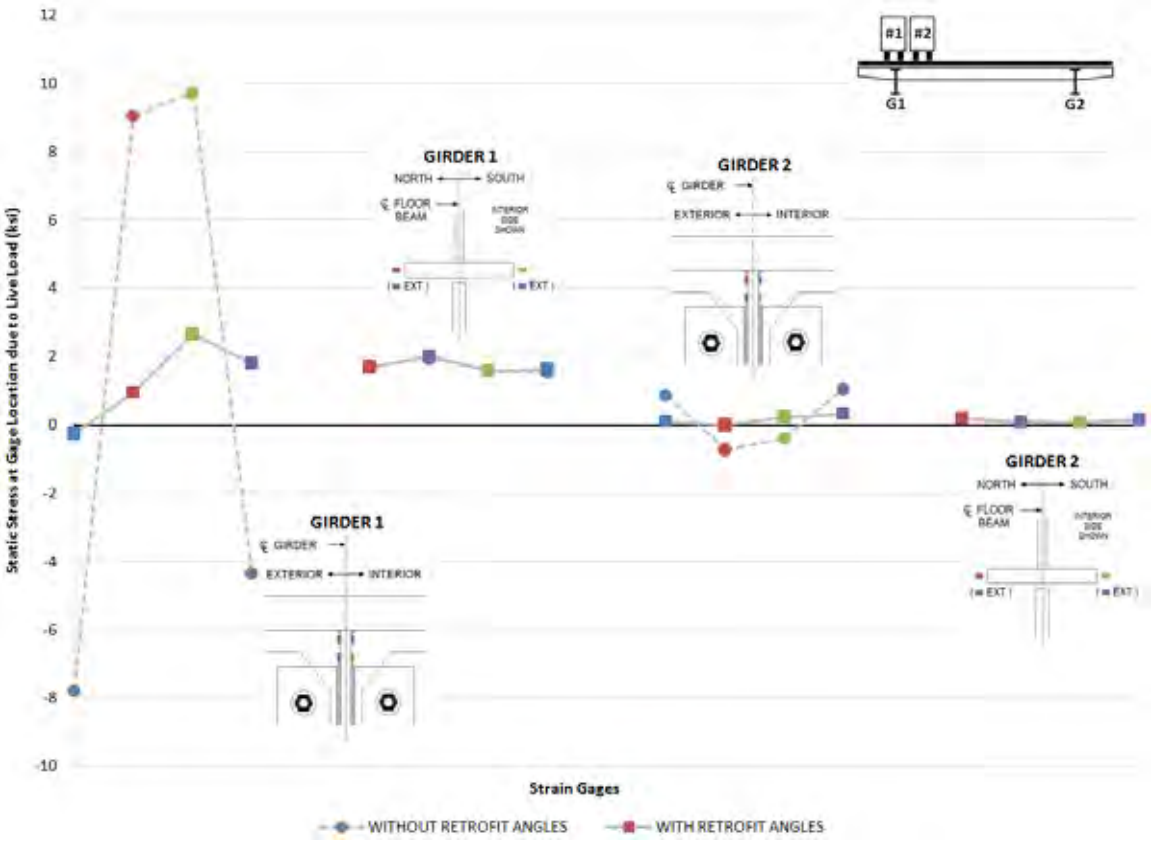

Figure 8.13: Comparison of Model Results with and without Retrofit Angles for Load Case with 2 Trucks on the Left

Figure 8.14 shows a view of the connection in the deformed state with the retrofit angles. If this figure is compared to Figure 8.10, which does not include the retrofit angles, it can be seen that the angles significantly reduce bending in the web gap, thus reducing the stress in that area.

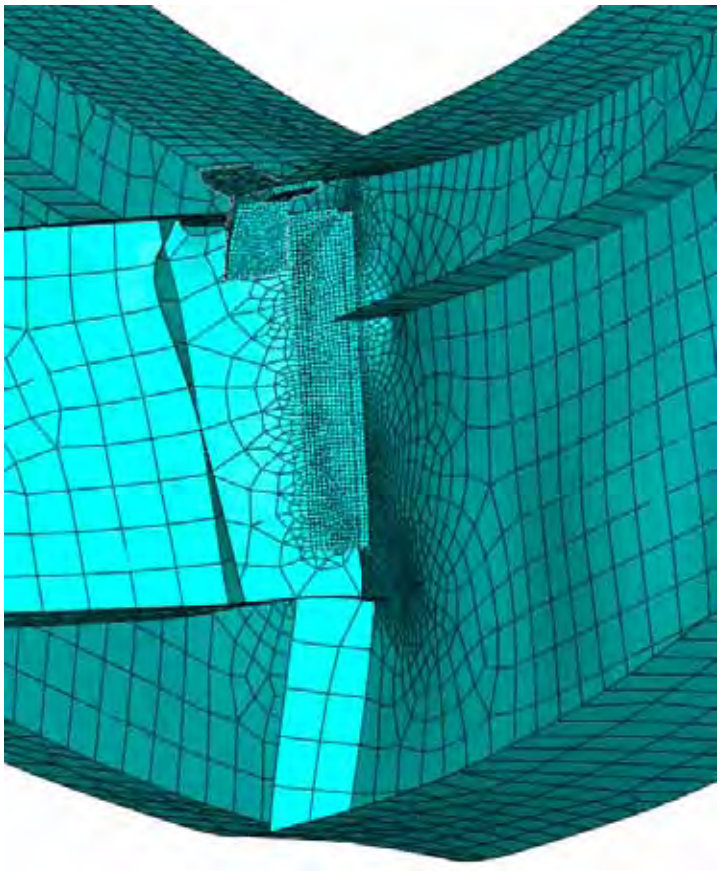

(a) Deformed Shape

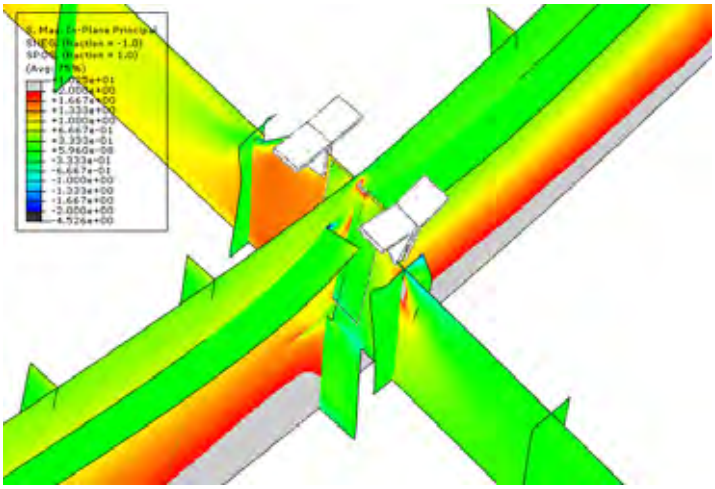

(b) Stress Contour

Figure 8.14: View of Connection in Deformed State with Retrofit Angles

The following two figures show stress contours and the deformed shape of the floor beam web near the floor beam cope. Figure 8.15 shows the floor beam before the retrofit angles and Figure 8.16 shows the floor beam with the retrofit angles. Although the retrofit angles decrease the bending in the web gap, it can be seen by comparing Figures 8.15 and 8.16 that the angles increase stresses in the floor beam web around the coped area, which is close to the area were the transverse stiffeners are attached to the floor beam. The increase in stress at the cope and at the transverse stiffener welds may lead to cracking at this location.

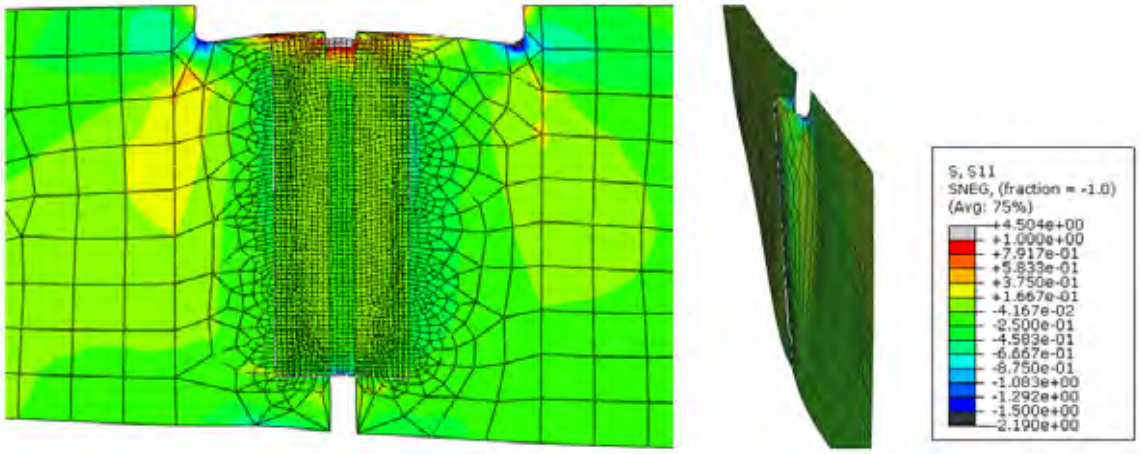

Figure 8.15: Stress Contours and Deformation near Floor Beam Cope with no Retrofit Angles

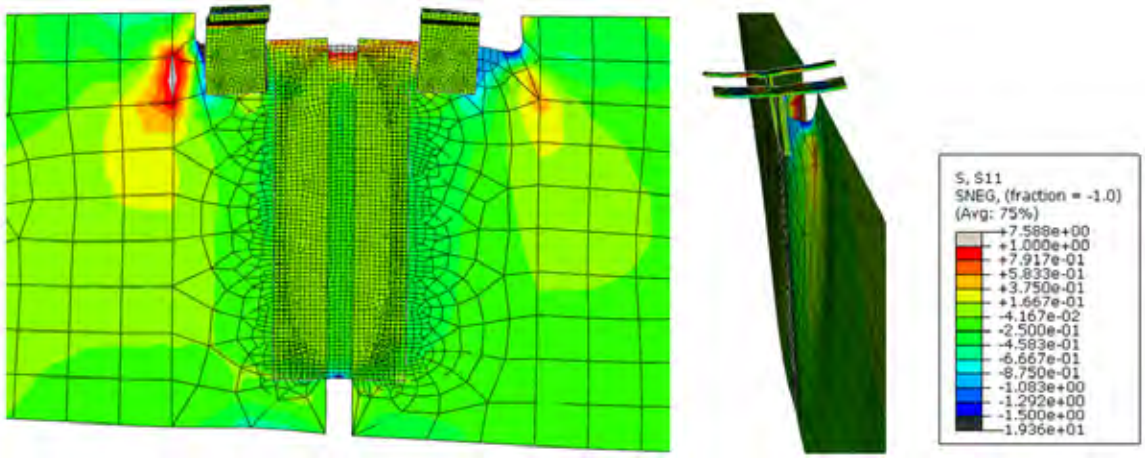

Figure 8.16: Stress Contours and Deformation near Floor Beam Cope with Retrofit Angles

8.4 Summary

In summary, the finite element model that most closely resembled the live load field tests results for Section F14N was the model with 4000 psi concrete and composite action between the slab and floor beams. One of the main differences between the model and the field test data is that the model shows the web gap bending in double curvature when the field test data shows that it bends in single curvature. The other difference is that the model does not show significant out-of-plane bending of the girder web around the area where the bottom flange of the floor beam frames into the girder.

Retrofit angles, one of the retrofit plans being considered for this bridge, were incorporated into the model to determine their effectiveness. The model shows that the angles decreased the bending stress in the web gap but increased the stress in the floor beam web around the coped area. The bolted connections of the angles were modeled assuming a rigid connection, no slip, between the angle and the members. If the bolts are not properly pretensioned in the field and the paint removed on the faying surfaces, the stiffness of the retrofit connection will be reduced, which will reduce its effectiveness.

Chapter 9. Finite Element Model Results for Section F17S

9.1 Introduction

After completing the field testing, a finite element model of Section F17S was created. The purpose of the model was to provide a comparison to the field test results. The model was also used to test the effectiveness of two of the retrofit ideas for this section. This chapter will explain the details of the finite element model as well as compare the model results with the field test data. The effectiveness of the retrofit plans will also be discussed by comparing the model results before and after the retrofits.

9.2 Finite Element Model Details

The model was created using the finite element software Abaqus. First, a full model of the bridge (shown in Figure 9.1 without the slab) was created. A ramp on the north end of this section causes the horizontal curvature of the bridge to change along the length of girder 2. The horizontal curvature of the bridge was simplified in the model by using a straight line for girder 1 and two straight lines for girder 2 to represent the flare caused by the ramp. In this simplified model of the bridge, the length of the girder 2 was maintained while the length of the girder 1 was reduced. Accordingly the locations of the floor beam connections on girder 2 were maintained while the locations on girder 1 were adjusted so that the floor beam intersects the girder 1 at 90 degree angle. The support conditions in the model are summarized in Table 9.1. The X direction runs transversely across the bridge, the Y direction is the vertical direction, and the Z direction runs longitudinally along the bridge. The location of vertical supports is on the bottom flanges of the girders between the bearing stiffeners. The support areas, that were below the connection of the floor beams 23 and 28 and girder 1 and the floor beams 16 and 25 on girder 2, were constrained to be rigid. While these rigid support areas can rotate, any translational movement was restrained.

In a preliminary analysis where the rotational movement of the rigid supports about the longitudinal axis of the girder was constrained, the deformation was concentrated more in the girder web near the floor beam to girder web connections. This resulted in higher stresses than the stresses measured in the field test. Therefore, as described in the support conditions, the restraint on the rotational movement of the rigid supports about the longitudinal axis of the girder was freed and the resulting flexibility of the girder reduced some of the deformation in the girder web and provided a closer match to the stresses from the field test. If the actual condition is close to the condition where the rotational movement about the longitudinal axis of the girder is restrained, the localized stress in the girder web is expected to be higher than the analysis indicates.

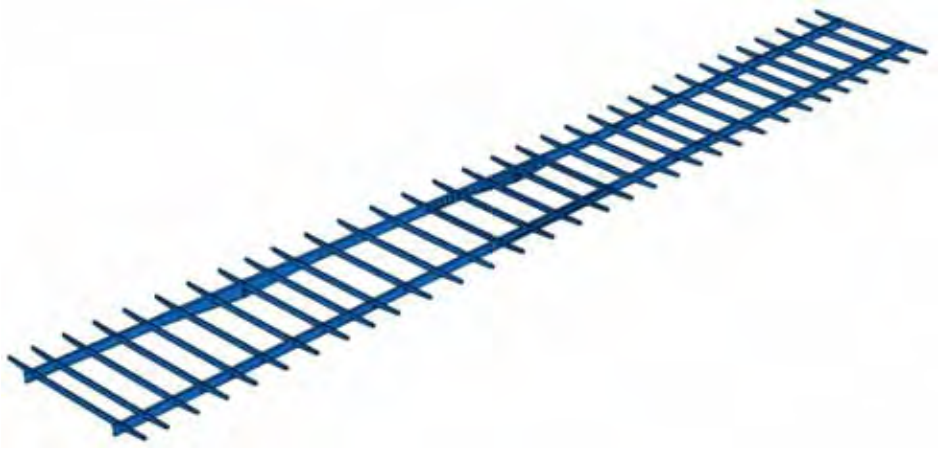

Figure 9.1: Full Finite Element Model of Section F17S

Table 9.1: Support Conditions for Section F17S

GIRDER	FLOOR BEAM	POINT	AREA	FIXED X	FIXED Y	FIXED Z
1	1	●			●	
1	7		●		●	
1	12		●		●	
1	18		●		●	
1	23		●	●	●	●
1	28		●	●	●	●
1	32	●			●	
2	1	●			●	
2	4		●		●	
2	10		●		●	
2	16		●	●	●	●
2	25		●	●	●	●
2	32	●			●	

As discussed in the previous sections, the field test results show that the slab and floor beams are most likely acting compositely due to a friction force between the slab and floor beams caused by a normal force on the interface from the traffic loads. The results from the model of Section F14N showed little difference between the composite and non-composite model results. Therefore, the model of Section F17S incorporates composite interaction between the floor beams and slab by using ties to connect the slab and floor beam elements together along the full length of the floor beam. While the traffic loads on the concrete slab induce composite action between the slab and the nearby floor beams and have influence on the behavior of the nearby floor beam to girder connections, possible non-composite action between the slab and the distant floor beams does not seem to have significant influence on the localized behavior in the connections of interest.

Considering the preliminary analysis results in the previous chapter, where results showed little difference in the stress values at the locations of interest for the different concrete strengths, 4000 psi concrete was used in the model of Section F17S as well.

To better understand the behavior at the connection of the floor beams to the girders, a sub model was created that uses the displacement field generated in the full model to derive its boundary conditions. The sub model, shown in Figure 9.2, focuses on the connection of floor beam 16 to girder 2, which is the location of one of the haunches along this girder. The sub model allowed for a finer mesh to be defined at the connections so that the behavior could be more accurately recorded.

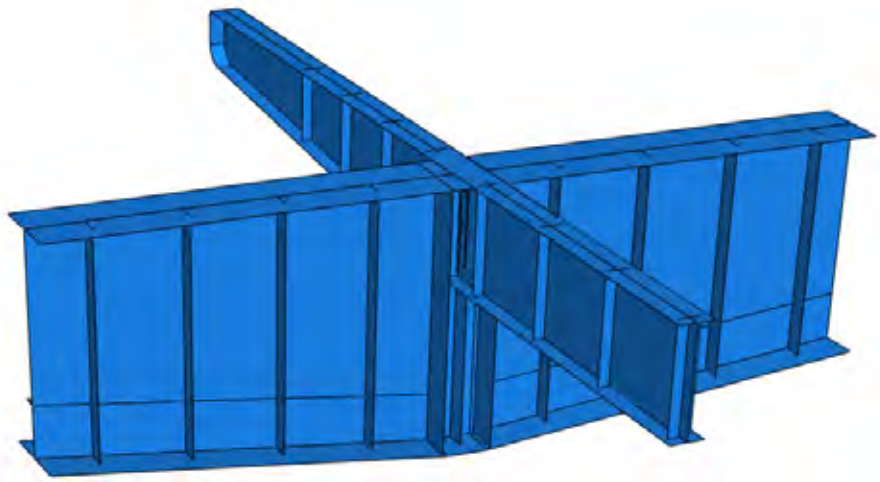

Figure 9.2: Sub Model Showing Connection of Floor Beam 16 to Girder 2

The sub model also incorporates two of the retrofit ideas that have been developed for this bridge. A detail of the first retrofit, which was developed by the Texas Department of Transportation, can be seen in Figure 9.3. The retrofit consists of using knee brace plates and angle brackets to connect the bearing stiffeners, the bottom flange of the floor beam and the bottom flange of the girder. This retrofit is intended for connections that are supported by columns and, therefore, have bearing stiffeners. Two knee brace plates are welded to the bearing stiffeners on either side of the floor beam. This is done on both the interior and exterior side of the girder. Thus, there are four knee brace plates required at every connection. Angle brackets, consisting of L8x8x1 angles and 1-inch plates, are welded to the backs of the brace plates and to the underside of the bottom flange of the floor beam. The brace plates continue down the bearing stiffener to the top side of the girder bottom flange. In the computer model, the brace plate was assumed to be 3/4 inches thick and the angles were assumed to be L8x8x3/4 as no dimension was specified in the details. Quadratic solid elements with reduced integration were used for the angles in the analysis. The plates and angles were tied along their edges to the bearing plates and floor beam flange to represent the welded connections specified in the detail. In addition, the surfaces of the angles, which are in contact with the floor beam bottom flanges, were tied to the flanges. Figure 9.4 shows two views of the retrofit brace plates and brackets in the sub model.

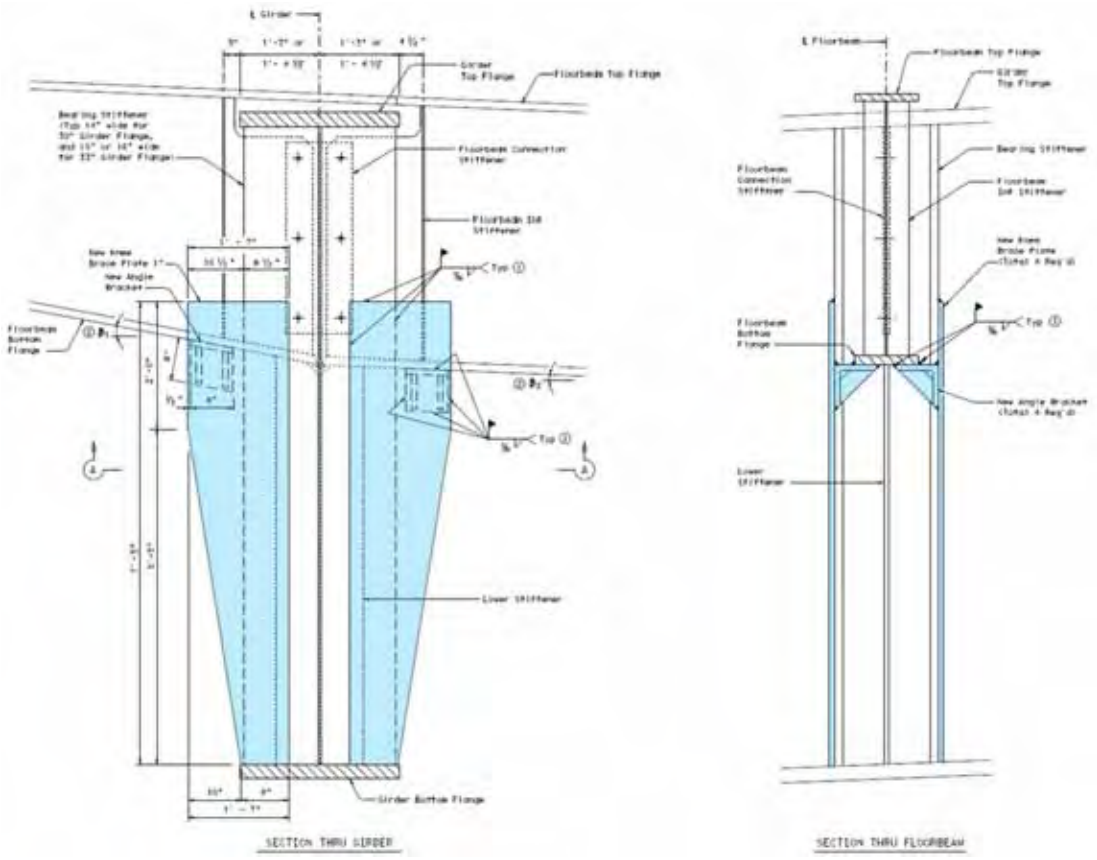

Figure 9.3: Detail Showing Proposed Retrofit Brace Plates and Brackets

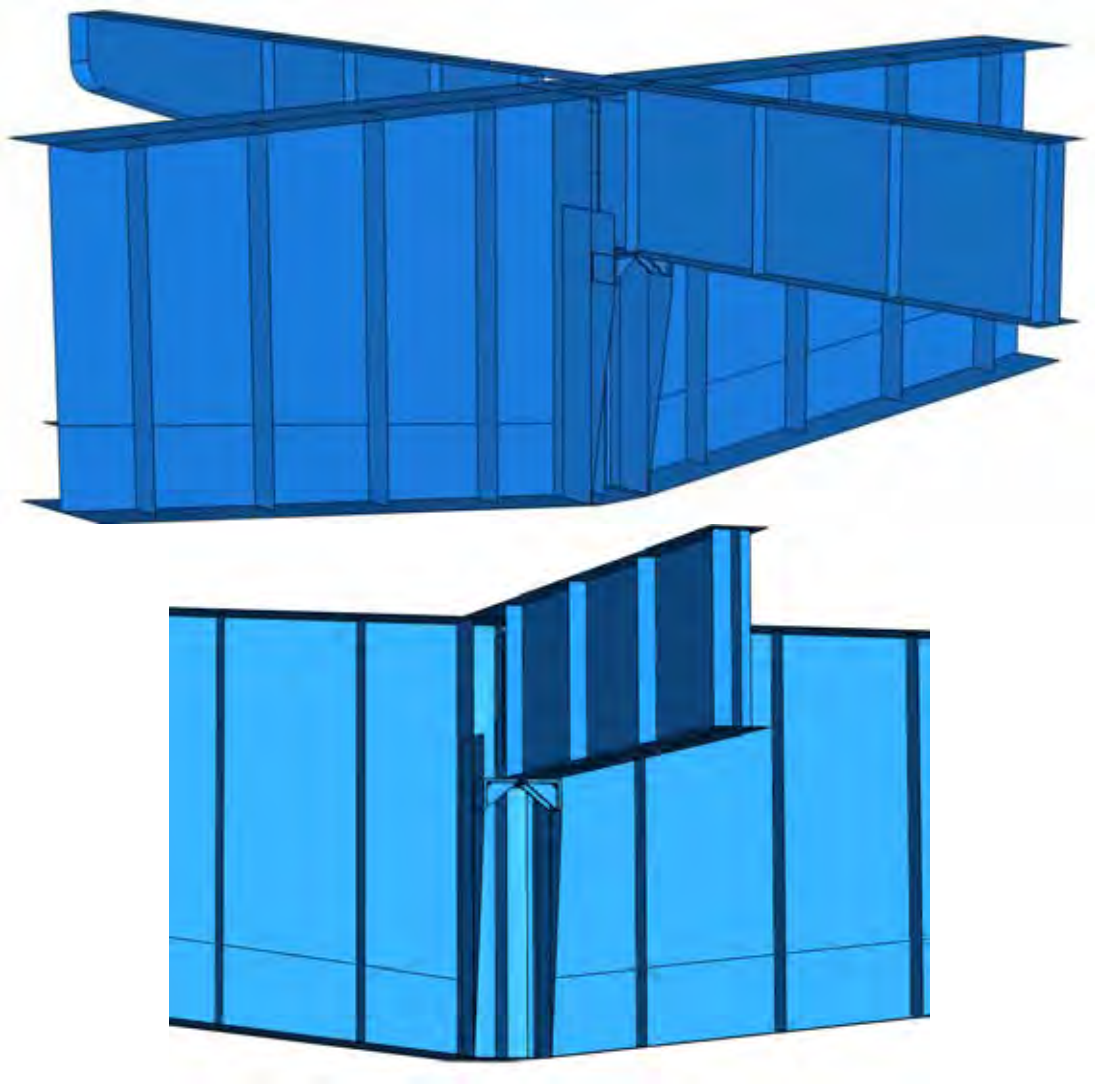

Figure 9.4: Views from Finite Element Model Showing Retrofit Brace Plates and Brackets

The second retrofit incorporated into the model involves cutting the bearing stiffeners at the connection of floor beam 16 to girder 2 in half. This eliminates the small gap that exists between the bearing stiffeners and the bottom flange of the connecting floor beam, which was shown to have relatively high stresses. A detail of this retrofit can be seen in Figure 9.5. The lower stiffener directly under the floor beam was left at its original height. Figure 9.6 shows this retrofit incorporated into the sub model.

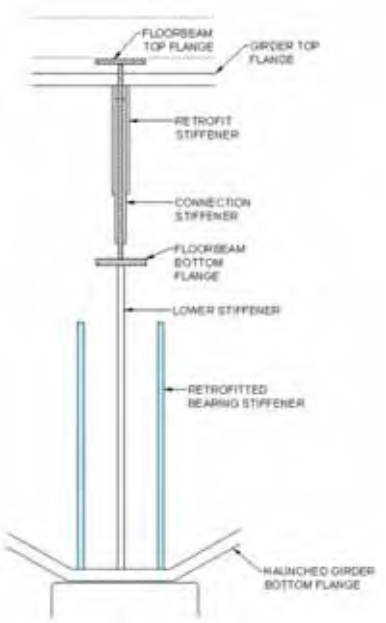

Figure 9.5: Detail Showing Proposed Retrofit Bearing Stiffeners

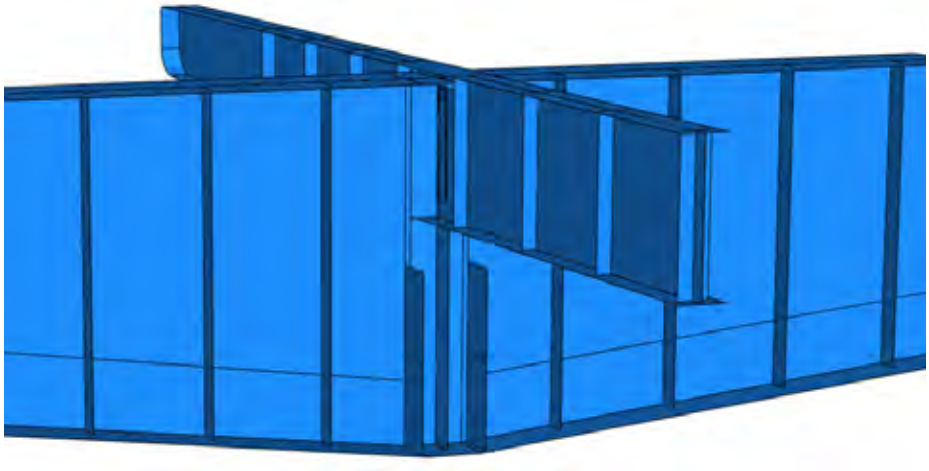

Figure 9.6: View from Finite Element Model Showing Retrofit Bearing Stiffeners

To be able to simulate the four live load truck runs that were performed in the field, the weights of the truck axles and the distances between those axles were recorded and were shown in Chapter 2. This information was then used to create loading conditions in the model that closely resembled the conditions in the field. This allowed for the model data and field data to be compared directly. Using the model, it was determined that the stresses measured at some of the gage locations changed significantly with slight changes in the locations of the trucks over the floor beam. During the field testing, it was intended that the trucks stop when the front drive axle was over the desired floor beam. However, this location was determined by the driver of the truck and is only an approximation. Thus, the loads simulating the trucks in the computer model were moved slightly forward, backward and transversely in order to determine a range of stress

values that were then compared to the field data. Figure 9.7 shows the various positions of the truck loads in the computer model.

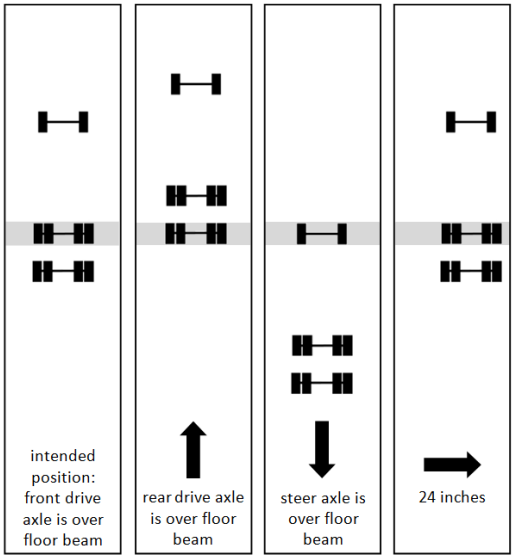

Figure 9.7: Locations of Trucks used in Analysis

9.3 Finite Element Model Results

9.3.1 Comparison of Composite Model and Field Test Results

Figure 9.8 shows the comparison of the model results to the field data for the test with two trucks on the right side of the bridge. The gage locations near the connection of floor beam 16 to girder 2 were used in the comparison and correspond to each of the data points in the figure. The color of the data point matches the color of the corresponding gage in the details within the figure. The model results show a range of values that was determined by slightly moving the truck loads as was discussed in the previous section. There are four locations where there is no field data point due to defective gages or inability to place a gage due to access issues: the gage on the south side of the interior retrofit stiffener, the gages on the girder web on the south side of the bottom floor beam flange, and the gage on the north side of the bottom flange of floor beam 16.

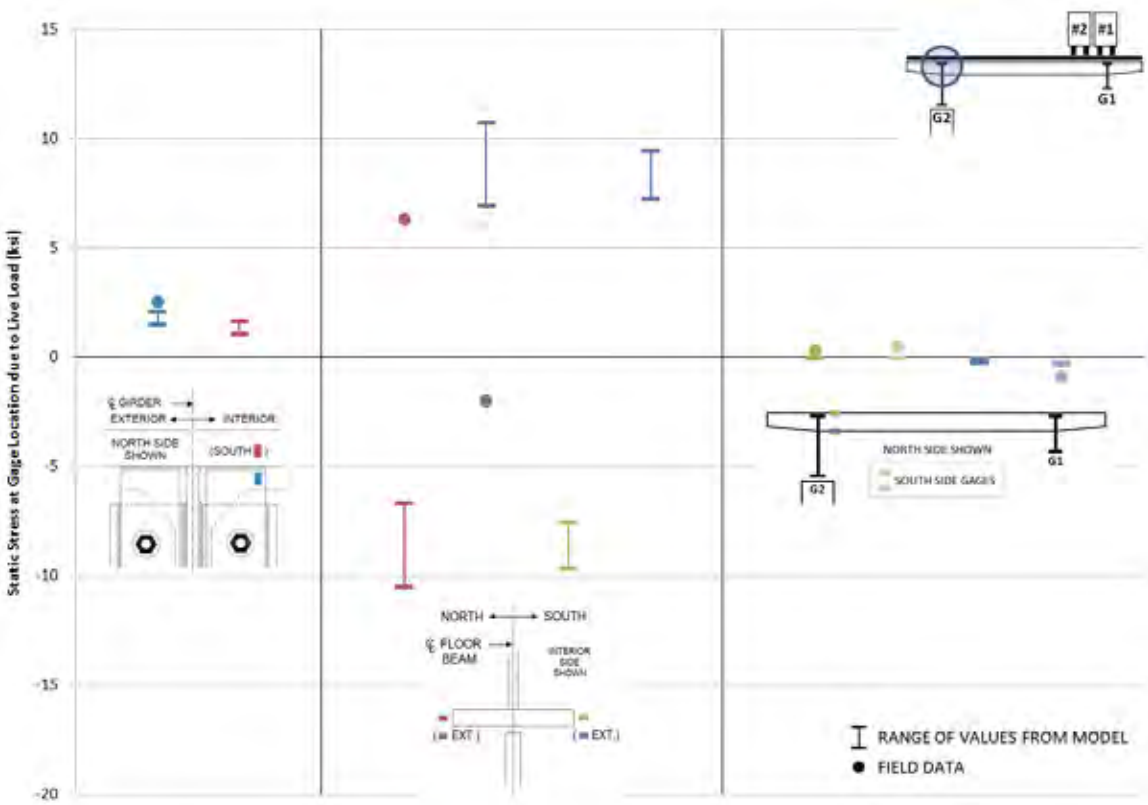

Figure 9.8: Comparison of Composite Model with Field Test Results for the Load Case with 2 Trucks on the Right

It can be seen from the figure that the stress values recorded by the retrofit stiffener gages and the floor beam gages correlate well with the computer model results. The main difference between the field and model data is shown by the girder web gages. The field data shows out-of-plane bending of the girder web toward the interior of the bridge while the computer model shows the web bending in the other direction. The reason for this can be seen in Figure 9.9, which shows stress contours on the girder web in the gap between the bearing stiffeners and bottom flange of the floor beam. Near the vertical bearing stiffener, the stress contours in the gap are red, which signifies tension. Near the bottom flange of the floor beam, the contours are blue, which signifies compression. The change from tension to compression means that the web is bending in double curvature within this gap. Because the gap is so small, this creates a very high stress gradient and any slight change in the location of the strain gage could result in a change in the sign of the stress recorded by the gage. Therefore, it is possible that the locations of the strain gages that were placed in this gap during the field testing do not exactly match the points where stress values were measured in the computer model. This would account for the difference in the direction of bending of the web between the field and model data. Thus, these discrepancies are likely to be the result of slight differences in the locations of the points used to compare the field data and computer model results.

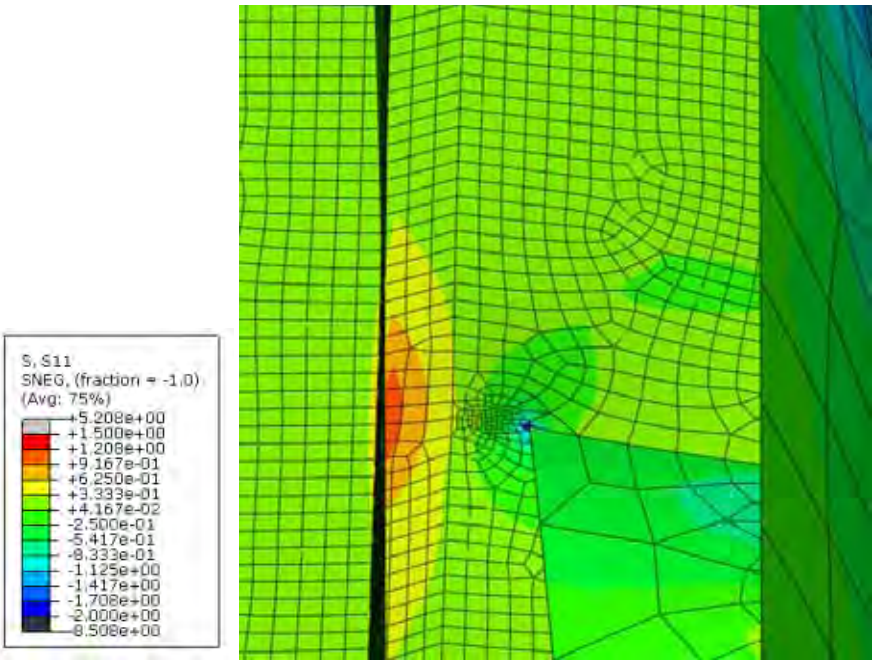

Figure 9.9: Stress Contours Showing Double Curvature in Web Gap

Figure 9.10 shows the comparison of the model to the field data for the test with two trucks on the left side of the bridge. These results show the good correlation in the retrofit stiffener and floor beam gages that was seen in the previous test. There is also good correlation in the girder web gages for this test. The range of values determined by the model is much larger for the girder web gages during this test. This is because the trucks are directly over the connection where the gages are located, which would make the gages more sensitive to slight changes in the locations of the trucks.

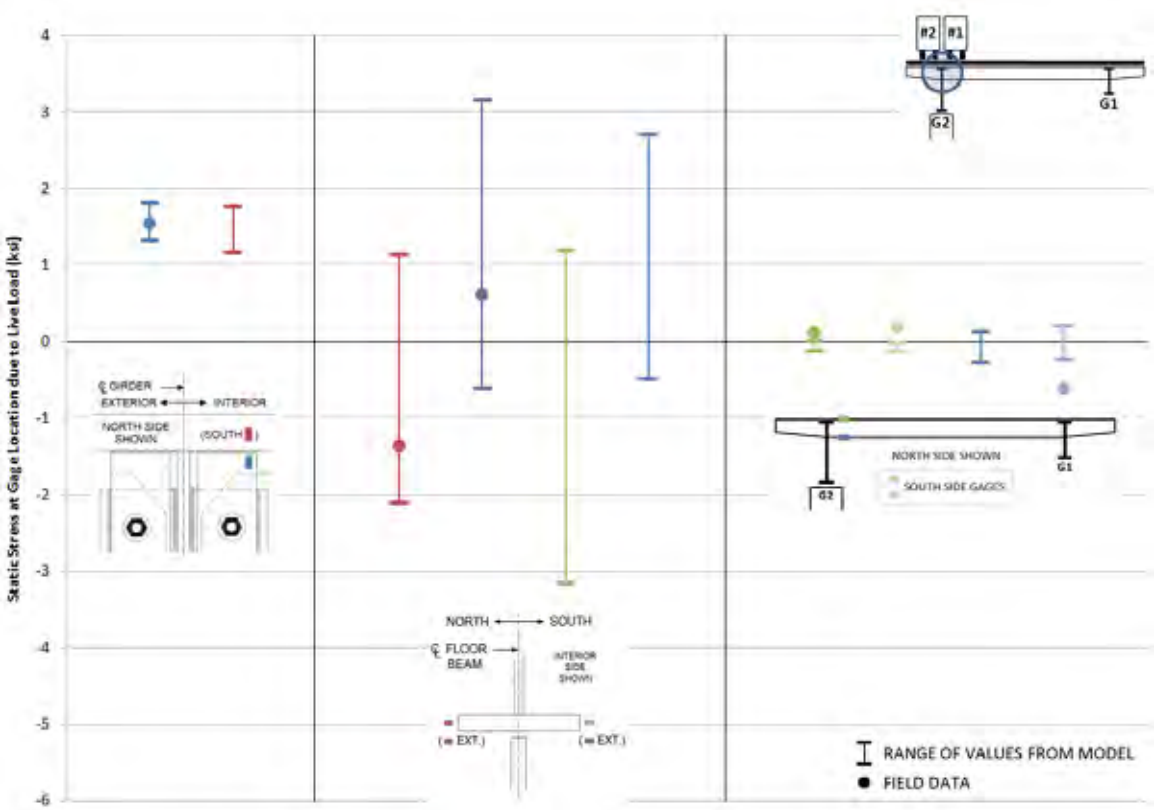

Figure 9.10: Comparison of Composite Model with Field Test Results for the Load Case with 2 Trucks on the Left

9.3.2 Effectiveness of Retrofits

The results from the composite model with and without the previously mentioned retrofits will be compared to determine if these retrofits are effective in reducing the stress at the connection. Figure 9.11 and Figure 9.12 show the results for the test with two trucks on the right and two trucks on the left, respectively. The squares in the plots represent that stress values from the model with no retrofits. The circles correspond to the stress values with the retrofit where the bearing stiffeners are cut in half and the Xs correspond to the retrofit with the knee brace plates and angle brackets. As can be seen from both figures, both retrofits were effective in reducing the stresses in most locations. When the trucks are over girder 1, the stresses in the web of girder 2 are significantly reduced with both retrofits. When the trucks are over girder 2, the stresses measured on opposite sides of the web of girder 2 are much closer in value with the retrofits, which means that the out-of-plane bending that was seen without the retrofits was reduced.

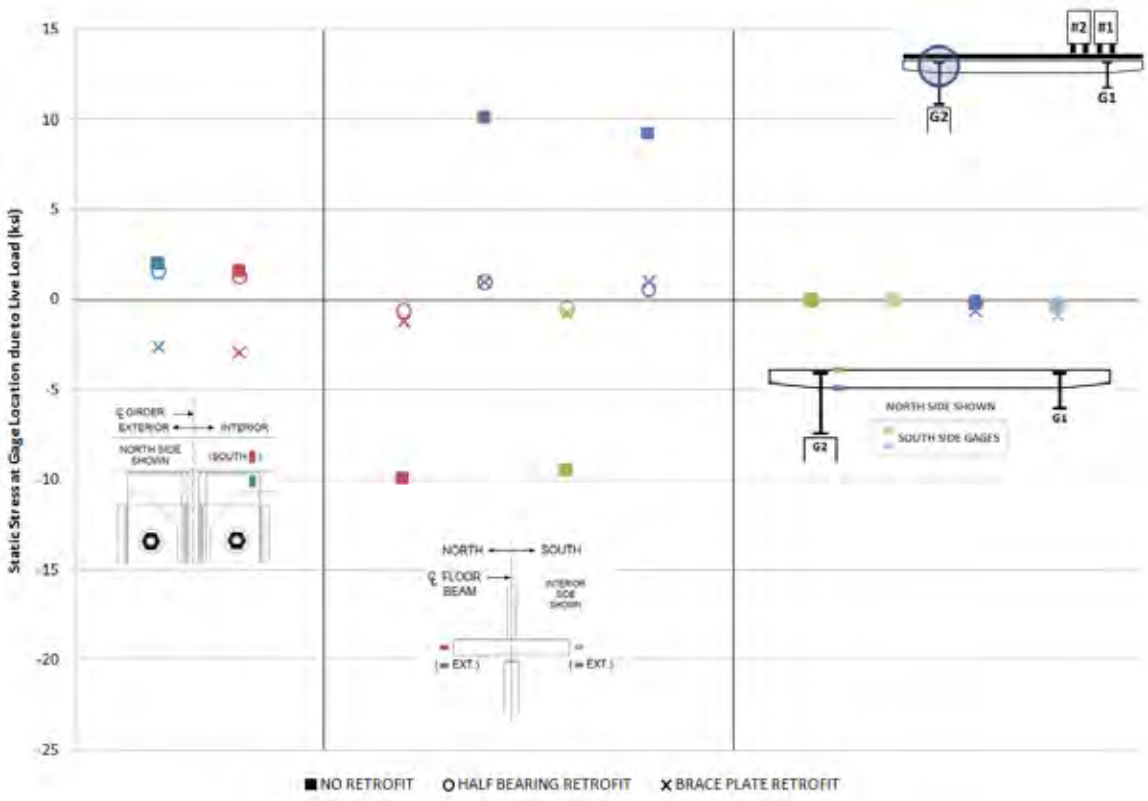

Figure 9.11: Comparison of Model Results with and without Retrofits for Load Case with 2 Trucks on the Right

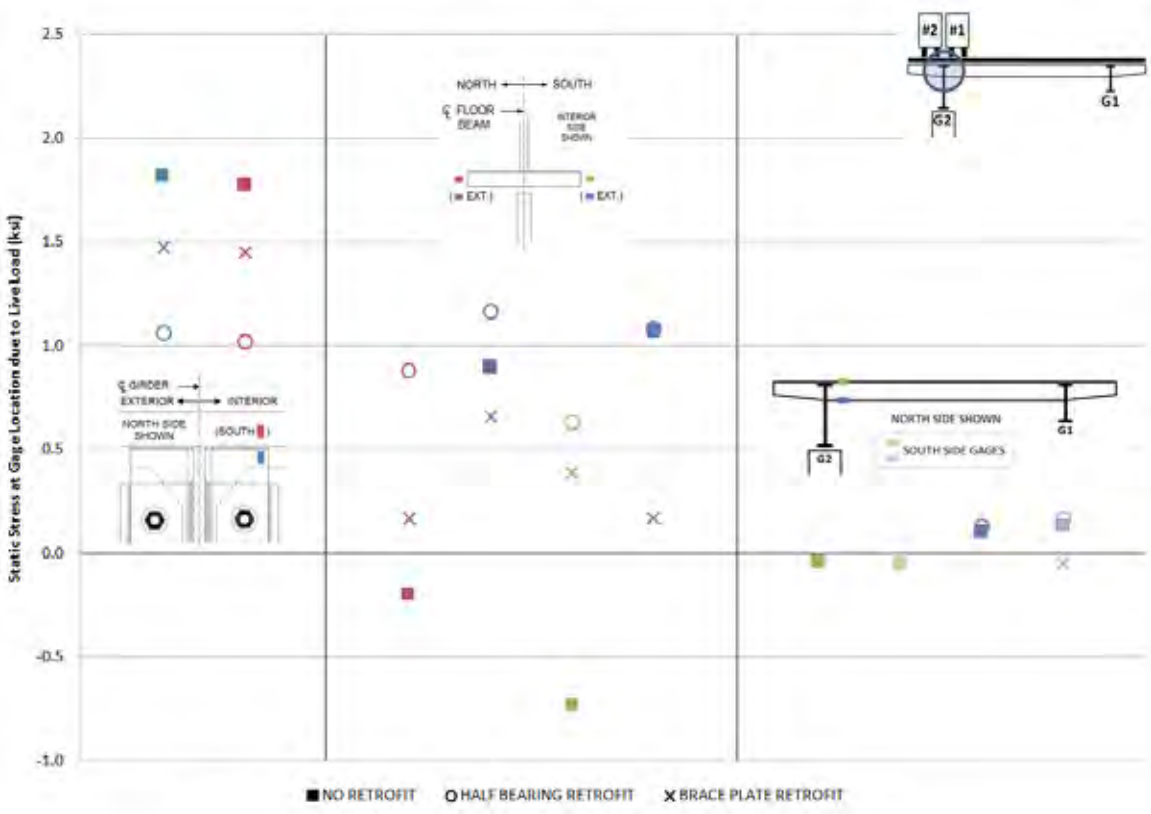

Figure 9.12: Comparison of Model Results with and without Retrofits for Load Case with 2 Trucks on the Left

Figure 9.13 shows a view of the connection in the deformed state with the retrofit braces and brackets. The stress contours in the gap between the bearing stiffeners and the bottom flange of the floor beam show that the magnitude of the stress in this area has decreased compared to Figure 9.9, which shows the connection without the retrofit. There are increased stresses in the bottom flange of the floor beam where the brackets are connected. These stresses are a result of the truck loads rotating the floor beam downward and the brackets pushing back up on the bottom flange. One possible way to reduce these stresses would be to place a continuous plate above both angle brackets between the brackets and the bottom floor beam flange. This would spread the stresses out and reduce the distortion that is seen in the bottom flange.

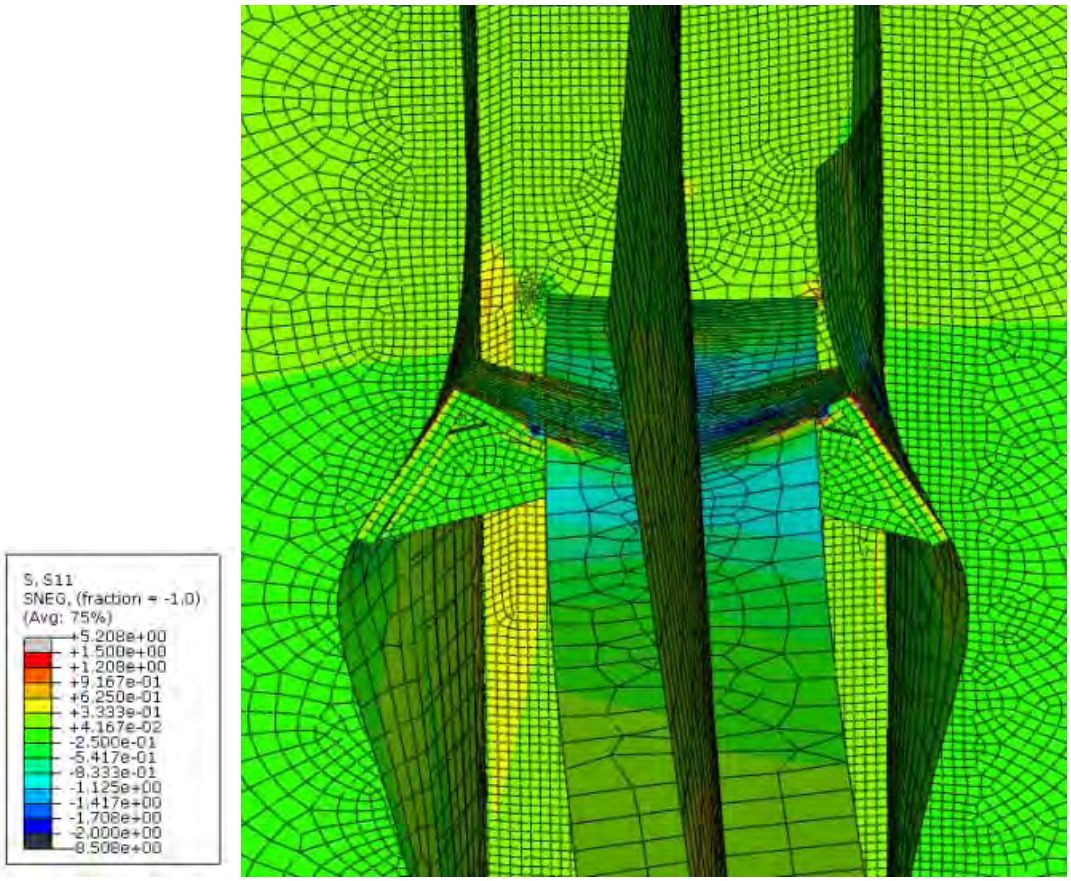

Figure 9.13: View of Connection in Deformed State with Retrofit Braces

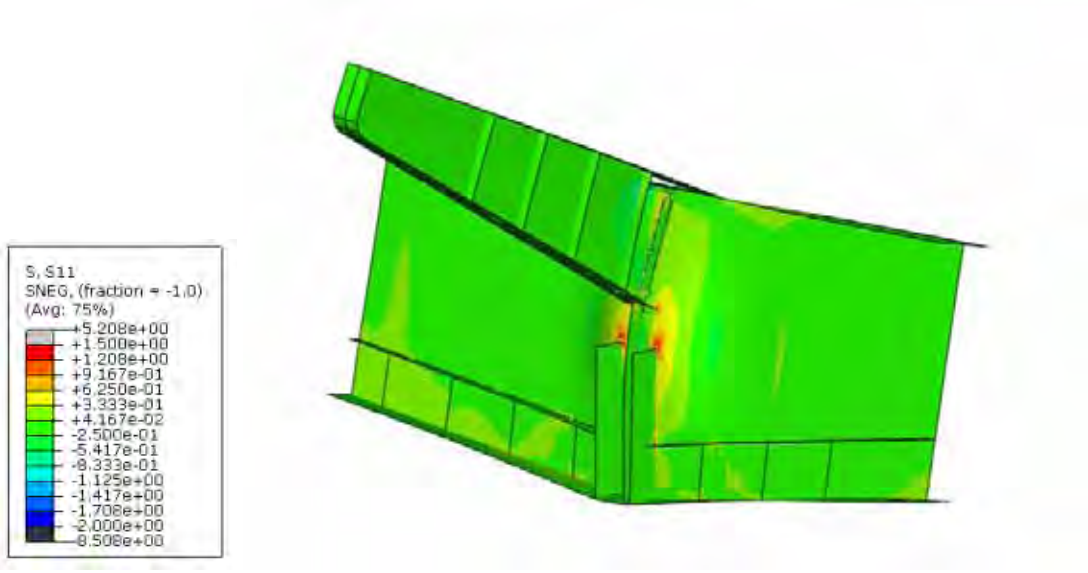

Figure 9.14: View of Connection in Deformed State with Retrofit Bearing Stiffeners

The two retrofits proposed for this section concentrate on reducing the stresses in the web of the girder near the location where the bottom flange of the floor beam frames into the girder.

It is important to note that the finite element model results show that there is also significant bending of the web of the floor beam near where the web is coped to go around the top girder flange. This bending is caused by rotation of the girder. Figure 9.15 shows the bending in the floor beam web near the cope without retrofits and Figure 9.16 shows similar bending in the floor beam web with the brace plate retrofit. The magnitude of the stresses near the cope is not reduced with the retrofit. Therefore, while the previously mentioned retrofits are effective in reducing the girder web stresses near the bottom flange of the floor beam, they do not help to reduce the stresses near the top of this connection when the distortion in the floor beam web is caused by the rotation of the girder.

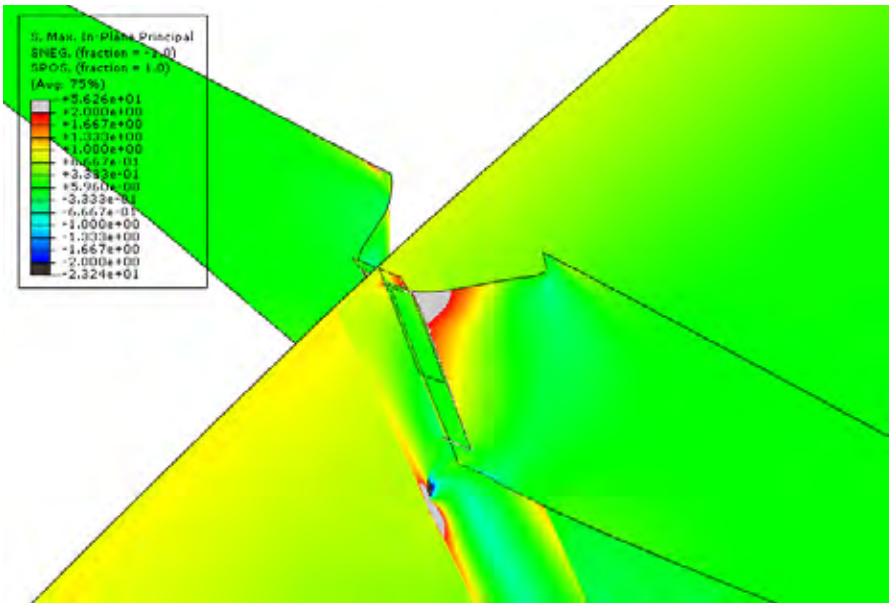

Figure 9.15: Floor Beam Web Bending due to Girder Rotation without Retrofits

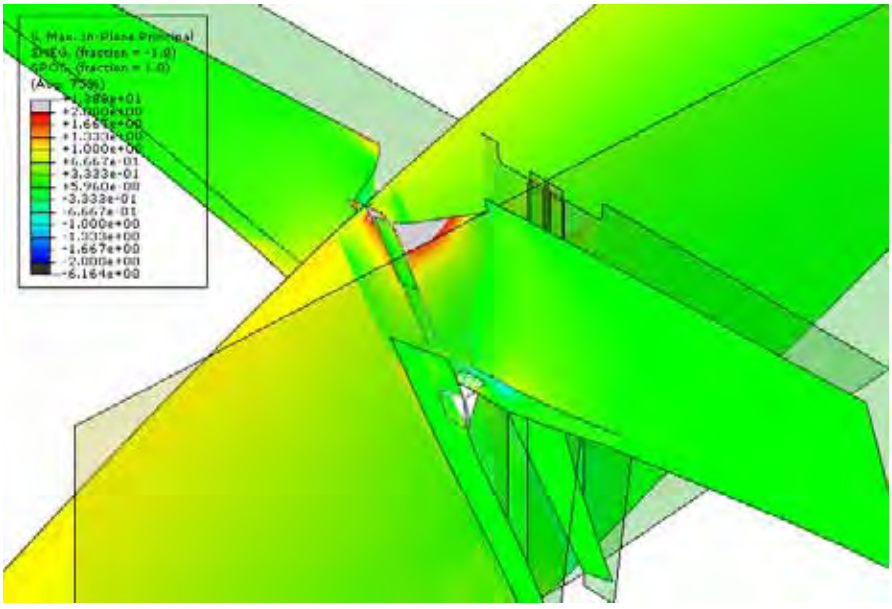

Figure 9.16: Floor Beam Web Bending due to Girder Rotation with Brace Plate Retrofit

9.4 Summary

In summary, a finite element model of Section F17S was created in order to verify the data collected during field testing and to test the effectiveness of two retrofits. The main difference between the model and the field test data is that the field data shows out-of-plane bending of the girder web toward the interior of the bridge while the computer model shows the web bending in the other direction. The reason for this is the double curvature that was shown to occur in the girder web in the small gap between the bearing stiffeners and the bottom flange of the floor beam. Because this gap is so small, any slight change in the location where the stress is measured could result in a change in the sign of that stress.

Two retrofits were incorporated into the model to determine their effectiveness. The first consists of adding knee brace plates over the existing bearing stiffeners, which are connected to the bottom floor beam flange using angle brackets and extend down to the bottom girder flange. The second involves cutting the existing bearing stiffeners in half in order to eliminate the previously mentioned small gap next to the bottom flange of the floor beam. The model shows that both retrofits were effective in reducing the stresses in these areas and also reduced the amount of out-of-plane bending of the girder web. However, these two retrofits are not effective in reducing the stresses and distortions in the floor beam web near the top of this connection.

Chapter 10. Conclusions

10.1 Introduction

This chapter summarizes the findings presented in the preceding chapters of this report. The results from the field tests performed on the two instrumented sections of the bridge will be summarized as well as the results from the finite element model of Section F14N. This chapter will also discuss what these results show to be the reasons for the cracking that has occurred in the bridge. Lastly, this chapter will give conclusions on the effectiveness of one possible retrofit for the bridge.

10.2 Summary of Field Test Results

10.2.1 Section F14N Results

In this section, floor beam 2 was the floor beam of interest. The connections of this floor beam to the girders had not been retrofitted with retrofit stiffeners. Cracks have formed in the girder web in the gap between the top flange of the girder and the web of the connecting floor beam. The field test results showed that the floor beam was bending in double curvature with the end of the floor beam under the trucks deflecting downward while the other end generally did not deflect. In addition to bending in the plane of the web, the floor beam also bends out of plane.

The girder was found to bend both in and out of the plane of the web at the location where the bottom flange of the floor beam frames into the girder. The in-plane bending is caused by the weight of the trucks deflecting the floor beams and girders downward. The out-of-plane bending is believed to be caused by the rotation of the floor beam under the weight of the trucks. Because the floor beams are connected to the web of the girder, this rotation is transferred to the girder in the form of out-of-plane bending of the web.

The gap in the girder web between the girder top flange and the web of the connecting floor beam was found to bend in single curvature. The stresses measured by the strain gages in this gap where the highest of all the gages on this section. The rotation of the floor beam under the truck loads is what is believed to cause the bending in this gap. Because of the small size of this gap, which measures between two and three inches, high stresses are occurring in this area, leading to the cracking.

10.2.2 Section F17S Results

In this section, floor beams 16 and 18 and their connections to the girders were instrumented. This section had staggered supports and two haunches along girder 2. The connections in this section had been retrofitted with retrofit stiffeners. This section experienced cracking in the web gap, on the girder web next to the bottom flange of the floor beam and at the weld connecting the retrofit stiffener to the top flange of the girder. The staggered supports allow the floor beams to deflect in such a way that creates a twisting motion in the bridge. Depending on the location of the trucks, the floor beams were shown to deflect vertically both up and down. The left side of floor beam 16 is connected to a haunched girder, which is supported by a column while the other side is connected to a girder that is neither haunched nor supported by a column. This creates a situation in which one side of the floor beam has a very stiff, rigid connection while the other side is fairly free to move. The haunch was shown to attract much of the stress caused by the weight of the trucks over this floor beam.

The webs of the girders were found to bend both in and out of the plane of the web at the location where the bottom flange of the floor beam frames into the girder. As was discussed in the previous section, the out-of-plane bending is believed to be the result of the rotation of the floor beam, which is connected to the girder web. At connections where the girder is supported by a column, the presence of bearing stiffeners creates a very small gap between the stiffeners and the bottom flange of the connecting floor beam. High stress concentrations in this gap are most likely the cause for the cracking that has been seen in this area.

The retrofit stiffeners were found to bend both in and out of the plane of the stiffener. In-plane bending was most likely caused by rotation of the floor beam-to-column connection due to deflection of the floor beams. Out-of-plane bending of the stiffeners was most likely due to vertical movement of the girder in the plane of the girder web.

10.2.3 Fatigue Test Results

The floor beams and retrofit stiffeners are of little concern with regard to fatigue. These details are experiencing relatively low stress ranges and perform fairly well under fatigue loading. The girder web details, including the small gap above the web of the connecting floor beam and adjacent to the bottom flange of the connecting floor beam, are details that perform very poorly under fatigue loading. These areas are experiencing very high stress ranges and many cycles, which results in very short fatigue lives. The poor fatigue performance of these details is confirmed by the presence of cracks in these areas.

10.3 Summary of Finite Element Model of Section F14N

The finite element model that most closely resembled the live load field tests results for Section F14N was the model with 4000 psi concrete and composite action between the slab and floor beams. One of the main differences between the model and the field test data is that the model shows the web gap bending in double curvature when the field test data shows that it bends in single curvature. The other difference is that the model does not show significant out-of-plane bending of the girder web around the area where the bottom flange of the floor beam frames into the girder.

Retrofit angles, one of the retrofit plans being considered for this bridge, were incorporated into the model to determine their effectiveness. The purpose of these angles is to connect the web of the floor beam to the top flange of the girder. The model shows that the angles decreased the bending stress in the web gap but increased the stress in the floor beam web around the coped area. This increase in stress at the cope and at the transverse stiffener welds may lead to cracking at this location.

10.4 Summary of Finite Element Model of Section F17S

A finite element model of Section F17S was created in order to verify the data collected during field testing and to test the effectiveness of two retrofits. The main difference between the model and the field test data is that the field data shows out-of-plane bending of the girder web toward the interior of the bridge while the computer model shows the web bending in the other direction. The reason for this is the double curvature that was shown to occur in the girder web in the small gap between the bearing stiffeners and the bottom flange of the floor beam. Because this gap is so small, any slight change in the location where the stress is measured could result in a change in the sign of that stress.

Two retrofits were incorporated into the model to determine their effectiveness. The first consists of adding knee brace plates over the existing bearing stiffeners, which are connected to the bottom floor beam flange using angle brackets and extend down to the bottom girder flange. The second involves cutting the existing bearing stiffeners in half in order to eliminate the previously mentioned small gap next to the bottom flange of the floor beam. The model shows that both retrofits were effective in reducing the stresses in these areas and also reduced the amount of out-of-plane bending of the girder web. However, these two retrofits are not effective in reducing the stresses near the top of this connection.